Impact of Endocrine and Nutritional Factors on White-to-Brown Conversion of Primary Human Adipocytes

Inaugural-Dissertation

zur
Erlangung des Doktorgrades

der Mathematisch-Naturwissenschaftlichen Fakultät
der Heinrich-Heine-Universität Düsseldorf

vorgelegt von
Manuela Fleckenstein-Elsen
aus Waldbröl

Düsseldorf, April 2015

Diese Arbeit wurde angefertigt am

Deutschen Diabetes-Zentrum
Paul-Langerhans-Gruppe für Integrative Physiologie
Leibniz-Zentrum für Diabetes-Forschung

an der Heinrich-Heine-Universität Düsseldorf

Gedruckt mit der Genehmigung der Mathematisch-Naturwissenschaftlichen Fakultät
der Heinrich-Heine-Universität Düsseldorf

Referent: Prof. Dr. Jürgen Eckel
Korreferent: Prof. Dr. Eckhard Lammert
Tag der mündlichen Prüfung: 13.07.2015

"Errare humanum est, in errore perseverare stultum"

Zusammenfassung

Adipositas, definiert als übermässige Ansammlung von Fettgewebe, ist ein bedeutendes weltweites Gesundheitsproblem und hat in Europa und anderen Regionen bereits epidemische Ausmaße erreicht. Neben der körperlichen Einschränkung ist Adipositas auch mit einem erhöhten Risiko für die Entwicklung zusätzlicher metabolischer Erkrankungen, wie z.B. Typ-2-Diabetes, verbunden. Das Fettgewebe spielt eine zentrale Rolle in der Regulation des Energiestoffwechsels und lässt sich prinzipiell in zwei funktional unterschiedliche Arten unterteilen: Weißes und braunes Fettgewebe. Weißes Fettgewebe speichert überschüssige Energie und stellt ein endokrines Organ dar, das eine Vielzahl aktiver Proteine, sogenannter Adipokine, freisetzt. Diese gelangen in die Zirkulation und üben so einen endokrinen Effekt auf andere Organe aus, wie z.B. die Entstehung von Insulinresistenz im Skelettmuskel. Die Funktion sowie Struktur des Fettgewebes verändert sich im Laufe der fortschreitenden Adipositas, und geht mit einer Veränderung des Adipokin-Sekretionsprofils einher. Die veränderte Freisetzung von Adipokinen im adipösen Zustand ist für das erhöhte Risiko zur Entstehung anderer metabolischer Erkrankungen verantwortlich. Daher ist die Charakterisierung von Adipokinen und deren Regulation im adipösen Zustand *in vivo* von besonderem Interesse. Basierend auf einer früheren Studie unserer Arbeitsgruppe wurde eine *in silico* Analyse durchgeführt, um die Regulation von mehr als 300 potentiellen Adipokinen in der Adipositas und deren funktionales Spektrum zu analysieren. Mit Hilfe eines Bewertungssystems wurden alle Adipokin-Kandidaten evaluiert, um diejenigen mit potentiell hoher Relevanz im Kontext der Adipositas zu selektieren. Die Faktoren mit der höchsten Bewertung könnten neue therapeutische Ansatzpunkte zur Eindämmung der Entwicklung von mit Adipositas assoziierten Erkrankungen darstellen.

Braunes Fettgewebe spielt ebenso wie weißes Fettgewebe eine bedeutende Rolle in der Regulation des Energiestoffwechsels. Die Funktion brauner Fettzellen ist die Bildung von Wärme im Rahmen der sogenannten zitterfreien Thermogenese unter Verbrennung von Energie, vermittelt durch das Protein *uncoupling protein-1* (UCP1). Es existieren zwei verschiedene Typen von braunen Fettzellen mit unterschiedlichem Entwicklungsursprung. Klassische braune Fettzellen mit myogenem Ursprung und beige Fettzellen, die aus weißen Präadipozyten durch bestimmte Faktoren induziert werden können. Beide Subtypen kommen im erwachsenen Menschen vor und exprimieren UCP1. Eine erhöhte Bildung brauner sowie beiger Fettzellen könnte den Gesamtenergieumsatz erhöhen und somit der Entstehung von Adipositas entgegenwirken. Primärer Fokus dieser Doktorarbeit war daher die Identifizierung von Faktoren, welche die Entwicklung beiger Fettzellen im weißen Fettgewebe fördern. In

diesem Rahmen wurde der Wachstumsfaktor *bone morphogenetic protein 4* (BMP4) als Vermittler der Induktion von beigen Adipozyten in einem primären humanen Zellsystem identifiziert. Weiterhin könnte BMP4 seine Wirkung in einer auto-/parakrinen Weise ausüben, da die Expression und Sekretion von BMP4 in primären humanen Adipozyten gezeigt wurde.

Eine überschüssige Energiezufuhr in Kombination mit Bewegungsmangel resultieren in einer positiven Energiebilanz und stellen die primären Ursachen für die weltweite Adipositas-Epidemie dar. Neben der absoluten Energiezufuhr spielt auch die Qualität der Nahrung, insbesondere die Fettsäurekomposition, eine bedeutende Rolle für die Funktion des weißen und braunen Fettes. In diesem Zusammenhang wird langkettigen mehrfach ungesättigten Fettsäuren (LC-PUFA, long-chain polyunsaturated fatty acid) der n-3 Familie ein hemmender Effekt auf die Gewichtszunahme zugesprochen, während n-6 LC-PUFAs die Entstehung von Adipositas fördern sollen. Diese Annahmen basieren hauptsächlich auf Studien in Mausmodellen und der direkte Effekt von n-3 und n-6 Fettsäuren auf die beige Adipozytendifferenzierung in humanen Präadipozyten war bisher nicht bekannt. Die Daten der vorliegenden Doktorarbeit zeigen, dass von den getesteten Fettsäuren ausschließlich die n-3 LC-PUFA Eicosapentaensäure (EPA) die Induktion beiger Adipozyten fördert. Im Gegensatz dazu hemmt die n-6 LC-PUFA Arachidonsäure (ARA) die Differenzierung beiger Adipozyten und führt zur Bildung eines weißen Adipozytenphänotyps. Dieser hier beschriebene Effekt von EPA auf die beige Adipogenese in einem primären humanen Zellsystem stellt einen neuen Mechanismus für die „anti-Adipositas“ Effekte von n-3 LC-PUFAs dar.

Kürzlich hat ein neues Hormon, welches die Bildung beiger Adipozyten induzieren soll, beachtliches Interesse hervorgerufen. Der Skelettmuskel stellt wie auch das Fettgewebe ein endokrines Organ da, das durch die Freisetzung von Faktoren in die Zirkulation mit anderen Geweben kommunizieren kann. Irisin soll ein solches Myokin sein und wurde erstmals 2012 beschrieben. Durch Spaltung des Transmembranproteins FNDC5 in der extrazellulären Domäne soll Irisin vermehrt nach sportlicher Betätigung freigesetzt werden und die Generierung beiger Fettzellen im weißen Fettgewebe fördern. Bis heute wurden bereits 207 Studien über Irisin publiziert, wobei die Datenlage sehr kontrovers ist. Diese Arbeit liefert einen bedeutenden Hinweis darauf, dass Irisin nicht oder nur marginal im Menschen exprimiert ist und weiterhin keinen Effekt auf die weiß-zu-beige Transdifferenzierung von primären humanen Adipozyten hat. Des Weiteren wurde die Literatur zu Irisin im Rahmen eines Übersichtsartikels aufgearbeitet und hohe Widersprüche zwischen verschiedenen

Studien aufgedeckt, welche die Relevanz von Irisin in der beigen Adipogenese im Menschen in Frage stellen.

Abschließend lässt sich sagen, dass die weiß-zu-beige Transdifferenzierung von humanen Adipozyten durch endogene Hormone, wie BMP4 gefördert wird. Darüber hinaus wurde gezeigt, dass auch mit der Nahrung zugeführte Komponenten, speziell die n-3 LC-PUFA EPA die Bildung beiger Adipozyten fördert. Im Gegensatz dazu hatte das vielversprechende Myokin Irisin keinen Effekt auf die beige Adipogenese und die Existenz von Irisin im Menschen ist fraglich. Die Daten dieser Arbeit tragen zum Verständnis der Regulation der beigen Adipozytendifferenzierung im Menschen bei und weisen darauf hin, dass eine ausgewogene EPA-reiche Ernährung eine potentielle Strategie gegen die fortschreitende Entwicklung von Adipositas darstellen könnte.

Summary

Obesity is a major global health problem associated with a higher risk to develop other severe metabolic complications, such as type 2 diabetes mellitus. The adipose organ plays a major role in the regulation of energy homeostasis and consists of two functionally different types: white and brown adipose tissue (WAT and BAT). WAT stores excess energy and has been recognized as an active endocrine organ, releasing several adipocyte-derived factors, the so-called adipokines. The progression of obesity and WAT growth is accompanied by morphological and functional changes of WAT. In this state, the adipokine secretion profile is concomitantly altered, providing a causal link between obesity and its associated metabolic diseases. The characterization and regulation of adipokines in human obesity is therefore of considerable interest. Based on a previous study from our group, an *in silico* analysis was performed aiming to evaluate the broad function of more than 300 recently identified adipokine candidates and to analyze their regulation in human obesity *in vivo*. Using a scoring system, potential adipokine candidates of high interest in the context of obesity were identified and selected. These high-score factors may represent novel therapeutic targets to prevent the development of obesity-associated diseases.

BAT as the second functional type of adipose tissue plays a major role in the regulation of energy homeostasis as well. The function of BAT is the generation of heat in response to a cold environment. This process called non-shivering thermogenesis expends energy and is mediated by uncoupling protein-1 (UCP1). Two types of UCP1-expressing thermogenically active adipocytes are currently known: Classical brown adipocytes derived from the myogenic lineage and brite (brown-in-white) or beige adipocytes which can be induced in WAT depots in response to certain stimuli. Both, classical brown and brite adipocytes are present in adult humans. Promoting the recruitment and activity of these adipocytes may increase energy expenditure and represent a strategy to counteract the development of obesity. As part of the search for approaches promoting white-to-brown conversion in human adipocytes, bone morphogenetic protein 4 (BMP4) was identified as an inducer of brite adipocyte differentiation in primary human adipose-derived stem cells (hASCs). Furthermore, BMP4 may regulate brite adipocyte differentiation in an auto-/paracrine manner, since it is expressed and secreted from hASCs.

Overnutrition and physical inactivity lead to a positive energy balance and are the main causes of weight gain. In addition to the energy content of diet, food composition and in particular the presence of certain fatty acids may have a specific impact on WAT and BAT

function. In particular, long-chain polyunsaturated fatty acids (LC-PUFAs) from the n-3 family exert anti-obesity effects in rodents, while n-6 LC-PUFAs are thought to promote obesity. However, the underlying mechanisms and the role of individual n-3 and n-6 LC-PUFAs in the white-to-brown conversion remain unclear. The present thesis reveals that the n-3 LC-PUFA eicosapentaenoic acid (EPA) and the n-6 LC-PUFA arachidonic acid (ARA) differentially regulate white versus brite adipocyte formation in hASCs. EPA induced a brite phenotype and improved mitochondrial function in hASCs, providing a novel mechanism for the anti-obesity effects of n-3 LC-PUFAs.

Recently, a novel hormone gained considerable interest as a potent inducer of WAT browning. Similar to WAT, skeletal muscle is considered as an endocrine organ releasing so-called myokines which enter the circulation and may affect adipose tissue function. Irisin is the cleavage product from the transmembrane protein FNDC5 and has been described in 2012 as an exercise-regulated myokine inducing the browning of WAT in mice. Until today, 207 studies have been published about this protein. However, the data of this thesis indicate that irisin is not expressed in humans and does not trigger brite adipogenesis in hASCs. As part of this thesis, a systematical review about the presence of irisin and its effect on WAT browning in humans was performed. Striking inconsistencies between studies were noted, questioning the relevance of irisin as a therapeutic tool in humans.

Taken together, white-to-brown conversion of primary human cells is regulated by endogenous hormonal factors like BMP4. This thesis further indicates that nutritional compounds, in particular the n-3 LC-PUFA EPA, promote brite adipocyte formation as well. In contrast, the promising exercise-regulated myokine irisin turned out to play a negligible role in humans, since it is likely to be not expressed and had no effect on white-to-brown conversion in primary human adipocytes. The here observed effect of EPA on white-to-brown conversion illustrates that diet quality is of importance and that a healthy diet may have beneficial effects on the development of obesity and its associated disorders in humans.

Table of contents

List of Figures

List of Tables

List of abbreviations

^{18}F-FDG	^{18}F-fluorodeoxyglucose
ALA	Alpha-linolenic acid
ARA	Arachidonic acid
ATF2	Activating transcription factor 2
BAT	Brown adipose tissue
BMI	Body mass index
BMP	Bone morphogenetic protein
C/EBP	CCAAT/enhancer-binding protein
cAMP	Cyclic adenosine monophosphate
COX	Cyclooxygenase
CPT1B	Carnitine palmitoyltransferase 1B (muscle type)
CREB	cAMP response element binding protein
DHA	Docosahexaenoic acid

List of abbreviations

EPA	Eicosapentaenoic acid
FABP	Fatty acid-binding protein
FNDC5	Fibronectin type III domain containing protein 5
FFA	Free fatty acids
HFD	High fat diet
HSL	Hormone-sensitive lipase
IL	Interleukin
LA	Linoleic acid
MAPK	Mitogen-activated protein kinase
NE	Norepinephrine
NST	Non-shivering thermogenesis
OA	Oleic acid
Pdgfrα	Platelet-derived growth factor receptor-alpha
PET-CT	Positron emission tomography – computed tomography
PGC1α	Peroxisome proliferator-activated receptor-gamma coactivator 1-alpha
PKA	cAMP-dependent protein kinase
PPARγ	Peroxisome proliferator-activated receptor-gamma
PRDM16	PR domain zinc finger protein 16
PUFA	Polyunsaturated fatty acid
RXR	Retinoid X receptor
TGF	Transforming growth factor
TMEM26	Transmembrane protein 26
TNFRSF9	Tumor necrosis factor receptor superfamily member 9
TNF	Tumor necrosis factor
TZD	Thiazolidinediones
UCP1	Uncoupling protein 1
WAT	White adipose tissue
WHO	World health organization
β-AR	β-adrenergic receptor
ECM	Extracellular matrix
WISP2	WNT1-inducible signaling pathway protein 2

1 Introduction

1.1 Obesity and associated diseases

1.1.1 Obesity

Obesity is a major global health problem with increasing prevalence mainly due to life style changes. Increased food intake and reduced physical activity result in a positive energy balance. Excess energy intake leads in consequence to the development of overweight and obesity, defined as abnormal or excessive fat accumulation (1). The body mass index (BMI) is the most commonly used measure to classify different levels of overweight. BMI, a simple relation of body weight to body height is defined as the weight in kg divided by the square of the height in m [kg/m^2]. According to the World Health Organization (WHO), a BMI greater or equal than 25 kg/m^2 is considered as overweight and a BMI greater or equal than 30 kg/m^2 is defined as obese (Table 1) (1). However, BMI is only a rough measure of weight and does not distinguish between fat and lean mass. The worldwide prevalence of obesity has dramatically increased over the last decades, with only 5% of men and 8% of women being obese in 1980 to a rate of 10 % for men and 14 % for women in 2008 (2). A high proportion of 35 % of adults aged over 20 years were estimated to be overweight (BMI $\geq$ 25 kg/m^2) in 2008. Overweight and obesity impair life quality and have severe consequences for health. Thus, overweight and obesity are associated with an increased risk for other metabolic disorders, such as insulin resistance, type 2 diabetes and cardiovascular diseases (3). The costs for treatment of obesity and its associated disorders are increasing and estimated between $147 and $210 billion per year, accounting for nearly 10 percent of all medical expenses (4).

Table 1: WHO weight classification according to BMI

Category	BMI range – kg/m^2
Very severely underweight	less than 15
Severely underweight	from 15.0 to 16.0
Underweight	from 16.0 to 18.5
Normal (healthy weight)	from 18.5 to 25
Overweight	from 25 to 30
Obese Class I (Moderately obese)	from 30 to 35
Obese Class II (Severely obese)	from 35 to 40
Obese Class III (Very severely obese)	over 40

1.1.2 White adipose tissue as an endocrine organ

Due to the increasing prevalence of obesity, the accompanied risk to develop other diseases and its impact on economic costs, research in the field of obesity is of particular relevance. In order to understand the link between obesity and the development of these associated disorders, research has focused on adipose tissue biology. Regarded for a long time as an inert depot to store excess energy, WAT is now considered as active endocrine organ, releasing a wide range of different bioactive factors, so-called adipokines (5;6). WAT is a complex organ composed of different cell types. Besides lipid-laden mature adipocytes, also macrophages, perivascular cells, preadipocytes, adipose-derived stem cells and blood cells coexist in the adipose organ and contribute to the whole secretory output (7). Classical adipokines, such as adiponectin and leptin are primarily secreted by mature adipocytes within WAT, while adipose-tissue resident macrophages and other cells from the stroma-vascular fraction release different cytokines and chemokines. Thus, the adipose tissue secretome is dependent on the tissue structure as well as cell composition (8). Moreover, the secretome differs between different anatomical locations and subcutaneous and visceral adipose tissue, the major WAT depots, display unique adipokine secretion profiles (9). In addition to their auto- and paracrine effects on adipose tissue-resident cells, adipokines are released into the circulation and thereby exert endocrine effects on peripheral organs (3). Several endocrine actions of adipokines are already known, including effects on skeletal muscle insulin sensitivity, vascular function, central regulation of food intake and pancreatic β-cell function (3). In order to understand this complex network, several studies aimed to characterize the human fat cell secretome (10;11). The identification of novel adipokines as potential therapeutic targets represents a relevant strategy to reduce obesity-associated disorders.

1.1.3 Impact of WAT-dysfunction on metabolic diseases

Weight gain and the progression of obesity are often accompanied by morphological and functional changes of WAT, defined as adipose tissue dysfunction. The main determinants of adipose tissue dysfunction are an enlargement of adipocytes (adipocyte hypertrophy) and a chronic low-grade inflammatory state, linking obesity to metabolic disturbances (12). Both, increasing the number as well as enlargement of adipocytes can occur during the expansion of adipose tissue mass (13). Increased energy intake and subsequent fat storage leads to increased adipocyte size and is thought to be the main mechanism contributing to adipose tissue growth (14;15). When enlarged adipocytes reach their maximum capacity to store triglycerides, postprandial circulating lipids cannot be buffered by WAT and remain in the circulation. In consequence, this may lead to the accumulation of fat in tissues originally not

conceived to store energy, such as the liver, skeletal muscle or the pancreas. This ectopic fat accumulation disturbs normal function of organs or tissues and represents a potential cause for the development of obesity-linked diseases (12). In particular, skeletal muscle insulin sensitivity is impaired by increased circulating levels of free fatty acids (FFA) (16). Interestingly, the number of fat cells stays relatively constant during adulthood and about 10% of adipocytes are annually renewed (13). Thus, *de novo* differentiation of adipocytes is an important process to maintain adipocyte number and to prevent adipocyte hypertrophy. Adipocyte size is highly variable between individuals within the same BMI range (17) and is linked to metabolic disturbances independently of BMI (18). Remarkably, individuals with hypertrophic adipose tissue display a reduced annual adipocyte turnover rate (17) and have a reduced capacity to recruit and differentiate new adipocytes (18). Such impairments of adipocyte turnover and adipogenesis may even promote the development of a hypertrophic adipose tissue phenotype.

Besides an impaired storage capacity of enlarged adipocytes, a shift towards a rather pro-inflammatory adipokine secretion profile occuring in hypertrophic obesity contributes to the development of metabolic dysfunction (3). This pro-inflammatory shift in the adipose tissue secretory output is the result of adipocyte size itself as well as changes in adipose tissue composition (8). Isolated human mature adipocytes which have been separated according to their size display a positive association between the secretion of pro-inflammatory adipokines and adipocyte size (19). Moreover, composition of WAT is concomitantly altered during the progression of obesity. Thus, macrophage marker expression is enhanced in WAT in different mouse models of genetic and diet-induced obesity (20). In contrast, weight loss results in a significant decrease of adipose tissue-resident macrophages in obese individuals (21). A histological feature of the obesity-associated chronic low-grade inflammation of WAT, especially in the visceral depot, is the accumulation of macrophages in so-called crown-like structures. In those arrangements, macrophages surround dead or non-functional adipocytes, probably in order to remove apoptotic cells (8). Not only quantity of macrophages is increased in obesity-associated adipose tissue inflammation, but macrophages also differ in their quality and function. In healthy adipose tissue from lean subjects, mainly macrophages from the "alternatively activated" M2 phenotype are present. M2 macrophages secrete anti-inflammatory cytokines, such as interleukin (IL)-10, and are involved in tissue repair and the resolution of inflammation. In obesity, a shift from M2 towards "classically activated" M1 macrophages occurs which secrete pro-inflammatory cytokines like tumor necrosis factor alpha (TNFα) and IL-6 (8).

Therefore, the increased release of pro-inflammatory factors from dysfunctional adipose tissue is due to both, secretory changes of the enlarged adipocyte as well as a higher abundance of macrophages, especially from the M1 phenotype. This low-grade chronic inflammation of WAT and a disturbed lipid-buffering capacity represent the major causal link between obesity and its associated metabolic diseases.

1.2 The adipose organ in the regulation of energy homeostasis

1.2.1 Functionality and distribution of white and brown adipose tissue

All adipose tissue depots, differing in their anatomical location and function, build the adipose organ (22). The adipose organ consists of two main functionally different types and plays an important role in the regulation of energy homeostasis. As explained in the previous chapter, WAT is the main site of energy storage and an endocrine organ. Due to their function to store excess energy in the form of triglycerides, white adipocytes consist of one large unilocular lipid droplet, a relatively low proportion of cytoplasm and a peripherally located nucleus (Figure 1a). During negative energy balance, breakdown of triglycerides leads to the release of glycerol and FFA into the circulation. This process called lipolysis guarantees nutrient supply for other tissues in starving times. Two major WAT depots can be distinguished according to their anatomical location: the subcutaneous and visceral depot. Subcutaneous WAT is located under the skin, while visceral WAT surrounds the inner organs. The latter can be further subdivided into the omental depot superficially lying on the intestines, the mesenteric depot deeply surrounding the intestines and the retroperitoneal depot close to the kidneys (Figure 1b). Moreover, several smaller depots such as pericardial, perivascular or epigastric adipose tissue exist surrounding specific organs (23). Several depot-specific differences between subcutaneous and visceral WAT have been described. Subcutaneous WAT harbors more preadipocytes with a higher capacity for adipogenesis than visceral WAT (24). In contrast, the visceral depot displays a lower ability to expand by hyperplasia, is more prone to develop obesity-associated chronic low-grade inflammation and secretes more cytokines than subcutaneous depots (25). Increased visceral WAT mass has been proposed to be a cause of reduced storage capacity or expandability of subcutaneous WAT and may be considered as ectopic fat accumulation (26). In line, body fat distribution is an important factor and visceral fat accumulation is accompanied with a high risk for metabolic complications (27).

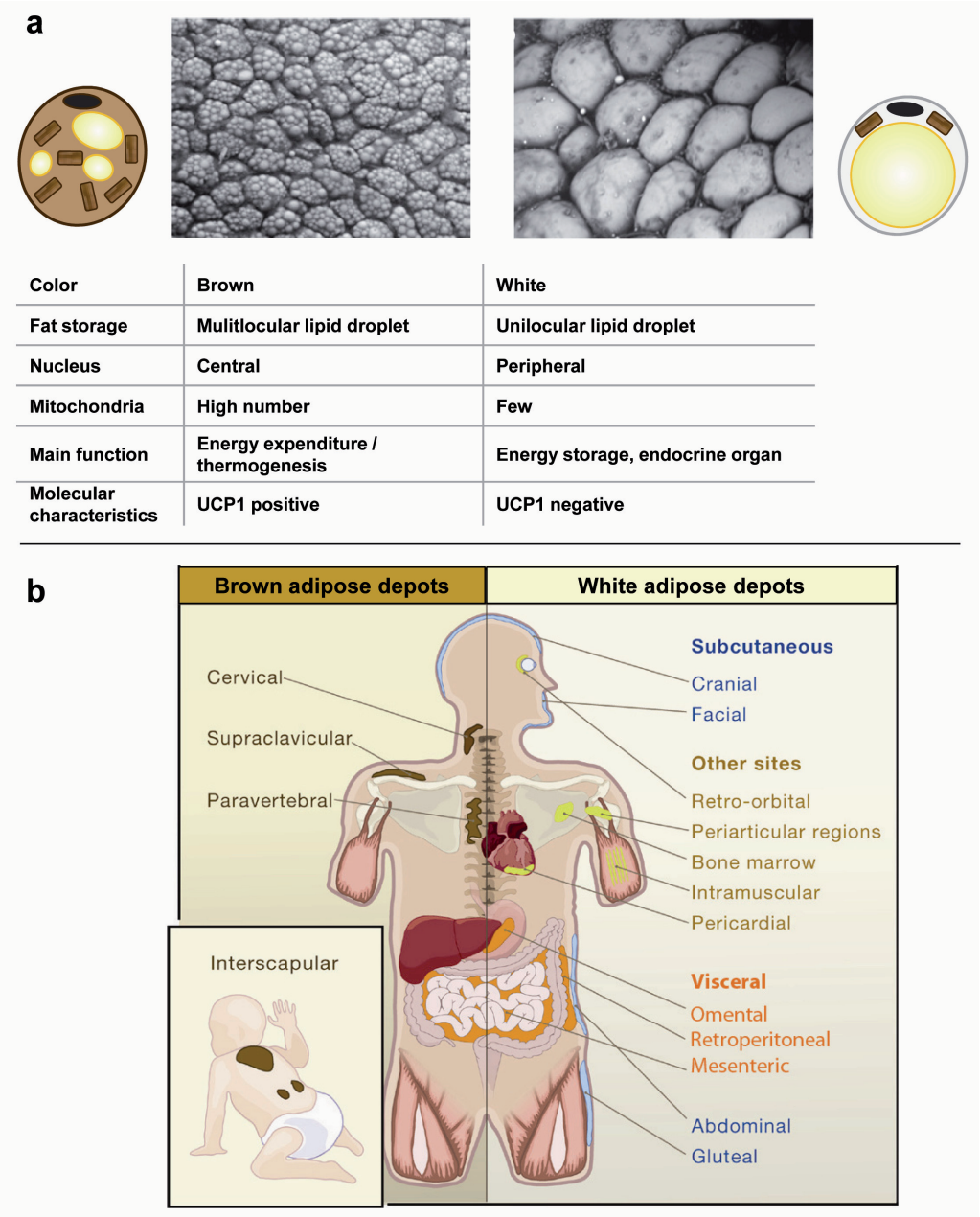

Color	Brown	White
Fat storage	Mulitlocular lipid droplet	Unilocular lipid droplet
Nucleus	Central	Peripheral
Mitochondria	High number	Few
Main function	Energy expenditure / thermogenesis	Energy storage, endocrine organ
Molecular characteristics	UCP1 positive	UCP1 negative

Figure 1: Characteristics and anatomical location of brown and white adipose tissue. (a) Electron micrograph of murine brown and white adipose tissue and schematic illustration of brown and white adipocyte morphology. Brown adipocytes are thermogenically active due to expression of uncoupling protein 1 (UCP1), have a high number of mitochondria and small multilocular lipid droplets. White adipocytes function as temporary energy storage site, have a unilocular lipid droplet and only few mitochondria. (b) Anatomical sites of brown and white adipose tissue depots in humans. Brown adipose tissue is abundant in newborns and still present in the adult human, located mainly in the interscapular region. The main sites of white adipose tissue are the subcutaneous and visceral depots (modified from Bartelt and Heeren, Nat Rev Endocrinol (2014) (a); and Gesta et al., Cell (2007) (b)).

In contrast to WAT, BAT dissipates energy to maintain body core temperature in a process called non-shivering thermogenesis (NST). This unique function of brown adipocytes is due to a high abundance of mitochondria, containing uncoupling protein 1 (UCP1) in the inner

mitochondrial membrane. During cold exposure, sympathetic neurons activate brown adipocytes which in turn oxidize lipids, stored in small multilocular lipid droplets, and generate heat by UCP1-mediated thermogenesis. Therefore, UCP1 dissipates the electrochemical proton gradient generated during oxidative phosphorylation under the generation of heat (28). The expression of ATP synthase, which also needs this electrochemical energy to generate ATP, is relatively low in BAT compared to WAT, reflecting the thermogenic function of brown adipocytes (29). In mice, BAT is mainly located in the interscapular, cervical and axillary depots (30). Until recently, BAT was believed to be absent in the adult human and only to play a role in newborns, where it is crucial to compensate for the decrease in ambient temperature after delivery. However, in 2009 five groups have independently discovered the presence of active BAT in adults by measuring uptake of the glucose analogue ^{18}F-fluorodeoxyglucose (^{18}F-FDG) using a combination of positron-emission tomography and computed tomography (PET-CT) (31-35). Similar to the anatomical location in mice, BAT depots in humans are found in the deep neck region, such as the supraclavicular and cervical localization (Figure 1b).

The presence of BAT and WAT allows mammals to adapt to changes in nutrient supply and ambient temperature, due to their ability to dissipate (BAT) or to store (WAT) energy. Interestingly, the adipose organ displays high plasticity in response to environmental changes. Especially the discovery of active BAT in the adult human led to high interest in this field and numerous studies have focused on the question, if BAT has a significant impact on energy expenditure in humans and therefore represents a potential target to treat obesity.

1.2.2 Control of BAT thermogenesis

The physiological function of BAT is the maintenance of body temperature. Thus, NST is only necessary when ambient temperature decreases and BAT has to be activated under these conditions. Similar to WAT, BAT is a complex organ consisting of different cell types surrounding the brown adipocytes and controlling their function. BAT is highly innervated with nerve fibers responsible for activation of brown adipocytes. Moreover, a high vascularization guarantees sufficient supply with oxygen and substrates needed for NST, and mediates the transport of heat into the periphery (28). The activation of UCP1-mediated thermogenesis in BAT is summarized in figure 2.

Upon cold exposure and excess energy intake, the catecholamine norepinephrine (NE) is released from sympathetic nerve ends leading to brown adipocyte activation via β-adrenergic receptor (β-AR) signaling. β-ARs are G protein-coupled receptors and three subtypes exist, the β1-, β2- and β3-AR. The latter being the most abundant in brown adipocytes and mainly responsible for thermogenesis. Upon binding of NE to the β-AR, adenylate cyclase is activated leading to increased cellular cylic AMP (cAMP) levels. Subsequently, cAMP triggers the activation of cAMP-dependent protein kinase (PKA) which in turn phosphorylates several downstream targets. PKA-mediated phosphorylation of lipid-droplet coating proteins, such as perilipins, allows triglyceride breakdown. Hormone-sensitive lipase (HSL), also activated by PKA, catalyzes the first step of lipolysis leading finally to the release of FFA and glycerol into the cytosol. Interestingly, the presence of FFAs in the cytosol is sufficient to induce UCP1-mediated thermogenesis independently of NE-stimulation (28). In the basal non-stimulated state, purine di- and triphosphate nucleotides, mainly ATP, bind to the cytosolic side of UCP1 and thereby prevent proton flux (36). When brown adipocytes are treated with FFA or lipolysis is induced by β-adrenergic stimulation, the inhibitory effect of ATP on UCP1 is overridden. Thus, UCP1 has been recently described as FFA/H^+ symporter and long-chain fatty acids directly bind to the cytoplasmic side of UCP1 and serve as substrates for the H^+ symport (37). Moreover, FFA levels must exceed ATP levels by roughly 100x to activate UCP1, indicating that UCP1 and thermogenesis are blocked under basal physiological conditions (37).

In white adipocytes, the process of lipolysis occurs in the fasted state and is driven by β-adrenergic stimulation as well. While white adipocytes release FFA into the circulation, brown adipocytes are able to retain most of the FFA as substrates for UCP1-mediated thermogenesis. This is due to a relatively high expression of fatty acid-binding proteins (FABPs) in brown adipocytes compared to white adipocytes and expression of the heart type of FABP (H-FABP) encoded by the *FABP3* gene (28). Furthermore, H-FABP expression is dramatically upregulated upon NE treatment preventing release of FFA from adipocytes (28). Additionally, a prominent expression of carnitine palmitoyltransferase 1B (CPT1B), mediating the transport of FFA from the cytosol into the mitochondria, assures substrate supply for β-oxidation and oxidative phosphorylation. Besides *FABP3* and *CPT1B* expression, several other genes encoding for proteins related to fatty acid metabolism and β-oxidation are differentially expressed in brown and white adipocytes, in line with their specialized metabolic functions (29).

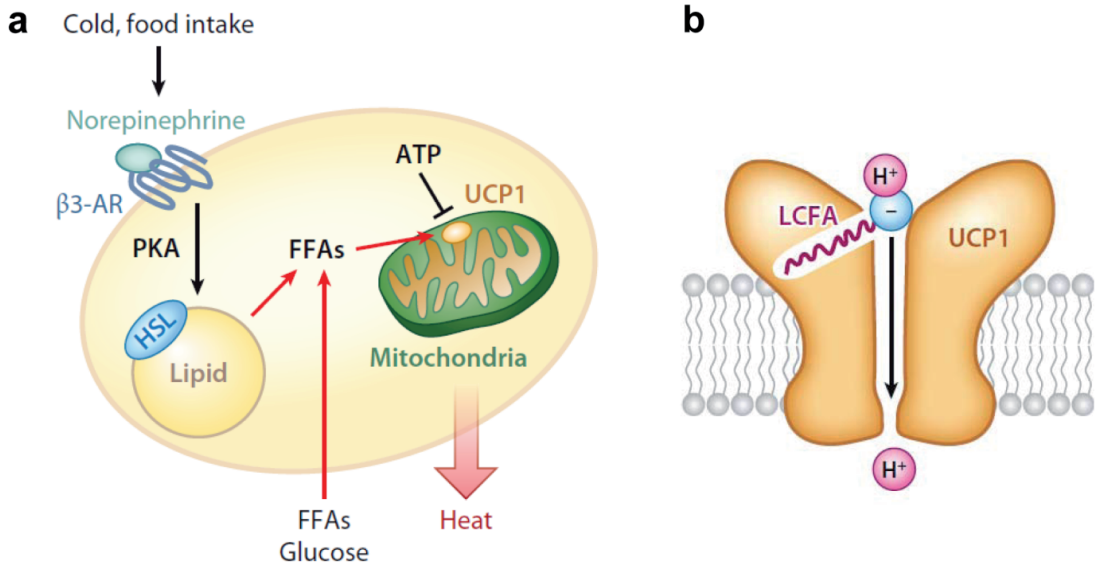

Figure 2: Activation of UCP1-mediated thermogenesis in brown adipocytes. (a) Upon cold exposure or excess food intake norepinephrine is released from sympathetic nerve fibers and binds to β-AR. Mainly mediated by the β3-AR, PKA is activated leading to phosphorylation and activation of downstream targets involved in lipolysis, such as HSL. FFAs released from lipolysis or taken up from the circulation serve as substrates for β-oxidation and activate UCP1, which is repressed in the basal state by binding of ATP. (b) Function of UCP1 as a symporter of long-chain fatty acids (LCFA) and H^+ (modified from Kajimura and Saito, Annu Rev Physiol (2014)).

1.2.3 Developmental origin of brown and brite adipocytes

Brown adipocytes

As putative therapeutic target, identification of the origin of brown adipocytes is of importance. The anatomy of BAT was already described in 1551 as "neither fat nor flesh" (38). In the recent decade, knowledge about the developmental origin and the regulation of white and brown adipocyte differentiation has highly advanced. One of the most striking observations in this field was the lineage determination of brown adipocytes. In contrast to previous assumptions, brown adipocytes to do not share a common progenitor with white adipocytes. Seale and colleagues reported by lineage tracing studies *in vivo*, that brown adipocytes derive from precursor cells expressing the muscle-specific *Myf5* gene (39;40). In this context, the transcriptional regulator PR domain zinc finger protein 16 (PRDM16) was identified as central regulator controlling cell fate of *Myf5*$^+$ progenitor cells. Thus, knockdown of PRDM16 in murine brown preadipocytes prevented adipocyte differentiation and abrogated expression of *UCP1* and other thermogenic genes. Vice versa, forced expression of *PRDM16* in myoblasts blocked myogenesis and allowed differentiation into brown adipocytes (39). Accordingly, classical brown adipocytes can be characterized by expression of myogenic marker genes, such *ZIC1* or *LHX8*, as well as the expression of *UCP1*

and other thermogenic genes (30) (Figure 3). From a functional point of view, it seems conclusive that white and brown adipocytes, which exert different functions, have no common precursor cell. Indeed, brown adipocytes are rather related to skeletal muscle cells which also take up and store macronutrients for their own consumption, whereas white adipocytes serve as a temporary energy storage depot for other tissues.

Brite adipocytes

In parallel to the lineage determination of brown adipocytes, a third type of adipocyte has previously been identified. So-called brite (brown-in-white) or beige adipocytes are found interspersed in classical WAT depots of mice after chronic cold exposure (41). Brite adipocytes share functional features of classical brown adipocytes due to expression of UCP1, a higher mitochondrial density and the ability to respond to β-adrenergic stimulation (42;43). In contrast to classical brown adipocytes arising from *Myf5*-expressing cells, brite adipocytes do not express muscle-specific genes and can be induced in preadipocytes isolated from WAT in response to certain stimuli (42;44-46). However, it is still unclear if brite adipocytes arise from white preadipocytes or even from a certain subpopulation of cells present in the stroma-vascular fraction (SVF). Petrovic and colleagues showed that only a subset of lipid-laden adipocytes treated with the anti-diabetic drug rosiglitazone display positive staining for UCP1 protein (42). Supporting the idea of a specific brite precursor cell, cloning of individual cells in the SVF isolated from the inguinal WAT of mice revealed differences in the gene expression pattern between the adipogenic clones. Clones classified as brite expressed selective genes allowing the differentiation from white and brown, in addition to the use of myogenic marker genes (43). In this context, tumor necrosis factor receptor superfamily member 9 (TNFRSF9) also called CD137 and transmembrane protein 26 (TMEM26) were identified as brite-enriched cell surface markers, allowing cell-sorting of brite precursor cells (43). On a molecular level, brite adipocytes can be characterized by a lack or low expression of myogenic markers, expression of thermogenic genes and enrichement of beige-selective genes, such as *CD137* (Figure 2). Nevertheless, the existence of a specific brite precursor cell is still unclear and several sources of brite adipocytes seem to exist. At least in the visceral fat pad of mice, bipotent plateled-derived growth factor receptor-α (Pdgfr-α) expressing precursor cells are present and give rise to both white and brite adipocytes (47).

Besides the aforementioned concept of *de novo* generation of brite adipocytes from several precursor cells, a second process resembling transdifferentiation might coexist. There is evidence from studies assessing morphological characteristics of adipose tissue, that direct

conversion of unilocular white adipocytes to multilocular brown-like adipocytes is possible (48). Cold exposure of mice for only 10 days leads to remodeling of WAT in mice containing multi-locular UCP1-positive adipocytes after this short cold period, suggesting direct conversion of mature white adipocytes (22). This idea is further supported by a recent study performing *in vivo* lineage tracing. Interestingly, brite fat cells in the inguinal WAT "whitened" after a period of warm acclimation and were able to regain their brite morphology after a subsequent period of cold adaptation (49).

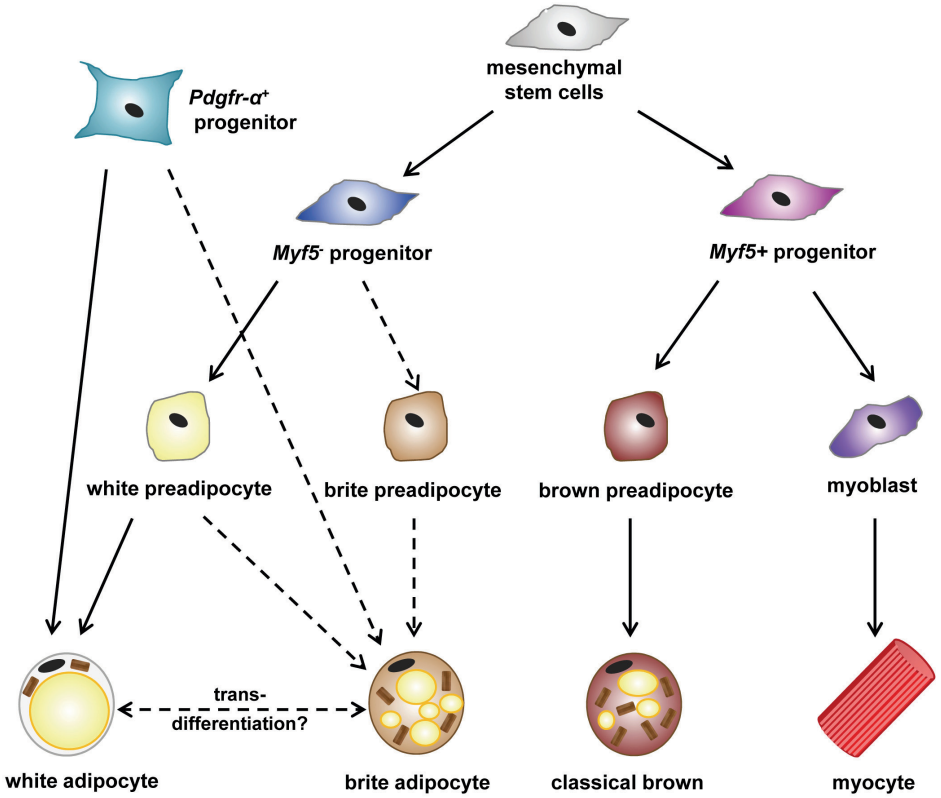

Leptin	*UCP1*	*UCP1*
HOXC9	*CD137*	*ZIC1*
TCF21	*TMEM26*	*LHX8*
	PGC1α	*PRDM16*
	CPT1B	*PGC1α*
		CPT1B

Enriched markers

Figure 3: Developmental origin of white, brite and classical brown adipocytes. Classical brown adipocytes share a common precursor with skeletal muscle cells and derive from *Myf5*+ progenitor cells. Besides *UCP1*, classical brown adipocytes express muscle-specific genes (*ZIC1* and *LHX8*) and display a high expression of mitochondria-related genes (*PGC1α* and *CPT1B*). White adipocytes on the other hand, are not derived from the myogenic lineage and exhibit a lack of myogenic marker gene as well as *UCP1* expression. Brite adipocytes share functional features with classical brown adipocytes, but develop from a non-myogenic origin. Several non-myogenic precursors may give rise to brite adipocytes, such as white preadipocytes, specific brite precursors or bipotential Pdgfr-α+ progenitors. Additionally, brite adipocytes may appear by direct conversion from mature white adipocytes. The absence of myogenic marker expression, enrichement of *UCP1* and mitochondrial genes, and expression of brite-specific genes such as *CD137* characterize brite adipocytes on a molecular level.

Taken together, brite adipocytes derive from different non-myogenic precursor cells in response to certain stimuli. Moreover, remodeling of WAT occurring during cold adaptation is likely to be due to both, *de novo* differentiation as well as transdifferentiation of mature white adipocytes.

1.2.4 Relevance of BAT as a therapeutic target in humans

BAT thermogenesis contributes to energy expenditure and protects against obesity in mice, since UCP1 (-/-) animals develop obesity under thermoneutrality (50) and UCP1 overexpression in adipose tissue protects against obesity (51). However, the role of BAT in humans and the contribution to whole body energy expenditure is less clear. Measuring the uptake of the glucose analogue ^{18}F-FDG by PET-CT is an indirect method to trace metabolic activity of tissues, such as BAT. The tracer ^{18}F-FDG enters glycolysis and is then trapped in the cell, since it cannot be further metabolized in the citric acid cycle. Using this method, active BAT has been discovered in humans and the regulation of BAT dependent on age, gender and obesity has been investigated. BAT mass and activity declines with increasing age and is higher in females compared to males (31). Moreover, a negative association between BAT activity and BMI was found in several studies (32;33;35), suggesting a potential protection against obesity by increasing BAT mass and activity (52). However, the simple presence of BAT and UCP1 protein does not mediate thermogenesis and BAT has to be activated by NE, which is released upon cold exposure. In consequence, only 7.5 % of women (n=1013) and 3.1 % of men (n=959) have been described to be positive for BAT under thermoneutral conditions (31), while 96 % of metabolically healthy male subjects (n=24) were BAT positive under mild cold exposure (16°C) (32).

Since the discovery of UCP1-positive BAT in the adult human and the description of the brite adipocyte, several studies have been performed in order to assess the nature and cell composition of human BAT. As described above, brown, white and brite adipocytes can be discriminated according to their unique gene expression pattern (Figure 2), allowing the characterization of the fat cell composition of a certain adipose tissue depot. In this context, human BAT from the supraclavicular region and proven to be BAT-positive by ^{18}F-FDG PET-CT imaging, has been shown to display a gene expression profile rather resembling that of murine beige adipose tissue (43). Thus, potential differences between the origin of murine and human BAT from the deep neck region may exist. However, recent studies revealed that classical brown adipocytes derived from a myogenic origin are still present in the adult

human. Cypess and colleagues assessed the gene expression pattern of paired biopsies taken from 5 different adipose tissue depots from adult individuals. They observed that the adipocytes from the deepest neck adipose tissue depot display a multilocular morphology and were stained positive for UCP1. Moreover, expression levels of *UCP1* and the classical brown marker genes *ZIC1* and *LHX8* were elevated in human deep neck fat, along with decreased leptin mRNA expression (53). Two other studies also confirmed the expression of classical brown marker genes in human deep neck fat (54;55), strongly indicating the presence of classical brown adipocytes in the adult human. Thus, classical brown and brite adipocytes probably coexist in human BAT and both types represent potential drug targets due to their thermogenic function.

Besides acute activation of BAT by cold exposure, little is known about the plasticity of the human adipose organ in response to chronic long-term interventions. Current clinical trials aim to assess if humans have the ability to recruit active BAT (comprising brown and brite adipocytes) in response to cold acclimation, similar as observed in mice (30;49). A recent study showed that daily cold exposure (10° C, 2h) for 4 weeks significantly increased BAT volume and oxidative capacity in young healthy lean males, providing evidence for the recruitment of active BAT in humans (56). Furthermore, morbidly obese patients being BAT-negative prior to bariatric surgery recruited BAT during weight loss after bariatric surgery (57). Taken together, active BAT is present in the adult human, is likely to be composed of both classical brown and brite adipocytes, and probably can be recruited during long-term interventions. Thus, BAT represents a very attractive therapeutic target in humans.

1.3 Regulation of brown and brite adipocyte development

1.3.1 Transcriptional control

PPARγ and C/EBPs

The major transcriptional regulators controlling adipocyte differentiation are peroxisome proliferator-activated receptor-gamma (PPARγ) and the family of CCAAT/enhancer-binding proteins (C/EBPs) (58). PPARγ is essential for both white and brown adipogenesis. Although required for brown adipocyte differentiation, PPARγ is not sufficient since ectopic expression of PPARγ in fibroblasts leads to the formation of white adipocytes (59). Moreover, PPARγ regulated distinct sets of target genes in brown and white adipocytes (60). In contrast to PPARγ, the C/EBP family member C/EBPα is only required for white adipocyte formation

but not for brown adipocyte development (61). C/EBPβ displays higher expression in BAT compared to WAT and plays a role in the regulation of brown adipocyte thermogenesis (62). Taken together, PPARγ and C/EBPs are important but not sufficient regulators of brown adipocyte differentiation, suggesting that other factors and co-regulators are necessary to drive the brown fat program (63).

PGC1α

PPARγ coactivator 1α (PGC1α) has been recognized as another transcriptional regulator of brown adipocyte function and a main driver of *UCP1* gene expression. Generally, PGC1α is a major regulator of mitochondrial biogenesis in many cell types (64). Intriguingly, PGC1α has been originally described as a cold-inducible transcription factor in brown adipocytes, suggesting a major role in adaptive thermogenesis (65). Indeed, ectopic expression of PGC1α in white adipocytes is able to increase mitochondrial biogenesis and to enhance thermogenic gene expression, including *UCP1* expression (65). The deletion of PGC1α in brown adipocytes leads to an impairment of cold-induced thermogenesis and β-adrenergic response. Interestingly, only thermogenic function but not brown adipocyte differentiation is affected in PGC1α-lacking cells (66). Mechanistically, PGC1α forms complexes with the nuclear receptors PPARα, PPARγ and retinoid X receptor (RXR) which drive *UCP1* expression by binding to PPAR response elements (PPRE) in the *UCP1* promotor (Figure 4).

PRDM16

As mentioned in the previous section, PRDM16 controls the developmental fate of *Myf5*$^{+}$ myogenic precursor cells to classical brown fat or muscle (39). Besides its role in the formation of classical BAT, PRDM16 may also be involved in the recruitment of brite adipocytes in mice. Expression of *PRDM16* has been shown in the subcutaneous inguinal but not in the visceral epididymal depot, a rather pure white depot, suggesting a specific role for PRDM16 in white-to-brown conversion of subcutaneous white adipocytes (67). The induction of thermogenic gene expression driven by PRDM16 is related to its direct interaction with PPARγ and C/EBPs (39). If PRDM16 plays a specific role in the white-to-brown conversion of human adipose-derived stem cells remains unclear (68).

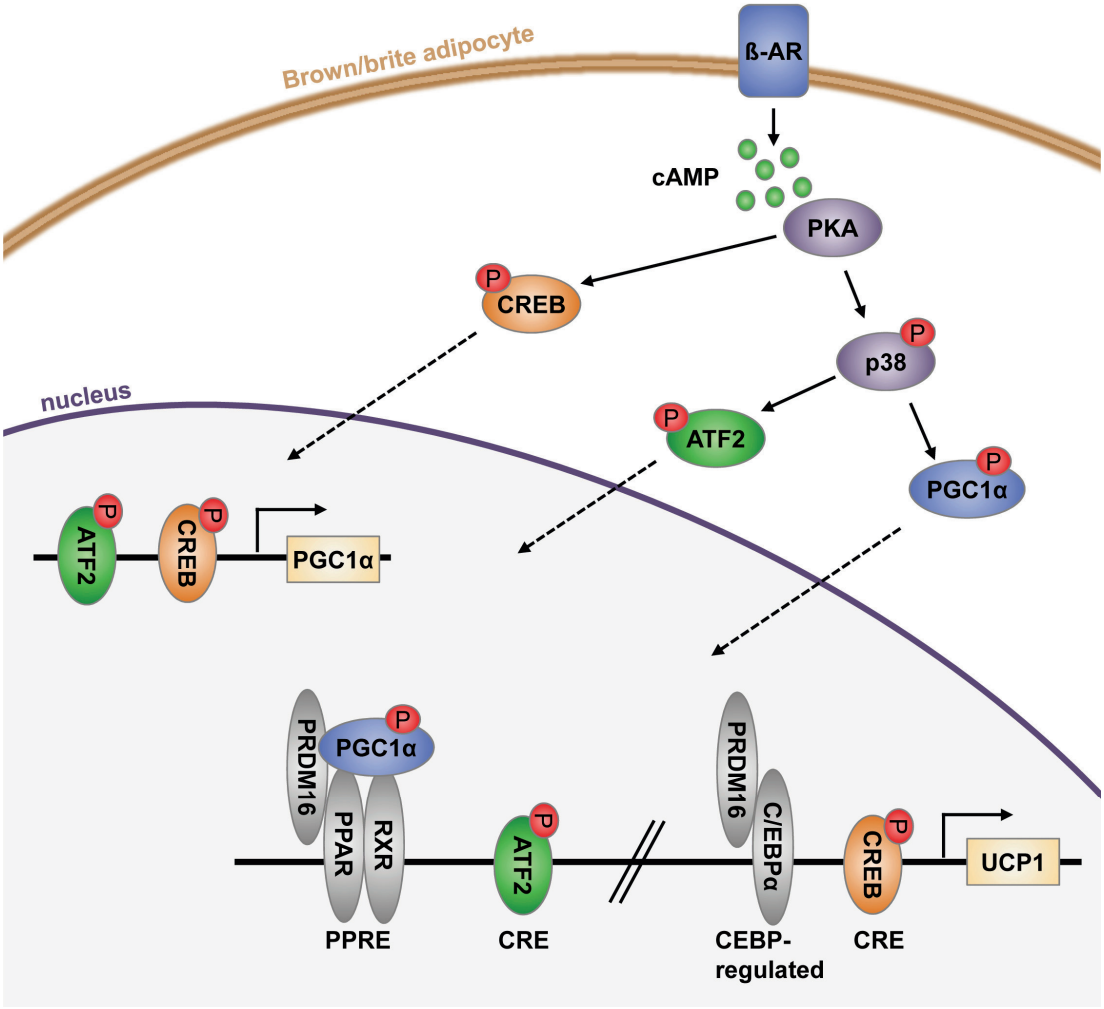

Figure 4: β-adrenergic control of UCP1 expression. Activation of β-AR leads to increased cytosolic cAMP levels which in turn activate PKA. Besides the acute effects of PKA on thermogenesis (figure 2), PKA mediates induction of *UCP1* gene transcription. P38 MAPK is a main downstream target of PKA and activates the transcription factors ATF2 and PGC1α, which directly bind to CRE in the *UCP1* promotor or interact with PPARγ.

1.3.2 Pharmacological agents and endogenous signaling pathways

Given that brown and brite adipocytes may protect against obesity due to their thermogenic function, there is a high interest to identify endogenous signals and pharmacological agents promoting browning of WAT. *UCP1* expression is the hallmark of thermogenic function in both brown and brite adipocytes. Many factors inducing *UCP1* expression drive other aspects of browning, such as increased mitochondrial biogenesis and oxidative metabolism (69). A selection of pharmacological factors and endogenous signals regulating browning and their potential mechanism are summarized below.

Catecholamines and β-adrenergic signaling

The thermogenic process in brown and brite adipocytes is mainly activated by NE-induced β-adrenergic signaling (Figure 2). As described above, cAMP levels are increased after NE binding to the β3-AR leading to PKA activation. In addition to the acute effects of PKA on lipolysis and UCP1-mediated thermogenesis, β3-AR signaling exerts effects on thermogenic gene expression allowing long-term adaptation to cold acclimation. In this context, p38 mitogen-activated protein kinase (MAPK) and the transcription factor cAMP response element binding protein (CREB) have been identified as central downstream targets of PKA (70). PKA-mediated p38 MAPK activation leads in turn to the phosphorylation and activation of activating transcription factor 2 (ATF2) and PGC1α, which induce *UCP1* transcription (Figure 4). Phosphorylated CREB directly binds to cAMP response elements (CRE) in the *UCP1* promotor and also induces transcription of type 2 iodothyronine deiodinase (DIO2) via CRE. These findings raised tremendous interest in the development of specific β3-AR agonists as anti-obesity drugs in humans. However, treatment of humans with these agonists turned out to be not as effective as expected and β3-AR agonists did not successfully enter the market of anti-obesity drugs (71). Nevertheless, the discovery of active BAT in humans has reactivated the development of effective β3-AR agonists and a novel agonist is currently in clinical trial phase 2 (ClinicalTrials.gov identifier: NCT01783470).

Thyroid hormones

Hyperthyroidism is associated with increased BAT thermogenesis in humans, while hypothyroidism reduces β-adrenergic response in BAT (72). DIO2 which is activated by β-adrenergic signaling mediates the conversion of thyroxine (T4) to the more active form triiodothyronin (T3). Moreover, DIO2 null mice display an impairment of cold-induced thermogenesis, suggesting an important role for thyroid hormones in the activation of thermogenesis. In line, T3 has recently been shown to increase *UCP1* expression, mitochondrial biogenesis and oxygen consumption in human mesenchymal adipose-derived stem cells (hMADS) (46). The *in vivo* effects of thyroid hormone treatment on BAT activity (NCT01379170, NCT01376648), mitochondrial function and insulin-sensitivity (NCT01379170) in humans are currently investigated in clinical trials.

PPARγ agonists

Thiazolidinediones (TZDs), such as rosiglitazone or pioglitazone, are synthetic PPARγ ligands and have insulin-sensitizing properties. TZD binding to PPARγ and activation increases expression of PPARγ target genes, such as *PGC1α* and *UCP1*. Though PPARγ is

crucial for white and brown adipocyte differentiation and not sufficient for the latter, TZDs have been shown to promote browning of WAT in rodents (73). In this context, chronic activation of PPARγ by rosiglitazone has been shown to be necessary to induce browning of primary murine white preadipocytes (42). The degree of agonism exerted by a certain PPARγ ligand seems to be a crucial determinant. Thus, full agonism (rosiglitazone) is required to promote browning, while PPARγ ligands with weak agonism fail to enhance expression of brown-specific genes (74). Stabilization and accumulation of PRDM16 protein has been proposed as potential reason for the browning effect of rosiglitazone (74). Despite promising effects on browning and whole energy metabolism in mice, the use of TZDs in humans is heavily discussed. Rosiglitazone has been authorized as drug for the treatment of type 2 diabetes in 1999 in the US, followed by Europe in 2000. Nevertheless, concerns about its cardiovascular safety have been raised leading to suspension of rosiglitazone from the European market in 2010 (75). Pioglitazone is the only TZD which is currently authorized in the EU and has been shown to increase WAT oxidative metabolism in humans (76). The specific effects of pioglitazone treatment on BAT activity are unknown so far, and pioglitazone is only authorized as anti-diabetic drug.

Bone morphogenetic proteins

Bone morphogenetic proteins (BMPs) belong to the transforming growth factor β superfamily (TGFβ) and play a role in the regulation of several developmental processes. Until now, more than 20 BMP family members are known (77). BMPs are synthesized as precursor proteins and cleavage by extracellular proteases leads to release of mature BMPs. Mature BMPs dimerize and bind to specific type 1 or type 2 Ser/Thr kinase receptors, mainly signaling via Smad1/5/8 but also through other non-canonical pathways. The specific BMP signaling is dependent on the ligand availability, the receptor composition and the presence of BMP antagonists (78). Several BMP members (BMP2, BMP4, BMP6, BMP7) are regulators of general adipocyte differentiation (79). In the context of BAT, BMP7 was the first BMP member described to be an important regulator of BAT function and whole-body energy expenditure. Thus, BMP7 knockout mice display decreased BAT mass (80) while systemic BMP7 administration to obese mice triggered weight loss, partly due to increased energy expenditure (81). BMP7 induces the full brown fat program in murine brown preadipocytes isolated from classical BAT depots, involving the activation of p38 MAPK and PCG1α (80). Besides its regulatory function in classical brown adipocyte differentiation, BMP7 also enhanced thermogenic gene expression in a subset of precursor cells isolated from murine subcutaneous WAT (82). In contrast to BMP7, the family member BMP4 was assumed to

promote white adipocyte differentiation while inhibiting BAT development (83). However, recent evidence from a transgenic mouse model and *in vitro* studies in murine cells suggest that BMP4 might also promote white-to-brown conversion (84). Further investigations are needed to clarify the role of BMP4 in the regulation of human adipose tissue plasticity, which is one focus of this thesis.

1.3.3 Life style factors

The major life style factors playing a role in the development of obesity are nutrition and physical activity. While overnutrition leads to growth of WAT and the development of obesity, physical activity is an energy consuming process leading to increased whole-body energy expenditure and thereby prevents the development of obesity. In addition to this simple evaluation of nutrition and exercise based on their contribution to energy balance, they exert additional effects on adipose tissue plasticity and function.

1.3.3.1 Nutrition and long-chain polyunsaturated fatty acids

The main determinants of a healthy diet are total energy content, food composition and quality. Chemical energy in diet is delivered by the three macronutrients, carbohydrates, fat and protein. Diets rich in fat and lipids display a high energy density and promote body weight gain in mice and men. Interestingly, mice fed a high fat diet (HFD) do not only gain weight and WAT mass, but also increase BAT mass and UCP1 protein content (50;85). Thus, excess energy intake may also impact white-to-brown transition. In addition to the total amount of dietary lipids, quality of lipids and especially fatty acids is an important factor for the specific effect of a HFD on adipose tissue (86-88).

Fatty acids are generally distinguished according to their length and degree of saturation. Polyunsaturated fatty acids (PUFAs) contain at least two double-bonds in their backbone. According to the position of the first double binding, counted from the methyl-end of the molecule, PUFAs can be subdivided into the n-3, n-6 and n-9 family. Due to the lack of a certain desaturase, introducing double bonds in the n-3 or n-6 position, PUFAs from the n-3 and n-6 family cannot be synthesized by mammals. Since n-3 and n-6 PUFAs possess several important biological functions, they are considered essential and have to be supplied by diet. Linoleic acid (LA; 18:2n-6) and alpha-linolenic acid (ALA; 18:3n-3) represent the basic members of the n-6 and n-3 PUFA family. After digestion, LA and ALA can be further metabolized by several elongation and desaturation steps, leading to the formation of long-

chain PUFAs (LC-PUFAs) (89). However, this conversion process may be inefficient and dietary supply of LC-PUFAs is recommended by the WHO and national health organizations, such as the German Society for Nutrition.

The best studied LC-PUFAs are arachidonic acid (ARA; 20:4n-6), eicosapentaenoic acid (EPA; 20:5n-3) and docosahexaenoic acid (DHA; 22:6n-3), which play a role in the development of several metabolic complications like obesity, cardiovascular diseases or type 2 diabetes (90-92). Most of the biological functions of LC-PUFAs are mediated by their lipid-derived mediators, the eicosanoids, including prostaglandins (PG), prostacyclins (PGI), leukotrienes (LT) and thromboxanes (TX). These molecules are synthesized upon release of LC-PUFAs from membrane phospholipids and further conversion by several oxygenation steps, mainly mediated by the enzymes cyclooxygenase type 1 (COX1) and type 2 (COX2). Both EPA (n-3) and ARA (n-6) are substrates for COX enzymes, leading to the formation of functionally different series of eicosanoids. While the n-6-derived eicosanoids (series 2 of PG, PGI and TX; series 4 of LT) are considered to be pro-inflammatory, n-3-derived eicosanoids (series 3 of PG, PGI and TX; series 5 of LT) have rather anti-inflammatory properties (93). In addition, the n-3 LC-PUFAs EPA and DHA signal by binding and activation of the G-protein coupled receptor GPR120 (alternatively called FFAR4). GPR120 is highly expressed in macrophages and mature adipocytes and mediates anti-inflammatory and insulin-sensitizing effects (94).

LC-PUFAs from the n-3 family possess other health benefits in addition to their anti-inflammatory effect. In mice, dietary supplementation with EPA and DHA reduces HFD-induced body weight gain, reduces WAT mass and improves systemic glucose metabolism (88;95). Interestingly, the anti-adipogenic effects of EPA and DHA were not accompanied by decreased food intake, but rather mediated by an improved oxidative metabolism in WAT (95). Moreover, it has also been shown that UCP1 expression in BAT is increased when diet was enriched with n-3 LC-PUFAs (87). Therefore, these animal studies suggest a positive effect of n-3 LC-PUFAs on white-to-brown conversion. This notion is supported by the fact, that LC-PUFAs and their metabolites represent potential ligands for PPARγ (96) and may therefore promote browning analogously to TZDs. Furthermore, the main enzyme of eicosanoid synthesis COX2 has been shown to be involved in adaptive thermogenesis and is upregulated in brown adipocytes after β-adrenergic stimulation (44;97).

In contrast to studies in mice, a potential relationship between n-3 LC-PUFA intake and decreased adiposity has been proposed by some studies in humans, but inconsistent results

exist (90). Since nutritional intervention studies in humans are difficult to control, *in vitro* studies assessing the direct effect of n-3 and n-6 LC-PUFAs in primary human cells may help to understand the role of LC-PUFAs on adipose tissue development and function in humans.

1.3.3.2 Physical activity

Physical activity and regular exercise have beneficial effects on the progression of several chronic-inflammatory diseases, such as cardiovascular diseases and type 2 diabetes. On the other hand, physical inactivity is associated with a high prevalence of these diseases (98). The positive effects of regular exercise can be partly explained by increasing whole-body energy expenditure and glucose clearance. In addition, skeletal muscle is also recognized as an endocrine organ, releasing several proteins termed myokines. Like adipokines, myokines are released into the circulation allowing the communication with other organs, such as adipose tissue (99). Changes of the myokine secretion pattern during and after exercise provide another mechanism of the beneficial effects of exercise (100).

Several studies in rodents have shown that regular training affects adipose tissue plasticity. While mass and UCP1 content of classical BAT has been found unchanged (101-103) or even decreased (85;104) after exercise intervention, alterations of the WAT phenotype have been observed. Hence, trained animals displayed a higher abundance of multilocular adipocytes and expression of brown marker genes in the epididymal WAT depot (103-105) and subcutaneous depot (85;106). Recently, the exercise-regulated myokine irisin has been identified and characterized in mice as a causal link between training and WAT browning (106). Irisin is released after cleaveage from fibronectin type III domain containing protein 5 (FNDC5), which was considered to be upregulated in skeletal muscle of mice and humans after exercise. Moreover, irisin induced browning of primary murine adipocytes isolated from the subcutaneous depot, indicated by increased expression of *UCP1*, *PGC1α* and other marker genes (106). Since irisin/FNDC5 also induced WAT browning accompanied by protection against diet-induced obesity and insulin-resistance *in vivo*, irisin gained a high interest as potential novel therapeutic target. However, the concept of exercise-induced browning of WAT has been questioned from a physiological point of view (107). Particularly, considering that muscle-contraction is an energy-consuming and heat-generating process itself, it seems puzzling that exercise would promote a WAT phenotype switch which also requires substrates for thermogenesis. The presence of the irisin peptide in humans, its regulation after exercise and its potential to induce browning in humans is still under discussion and has been a major topic of this thesis.

1.4 Objectives

A sedentary lifestyle and unhealthy nutrition represent the main causal factors for the worldwide growing prevalence of obesity. Obesity is associated with several metabolic disturbances, such as type 2 diabetes, hyperlipidemia and cardiovascular complications. WAT dysfunction, characterized by a chronic low-grade WAT inflammation, adipocyte hypertrophy and a shift in the adipokine secretion profile, has been identified as pathogenic link between obesity and its associated diseases. In the light of the obesity epidemics, WAT as endocrine organ and the characterization of adipokines as potential therapeutic targets to prevent the development of metabolic disturbances has been a major research focus in the recent decade. Our group previously described the WAT secretome and identified more than 300 proteins potentially secreted from WAT. Among those, 44 were described as novel adipokines.

The first aim of the thesis was the functional evaluation of the adipose tissue secretome in order to identify highly interesting candidates in the context of obesity.

While WAT is the main site of energy storage, BAT expends energy to generate heat. Besides classical brown adipocytes derived from the myogenic lineage, the brite adipocyte has been discovered as a second type of thermogenically competent adipocyte, with a distinct developmental origin. Due to their function, both increasing the recruitment of brown as well as brite adipocytes may increase energy expenditure and counteract the development of obesity. Since both types of adipocytes are present in the adult human, this may also represent a relevant strategy in humans. Not surprisingly, the identification of factors involved in the regulation of brite adipocyte formation and activity has been a major research focus since the discovery of the brite adipocyte in 2009. Several hormonal and pharmacological factors promoting white-to-brown conversion have been described until now. Though, most of these factors have been characterized in mouse models and their role in humans still remains unclear.

The second aim of the thesis was to validate potential endogenous regulators of white-to-brown conversion in primary human adipocytes.

Besides endocrine regulation, life style factors have a major impact on adipose tissue function and the development of obesity. Overnutrition leads to a positive energy balance and subsequent storage of excess energy in WAT. Besides food quantity, also diet composition and quality is of importance. In particular, fatty acid composition has been shown to influence WAT growth and weight gain in rodents.

The third aim of the thesis was to assess the effect of n-3 LC-PUFAs, which are considered to have anti-obesity effects in rodents, on white-to-brown conversion in human adipocytes.

Regular exercise is another life style aspect exerting several beneficial effects. First, muscle contraction during physical activity is an energy consuming process, increasing whole body energy expenditure. Secondly, skeletal muscle has been recognized as active endocrine organ, releasing several so-called myokines. In a multi-directional inter-organ crosstalk *scenario*, myokines may also affect adipose tissue function and plasticity. Similar to WAT as an endocrine organ, the myokine secretion pattern varies dependent on the skeletal muscle type and is also influenced by exercise and contraction. Irisin has previously been proposed to be an exercise-regulated myokine in mice, mediating browning of WAT.

The fourth aim of the thesis was to determine if irisin is an inducer of brite adipogenesis in humans as well. Moreover, general effects of exercise on white-to-brown conversion and the role of irisin in humans were reviewed.

2 Published Articles

2.1 Functional annotation of the human fat cell secretome.

Dahlman I, **Elsen M**, Tennagels N, Korn M, Brockmann B, Sell H, Eckel J, Arner P. Arch Physiol Biochem (2012) 118(3):84-91.

2.2 BMP4 and BMP7 induce the white-to-brown transition of primary human adipose stem cells

Elsen M, Raschke S, Tennagels N, Schwahn U, Jelenik T, Roden M, Romacho T, Eckel J. Am J Physiol Cell Physiol (2014) 306(5):C431-40.

2.3 Eicosapentaenoic acid and arachidonic acid differentially regulate white-to-brown conversion and mitochondrial function in primary human adipocytes

Fleckenstein-Elsen M, Dinnies D, Jelenik T, Roden M, Romacho T, Eckel J. Int J Obesity (2015) submitted

2.4 Evidence against a beneficial effect of irisin in humans

Raschke S, **Elsen M**, Gassenhuber H, Sommerfeld M, Schwahn U, Brockmann B, Jung R, Wisløff U, Tjønna AE, Raastad T, Hallén J, Norheim F, Drevon CA, Romacho T, Eckardt K, Eckel J. PLoS One (2013) 8(9):e73680.

2.5 Browning of white fat: does irisin play a role in humans?

Elsen M, Raschke S, Eckel J. J Endocrinol. (2014) 222(1):R25-38.

Functional annotation of the human fat cell secretome

Ingrid Dahlman[1], **Manuela Elsen**[2], Norbert Tennagels[3], Marcus Korn[3], Barbara Brockmann[3], Henrike Sell[2], Juergen Eckel[2], and Peter Arner[1]

[1]Karolinska Institutet, Department of Medicine, Huddinge, 141 86 Stockholm, Sweden,
[2]Paul-Langerhans-Group, German Diabetes Center, Duesseldorf, Germany
[3]Sanofi-Deutschland GmbH, Diabetes Division, Industriepark Höchst, H821

Abstract

Context: Recent secretome analyses suggest that human fat cells secrete hundreds of proteins (adipokines)

Objective: We made an overall analysis of their potential functional importance.

Materials and methods: A secretome of 347 adipokines was evaluated by *in silico* analysis of their expression during adipocyte differentiation, regulation by obesity and adipose region. The gene expression in human adipose tissue was investigated in microarray studies using samples from different adipose depots from lean or obese patients.

Results: 60% of the adipokines were regulated by obesity and 50% between visceral and subcutaneous adipose region. Eight adipokines, all novel, scored particularly high in the *in silico* analysis. Among those, four were both regulated by obesity and adipose region, namely WNT1-inducible-signaling pathway protein 2, transmembrane glycoprotein NMB, inter-alpha-trypsin inhibitor heavy chain H5, and complement C4-A. Furthermore, many adipokines were extracellular matrix proteins.

Conclusion: Several novel adipokines have potential important functional features warranting in depth analysis.

Keywords: adipokines, gene expression, obesity, adipose region, microarray

Introduction

Obesity is associated with increased risk of type 2 diabetes and cardiovascular disease, which has been related to metabolic disturbances in adipose tissue (Arner, 2005b; Reaven *et al*., 2004). Human white adipose tissue (WAT) participates in regulation of whole body metabolism by secretion of hormones and other peptides, i.e. adipokines (Arner, 2005b). Some of these proteins are inflammatory mediators, which are believed to promote fat cells specific insulin resistance (Hotamisligil *et al*., 1995). Others directly regulate insulin sensitivity. One example is adiponectin which, in experimental models, have been shown to promote insulin sensitivity (Koerner *et al*., 2005). Among adipose tissue depots, the intra-abdominal WAT is believed to be the most important contributor to the metabolic disturbances in obesity (Wajchenberg, 2000). This may be related to depot differences in adipokine secretion (Arner, 2001). Some adipokines are primarily expressed by fat cells. However, the stroma vascular fraction contributes to WAT endocrine and paracrine function.

Global transcriptome profiling has successfully been used to define obesity-associated disturbances in human WAT such as increased expression of proinflammatory and extracellular matrix genes (Clement *et al*., 2004; Henegar *et al*., 2008). However, there is limited information about global expression of potential adipokines in adipocytes and other cells of adipose tissue. Recently, proteomics have been applied to determine the secretion pattern of peptides from human subcutaneous progenitor cells undergoing *in vitro* differentiation to fat cells (Kim *et al*., 2010; Zhong *et al*., 2010). We recently identified 347 proteins in a profiling on concentrated conditioned medium derived from primary human *in vitro* differentiated adipocytes using SDS-PAGE/LC-ESI-MS/MS and 2-dimensional SDS-PAGE/MALDI-MS (Lehr *et al*., 2012). However, the *in vivo* expression pattern of these newly detected adipokines in relation to various clinical measures is largely unknown.

Outgoing from the 347 proteins identified in our own proteomic analysis of human fat cells (Lehr *et al*., 2012), henceforward termed adipocyte secretome, we

here attempt by *in silico* analysis of the corresponding genes to narrow down the list of putative important new adipokines to a few interesting candidates for future in depth functional evaluation. In one analysis, we use our own global transcriptome profiles on adipose tissue from large cohorts of obese and lean women to determine to what extent genes that are regulated by obesity and adipose tissue depot are included in the adipocyte secretome. In a second analysis, we exploited public databases and proprietary gene expression datasets to rank the adipocyte secretome proteins taking into account whether specific proteins are annotated as secreted, and whether gene expression is enriched in fat cells, and/or regulated by adipogenesis and adiposity.

Methods

Patients and clinical investigation

Subjects were recruited by local advertisement for the purpose of studying genes regulating obesity and fat cell function. Morbid obesity was defined as having a BMI ≥ 40 kg/m^2, whereas leanness was defined as having a BMI ≤25 kg/m^2. Informed consent was received from all subjects involved in the study. The project was approved by the Regional Ethics committee in Stockholm. Transcriptome profiling in relation to obesity was performed on 17 lean women (age 40 ± 14 years, BMI 23 ± 1 kg/m^2) and 17 morbidly obese woman with BMI > 40 kg/m^2 (age 40 ± 6 years, BMI 46 ± 4 kg/m^2). An abdominal subcutaneous fat biopsy was obtained by needle biopsy in the morning after an overnight fast. Comparison of gene expression between paired samples of abdominal subcutaneous and visceral adipose tissue was based on a previously published microarray study on 24 women with a wide variation in BMI (age 40±11 years, BMI 37±10 kg/m^2); eight of these women had type 2 diabetes (Dahlman *et al*., 2006). The obese subjects in these cohorts were operated with anti-obesity surgery and the non-obese for uncomplicated gall stone disease. Pieces of adipose tissue were obtained at the beginning of surgery. Tissue pieces were rapidly rinsed in saline and frozen in liquid nitrogen and kept at −70°C.

RNA preparation

RNA for the obesity project was extracted using the Nucleospin RNAII kit (Macherey-Nagel, Düren, Germany). RNA from the adipose tissue depot samples were extracted using the RNeasy kit (QIAGEN, Hilden, Germany). RNA concentration, as well as purity was measured spectrophotometrically using a Nanodrop ND-1000 Spectrophotometer (Thermo Fisher Scientific, Lafayette, CO). High-quality RNA was confirmed using an Agilent 2100 Bioanalyzer (Agilent Technologies, Palo Alto, CA).

Microarray analysis

From non-degraded high-quality total RNA we prepared and hybridized biotinylated complementary RNA to Gene 1.0 ST arrays (obesity project) or U133 array sets (adipose tissue depot samples) using standardized protocols (Affymetrix Inc., Santa Clara, CA). Preprocessing of the Gene 1.0 ST arrays were performed using the Affymetrix Expression Console version 1.1 and the following settings. Summarization: PLIER, Background Correction: PM-GCBG, Normalization: Global Median. Processing of the U133 array set has been described (Dahlman *et al*., 2006).

We used Gene Set Analysis Toolkit v2 (http://bioinfo. vanderbilt.edu/webgestalt/) to determine if specific gene sets were over-represented in the adipocyte secretome. In this analysis we applied a hypergeometric test and the Benjamini-Hochberg procedure for multiple comparisons, and limited the analysis to gene sets containing a minimum of three adipokines, and the top 10 over-represented gene sets. The Affymetrix 1.0 ST array, which contains >22,000 annotated transcripts, was used as reference in the analysis.

In silico analysis

In order to prioritize candidates for further in depth functional evaluation, we have to narrow down the list of putative new adipokines. Therefore, keeping the known properties of adipokines like leptin in mind, which is, for example, highly specifically expressed in adipocytes and highly regulated on mRNA level during adipocyte differentiation, we defined criteria that could characterize such an adipokine. We assigned these priorities through two major types of annotation: (1) what is known about the putative adipokine itself as a protein and (2) is there information at the gene expression level which may allow us to speculate about a function in adipocyte biology. To address the first classification, the proteins were annotated with all available information regarding cellular localization and secretory sequences (Gene Ontology, UniProt, Ensembl, NCBI). To examine a possible role in adipocyte biology, we exploited proprietary gene expression datasets for all proteins found in the supernatant of adipocytes with the following criteria in mind:

A.

Regulation (at least 2-fold, $p < 0.001$, no differentiation between up- or down-regulation) during the *in vitro* differentiation of subcutaneous or visceral human adipocytes.

B.
mRNA level in adipocytes (subcutaneous and/or visceral) display tissue selectivity (in comparison to expression data from 20 other tissues: brain, breast, cartilage, cerebellum, colon, dorsal root ganglion, heart, kidney, leucocyte, liver, lung, pancreas, pancreatic islet, platelet, prostate, skeletal muscle, spinal cord, spleen, testis, thyroid).

C.
Regulation (at least 1.5 fold, $p < 0.001$, no differentiation between up- or down-regulation) in obese patients in subcutaneous or visceral depots (comparison lean vs obese)

D.
Regulation in epididymal WAT (at least 1.5 fold, $p < 0.05$, no differentiation between up- or down-regulation) in an animal disease model (ZDF rats versus lean controls).

In total, six searches were performed. If the search criteria were fulfilled for a gene, a pre-assigned score was assigned to the hit. The search criteria and the assigned scores were as follows:

(1) Genes expressed highest in human subcutaneous and/or visceral adipose tissue in comparison to the tissues described above and found to be regulated during *in vitro* adipocyte differentiation. (Score 1.5)

(2) Genes annotated as described above coding for secreted proteins and found to be regulated during *in vitro* adipocyte differentiation. (Score 1.5)

(3) Genes not known to be a secreted protein (no information available) and found to be regulated during *in vitro* adipocyte differentiation. (Score 1)

(4) Genes highly expressed in human subcutaneous or visceral adipocytes and considered as present in a maximum of 10 of 22 tissues. (Score 1)

(5) Genes found regulated as described above in subcutaneous or visceral adipose tissue in comparison of obese versus lean patients. (Score 1)

(6) Genes found regulated in epididymal adipose tissue of ZDF rats compared to lean controls when analyzed at 6, 7, 9, 12 or 20 weeks of age. (Score 1)

The final ranking for each gene was the sum of the assigned scores. Matrix-protein genes and well known enzymes/pharmacological targets were excluded from the ranking since an in depth validation seems not to be desirable, possible or is already under evaluation for such genes.

Statistical analysis
Gene expression between two groups were compared by t test (two sided). We used the Benjamini-Hochberg procedure with a 5% FDR to adjust for multiple comparisons due to analysis of multiple genes.

Results

As previously reported a comprehensive proteomic profiling of the human adipocyte secretome has identified 347 proteins (Lehr *et al*., 2012). We here first examined adipose tissue expression of all adipocyte secretome genes in relation to human obesity; 222 genes displayed significantly altered expression in obesity; 217 genes were up-regulated and five down-regulated, Table 1. Nine genes were not represented on the arrays. We performed pathway analysis of the 217 up-regulated genes using the Gene Set Analysis Toolkit. The most significantly up-regulated gene sets at mRNA level included extracellular matrix organization, biological adhesion, and acute inflammatory response, Table 2.

Bioinformatic analysis of the 347 adipose secretome proteins identified 48 proteins with independent evidence as secreted proteins, and expression regulated by fat cell differentiation or adiposity in humans or rats; that is with a score ≥2 according to our *in silico* analysis described in the methods section (Table 3). The eight genes with the top score, score >3, are considered the most promising for further characterization in adipose tissue (for comparison: for leptin and adiponectin the scores 6 and 3 were assigned, respectively). Thirty-two of the 48 genes with a score ≥2 are up-regulated and one gene, adiponectin, down-regulated at mRNA level in subcutaneous adipose tissue of obese versus lean women with FDR 5%. In the top score group, five genes are up-regulated in obese women (Table 3). The five genes are WNT1-inducible-signalling pathway protein 2 *(WISP2)*, transmembrane glycoprotein NMB *(GPNMB)*, inter-alpha-trypsin inhibitor heavy chain H5 *(ITIH5)*, glia-derived nexin *(SERPINE2)* and complement C4-A *(C4A)* (Table 4).

Table 1. Adipose tissue expression of secretome genes in relation to obesity and depot.

	Obese vs lean	Visceral vs subcutaneous
Up regulated	217	62
Down regulated	5	127
Not regulated	116	153

Note: Groups were compared with *T*-test with BH-adjustment for multiple comparisons.

Table 2. Extracellular matrix components, adhesion molecules and inflammatory mediators expressed as proteins in primary human adipocytes and upregulated at mRNA level in adipose tissue of obese subjects.

Extracellular matrix organization			Biological adhesion (continued)		
O = 19; E = 1.28; adjP = 1.11×10^{-14}			COL5A3	Collagen/type V/alpha 3	1.30
MMP9	Matrix metallopeptidase 9	3.34	CD44	CD44 molecule	1.69
NID1	Nidogen 1	1.41	VCL	Vinculin	1.26
COL6A2	Collagen/type VI/alpha 2	1.61	NID1	Nidogen 1	1.41
COL5A2	Collagen/type V/alpha 2	1.82	COL6A2	Collagen/type VI/alpha 2	1.61
COL4A2	Collagen/type IV/alpha 2	1.31	LAMC1	Laminin/gamma 1	1.16
LAMC1	Laminin/gamma 1	1.16	THBS2	Thrombospondin 2	1.56
HSPG2	Heparan sulphate proteoglycan 2	1.24	COL1A1	Collagen/type I/alpha 1	1.61
COL1A1	Collagen/type I/alpha 1	1.61	CLSTN1	Calsyntenin 1	1.29
LUM	Lumican	1.46	ACTN1	Actinin/alpha 1	1.55
COL18A1	Collagen/type XVIII/alpha 1	1.30	LAMA2	Laminin/alpha 2	1.24
B4GALT1	UDP-Gal:betaGlcNAc beta 1.4- galactosyltransferase	1.30	GPNMB	Glycoprotein nmb	1.70
TGFBI	Transforming growth factor	1.63	TGFBI	Transforming growth factor/beta	1.63
COL3A1	Collagen/type III/alpha 1	1.71	NID2	Nidogen 2	1.40
FKBP1A	FK506 binding protein 1A/12kDa	1.39	THY1	Thy-1 cell surface antigen	1.89
CCDC80	Coiled-coil domain containing 80	1.87	CCDC80	Coiled-coil domain containing 80	1.87
COL5A1	Collagen/type V/alpha 1	1.53	MFAP4	Microfibrillar-associated protein 4	1.48
CST3	Cystatin C	1.38	VCAN	Versican	1.94
COL5A3	Collagen/type V/alpha 3	1.30	CSF1	Colony stimulating factor 1	1.48
COL1A2	Collagen/type I/alpha 2	1.59	COL15A1	Collagen/type XV/alpha 1	1.41
			LAMB1	Laminin/beta 1	1.26
Biological adhesion			ARHGDIA	Rho GDP dissociation inhibitor alpha	1.27
O=43; E=10.45; R=4.11; adjP=1.64×10^{-13}			DPP4	Dipeptidyl-peptidase 4	1.38
AEBP1	AE binding protein 1	1.49	SVEP1	Sushi/von Willebrand factor type A/	1.51
FN1	Fibronectin 1	2.15	ISLR	Immunoglobulin superfamily containing leucine-rich repeat	1.37
HSPG2	Heparan sulphate proteoglycan 2	1.24			
CPXM1	Carboxypeptidase X/member 1	1.41	*Acute inflammatory response*		
COL18A1	Collagen/type XVIII/alpha 1	1.30	O = 13; E = 1.37; adjP = 7.35×10^{-8}		
B4GALT1	UDP-Gal:betaGlcNAc beta 1.4- galactosyltransferase	1.30	C1QB	Complement component 1/q subcomponent/B	2.07
TNC	Tenascin C	2.49	C3	Complement component 3	1.51
COL3A1	Collagen/type III/alpha 1	1.71	SERPINA1	Serpin peptidase inhibitor/clade A/ member 1	1.54
LGALS3BP	Lectin/galactoside-binding/soluble/3 BP	1.19	CFH	Complement factor H	1.76
COL6A3	Collagen/type VI/alpha 3	1.35	FN1	Fibronectin 1	2.15
WISP2	WNT1 inducible signalling pathway protein 2	1.77	A2M	Alpha-2-macroglobulin	1.27
IGFBP7	Insulin-like growth factor binding protein 7	1.34	B4GALT1	UDP-Gal:betaGlcNAc beta 1.4- galactosyltransferase	1.30
THBS1	Thrombospondin 1	1.77	C1R	Complement component 1/r subcomponent	1.51
MCAM	Melanoma cell adhesion molecule	1.23	C1S	Complement component 1/s subcomponent	1.62
COL5A1	Collagen/type V/alpha 1	1.53	CFB	Complement factor B	1.80
SPON2	Spondin 2/extracellular matrix protein	1.61	CLU	Clusterin	1.57
COL6A1	Collagen/type VI/alpha 1	1.65	C2	Complement component 2	2.55
LAMB2	Laminin/beta 2	1.33	PRDX2	Peroxiredoxin 2	1.26

Notes: Among 347 proteins identified in a proteomic analysis of medium from primary human adipocyte culture, 217 were up-regulated at mRNA level in adipose tissue from obese versus lean subjects. These 217 genes were analysed using the Gene Set Analysis Toolkit and the genes in the most significantly up-regulated gene sets listed above. O = observed number of genes. E = expected number of genes.

We next examined adipose tissue expression of the 347 adipocyte secretome genes in relation to human adipose depot. Sixty-two genes were up-regulated and 127 genes down-regulated in visceral as compared to subcutaneous human adipose tissue (Table 1). Five genes were not represented on the arrays. Pathway analysis of these genes did not highlight any clear biological differences between these adipose depots (results not shown). Analysis of the 48 proteins with score ≥2 in our *in silico* analysis revealed that 33 were differentially expressed between subcutaneous and visceral adipose tissue with 5% FDR (Table 3). The eight genes with the top score, score >3, of which six are differentially expressed between adipose depots, are considered the most promising for further characterization in adipose tissue (Table 3). The genes down-regulated in visceral as compared to subcutaneous adipose tissue are vascular endothelial growth factor D

Table 3. Adipose tissue expression of top-score secretome genes (≥2) in relation to obesity and depot.

	Obese vs lean		Visceral vs subcutaneous	
Score	>3	2–3	>3	2–3
Up regulated	5	27	1	10
Down regulated	0	1	5	17
Not regulated	3	12	2	13

Note: Groups were compared with *t*-test with BH-adjustment for multiple comparisons.

(FIGF), *ITIH5*, *WISP2*, complement factor D *(CFD)* and *GPNMB* (Table 4). Complement C4-A *(C4A)* is up-regulated in visceral adipose tissue. Four of the top ranked genes *WISP2*, *GPNMB*, *ITIH5*, and *C4A* were regulated by both adipose region and obesity.

Discussion

Proteomic analysis of culture medium from *in vitro* differentiated human fat cells have identified several new fat cell produced proteins (Lehr *et al*., 2012). Their clinical role is in most cases unknown. We presently show a number of potentially important features of these adipokines. The gene expression of the majority of the adipokines is regulated by obesity and/or adipose region. Most of the genes are up-regulated in obesity. Many are either up- or down-regulated in visceral versus subcutaneous adipose tissue. Adipocytes are shown to be an important source of adipose tissue extracellular matrix and adhesion proteins as regards their gene expression pattern. Furthermore, our ranking of the adipocyte secretome genes, based on annotation and expression pattern of the genes, have identified a handful of novel adipokine genes that, in our opinion, should be prioritized for future functional evaluation. Of particular importance might be *WISP2*, *GPNMB*, *ITIH5* and *C4A*. These genes both scored among the highest in the *in silico* analysis of potential important adipokines, and were regulated by obesity, and well as adipose region.

Recent findings have highlighted the importance of extracellular matrix genes in human adipose tissue. Weight loss of obese reduces extracellular matrix expression (Henegar *et al*., 2008; Kolehmainen *et al*., 2008). Furthermore, these genes are down-regulated by cancer cachexia in human adipose tissue (Dahlman *et al*., 2010). Extracellular matrix could also be involved in obesity associated insulin resistance. As mentioned adipose tissue inflammation is believed to be an important cause of adipose tissue insulin resistance. However, the inflammatory mediators are primarily expressed in adipose tissue resident macrophages and not in the fat cells themselves (Clement *et al*., 2004). It is thus unknown what triggers expression of inflammatory mediators in adipose tissue. Adipose tissue extracellular matrix protein expression has been proposed to be linked to adipose inflammation (Henegar *et al*., 2008). Collagen expression is associated with markers of adipose inflammation (Spencer *et al*., 2010) and in rodents depletion of specific extracellular matrix proteins protect against insulin resistance (Li *et al*., 2011). From this perspective, our finding that adipocytes are a source of many extracellular matrix proteins are compatible with a model in which adipocyte, via expression of extracellular matrix proteins, can trigger adipose inflammation and insulin resistance in obesity.

For our *in silico* analysis, we defined a scoring in order to prioritize proteins for a further in depth validation. This scoring is mainly based on gene expression data obtained from gene array experiments and therefore could be, especially if gene expression changes are included in the scoring criteria, biased, for example, by sensitivity. We therefore validate our scoring criteria, for example, for leptin or adiponectin, for those well known adipokines we estimate a score of 6 and 3, respectively. In order to broaden the base of datasets for the scoring, we include also data from gene expression profiling studies from ZDF rats. This animal model has been used for the characterization of anti-diabetic drug candidates in numerous pharmacological experiments and is therefore considered as a validated Type 2 Diabetes animal model on the path to the clinic.

Our *in silico* analysis of the adipocyte secretome genes, based on known annotation and pattern of expression in adipose tissue, identified nine genes with top score (>3). Within this group, the six genes which display altered mRNA expression in adipose in obesity are particularly interesting and constitute candidates for further studies in obesity. These genes include *WISP2*, which is a member of the WNT signalling cascades. WNT signalling is known to be involved in pre-adipocyte differentiation (Cristancho and Lazar, 2011). The second gene is the extracellular matrix protein *ITIH5*. Although *ITIH5* has to our knowledge not been studied in adipose tissue previously, extracellular matrix has a potentially important role in obesity associated adipose inflammation and insulin resistance as described above. The third gene, *SERPINE2*, is a serine protease inhibitor that modulates the activity of plasminogen activators. The fourth protein is *C4A*. The detection of a complement factor is in agreement with the emerging evidence of adipose

Table 4. Top-score secretome genes (≥2) in relation to obesity and depot.

Gene	Score	Obese/lean	BH P	Gene	Score	Visceral/ subcutaneous	BH P
Up regulated in obesity				Down regulated in visceral adipose tissue			
WISP2	4.0	1.77	0.0001	FIGF	6.0	0.82	0.005000
GPNMB	3.5	1.70	0.0036	ITIH5	4.0	0.41	2.6×10^{-08}
ITIH5	4.0	1.50	0.0007	WISP2	4.0	0.43	1.4×10^{-06}
SERPINE2	3.5	1.78	0.0002	CFD	4.0	0.73	1.2×10^{-07}
C4A	3.5	1.36	0.0027	GPNMB	3.5	0.91	0.033000
AKR1C3	3.0	1.39	0.0007	AKR1C3	3.0	0.37	8.0×10^{-10}
SEMA3G	3.0	1.67	0.0001	SEMA3G	3.0	0.39	4.1×10^{-10}
SVEP1	3.0	1.51	0.0006	CRYAB	3.0	0.73	0.00094
SLIT3	3.0	1.50	0.0001	CHRDL1	3.0	0.89	0.014000
CHRDL1	3.0	1.31	0.0036	VCAN	2.5	0.45	9.2×10^{-06}
CHI3L1	2.5	5.68	0.0011	CLU	2.5	0.53	1.7×10^{-06}
SERPINE1	2.5	2.40	0.0006	ENPP2	2.5	0.54	6.0×10^{-09}
TIMP1	2.5	2.29	0.0000	MCAM	2.5	0.57	2.6×10^{-08}
VCAN	2.5	1.94	0.0002	PDXK	2.5	0.60	1.7×10^{-08}
CFH	2.5	1.76	0.0002	CFH	2.5	0.65	0.000400
CTSD	2.5	1.71	0.0001	CHI3L1	2.5	0.82	0.003800
ANPEP	2.5	1.62	0.0006	CTSD	2.5	0.85	0.036000
CLU	2.5	1.57	0.0000	ERAP1	2.5	0.87	0.021000
C3	2.5	1.51	0.0008	RARRES2	2.5	0.88	0.017000
PCOLCE	2.5	1.44	0.0021	ASAH1	2.0	0.58	6.8×10^{-07}
TPSAB1	2.5	1.41	0.0068	S100A4	2.0	0.66	4.7×10^{-05}
CPE	2.5	1.39	0.0106	CD44	2.0	0.70	9.7×10^{-06}
DPP4	2.5	1.38	0.0270	Up regulated in visceral adipose tissue			
IGFBP4	2.5	1.33	0.0013	C4A	3.5	1.33	3.1×10^{-05}
ERAP1	2.5	1.27	0.0043	SVEP1	3.0	1.78	3.8×10^{-05}
MCAM	2.5	1.23	0.0055	IGFBP4	2.5	1.27	0.001700
CD44	2.0	1.69	0.0001	AGT	2.5	1.54	0.002800
S100A4	2.0	1.53	0.0075	DPP4	2.5	2.07	9.59E-06
PEA15	2.0	1.48	0.0001	PCOLCE	2.5	2.32	0.002694
ABI3BP	2.0	1.45	0.0090	CPE	2.5	3.09	6.66E-08
ASAH1	2.0	1.39	0.0001	TIMP1	2.5	3.67	1.65E-08
IGFBP7	2.0	1.34	0.0046	C3	2.5	3.92	5.89E-08
Down regulated in obesity				C7	2.5	13.07	1.36E-10
ADIPOQ	3.0	0.89	0.0299	SELENBP1	2.0	1.42	2.6E-06
Not regulated				Not regulated			
FIGF	6.0	0.76	0.0756	CALB2	3.5	1.07	0.955520
CFD	4.0	1.15	0.1393	SERPINE2	3.5	1.09	0.793270
CALB2	3.5	1.02	0.8468	ADIPOQ	3.0	0.90	0.060796
CRYAB	3.0	1.09	0.3500	SLIT3	3.0	1.10	0.469813
TIMP4	3.0	1.04	0.7719	TIMP4	3.0	1.19	0.256568
AGT	2.5	1.19	0.1356	SOD3	2.5	0.88	0.056055
ENPP2	2.5	1.18	0.0599	ANPEP	2.5	0.92	0.056434
GGH	2.5	1.17	0.2445	HEBP2	2.5	0.92	0.119572
PDXK	2.5	1.10	0.2170	GGH	2.5	1.10	0.770743
IGFBP5	2.5	1.09	0.4514	IGFBP5	2.5	1.13	0.315896
C7	2.5	1.08	0.7555	SERPINE1	2.5	1.16	0.380438
HEBP2	2.5	0.95	0.6162	TPSAB1	2.5	1.27	0.398775
RARRES2	2.5	0.90	0.2412	PEA15	2.0	0.97	0.396736
SOD3	2.5	0.84	0.0927	IGFBP7	2.0	1.01	0.769020
SELENBP1	2.0	1.05	0.6249	ABI3BP	2.0	1.49	0.133261

tissue and adipocytes as a source of complement components, which have been proposed to be important in tissue maintenance and apoptosis (van Greevenbroek, 2009). The fifth gene *GPNMB* has been shown to be important for osteoblast differentiation (Singh *et al*., 2012). To our knowledge *SERPINE2*, *C4A* and *GPNMB* have not been studied in adipose tissue previously.

Visceral adipose tissue displays an unfavourable metabolic profile and is believed to be an important mediator of the metabolic disturbances in obesity (Wajchenberg, 2000; Arner, 2005a). A better understanding of the gene sets that underlie the metabolic difference between subcutaneous and visceral adipose tissue may highlight new targets for treating the metabolic disturbances in visceral adipose tissue. Our

in silico analysis of the adipocyte secretome genes, based on known annotation and pattern of expression in adipose tissue, identified six genes with top score (>3) that were also differentially expressed between visceral and subcutaneous adipose tissue. These genes potentially contribute to the adipose tissue depot differences in metabolism. They include the above-mentioned *ITIH5*, *WISP2*, and *GPNMB*, which are expressed at lower levels in visceral adipose tissue, and *C4A* which is expressed at higher levels in visceral adipose tissue. In addition, the top-score genes include *FIGF*, which is expressed at higher levels in visceral adipose tissue and promote angiogenesis (Bahram and Claesson-Welsh, 2010) and *CFD*, another complement component.

Expression profiling has previously been used to predict new adipokines. We compared our results with those adipose secretome genes predicted by microarray. Mutch *et al*. (2009) used global transcriptome profiling and bio-informatics to predict secreted proteins among genes differentially expressed in human primary pre-adipocytes undergoing adipogenesis (Mutch *et al*., 2009). Among genes up-regulated during differentiation of adipocytes, Mutch *et al*. (2009) noted enrichment for complement genes. Similarly, we observed nine complement genes in our list of 347 adipose secretome proteins (C1QB, C1R, C1S, C2, C3, C4A, C7, CFD and CFH). The up-regulation of complement genes during adipocyte differentiation points to an important role in fat cells. A total of 33 predicted adipocyte secreted proteins that are found in human plasma are listed in the paper by Mutch *et al*. (2009) 11 of the 33 genes were confirmed in our list of 347 adipose secretome genes, i.e. *CD44, TIMP1, SERPINE1, GGH, C7, PTGDS, MMP9, THBS1, C1QB, CFD* and *CLEC3B*. These findings validate the use of global transcriptome profiling together with bioinformatics to detect new secreted proteins. In another study Hoggard *et al*. (2012) have used transcriptome profiling and bioinformatics to identify 11 genes that are differentially expressed between omental and subcutaneous adipose tissue and are predicted to code for secreted proteins (Hoggard *et al*. 2012). These 11 genes do not overlap with our list of 347 adipose secretome genes. The different results may be due to the different approaches used, i.e. Hoggard *et al*. (2012) limited his analysis to genes differentially expressed between adipose depots only.

This study pinpoints potential novel adipocyte proteins whose expression pattern suggests that they have important functional features in adipose tissue. However, the study has several limitations. First, for most of the proteins a time-dependent release from fat cells has not yet been established. The presence of a protein in medium from adipocyte cultures does not necessarily mean that the protein is secreted (Lehr *et al*., 2012). The protein could origin from fragmenting cells. Second, mRNA expression pattern is not the only mean of assaying functional importance. Post-translational changes in proteins (phosphorylation, protein interactions, etc) also indicate altered protein action. Third, proteomic screens cannot identify all proteins in a solution.

In conclusion, analysis of the adipocyte protein secretome highlights the importance of fat cells as a source of extracellular matrix proteins in adipose tissue, and identifies *ITIH5, WISP2, GPNMB, SERPINE2, C4A* and *FIGF* as novel potential adipokine candidate regulators of obesity and adipose regions. These genes should be prioritized in future functional adipokine studies. The functions ascribed to these genes pinpoints extracellular matrix, adipogenesis, and angiogenesis as potentially important function of adipocyte secretome genes. Finally, the majority of the adipokines are regulated by obesity, and/or adipose depot.

Declaration of interest

This study was supported by a grant from the 7th Framework of the European Union ADAPT FP-7-Health-2007-A (http://www.adapt-eu.net), the Novonordisk foundation, the Swedish Research Council, Marianne and Marcus Wallenbergs' foundation and The Stockholm County Council (ALF). I.D., M.E., H.S., and P.A. report no declaration of interest. J.E. was supported by a grant from Sanofi-Aventis. B.B., M.K. and N.T. are employees of Sanofi-Aventis.

References

Arner P . (2001). Regional differences in protein production by adipose tissue. Biochem Soc Trans 29:72–5.

Arner P. (2005a). Human fat cell lipolysis: biochemistry, regulation and clinical role. Best Pract Res Clin Endocrinol Metab 19:471–82.

Arner P. (2005b). Insulin resistance in type 2 diabetes – role of the adipokines. Curr Mol Med 5:333–9.

Bahram F, Claesson-Welsh L. (2010). VEGF-mediated signal transduction in lymphatic endothelial cells. Pathophysiology 17:253–61.

Clement K, Viguerie N, Poitou C, Carette C, Pelloux V, Curat CA, Sicard A, Rome S, Benis A, Zucker JD, et al. (2004). Weight loss regulates inflammation-related

genes in white adipose tissue of obese subjects. FASEB J 18:1657–69.

Cristancho AG, Lazar MA. (2011). Forming functional fat: a growing understanding of adipocyte differentiation. Nat Rev Mol Cell Biol 12:722–34.

Dahlman I, Forsgren M, Sjogren A, Nordstrom EA, Kaaman M, Naslund E, Attersand A, Arner P. (2006). Downregulation of electron transport chain genes in visceral adipose tissue in type 2 diabetes independent of obesity and possibly involving tumor necrosis factor-alpha. Diabetes 55:1792–9.

Dahlman I, Mejhert N, Linder K, Agustsson T, Mutch DM, Kulyte A, Isaksson B, Permert J, Petrovic N, Nedergaard J, et al. (2010). Adipose tissue pathways involved in weight loss of cancer cachexia. Br J Cancer 102:1541–8.

Eisen MB, Spellman PT, Brown PO, Botstein D. (1998). Cluster analysis and display of genome-wide expression patterns. Proc Natl Acad Sci USA 95:14863–8.

Henegar C, Tordjman J, Achard V, Lacasa D, Cremer I, Guerre-Millo M, Poitou C, Basdevant A, Stich V, Viguerie N, et al. (2008). Adipose tissue transcriptomic signature highlights the pathological relevance of extracellular matrix in human obesity. Genome Biol 9:R14.

Hoggard N, Cruickshank M, Moar KM, Bashir S, Mayer CD. (2012). Using gene expression to predict differences in the secretome of human omental vs. subcutaneous adipose tissue. Obesity January [Epublished ahead of print].

Hotamisligil GS, Arner P, Caro JF, Atkinson RL, Spiegelman BM. (1995). Increased adipose tissue expression of tumor necrosis factoralpha in human obesity and insulin resistance. J Clin Invest 95: 2409–15.

Kim J, Choi YS, Lim S, Yea K, Yoon JH, Jun DJ, Ha SH, Kim JW, Kim JH, Suh PG, et al. (2010). Comparative analysis of the secretory proteome of human adipose stromal vascular fraction cells during adipogenesis. Proteomics 10:394–405.

Koerner A, Kratzsch J, Kiess W. (2005). Adipocytokines: leptin – the classical, resistin – the controversical, adiponectin – the promising, and more to come. Best Pract Res Clin Endocrinol Metab 19:525–46.

Kolehmainen M, Salopuro T, Schwab US, Kekalainen J, Kallio P, Laaksonen DE, Pulkkinen L, Lindi VI, Sivenius K, Mager U, et al. (2008). Weight reduction modulates expression of genes involved in extracellular matrix and cell death: the GENOBIN study. Int J Obes (Lond) 32:292–303.

Lehr S, Hartwig S, Lamers D, Famulla S, Mueller S, Hanisch FG, Cuvelier C, Ruige J, Eckardt K, Ouwens DM, et al. (2012). Identification and validation of novel adipokines released from primary human adipocytes. Mol Cell Proteomics 11: M111.010504.

Li Y, Tong X, Rumala C, Clemons K, Wang S. (2011). Thrombospondin1 deficiency reduces obesity-associated inflammation and improves insulin sensitivity in a diet-induced obese mouse model. PLoS One 6:e26656.

Mutch DM, Rouault C, Keophiphath M, Lacasa D, Clement K. (2009). Using gene expression to predict the secretome of differentiating human preadipocytes. Int J Obes (Lond) 33:354–63.

Reaven G, Abbasi F, McLaughlin T. (2004). Obesity, insulin resistance, and cardiovascular disease. Recent Prog Horm Res 59:207–23.

Singh M, del Carpio-Cano FE, Monroy MA, Popoff SN, Safadi FF. (2012). Homeodomain transcription factors regulate BMP-2-induced osteoactivin transcription in osteoblasts. J Cell Physiol 227:390–99.

Spencer M, Yao-Borengasser A, Unal R, Rasouli N, Gurley CM, Zhu B, Peterson CA, Kern PA. (2010). Adipose tissue macrophages in insulin-resistant subjects are associated with collagen VI and fibrosis and demonstrate alternative activation. Am J Physiol Endocrinol Metab 299:E1016–27.

Wajchenberg BL. (2000). Subcutaneous and visceral adipose tissue: their relation to the metabolic syndrome. Endocr Rev 21: 697–738.

van Greevenbroek MM. (2009). The expanding role of complement in adipose tissue metabolism and lipoprotein function. Curr Opin Lipidol 20:353–4.

Zhong J, Krawczyk SA, Chaerkady R, Huang H, Goel R, Bader JS, Wong GW, Corkey BE, Pandey A. (2010). Temporal profiling of the secretome during adipogenesis in humans. J Proteome Res 9:5228–38.

BMP4 and BMP7 induce the white-to-brown transition of primary human adipose stem cells

Manuela Elsen,[1] Silja Raschke,[1] Norbert Tennagels,[2] Uwe Schwahn,[2] Tomas Jelenik,[3] Michael Roden,[3,4], Tania Romacho,[1] and Jürgen Eckel[1]

[1]*Paul-Langerhans-Group for Integrative Physiology, German Diabetes Center, Düsseldorf, Germany;*
[2]*R&D Diabetes Division, Sanofi-Aventis Deutschland, Frankfurt, Germany;*
[3]*Institute for Clinical Diabetology, German Diabetes Center, Düsseldorf, Germany;*
[4]*Department of Endocrinology and Diabetology, Heinrich-Heine University Düsseldorf, Düsseldorf, Germany*

Abstract

While white adipose tissue (AT) is an energy storage depot, brown AT is specialized in energy dissipation. Uncoupling protein 1 (UCP1)-expressing adipocytes with a different origin than classical brown adipocytes have been found in white AT. These "brite" (brown-in-white) adipocytes may represent a therapeutic target to counteract obesity. Bone morphogenetic proteins (BMPs) play a role in the regulation of adipogenesis. Based on studies with murine cells, BMP4 is assumed to induce stem cell commitment to the white adipocyte lineage, whereas BMP7 promotes brown adipogenesis. There is evidence for discrepancies between mouse and human AT. Therefore we compared the effect of BMP4 and BMP7 on white-to-brown transition in primary human adipose stem cells (hASCs) from subcutaneous AT. Long-term exposure of hASCs to recombinant BMP4 or BMP7 during differentiation increased adipogenesis, as determined by lipid accumulation and *PPARγ* expression. Not only BMP7, but also BMP4 increased *UCP1* expression in hASCs and decreased expression of the white-specific marker *TCF21*. The ability of hASCs to induce *UCP1* in response to BMP4 and BMP7 markedly differed between donors and could be related to the expression of the brite marker *CD137*. However, mitochondrial content and oxygen consumption was not increased in hASCs challenged with BMP4 and BMP7. In conclusion, we showed for the first time that BMP4 has similar effects on white-to-brown transition as BMP7 in our human cell model. Thus, the roles of BMP4 and BMP7 in adipogenesis cannot always be extrapolated from murine to human cell models.

Keywords: bone morphogenetic proteins; primary human preadipocytes; adipogenesis; brite adipocytes.

Introduction

Adipose tissue (AT) plays a crucial role in the regulation of energy homeostasis. Functionally, AT can be subdivided into white AT and brown AT. While white AT is the main site of energy storage and provides substrates in terms of energy needs by releasing free fatty acids and glycerol, brown AT metabolizes triglycerides to generate heat in adaptation to a cold environment (32). This unique function of brown AT is due to a high mitochondrial density and to the presence of uncoupling protein 1 (UCP1). Until recently, brown AT was believed to play a negligible role in the adult human. However, it gained substantial interest since active brown AT has been shown to be present in adults by five independent groups (4; 23; 38; 40; 43), and brown AT activity was negatively associated with increasing BMI (23; 38; 43). Furthermore, *UCP1*-expressing brown-like adipocytes have been discovered within white AT after cold exposure (31). These so called "brite" (brown-in-white) adipocytes arise from white preadipocytes (19), whereas classical brown adipocytes are derived from the myogenic lineage (29; 35). Both increasing brown AT activity and promoting the induction of brite adipocytes in white AT represent strategies to counteract obesity. Pharmacological agents, like peroxisome proliferator-activated receptor γ (PPARγ) agonists (8; 20), triiodothyronine (T3) (12), cardiac natriuretic peptides (CNPs) (1) and bone morphogenetic protein (BMP) 7 (27) have been reported to induce brite adipocytes in humans.

BMPs belong to the transforming growth factor beta (TGF-β) superfamily and are important regulators of developmental processes. BMP signaling is complex and dependent on the receptor composition of a cell and the presence of intra- and extracellular antagonists (3). Selected members of the BMP family play an important role in the regulation of white vs. brown adipogenesis and energy homeostasis (16). While BMP4

induces commitment of pluripotent stem cells to the white adipocyte lineage (2; 10) and promotes differentiation of white preadipocytes (9), BMP7 plays an important role in brown adipocyte lineage determination of the multipotent C3H10T1/2 cell line and promotes differentiation of murine brown preadipocytes (37). Evidence from transgenic mouse models suggests, that BMP7 plays an important role in whole energy homeostasis, since BMP7 knockout mice displayed a decrease in brown AT mass (37) and systemic BMP7 administration to ob/ob mice led to increased energy expenditure and reduced food intake accompanied by weight loss (36). Therefore, it is currently assumed that BMP4 and BMP7 differentially regulate white vs. brown adipogenesis. However, BMP4 might also induce a white-to-brown switch and have positive effects on energy homeostasis (21). Qian and colleagues showed that adipose tissue-specific overexpression of BMP4 leads to induction of brite adipocytes and increased energy expenditure in mice. Furthermore, murine 3T3-L1 adipocytes challenged with BMP4 during differentiation displayed a brite phenotype with increased mitochondrial content and expression of brown adipose tissue markers (21).

There is evidence that the molecular signature from human adipose tissue depots differ from mouse adipose tissue depots (42), raising the question if results from mouse studies investigating mechanisms of browning of white AT can be extrapolated to humans. Furthermore, the effects of different BMPs on white vs. brown adipogenesis seem to be dependent on the AT depot and species studied. The impact of BMP4 and BMP7 on browning of white preadipocytes has not yet been explored in parallel in a human cell culture model. Therefore, we aimed to investigate for the first time the effect of BMP4 on the white-to-brown transition of primary human adipose stem cells (hASCs) in comparison to the known browning factor BMP7. In this study, hASCs were isolated from the subcutaneous depot of different donors and challenged with BMP4 or BMP7. In contrast to mice, in humans both BMP4 and BMP7 we found to induce a brite adipocyte phenotype, suggesting substantial differences in adipose tissue plasticity between different species.

Material and methods

Isolation and culture of primary hASCs

Subcutaneous AT (from the abdominal and mammary region) was obtained from healthy lean or overweight women (n = 38, body mass index 28.8 ± 0.7 kg/m^2, age 39 ± 3 years) undergoing plastic surgery. The procedure was approved by the ethical board of Heinrich-Heine-University, Düsseldorf, Germany. Human adipose stem cells (hASCs) were isolated by collagenase digestion of AT as previously described by our group (6). Isolated cell pellets were resuspended in adipocyte basal medium (BM) which was DMEM/F-12 (GIBCO, Grand Island, NY) supplemented with 14 nmol/l NaHCO3, 33 mmol/l biotin, 17 mmol/l D-panthothenic-acid containing 10 % FCS (GIBCO) pH 7.4, seeded in six-well plates and maintained at 37°C and 5 % CO2. When cells reached confluence differentiation was induced with adipocyte differentiation medium (BM supplemented with 66 nM insulin, 1 nM triiodo-L-thyronine, 100 nM cortisol, 10 mg/ml apotransferrin, 50 mg/ml gentamycin) with the addition of 5 µM troglitazone during the first 3 days. Medium was changed every 2-3 days and cells were differentiated for 14 days or as indicated. Recombinant human BMP4 or BMP7 (R&D Systems, Minneapolis, MN) were added to the differentiation medium at a final concentration of 50 ng/ml.

Oil Red O Staining

For Oil Red O Staining cells were cultured in 6-well plates and differentiated with or without BMP4 or BMP7. After 14 days, cells were washed in PBS and fixed for 2 h with a solution containing 71% picric acid (v/v), 24% acetic acid (v/v) and 5% formaldehyde (w/v). Afterwards, cells were washed three times with PBS and lipids were subsequently stained with 0.3% Oil Red O dissolved in 60% isopropanol for 10 min. The staining was quantified by dissolving Oil Red O with 100% isopropanol and measuring absorbance at 500 nm.

Immunofluorescence Staining

For immunocytochemistry, hASCs were cultured on 12x12 mm coverslips coated with 0.1 % gelatine. After 12 days of differentiation, adipocytes were washed with PBS and fixed with 3 % formaldehyde for 15 min at room temperature. Afterwards, cells were washed three times with PBS for 5 min and incubated with blocking solution (PBS containing 1 % BSA and 0.1 % Triton X-100) for 1 h at room temperature. Mouse anti-human MTCO2 (Abcam, Cambridge, UK) was diluted 1:100 in blocking solution and incubated at 4°C over night. After 3 washes for 5 min with PBS, cells were incubated with anti-mouse Alexa Fluor 488 (Life Technologies, Carlsbad, CA) diluted 1:500 in blocking solution for 1 h at room temperature. Nuclei were stained with 1 µg/ml DAPI (Life Technologies) in PBS for 10 min at room temperature. Finally, coverslips were mounted with ProLong Gold Antifade reagent (Life Technologies). Cells were analyzed using a Zeiss fluorescence microscope (Oberkochen,

Germany) equipped with a Axio Cam MRc5. Images were acquired with AxioVision rel. 4.3 with equal settings for contrast/brightness and merged by use of the Image J software.

Generation of concentrated supernatants

For generation of supernatants, hASCs were seeded in 75 cm^2 flasks and underwent adipogenic differentiation for 14 days. Subsequently, cells were incubated with 10 ml of αMEM (GIBCO) for 24 h. Afterwards, supernatants were collected, centrifuged at 1200 rpm and concentrated 100-fold by using Amicon® Ultra-4 Centrifugal Filter Units with Ultracell 3 membrane (Millipore, Billerica, MA). Concentrated supernatants were diluted in Laemmli buffer and subjected to immunoblot analysis.

Immunoblot analysis

Total cellular proteins were dissolved in lysis buffer containing 20 mM MOPS, 2 mM EGTA, 5 mM EDTA, 1 mM dithiothreitol, 1% Triton X-100, complete protease inhibitor cocktail (Roche, Basel, Switzerland) and PhosStop phosphatase inhibitor cocktail (Roche), pH 7.0. Lysates were shaken for 2 h at 4°C and centrifuged at 10.000 x g for 20 min. Protein concentration was determined by using Bradford protein assay (Bio-Rad, Hercules, CA) and 10 µg protein was seperated by SDS-PAGE using 10% horizontal gels. Proteins were transferred to a polyvinylidene difluoride membrane (Millipore) in a semidry blotting system. Membranes were blocked with 5 % non-fat dry milk or BSA in TBS containing 0.1% Tween for 1 h at RT and probed with the indicated primary antibodies overnight at 4°C. After washing, membranes were incubated with a secondary HRP-coupled antibody and processed for enhanced chemiluminescence detection using Immobilon HRP substrate (Millipore). Signals were visualized and analyzed on a BioRad VersaDoc 4000 MP work station. Antibodies were used as follows: anti-BMP4 (ab93939, Abcam) diluted 1:1000, anti-BMP7 (sc-9305, Santa Cruz Biotechnology, Santa Cruz, CA) diluted 1:200, anti-phospho SMAD1/5/8 (#9511, Cell Signaling, Danvers, MA) diluted 1:1000 and anti-OXPHOS cocktail (MS604, Abcam) diluted 1:1000, anti-beta actin (ab6276, Abcam).

High-resolution respirometry

For oxygen consumption measurements, hASCs were seeded in T25 cm^2 flasks and differentiated for 14 days under control conditions or with the addition of 50 ng/ml BMP4 or BMP7 (R&D Systems). Oxygen consumption was measured using the Oroboros Oxygraph-2k (Oroboros Oxygraph, Insbruck, Austria). Chambers were equilibrated with BM for 30 min before addition of freshly trypsinized cells. Measurements were done in duplicates and performed in 2 ml of adipocyte BM supplemented with 10 % FCS at 37°C under continuous stirring. After observing a steady-respiratory flux, cells were titrated with the uncoupler carbonyl cyanide-4-trifluoromethoxyphenylhydrazone (C2920, Sigma-Aldrich, St. Louis, MO) to obtain maximal respiration. Finally, respiration was inhibited with 2.5 µM of the complex III inhibitor, Antimycin A (A8674, Sigma-Aldrich). Oxygen consumption was normalized to cell number and analyzed with the Oroboros software. Antimycin A-sensitive oxygen consumption was considered as basal respiration.

RNA isolation and quantitative real-time PCR

hASCs underwent adipogenic differentiation for 14 days with or without the addition of BMP4 and BMP7 and total RNA was isolated by using the RNeasy Lipid Tissue kit (Qiagen, Hilden, Germany). Equal amounts of RNA were reverse transcribed with the Omniscript Reverse Transcription kit (Qiagen) according to the manufacturer's protocol. To determine mRNA expression levels of genes, quantitative RT-PCR was performed using GoTaq qPCR Master Mix (Promega, Madison, WI) and QuantiTect Primer Assays (Qiagen) for PPARγ (Hs_PPARG_1 SG), UCP1 (Hs_UCP1_3_SG), TCF21 (Hs_TCF21_2_SG), ZIC1 (Hs_ZIC1_1_SG), PGC-1α (Hs_PPARGC1A_1 SG), and ß-actin (Hs_ACTB_2_SG) and primer pairs for CD137 (Eurofins MWG, Hamburg, Germany, forward 5'- AGCTGTTACAACATAGTAGCCAC, reverse 5'-TCCTGCAATGATCTTGTCCTCT) on a Step One Plus cycler (Applied Biosystems, Carlsbad, CA). Amplification was done as follows: One step at 95°C 2 min, 40 cycles at 95°C 15 s, 55-58 °C 30 s and 60°C 30 s. All samples were analyzed in triplicate. Expression of genes was normalized to ß-actin mRNA according to the comparative threshold method (ΔCT).

Microfluidic card TaqMan gene expression assay

RNA integrity was tested on an Agilent 2100 Bioanalyzer (Agilent Technologies, Santa Clara, CA) using Agilent RNA Nano chips. Only RNAs with a RIN score of 7.5 or higher were used for analysis. Synthesis of cDNA was done from 0.5 µg of each total RNA preparation in a volume of 20 µl with the QuantiTect Reverse Transcription Kit (Qiagen) according to the manufacturer's instructions. Thermal cycling of the PCR reactions was done in microfluidic cards on a ViiA7 Real Time PCR 384 well cycler and fluorescence plate reader (Applied Biosystems). Specific TaqMan® Gene Expression Assays (Applied Biosystems) for PRDM16 (Hs00922674_m1), PPARA (Hs00947539_m1), PGC-1ß (Hs00991677_m1),

NRF1 (Hs00192316_m1), TFAM (Hs00273372_s1), OXR1 (Hs00250562_m1), UCP2 (Hs01075227_m1), UCP3 (Hs01106052_m1), CYCS (Hs01588974_g1), VDAC1 (Hs01631624_gH), GAPDH (Hs02758991_g1) and ß-actin (Hs01060665_g1) were used. Expression levels of genes were normalized to GAPDH and ß-actin as housekeeping genes and related to control samples.

Statistics

Results are expressed as mean ± SEM. One-way ANOVA (post-hoc test: Bonferroni or Dunnett's) was used to determine statistical significances. All statistical analyses were done using GraphPad Prism 5 considering a p-value of less than 0.05 as statistically significant.

Results

BMP4 is secreted by human adipocytes.

BMP4 has been shown to induce commitment of pluripotent C3H10T1 cells to the adipocyte lineage (2; 33). Furthermore, *BMP4* mRNA is induced in primary human preadipocytes undergoing adipogenic differentiation (9), suggesting that BMP4 may be a secreted factor acting on adipocyte differentiation in a paracrine manner. Thus, we first examined BMP4 protein levels in primary hASCs undergoing adipogenic differentiation. BMP4 is constitutively expressed during differentiation of primary hASCs, with a trend towards a decrease at later stages of differentiation (Figure 1 A). Moreover, we show for the first time that BMP4 is secreted from differentiated hASCs, as determined by immunoblot of concentrated supernatants from 7 different donors (Figure 1C). The detected band for BMP4 has a molecular weight of 47 kDa, corresponding to the uncleaved propeptide of BMP4 (UniProt entry P12644). We also assessed BMP7 protein levels during adipogenesis of hASCs. We found that BMP7 (UniProt entry P18075) is present as a 50 kDa form, representing the precursor (data not shown), and as smaller 15.7 kDa protein, reflecting the cleaved mature protein (Figure 1B). Levels of mature BMP7 were slightly, but not significantly upregulated during adipogenesis (Figure 1B). Interestingly, we could not

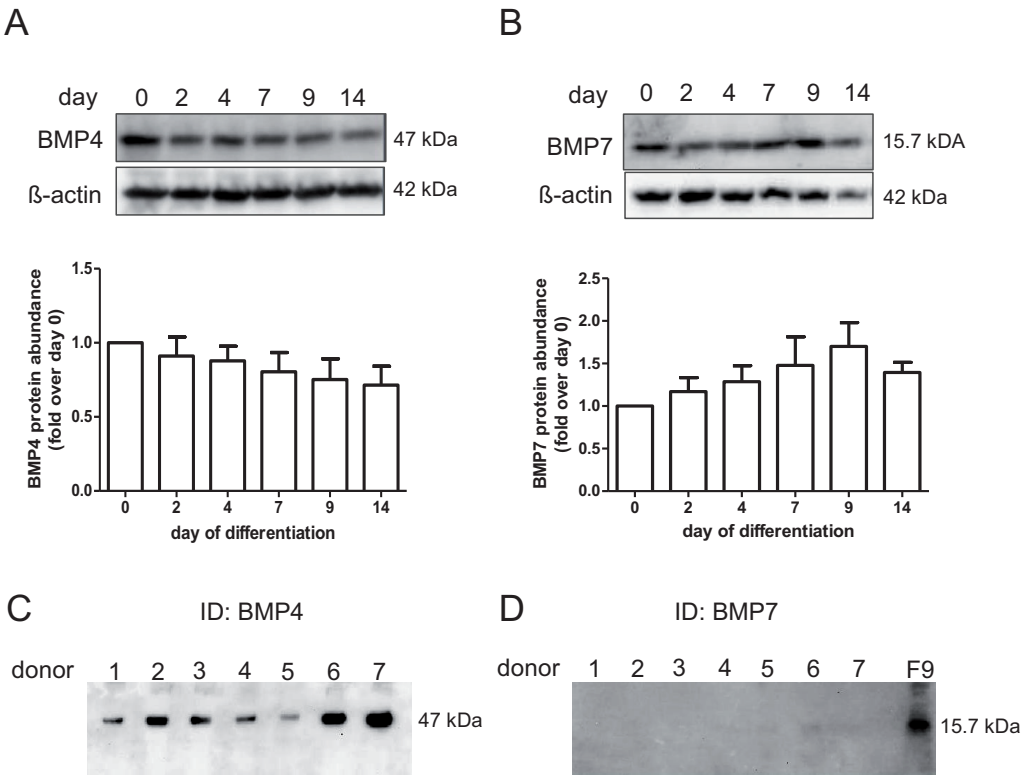

Figure 1: BMP4 but not BMP7 is secreted from differentiated hASCs. *(A+B) hASCs were differentiated for the indicated time points and BMP4 (A) and BMP7 (B) protein levels were analyzed by immunoblot. All data are normalized to β-actin and expressed relative to day 0. Data are expressed as mean values ± SEM, n= 5, * p<0.05 in comparison to day 0. (C+D) To analyze secretion of BMP4 and BMP7 from adipocytes, supernatants of hASCs from 7 different donors at day 14 of differentiation were collected after 24 hours, 100x concentrated and subsequently analyzed by Western Blot for BMP4 (C) and BMP7 (D). F9: F9 cell lysate (Santa Cruz Biotechnology, sc-2245) was used as a positve control for BMP7. ID: Immunodetection.*

show secretion of BMP7 from differentiated hASCs, since BMP7 was not detectable in the same concentrated supernatants used for detection of BMP4 (Figure 1D).

In order to compare the effect of BMP4 to BMP7 on the white-to-brown shift of hASCs, we determined equipotent concentrations of BMP4 and BMP7. Therefore, undifferentiated hASCs were challenged with different concentrations of BMP4 or BMP7 for 30 min and SMAD1/5/8 phosphorylation, the main signaling pathway activated by BMPs, was measured. We observed a dose-dependent increase of BMP4- and BMP7-induced SMAD1/5/8 phosphorylation with similar maximal BMP4/7 concentrations (Figure 2A). Furthermore, SMAD1/5/8 phoshporylation induced by BMP4 and BMP7 was time-dependent (Figure 2B). For long-term treatments we chose a concentration of 50 ng/ml for BMP4 and BMP7, which induced maximal SMAD1/5/8 phosphorylation. Previous studies in preadipocytes and mesenchymal stem cells used similar BMP concentrations (9; 10; 15; 21; 27; 37).

BMP4 and BMP7 induce a brite-like expression profile in hASCs

It is known that BMPs play a role in preadipocyte commitment and also promote differentiation of already committed preadipocytes (28). Therefore, we first investigated the effect of chronic BMP4/7 exposure on hASC differentiation. Differentiation efficiency of hASCs was significantly increased by long-term

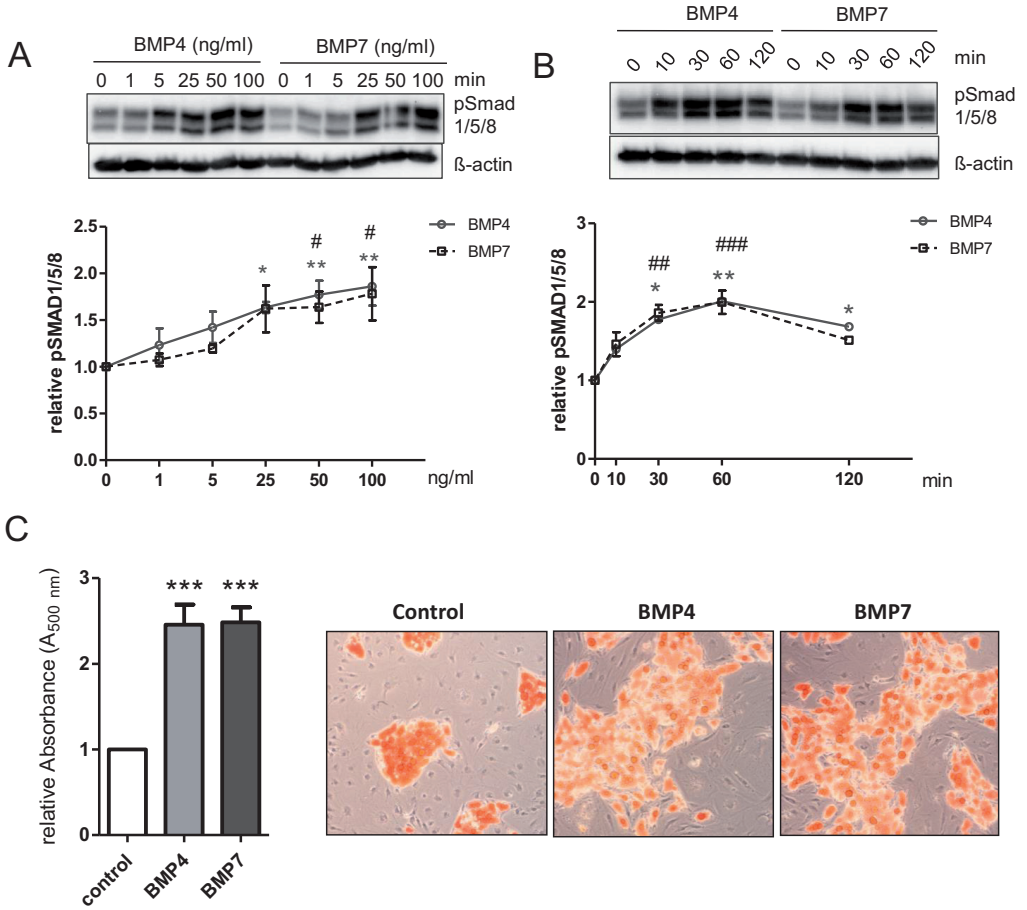

Figure 2: Equipotent concentrations of BMP4 and BMP7 result in a similar long-term effect on adipogenic differentiation of hASCs. *(A+B) In order to assess the activity of BMP4 and BMP7 on SMAD 1/5/8 signaling, non-differentiated hASCs from different donors were acutely stimulated with different concentrations (0 – 100 ng/ml) of recombinant human BMP4 or BMP7 for 30 min (A) and with 10 ng/ml BMP4 or BMP7 for the indicated time points (B). Subsequently, cells were lysed and SMAD1/5/8 phosphorylation was analyzed by immunoblot. Results are normalized to ß-actin and expressed related to control. Data are expressed as mean values ± SEM, n=3-4, **p<0.01, *p<0.05 refer to hASCs treated with BMP4 in comparison to untreated cells. ###p<0.001, ##p<0.01, #p<0.05 refers to hASCs exposed to BMP7 in comparison to untreated cells. Representative blots are shown on top. (C) hASCs from different donors were induced for adipogenic differentiation under standard conditions or with the addition of recombinant human BMP4 or BMP7 (50 ng/ml). On day 14 of differentiation, cells were stained with Oil Red O, the dye was extracted with 100 % isopropanol and absorption was measured at 500 nm. Each column represents mean values ± SEM and is expressed related to control, n=8, ***p<0.001. Representative pictures are shown on the right.*

BMP4 and BMP7 treatment, as indicated by Oil Red O Staining (Figure 2C) and *PPARγ* expression (Figure 3A).

Moreover, BMP4 and BMP7 induced a brown-like mRNA expression profile in hASCs, as determined by significantly increased *UCP1* expression (Figure 3B) and reduced expression of the white-specific marker *TCF21* (Figure 3C). *ZIC1*, a marker for classical brown adipocytes derived from the myogenic lineage was not altered (Figure 3D). The transcription factor PRDM16 is a key regulator of brown adipogenesis and activates the PPARγ coactivator 1 (PGC-1) family members PGC-1α and PGC-1β (30), which play a role in the regulation of mitochondrial function (24). The key regulator *PRDM16* was slightly, but not significantly upregulated by BMP4 and BMP7 (Figure 3F). While *PGC-1α* expression was also not enhanced by BMP4 and BMP7 (Fig. 3E), *PGC-1β* expression was significantly increased by BMP4 and BMP7 (Fig. 3F). Since mitochondrial content and function is enhanced in brite adipocytes (19), we studied mRNA expression levels of further genes encoding for transcriptional regulators of mitochondrial function and mitochondrial proteins. The transcription factors *NRF1* and *TFAM*, which are involved in mitochondrial biogenesis (25), were not affected by BMP4 or BMP7. Expression of some genes like *CYCS* and *UCP2* was significantly enhanced by BMP4 and BMP7, whereas expression of *OXR1* and *UCP3* was downregulated in BMP4- and BMP-treated hASCs (Figure 3F).

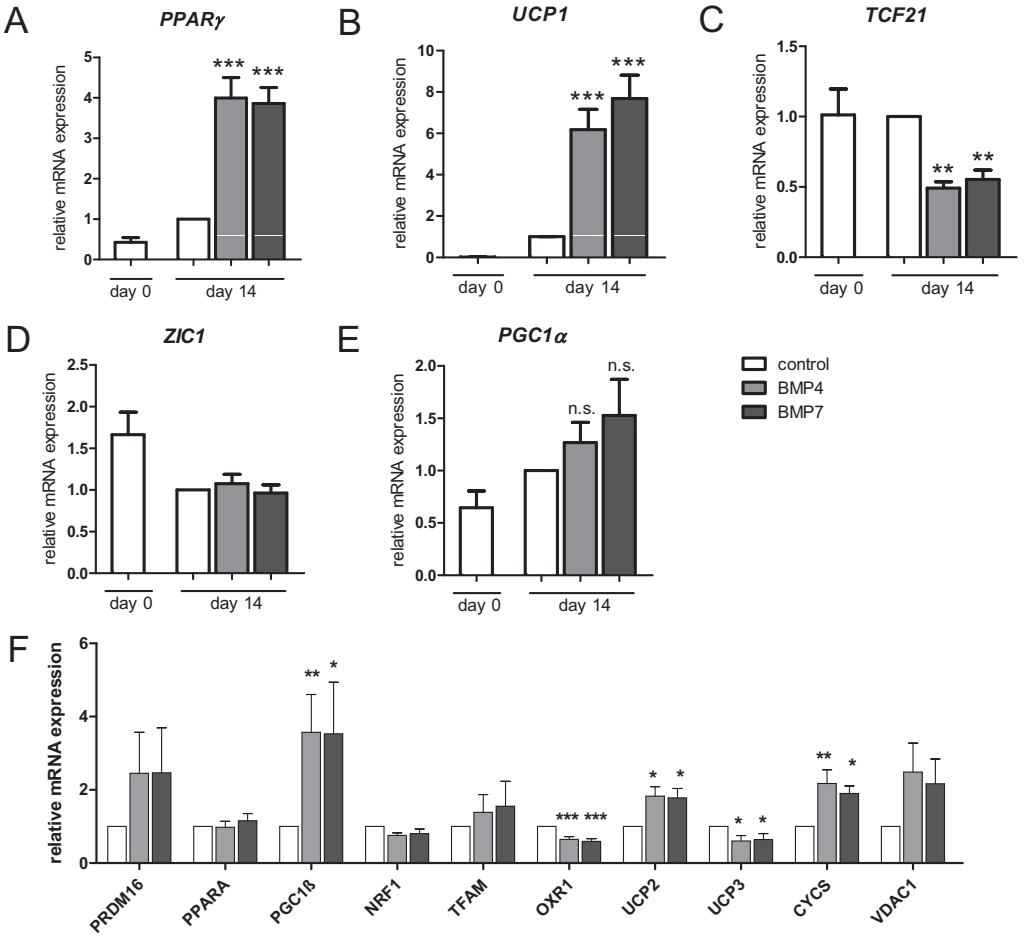

Figure 3: BMP4 and BMP7 induce a brite gene expression pattern in hASCs. *hASCs from different donors were induced for adipogenic differentiation under standard conditions or with the addition of recombinant human BMP4 or BMP7 (50 ng/ml). Medium and recombinant BMP4/7 were replaced every 2-3 days and cells were differentiated for 14 days. (A-E) total mRNA was isolated and mRNA expression of the general marker for adipogenesis PPARγ (A), the brite marker UCP1 (B), and PGC1α (C), the myogenic marker ZIC1 (D) and the white-specific marker transcription factor 21 (TCF21) (E) were analyzed via quantitative real-time PCR. Data are normalized to ß-actin mRNA levels and expressed relative to control on day 14. Data are mean values ± SEM, n=7-14, ***p<0.001, **p<0.01, *p<0.05. (F) Further transcription factors involved in white-to-brown transition and mitochondria-related genes were analyzed in hASCs at day 14 of differentiation with a microfluidic card TaqMan gene expression assay. Expression levels of PRDM16, PPARA, PGC1ß, NRF1, TFAM, OXR1, UCP2, UCP3, CYCS and VDAC1 were determined in relation to GAPDH and ß-actin mRNA levels and expressed related to control. Data represent mean values ± SEM, n=4-9, ***p<0.001, **p<0.01, *p<0.05.*

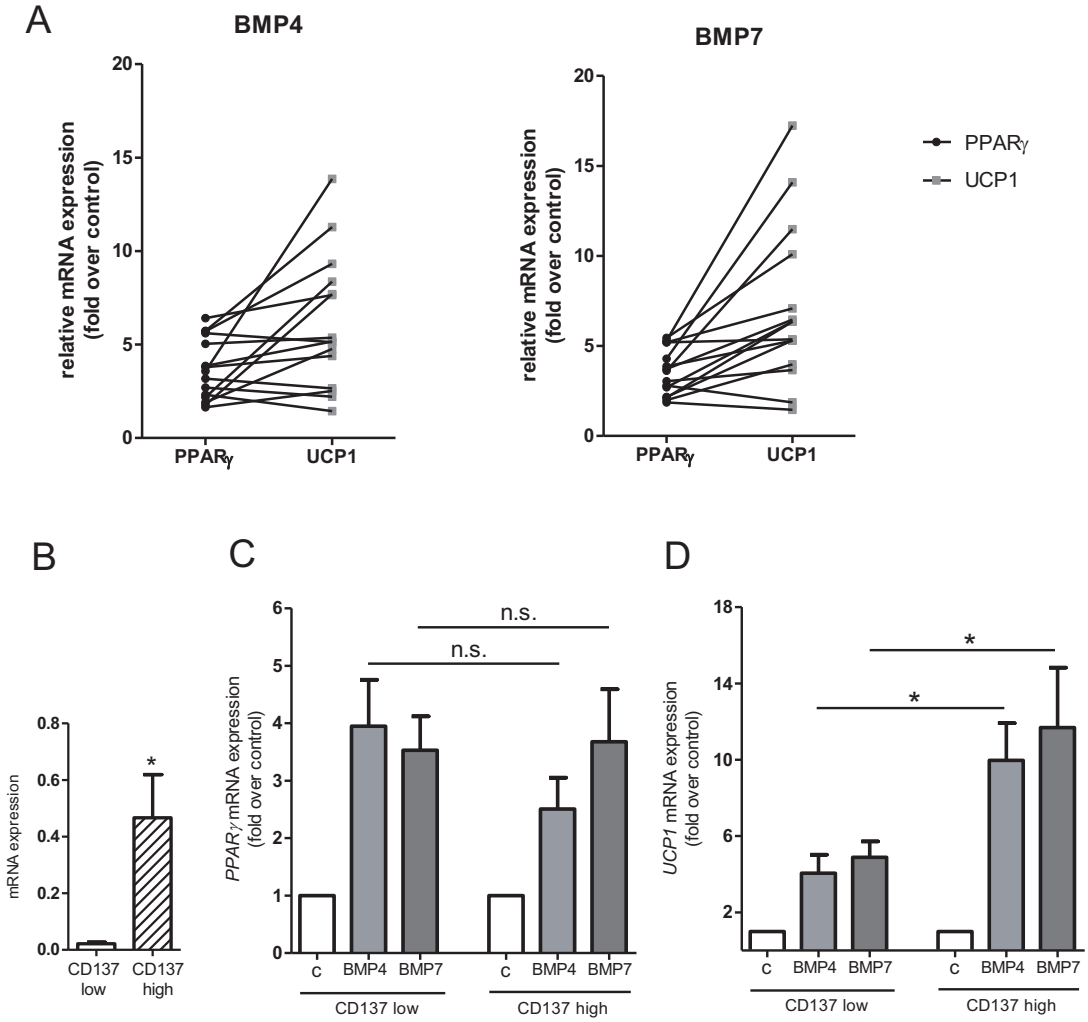

Figure 4: The ability to induce UCP1 in response to BMP4/7 is variable between donors and related to CD137 expression. *(A) PPARγ and UCP1 expression in hASCs at day 14 of differentiation in response to BMP4 and BMP7 was assessed by qRT-PCR. Some donors show a very strong induction of UCP1 in response to BMP4/7, while the effect on PPARγ is comparable between donors. Date are normalized to ß-actin and expressed related to control, n=16. (B) Undifferentiated hASCs from nine different donors were analysed for CD137 expression by qRT-PCR and seperated into CD137 high (n=3) and low (n=6) expressing donors. There was no significant difference in BMI between the CD137 low and CD137 high group (29.3 ± 1.3 kg/m² and 28.9 ± 1.2 kg/m², respectively). (C+D) Comparison of UCP1 (C) and PPARγ (D) mRNA expression levels between CD137 low and high expressing donors on day 14 of differentiation. Donors expressing high levels of CD137 show a significant stronger induction of UCP1 in response to BMP4 and BMP7 compared to CD137 low expressing donors. Data are mean values ± SEM and expressed related to control, *p<0.05 CD137 low vs. CD137 high.*

The ability to induce UCP1 in response to BMP4 and BMP7 was highly variable between donors (1.4 – 13.9 fold and 1.5 – 17.2 fold, respectively) (Figure 4A). Recently, *CD137* and *TMEM26* have been described as brite adipocyte-selective markers and murine precursor cells expressing high levels of *CD137* showed a higher potential to induce browning in response to the newly identified myokine irisin (42). Therefore, we measured *CD137* mRNA levels in undifferentiated hASCs of nine donors and separated them into *CD137* low and high expressing donors (Figure 4B). Interestingly, the mean BMI was similar in the *CD137* low and high expressing group (29.3 ± 1.3 kg/m² and 28.9 ± 1.2 kg/m², respectively). *CD137* high expressing donors showed a significantly higher induction of *UCP1* in response to BMP4 and BMP7 than *CD137* low expressing donors (Figure 4D), while there is no significant difference in *PPARγ* expression between the two groups (Figure 4C).

Mitochondrial content and function are not increased in hASCs by BMP4 and BMP7

Next we aimed to assess if the observed browning effects of BMP4 and BMP7 on *UCP1* and mitochondrial gene expression resulted in a higher mitochondrial content and respiratory capacity. Using an OXPHOS antibody cocktail, we observed that BMP4 and BMP7

significantly increased OXPHOS complexes in total by 2-fold, as well as the single complexes I-IV by 1.6-3-fold (Figure 5A). We also showed that OXPHOS complexes were upregulated during adipocyte differentiation (Figure 5B). Upregulation of mitochondrial content during adipogenesis of hASCs was also confirmed by immunofluorescene staining using anti-Mitochondria antibody (MTC02), which showed a stronger staining in differentiated, lipid-loaden hASCs compared to undifferentiated hASCs (Figure 5D). Furthermore, MTC02 abundance was not higher in BMP4 and BMP7 treated differentiated hASCs compared to control differentiated hASCs (Figure 5D).

In addition to mitochondrial protein content, mitochondrial function was measured by high-resolution respirometry. Basal and uncoupled respiration were increased by 2-fold in BMP4 and BMP7 challenged hASCs compared to untreated hASCs (Figure 5C).

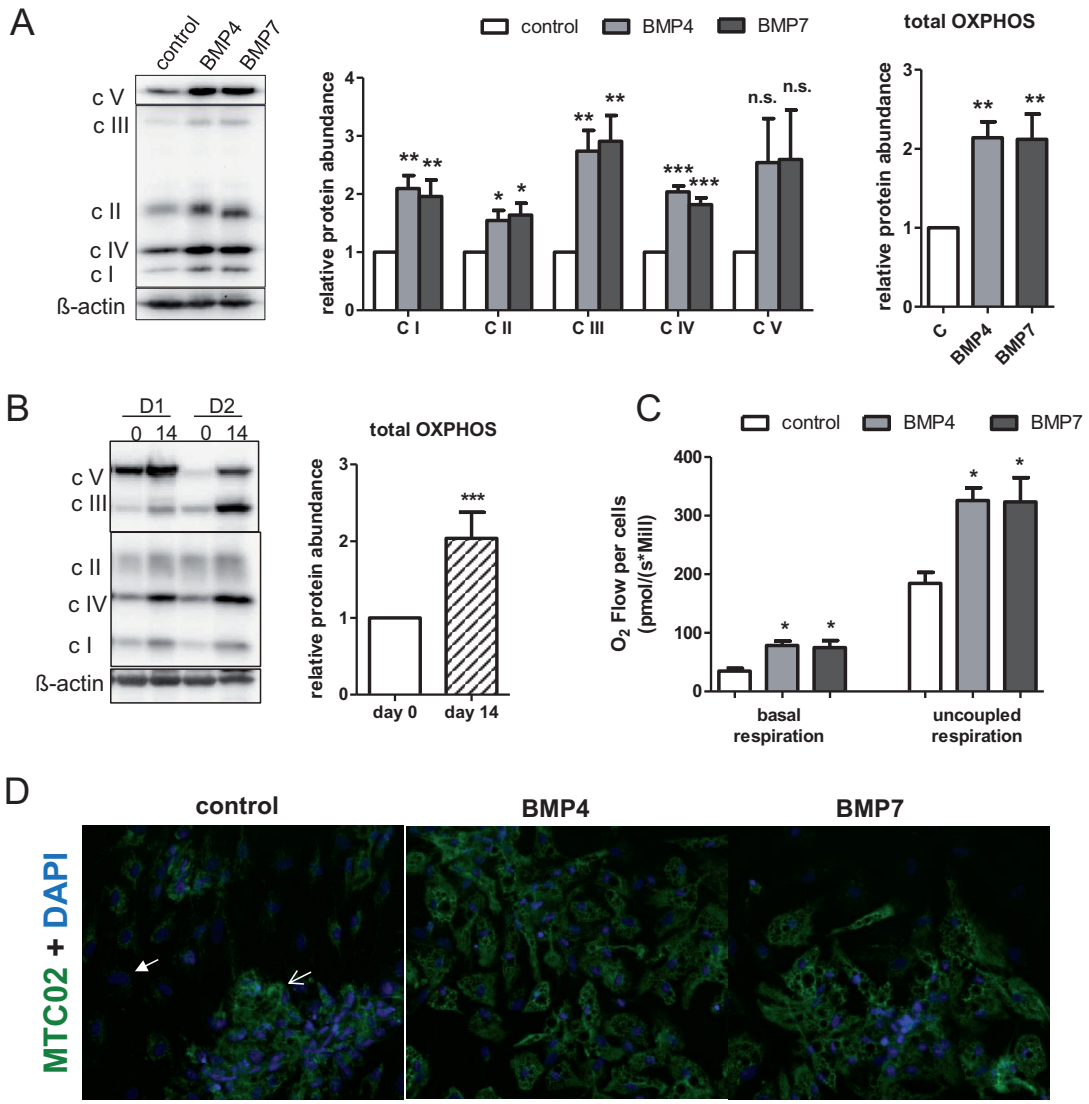

Figure 5: Mitochondrial content and function in differentiated hASCs is not increased by BMP4 and BMP7*. hASCs from different donors were induced for adipogenic differentiation under standard conditions or with the addition of recombinant human BMP4 or BMP7 (50 ng/ml). Medium and recombinant BMP4 and BMP7 were replaced every 2-3 days. (A) On day 14 of differentiation cells were lysed and analyzed for OXPHOS complexes by immunoblot with a commercially available OXPHOS antibody cocktail. BMP4 and BMP7 increased protein levels of the single complexes and of OXPHOS complexes in total. Results are normalized to ß-actin protein levels and expressed relative to control. Data are mean values ± SEM, n=9, ***p<0.001, **p<0.01, *p<0.05. Representative blots are shown. (B) OXPHOS complexes in differentiated hASCs (days 14) in comparison to undifferentiated hASCs (day 0). Results are normalized to ß-actin and expressed relative to day 0. Data are mean values ± SEM, n=5-6 *p<0.05. Representative blots are shown. (C) Basal and uncoupled respiration was measured in differentiated hASC at day 14. Data are mean values ± SEM, n=4, *p<0.05 vs. control. (D) Immunofluorescene staining against mitochondrial marker MTC02 (green) and staining of nuclei with DAPI (blue) in hASCs differentiated under control conditions and challenged with BMP4 or BMP7. MTC02 abundance is higher in differentiated hASCs (opened arrowhead) in comparison to non-differentiated hASCs (closed arrowhead).*

Discussion

A large number of adipokines act on adipose tissue in an auto-/paracrine manner and exert endocrine effects (7; 34). Here we show that BMP4 is a novel adipokine secreted from hASCs. BMP4 is expressed and secreted from proliferating A33 cells, which is an adipogenic subline of the pluripotent 10T1/2 cell line (2). Furthermore, BMP4 mRNA is induced in human preadipocytes undergoing differentiation. The inhibition of adipogenic differentiation by the BMP4 inhibitor noggin strongly suggests a paracrine function for BMP4 in adipogenesis (9). Our results confirm that BMP4 is secreted from differentiated hASC and promotes adipogenic differentiation of hASCs. It should be noted, that we observed secretion of a 47 kDa BMP4 peptide, corresponding to the uncleaved propeptide of BMP4. BMPs are described to be fully processed to their mature form before secretion (26). However, BMP4 and other BMP members can form complexes with their prodomains after cleavage and be secreted in this form (3). Since we were not able to show BMP7 secretion, BMP7 does probably not act on adipogenesis in an auto-/paracrine manner. In line with our findings, BMP4 and BMP7 increased lipid accumulation in murine brown preadipocytes (37) and BMP7 promoted adipogenesis of human preadipocytes derived from WAT (27).

Besides the effect of BMP4 and BMP7 on adipogenic differentiation of hASCs, we observed gene expression patterns which have been described for brite adipocytes (19; 20). *TCF21* has been described as a white-specific marker gene, which is downregulated in white murine preadipocytes chronically challenged with rosiglitazone triggering functional features of brown adipocytes (19). We observed reduced expression of *TCF21* in hASCs treated with BMP4 and BMP7. Importantly, *TCF21* was a marker independent of differentiation in our model system. However, *UCP1* mRNA expression was differentiation-dependent and is upregulated in mature adipocytes (12; 19; 27). This raises the question whether the observed increase of *UCP1* expression induced by BMP4 and BMP7 is solely related to the BMP4 and BMP7 mediated promotion of adipogenic differentiation. Nevertheless, the BMP4 and BMP7 induced increase of *UCP1* mRNA (6.2 and 7.7 fold, respectively) was higher than their effect on differentiation, as determined by lipid accumulation (2.5 and 2.6 fold, respectively) and *PPARγ* mRNA level (4.2 and 4.1 fold, respectively). Thus, increased expression levels of *UCP1* together with decreased expression levels of the differentiation-independent marker *TCF21* indicate a white-to-brown switch of hASCs challenged with BMP4 and BMP7. A previous study in primary human preadipocytes derived from the subcutaneous depot, showed similar effects of BMP7 on *UCP1* and a differentiation marker. Furthermore, this study provided evidence that the subcutaneous depot in mouse and human AT displays the highest capacity to undergo a white-to-brown transition (27). All hASCs used for this study were isolated from the subcutaneous AT.

An interesting observation of this study was the variable ability of different donors to induce *UCP1* expression in response to BMP4/7. Recently, the cell surface protein CD137 has been described as a new brite-selective marker gene in mice. CD137-selected murine preadipocytes displayed elevated expression levels of *UCP1* and a higher ability to induce a brite phenotype in response to the recently described hormone irisin (42). We detected a stronger potential to induce *UCP1* expression in response to BMP4/7 in those donors highly expressing *CD137*. Thus, *CD137* might also be a marker for brite precursor cells in humans. However, the comparability between mouse and human AT depots is currently puzzling. Wu and colleagues suggested, that brown AT from the adult human consists of brite adipocytes rather than of classical brown adipocytes derived from a myogenic origin (42). However, recent studies provided evidence for the existence of classical brown AT in humans (5; 11; 13), indicating that human brown AT is composed of brite and classical brown adipocytes. It should be noted that active brown AT cannot be found in all humans and decreases with increasing BMI (23; 38; 43). Vice versa, brown AT can be recruited in humans and morbidly obese patients negative for brown AT became brown AT-positive after weight loss. Interestingly, not all patients were able to recruit brown AT (39). In line with that, our results indicate, that not all individuals might have the ability to induce thermogenically active adipocytes. To counteract human obesity by targeting brown/brite AT, it is of importance to identify the developmental origins of these tissues in humans and to identify markers which label cells capable to induce thermogenically active adipocytes.

Assessment of white-to-brown transition solely based on *UCP1* expression without any functional readout is critical, since expression of *UCP1* mRNA does not necessarily lead to increased energy dissipation (17). To strengthen this study we analyzed mitochondrial biogenesis and function, which are enhanced in brite adipocytes. Increased mitochondrial biogenesis can be induced in human adipocytes by certain stimuli, such as CNPs (1), T3 (12) and PPARγ agonists (8; 20).

Here, we found that BMP4 and BMP7 upregulate OXPHOS complexes in hASCs. This effect probably reflects the increased differentiation induced by BMP4 and BMP7, since mitochondrial content is upregulated during differentiation of 3T3-L1 adipocytes (41), rat adipocytes (14) and also in our human cell model. Immunofluorescence staining for MCT02 confirmed that there is no difference in MCT02 abundance between the differentiated lipid-loaden hASCs treated with and without BMP4/7. The increased oxygen consumption in BMP4/7 challenged hASCs can therefore also be related to the differentiation effect of the BMPs. Mitochondrial biogenesis in AT is mainly controlled by members of the PGC-1 family (24). Of note, *PGC-1β*, but not *PGC-1α* was upregulated in differentiated hASCs by BMP4/7 treatment. In line with that, PGC-1β has been proposed to be involved in general mitochondrial biogenesis in white AT, while PGC-1α plays a role in brown AT mitochondrial function (18). Nevertheless, BMP7 is able to enhance mitochondrial biogenesis in murine brown preadipocytes accompanied by increased *PGC-1α* expression (37) and overexpression of BMP4 in murine white AT increased *PGC-1α* mRNA levels and mitochondriogenesis (21). Thus, BMP4 and BMP7 can affect mitochondrial biogenesis in murine models, but were not able to increase brown-related mitochondrial biogenesis in our human cell model. To our knowledge, there are no reports on the role of BMP4 and BMP7 on mitochondria in primary human adipocytes. Taken together, we showed here that BMP4 and BMP7 induce a brite gene expression pattern in hASCs, but do not induce a full white-to-brown transition with increased mitochondrial function. AT plasticity is a complex scenario and other AT-derived factors may be necessary to synergize with BMP4 and BMP7 to induce complete browning in human white AT.

Our findings differ from the current view of BMP4 as a player in white adipogenesis and BMP7 as promoter of brown adipogenesis (16; 28; 37). Importantly, this view is based on different studies using different cell model systems (murine vs. human; brown AT vs. white AT) and the effects of BMP4 and BMP7 have been compared only in a few cases. In the study by Tseng et al. (2008) (37), BMP4 and BMP7 had the same effect on lipid accumulation in murine brown preadipocytes, but only BMP7 was able to significantly induce *UCP1* expression whereas BMP4 suppressed expression of *UCP1* in these brown preadipocytes. The induction of *UCP1* mRNA expression by BMP7 has also been shown in primary human preadipocytes derived from subcutaneous AT. But a longer treatment with BMP7 was necessary to induce browning in human preadipocytes than in murine preadipocytes and the effect on *UCP1* expression was less strong (27). Furthermore, only a slight effect of BMP7 on UCP1 expression has been observed in human multipotent adipose-derived stem cells (20). We also show a slight effect of BMP7 on *UCP1* expression and no enhancement of mitochondrial biogenesis, suggesting a lower potency of BMP7 to induce browning in human preadipocytes compared to murine cells. Moreover, BMP4 did not suppress *UCP1* expression in hASCs, but exerted similar effects as BMP7 on all aspects of white-to-brown transition in primary hASCs. The inhibitory effect of BMP4 on brown adipogenesis, as shown in murine brown preadipocytes (37), has never been investigated in human white preadipocytes. Furthermore, there was recent evidence that BMP4 plays a different role in white and brown AT. In transgenic mice with AT-specific overexpression of *BMP4*, mRNA levels of *UCP1* and the key factors of brown adipogenesis *PGC-1α* and *PRDM16* were strongly increased in white AT, while the expression of these genes were decreased in brown AT (21). The myokine irisin is another example uncovering differences between mice and humans. While irisin induced browning in murine preadipocytes derived from white AT (42), we recently showed that irisin has no effect on white-to-brown transition in human white preadipocytes (22). Comparing our results with these previous studies supports the idea, that there are discrepancies of the action of BMPs between human vs. murine models and white vs. brown AT precursor cell origin (summarized in Figure 6). Additionally, AT plasticity is a complex scenario and rather a cocktail of factors than BMP4 and BMP7 alone may be necessary to induce a complete white-to-brown transition in human white AT.

Given this and taking into account, that BMP signaling is dependent on the receptor composition, the presence of ligands and extracellular antagonists (3), it is likely that BMP4 and BMP7 might have a similar effect on precursor cells derived from white AT but play a differential role in brown precursor cells. In addition, BMP4 and BMP7 may be more potent inducers of browning in mice than in humans. Furthermore, we here show that BMP4 is a new adipokine and acts on adipogenesis and white-to-brown transition in an auto-/paracrine manner. It has been shown recently, that *BMP4* expression is higher in WAT from lean compared to obese humans (21). Therefore, BMP4 represents a potential target in the fight against obesity and its regulation in states of AT inflammation, should

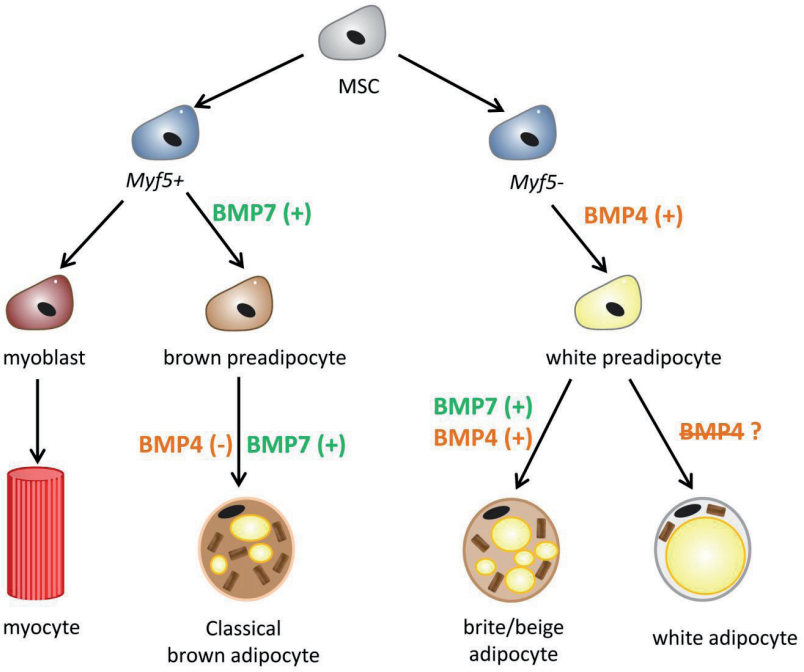

BMP member	Mouse		Human	
	White preadipocyte	brown preadipocyte	White preadipocyte	Brown preadipocyte
BMP4	UCP1 ↑ (Qian et al. 2013)	UCP1 ↓ (Qian et al. 2013)	UCP1↑ (Figure 3)	-
BMP7	UCP1 ↑ (Schulz et al. 2011)	UCP1 ↑ (Tseng et al. 2008)	UCP1↑ (Figure 3) UCP1↑ (Schulz et al. 2011) UCP1↗ (Pisani et al. 2011)	-

Figure 6: The effect of BMP4 and BMP7 on AT precursor cells is dependent on the AT depot and species. *BMP4 and BMP7 are able to induce UCP1 in murine and human white preadipocytes. In brown preadipocytes/AT, exclusively BMP7 promotes brown adipogenesis, while BMP4 suppresses UCP1 expression. Comparing murine and human models, BMP4 and BMP7 show a stronger effect on browning in murine model systems. ↗ slight UCP1 upregulation, ↑ strong UCP1 upregulation.*

be addressed in further studies. Finally, our results indicate that not all donors have the ability to strongly induce *UCP1* in response to BMP4/7 and this feature was related to *CD137* expression. To promote white-to-brown transition of human white AT as a therapeutic approach, it is essential to know which cells can be targeted. Thus, markers labeling human cells which possess a high potential to undergo browning should be investigated.

Acknowledgements

We thank J. Liebau (Department of Plastic Surgery, Florence-Nightingale-Hospital, Düsseldorf, Germany) and C. Andree (Department of Plastic Surgery, Sana-Hospital, Düsseldorf-Gerresheim, Germany) for support in obtaining AT samples. The secretarial assistance of B. Hurow and the technical help of A. Cramer, M. Esser, I. Rokitta, S. Kauffelt and A. Schlüter are gratefully acknowledged.

Grants

This work was supported by the Ministerium für Wissenschaft und Forschung des Landes Nordrhein-Westfalen (Ministry of Science and Research of the State of North Rhine-Westphalia), the Bundesministerium für Gesundheit (Federal Ministry of Health). TR is the recipient of a FP7 Marie Curie Intra-European fellowship. This study was supported in part by a grant from the German Federal Ministry of Education and Research (BMBF) to the German Center for Diabetes Research (DZD e.V.) and the European Foundation for the Study of Diabetes (EFSD).

Disclosure

The authors declare no conflict of interest.

Author contributions

M.E., S.R., T.R. and T.J. performed experiments; M.E., S.R. and U.S. analyzed experiments; M.E., S.R., N.T., T.R. and J.E. interpreted results of experiments; M.E. prepared figures; M.E. and J.E. drafted manuscript; M.E., S.R., N.T., U.S., T.J., M.R., T.R. and J.E. edited and revised the manuscript; M.E., S.R., N.T., U.S., T.J., M.R., T.R. and J.E. approved final version of manuscript; M.E., T.R. and J.E. conception and design of research.

Reference List

1. Bordicchia M, Liu D, Amri EZ, Ailhaud G, Dessi-Fulgheri P, Zhang C, Takahashi N, Sarzani R and Collins S. Cardiac natriuretic peptides act via p38 MAPK to induce the brown fat thermogenic program in mouse and human adipocytes. Journal of Clinical Investigation 122: 1022-1036, 2012.

2. Bowers RR, Kim JW, Otto TC and Lane MD. Stable stem cell commitment to the adipocyte lineage by inhibition of DNA methylation: Role of the BMP-4 gene. Proceedings of the National Academy of Sciences of the United States of America 103: 13022-13027, 2006.

3. Bragdon B, Moseychuk O, Saldanha S, King D, Julian J and Nohe A. Bone Morphogenetic Proteins: A critical review. Cellular Signalling 23: 609-620, 2011.

4. Cypess AM, Lehman S, Williams G, Tal I, Rodman D, Goldfine AB, Kuo FC, Palmer EL, Tseng YH, Doria A, Kolodny GM and Kahn CR. Identification and importance of brown adipose tissue in adult humans. N Engl J Med 360: 1509-1517, 2009.

5. Cypess AM, White AP, Vernochet C, Schulz TJ, Xue R, Sass CA, Huang TL, Roberts-Toler C, Weiner LS, Sze C, Chacko AT, Deschamps LN, Herder LM, Truchan N, Glasgow AL, Holman AR, Gavrila A, Hasselgren PO, Mori MA, Molla M and Tseng YH. Anatomical localization, gene expression profiling and functional characterization of adult human neck brown fat. Nat Med 19: 635-639, 2013.

6. Dietze-Schroeder D, Sell H, Uhlig M, Koenen M and Eckel J. Autocrine action of adiponectin on human fat cells prevents the release of insulin resistance-inducing factors. Diabetes 54: 2003-2011, 2005.

7. Eckardt K, Sell H and Eckel J. Novel aspects of adipocyte-induced skeletal muscle insulin resistance. Arch Physiol Biochem 114: 287-298, 2008.

8. Elabd C, Chiellini C, Carmona M, Galitzky J, Cochet O, Petersen R, Penicaud L, Kristiansen K, Bouloumie A, Casteilla L, Dani C, Ailhaud G and Amri EZ. Human Multipotent Adipose-Derived Stem Cells Differentiate into Functional Brown Adipocytes. Stem Cells 27: 2753-2760, 2009.

9. Gustafson B and Smith U. The WNT Inhibitor Dickkopf 1 and Bone Morphogenetic Protein 4 Rescue Adipogenesis in Hypertrophic Obesity in Humans. Diabetes 61: 2012.

10. Huang HY, Song TJ, Li X, Hu LL, He Q, Liu M, Lane MD and Tang QQ. BMP signaling pathway is required for commitment of C3H10T1/2 pluripotent stem cells to the adipocyte lineage. Proceedings of the National Academy of Sciences of the United States of America 106: 12670-12675, 2009.

11. Jespersen NZ, Larsen TJ, Peijs L, Daugaard S, Homoe P, Loft A, de JJ, Mathur N, Cannon B, Nedergaard J, Pedersen BK, Moller K and Scheele C. A classical brown adipose tissue mRNA signature partly overlaps with brite in the supraclavicular region of adult humans. Cell Metab 17: 798-805, 2013.

12. Lee JY, Takahashi N, Yasubuchi M, Kim YI, Hashizaki H, Kim MJ, Sakamoto T, Goto T and Kawada T. Triiodothyronine induces UCP-1 expression and mitochondrial biogenesis in human adipocytes. American Journal of Physiology-Cell Physiology 302: C463-C472, 2012.

13. Lidell ME, Betz MJ, Dahlqvist LO, Heglind M, Elander L, Slawik M, Mussack T, Nilsson D, Romu T, Nuutila P, Virtanen KA, Beuschlein F, Persson A, Borga M and Enerback S. Evidence for two types of brown adipose tissue in humans. Nat Med 19: 631-634, 2013.

14. Lu RH, Ji H, Chang ZG, Su SS and Yang GS. Mitochondrial development and the influence of its dysfunction during rat adipocyte differentiation. Mol Biol Rep 37: 2173-2182, 2010.

15. Luo X, Hutley LJ, Webster JA, Kim YH, Liu DF, Newell FS, Widberg CH, Bachmann A, Turner N, Schmitz-Peiffer C, Prins JB, Yang GS and Whitehead JP. Identification of BMP and Activin Membrane-Bound Inhibitor (BAMBI) as a Potent Negative Regulator of Adipogenesis and Modulator of Autocrine/Paracrine Adipogenic Factors. Diabetes 61: 124-136, 2012.

16. Modica S and Wolfrum C. Bone morphogenic proteins signaling in adipogenesis and energy homeostasis. Biochim Biophys Acta 1831: 915-923, 2013.

17. Nedergaard J and Cannon B. UCP1 mRNA does not produce heat. Biochim Biophys Acta 1831: 943-949, 2013.

18. Pardo R, Enguix N, Lasheras J, Feliu JE, Kralli A and Villena JA. Rosiglitazone-Induced Mitochondrial Biogenesis in White Adipose Tissue Is Independent of Peroxisome Proliferator-Activated Receptor gamma Coactivator-1 alpha. Plos One 6: 2011.

19. Petrovic N, Walden TB, Shabalina IG, Timmons JA, Cannon B and Nedergaard J. Chronic Peroxisome Proliferator-activated Receptor gamma (PPAR gamma) Activation of Epididymally Derived White Adipocyte Cultures Reveals a Population of Thermogenically Competent, UCP1-containing Adipocytes Molecularly Distinct from Classic Brown Adipocytes. Journal of Biological Chemistry 285: 7153-7164, 2010.

20. Pisani DF, Djedaini M, Beranger GE, Elabd C, Scheideler M, Ailhaud G and Amri EZ. Differentiation of Human Adipose-Derived Stem Cells into „Brite“ (Brown-in-White) Adipocytes. Front Endocrinol (Lausanne) 2: 87, 2011.

21. Qian SW, Tang Y, Li X, Liu Y, Zhang YY, Huang HY, Xue RD, Yu HY, Guo L, Gao HD, Liu Y, Sun X, Li YM, Jia WP and Tang QQ. BMP4-mediated brown fat-like changes in white adipose tissue alter glucose and energy homeostasis. Proc Natl Acad Sci U S A 2013.

22. Raschke S, Elsen M, Gassenhuber H, Sommerfeld M, Schwahn U, Brockmann B, Jung R, Wisloff U, Tjonna AE, Raastad T, Hallen J, Norheim F, Drevon CA, Romacho T, Eckardt K and Eckel J. Evidence against a beneficial effect of irisin in humans. Plos One 2013.

23. Saito M, Okamatsu-Ogura Y, Matsushita M, Watanabe K, Yoneshiro T, Nio-Kobayashi J, Iwanaga T, Miyagawa M, Kameya T, Nakada K, Kawai Y and Tsujisaki M. High incidence of metabolically active brown adipose tissue in healthy adult humans: effects of cold exposure and adiposity. Diabetes 58: 1526-1531, 2009.

24. Scarpulla RC. Metabolic control of mitochondrial biogenesis through the PGC-1 family regulatory network. Biochim Biophys Acta 1813: 1269-1278, 2011.

25. Scarpulla RC, Vega RB and Kelly DP. Transcriptional integration of mitochondrial biogenesis. Trends Endocrinol Metab 23: 459-466, 2012.

26. Schmierer B and Hill CS. TGFbeta-SMAD signal transduction: molecular specificity and functional flexibility. Nat Rev Mol Cell Biol 8: 970-982, 2007.

27. Schulz TJ, Huang TL, Tran TT, Zhang H, Townsend KL, Shadrach JL, Cerletti M, McDougall LE, Giorgadze N, Tchkonia T, Schrier D, Falb D, Kirkland JL, Wagers AJ and Tseng YH. Identification of inducible brown adipocyte progenitors residing in skeletal muscle and white fat. Proc Natl Acad Sci U S A 108: 143-148, 2011.

28. Schulz TJ and Tseng YH. Emerging role of bone morphogenetic proteins in adipogenesis and energy metabolism. Cytokine & Growth Factor Reviews 20: 523-531, 2009.

29. Seale P, Bjork B, Yang W, Kajimura S, Chin S, Kuang S, Scime A, Devarakonda S, Conroe HM, Erdjument-Bromage H, Tempst P, Rudnicki MA, Beier DR and Spiegelman BM. PRDM16 controls a brown fat/skeletal muscle switch. Nature 454: 961-967, 2008.

30. Seale P, Kajimura S, Yang W, Chin S, Rohas LM, Uldry M, Tavernier G, Langin D and Spiegelman BM. Transcriptional control of brown fat determination by PRDM16. Cell Metabolism 6: 38-54, 2007.

31. Smorlesi A, Frontini A, Giordano A and Cinti S. The adipose organ: white-brown adipocyte plasticity and metabolic inflammation. Obes Rev 13 Suppl 2: 83-96, 2012.

32. Stephens M, Ludgate M and Rees DA. Brown fat and obesity: the next big thing? Clinical Endocrinology 74: 661-670, 2011.

33. Tang QQ, Otto TC and Lane MD. Commitment of C3H10T1/2 pluripotent stem cells to the adipocyte lineage. Proceedings of the National Academy of Sciences of the United States of America 101: 9607-9611, 2004.

34. Taube A, Schlich R, Sell H, Eckardt K and Eckel J. Inflammation and metabolic dysfunction: links to cardiovascular diseases. Am J Physiol Heart Circ Physiol 302: H2148-H2165, 2012.

35. Timmons JA, Wennmalm K, Larsson O, Walden TB, Lassmann T, Petrovic N, Hamilton DL, Gimeno RE, Wahlestedt C, Baar K, Nedergaard J and Cannon B. Myogenic gene expression signature establishes that brown and white adipocytes originate from distinct cell lineages. Proc Natl Acad Sci U S A 104: 4401-4406, 2007.

36. Townsend KL, Suzuki R, Huang TL, Jing E, Schulz TJ, Lee K, Taniguchi CM, Espinoza DO, McDougall LE, Zhang H, He TC, Kokkotou E and Tseng YH. Bone morphogenetic protein 7 (BMP7) reverses obesity and regulates appetite through a central mTOR pathway. Faseb Journal 26: 2012.

37. Tseng YH, Kokkotou E, Schulz TJ, Huang TL, Winnay JN, Taniguchi CM, Tran TT, Suzuki R, Espinoza DO, Yamamoto Y, Ahrens MJ, Dudley AT, Norris AW, Kulkarni RN and Kahn CR. New role of bone morphogenetic protein 7 in brown adipogenesis and energy expenditure. Nature 454: 1000-1004, 2008.

38. van Marken Lichtenbelt WD, Vanhommerig JW, Smulders NM, Drossaerts JM, Kemerink GJ, Bouvy ND, Schrauwen P and Teule GJ. Cold-activated brown adipose tissue in healthy men. N Engl J Med 360: 1500-1508, 2009.

39. Vijgen GH, Bouvy ND, Teule GJ, Brans B, Hoeks J, Schrauwen P and van Marken Lichtenbelt WD. Increase in brown adipose tissue activity after weight loss in morbidly obese subjects. J Clin Endocrinol Metab 97: E1229-E1233, 2012.

40. Virtanen KA, Lidell ME, Orava J, Heglind M, Westergren R, Niemi T, Taittonen M, Laine J, Savisto NJ, Enerback S and Nuutila P. Brief Report: Functional

Brown Adipose Tissue in Healthy Adults. New England Journal of Medicine 360: 1518-1525, 2009.

41. Wilson-Fritch L, Burkart A, Bell G, Mendelson K, Leszyk J, Nicoloro S, Czech M and Corvera S. Mitochondrial biogenesis and remodeling during adipogenesis and in response to the insulin sensitizer rosiglitazone. Mol Cell Biol 23: 1085-1094, 2003.

42. Wu J, Bostrom P, Sparks LM, Ye L, Choi JH, Giang AH, Khandekar M, Virtanen KA, Nuutila P, Schaart G, Huang K, Tu H, Lichtenbelt WD, Hoeks J, Enerbaeck S, Schrauwen P and Spiegelman BM. Beige Adipocytes Are a Distinct Type of Thermogenic Fat Cell in Mouse and Human. Cell 150: 2012.

43. Zingaretti MC, Crosta F, Vitali A, Guerrieri M, Frontini A, Cannon B, Nedergaard J and Cinti S. The presence of UCP1 demonstrates that metabolically active adipose tissue in the neck of adult humans truly represents brown adipose tissue. FASEB J 23: 3113-3120, 2009.

Eicosapentaenoic acid and arachidonic acid differentially regulate white-to-brown conversion and mitochondrial function in primary human adipocytes

Manuela Fleckenstein-Elsen[1], Daniela Dinnies[1], Tomas Jelenik[2], Michael Roden[2,3], Tania Romacho[1], Jürgen Eckel[1]

[1]*Paul-Langerhans-Group for Integrative Physiology, German Diabetes Center, Düsseldorf, Germany*
[2]*Institute for Clinical Diabetology, German Diabetes Center, Düsseldorf, Germany*
[3]*Department of Endocrinology and Diabetology, Medical Faculty, Heinrich-Heine University Düsseldorf, Germany*

Abstract

Background/Objectives: Promoting the induction of UCP1-expressing brown-like (brite/beige) adipocytes within white adipose tissue (WAT) may increase energy expenditure and represent a strategy to counteract obesity. Long-chain polyunsaturated fatty acids (LC-PUFAs) from the n-3 family exert beneficial effects on WAT oxidative metabolism and may impact white-to-brown conversion of adipocytes. Since serum n-3/n-6 LC-PUFA ratios are decreased in obese and type 2 diabetic subjects, we aimed to compare the effect of n-3 and n-6 LC-PUFAs on white-to-brown conversion in human adipocytes.

Subjects/Methods: Primary human adipose-derived stem cells (hASCs) isolated from the subcutaneous depot of different female donors were exposed to 20 μM of the n-3 PUFAs eicosapentaenoic acid (EPA) and docosahexaenoic acid (DHA), arachidonic acid (ARA,n-6) and oleic acid (OA,n-9) during adipocyte differentiation (12 days) or from day 8 to 12 of differentiation. A potential white-to-brown conversion was assessed on the molecular and functional level.

Results: Treatment of hASCs during adipogenesis with EPA, DHA and ARA increased adipocyte differentiation. Exclusively EPA upregulated *UCP1* and *CPT1B* mRNA expression, along with increased citrate synthase activity and maximal cellular respiration. ARA had no effect on brite marker genes, but increased mRNA expression of the white-specific marker *TCF21*, led to enlarged lipid droplets and decreased spare respiratory capacity in hASCs. The beneficial effects of EPA on *UCP1* and *CPT1B* expression were abrogated when hASCs were exposed to combined EPA and ARA (ratio 1:2). Moreover, EPA even triggered brite gene expression in hASCs when applied from day 8 to 12 of differentiation.

Conclusion: EPA induces browning of primary hASCs, providing a novel mechanism for the anti-obesity effects of dietary n-3 LC-PUFAs. Moreover, we observed a divergent regulation of brite and white adipogenesis by EPA and ARA, indicating that the low EPA/ARA ratios in plasma of obese patients may even enhance the progression of obesity and associated disorders.

Keywords: Polyunsaturated fatty acids, bone morphogenetic protein 4, adipogenesis, brite adipocyte, mitochondrial function

Introduction

Obesity is a major global health problem resulting from excess energy intake. The adipose organ, consisting of two functionally different types, plays an important role in the regulation of energy homeostasis. Excess energy is stored as lipids in white adipose tissue (WAT), while brown adipose tissue (BAT) maintains body core temperature by producing heat in a process called non-shivering thermogenesis (NST) (1). This unique function of brown adipocytes is due to a high density of mitochondria, containing uncoupling-protein 1 (UCP1) in the inner mitochondrial membrane. During cold exposure, sympathetic neurons activate brown adipocytes, which in turn oxidize stored lipids and produce heat by UCP1-mediated uncoupling of ATP synthesis (2). Recent studies showed that brown adipocytes derive from *Myf-5* positive myogenic precursor cells, distinct from that of white adipocytes (3;4). In addition to these classical brown adipocytes,

brite (brown-in-white) or beige adipocytes have been described as second type of *UCP1*-expressing adipocytes, not derived from the myogenic lineage (5). In mice, brite adipocytes appear in WAT depots in response to a cold environment (6) or can be induced by several pharmacological and hormonal stimuli (7). Increasing the abundance of classical brown or brite adipocytes might augment energy expenditure and represent potential strategies to fight obesity. Importantly, this may also be of high relevance in humans, since active BAT (8-12) and both classical brown and brite adipocytes are present in adult humans (13-15).

Besides pharmacological and hormonal stimulation, nutritional factors such as long-chain polyunsaturated fatty acids (LC-PUFAs) may also affect white-to-brown conversion of adipose tissue (16). LC-PUFAs from the n-3 and n-6 family possess several opposing biological functions. In particular, the n-3 LC-PUFAs eicosapentaenoic acid (EPA, 20:5n-3) and docosahexaenoic acid (DHA, 22:6n-3) exert anti-obesity effects (17;18), potentially resulting from increased oxidative metabolism in WAT (19). In contrast, the n-6 LC-PUFA arachidonic acid (ARA, 20:4n-6) is discussed to promote the development of obesity (20). EPA and ARA are both substrates for cyclooxygenase type 1 (COX1) and type 2 (COX2), giving rise to different series of prostaglandins which partly mediate the divergent effects of EPA and ARA (17). Interestingly, it has recently been shown that COX2 is involved in the regulation of cold-induced white-to-brown conversion in mice (21).

The effects of n-3 LC-PUFAs on WAT oxidative metabolism, as well as the role of COX2 in WAT browning suggest an impact of LC-PUFAs on brite and white adipogenesis. However, the effect of n-3 and n-6 LC-PUFAs on WAT browning in humans remains unclear. This may be of substantial relevance, since plasma EPA/ARA ratios have been found to be decreased in obese and type 2 diabetic subjects (22;23). Therefore, the aim of this study was to compare the effects of specific n-3 and n-6 LC-PUFAs on brite adipogenesis in primary human adipose-derived stem cells (hASCs). Herein, we found a differential regulation of white versus brite adipogenesis by the n-3 member EPA and the n-6 member ARA. Moreover, EPA can even trigger white-to-brite conversion at a late stage of adipocyte differentiation. Our results highlight the importance of a balanced EPA/ARA ratio in diet for adipose tissue functionality and energy homeostasis, and contribute to explain the association of a high n-6 intake with obesity and type 2 diabetes.

Materials & Methods

Isolation and culture of primary hASCs

Subcutaneous AT (from the abdominal and mammary region) was obtained from healthy lean or moderately overweight women undergoing plastic surgery. The procedure was approved by the ethics board of Heinrich-Heine-University, Düsseldorf, Germany. hASCs were isolated by collagenase digestion of AT as previously described by our group (24). Isolated cell pellets were resuspended in adipocyte basal medium (BM), which was DMEM/F-12 (GIBCO, Grand Island, NY) supplemented with 14 nmol/l NaHCO3, 33 mmol/l biotin and 17 mmol/l D-panthothenic-acid and 10% FCS (GIBCO) at pH 7.4. Cells were maintained at 37°C and 5% CO2. Three days after seeding, hASCs were induced for adipocyte differentiation with a differentiation induction cocktail (BM supplemented with 2.5 % FCS, 100 nmol/l insulin, 1 µmol/l dexamethasone, 0.25 µmol/l troglitazone and 200 µmol/l isobutylmethylxanthine (all from Sigma-Aldrich, St. Louis, MO). At day 7 of differentiation, medium was switched to a maintenance medium without the addition of troglitazone and IBMX. Cells were challenged during the whole differentiation period of 12 days with fatty acids or BMP4 (R&D Systems, Minneapolis, MN) as indicated. Medium and treatments were replaced every 48 hours.

Preparation and handling of fatty acids

Stock and working solutions of EPA, DHA, ARA and OA (all obtained from Sigma-Aldrich) were prepared as previously described by us (25). If not indicated otherwise, hASCs were treated with 20 µM of fatty acids and DMSO/BSA as vehicle (veh) according to the fatty acid concentration used. Fatty acids were replaced freshly every 48 hours to prevent lipid peroxidation.

Neutral red uptake assay

To test the effect of fatty acids on cell vitality, hASCs were seeded in 12-well cell culture plates (100.000 cells/well), treated as indicated and neutral red uptake (NRU) assay was performed as previously described (25). After elution of the neutral red dye, staining was quantified by measuring the absorbance at 540 nm.

Oil Red O Staining

hASCs were cultured in six-well plates and differentiated for 12 days with the indicated treatments and Oil Red O staining was perfomed as described (24). The staining was quantified by dissolving Oil Red O with 100% isopropanol and measuring absorbance at 500 nm.

Nile Red Staining and assessment of lipid droplet size

For microscopy, hASCs were seeded and differentiated on 12 x 12 mm coverslips coated with 0.1 % gelatine. At day 12 of adipocyte differentiation, cells were washed twice with PBS and fixed with 3 % formaldehyde for 15 min at RT. Afterwards, cells were washed 3x for 5 min with PBS and incubated with 10 µg/ml Nile Red dissolved in PBS for 20 min. After washing twice with PBS coverslips were mounted with ProLong Gold Antifade reagent (Life Technologies, Carlsbad, CA). Lipid droplets were analyzed using a Zeiss fluorescence microscope (Oberkochen, Germany) equipped with a Axio Cam MRc5. Five randomly taken images were acquired per condition with AxioVision rel. 4.3 at 40x magnification. Lipid droplet diameter was measured using the Image J software.

Western Blot

Total cellular proteins were extracted and separated by SDS-PAGE as previously described (24). Membranes were probed over night at 4°C with the following primary antibodies: Adiponectin 1:2000 in 5% BSA (Abcam, Cambridge, UK, ab22554), HSL 1:5000 in 5% BSA (Cell signaling, Danvers, MA, #4107), anti-OXPHOS cocktail (Abcam, MS604) diluted 1:1,000, and anti-beta actin (Abcam, ab6276).

Quantitative RT-PCR

Total RNA of hASCs was isolated by using the RNeasy Lipid Tissue kit (Qiagen, Hilden, Germany) according to the manufacturer's protocol. Equal amounts of RNA were reverse transcribed with the Omniscript Reverse Transcription kit (Qiagen) and mRNA expression levels measured by quantitative RT-PCR using SYBR green Master Mix and QuantiTect Primer Assays (Qiagen) as described (24).

Measurement of cellular respiration

For assessment of cellular oxygen consumption rate (OCR), hASCs were plated (10.000 cells/well) in XF96 V3-PS cell culture microplates (Seahorse Bioscience, North Billerica, MA) and started for adipogenic differentiation 2 days after seeding. Prior to the assay, cells were washed twice with assay medium (XF-DMEM containing 17.5 mM D-Glucose, 2 mM sodium pyruvate and 2 mM glutamine) and maintained in 180 µl of assay medium per well for 1h at 37°C without CO2. After 1 h in a CO2-free environment, cellular OCR was measured in the XFe96 flux analyzer (Seahorse Bioscience). After equilibration, basal respiration was measured, followed by injection of several mitochondrial inhibitors (Seahorse Bioscience): ATP synthase inhibitor oligomycin (1 µM), uncoupler FCCP (1 µM) and a cocktail of Antimycin A and Rotenone to block mitochondrial respiration (1 µM each). OCR values were normalized to cell number, which was determined after the assay using the CyQUANT® Cell Proliferation Assay Kit (Life Technologies). Basal OCR and maximal OCR (after injection of FCCP) were corrected for non-mitochondrial respiration (after Antimycin A/Rotenone injection). Spare respiratory capacity, an indicator of metabolic flexibility, was calculated as the quotient of FCCP-induced maximal OCR and basal OCR.

Citrate synthase assay

Total protein was extracted at day 12 of differentiation using the CellLytic MT Lysis Reagent (Sigma-Aldrich, C3228) and citrate synthase activity was measured as indicator of mitochondrial content and function with a commercially available Citrate Synthase (CS) assay kit (Sigma-Aldrich, CS0720) according to the manufacturer's protocol. Total CS activity was measured after the injection of 100 µM oxaloacetate as substrate and normalized to protein content of each sample.

Statistics

Results are expressed as mean ± SEM. One-way ANOVA (post-hoc test: Bonferroni or Dunnett's) was used to determine statistical significances. All statistical analyses were done using GraphPad Prism 5 considering a p-value of less than 0.05 as statistically significant.

Results

Effect of n-3 and n-6 LC-PUFAs on adipocyte differentiation and morphology

LC-PUFAs are prone to lipid peroxidation and DHA has been shown to induce apoptosis in 3T3-L1 preadipocytes (26). Long-term treatment of hASCs with 20 µM of EPA, DHA and ARA did not impair cell vitality (Suppl. figure 1a). LC-PUFAs and their derived mediators, the eicosanoids, are potential ligands for PPARγ and have been reported to play a role in the regulation of 3T3-L1 adipocyte differentiation (27). Here, both, the n-3 LC-PUFAs EPA and DHA, as well as the n-6 LC-PUFA ARA significantly increased lipid accumulation in differentiated hASCs, to a comparable extent as the well-known promotor of adipogenesis BMP4 (28;29) (Figure 1a). Moreover, levels of the adipocyte-specific enzyme hormone sensitive lipase (HSL) were increased after EPA, DHA, ARA and BMP4 treatment (Figure 1b+c). In line with recent studies in mouse (30), rat (31) and human adipocytes (32), only

the n-3 LC-PUFAs EPA and DHA increased adiponectin protein expression in differentiated hASCs (Figure 1b+d). In addition, a shift towards larger lipid droplets and a significant increase of mean lipid droplet diameter was observed in ARA challenged hASCs compared to vehicle (Figure 1e+f). The non-essential monounsaturated fatty acid OA had no effect on any of the investigated aspects of adipocyte differentiation.

Treatment with EPA during differentiation promotes a brite gene expression pattern

Despite similar effects of EPA, DHA (n-3) and ARA (n-6) on parameters of adipocyte differentiation, specific differences of these LC-PUFAs on white and brown marker gene expression were observed. Expression levels of the transcription factors *PPARγ* and *C/EBPα*, which are crucial for white and brown adipogenesis, were increased in hASCs challenged with EPA and DHA, but not with ARA or OA (Figure 2a+b). Interestingly, solely the n-3 LC-PUFA EPA, but not DHA or ARA significantly enhanced *UCP1* and *CPT1B* mRNA expression (Figure 2c+d). In contrast, ARA treatment upregulated expression of the white-specific marker *TCF21* in differentiated hASCs (Figure 2e). Since EPA and ARA are COX2 substrates and COX2 has recently been shown to be involved in ad-

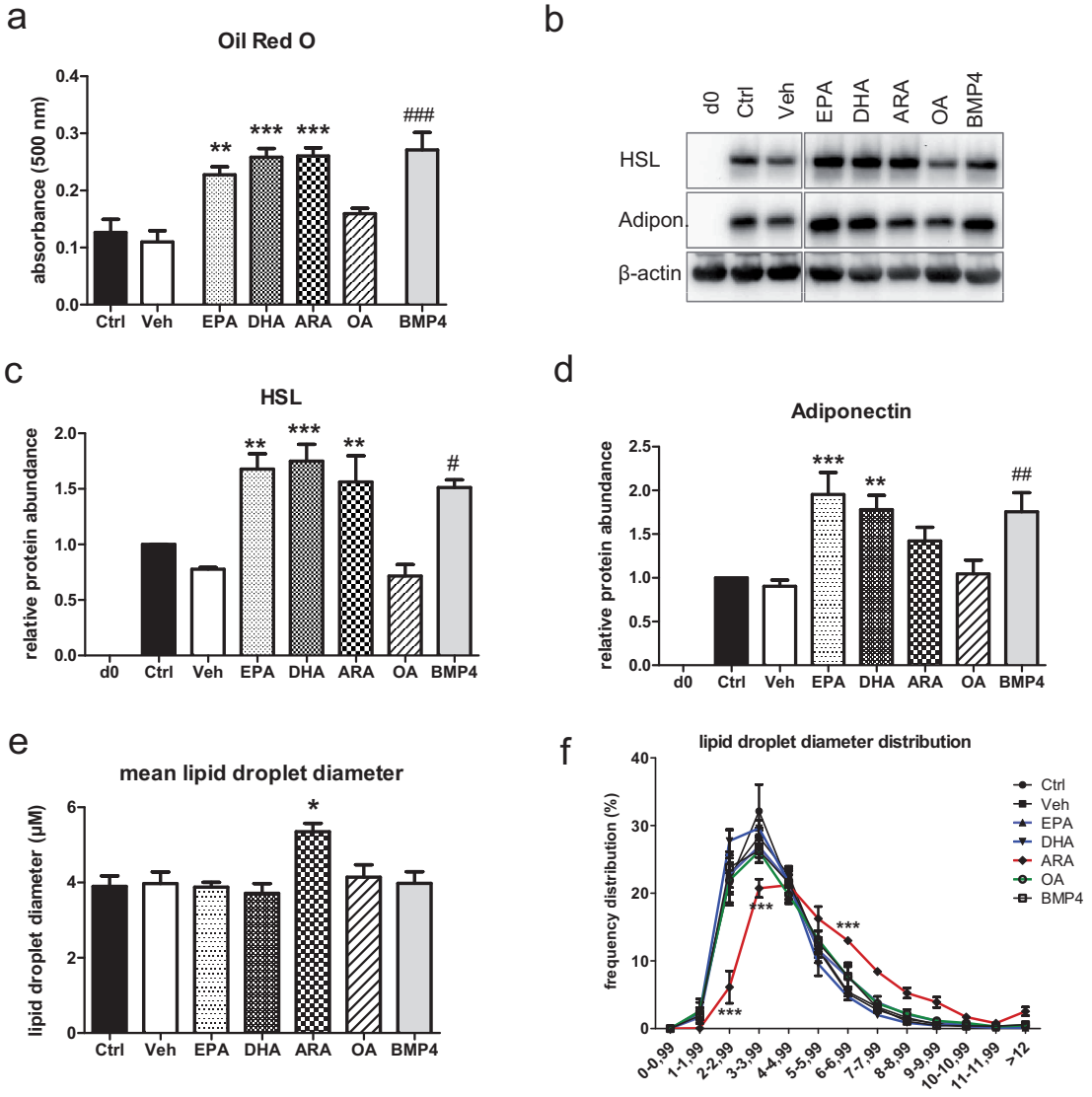

*Figure 1: Effect of LC-PUFAs on adipogenesis and lipid droplet size. hASCs were challenged with the fatty acids EPA, DHA, ARA and OA (20 µM) or BMP4 (50 ng/ml) during the differentiation period of 12 days. (a) Cells were stained with Oil Red O, the dye was extracted with 100% isopropanol and absorbance was measured at 500 nm. Data are mean values ± SEM and expressed relative to control, n=5. (b-d) Protein abundance of HSL (c) and adiponectin (d) was assessed by Western blot. Data are normalized to β-actin protein levels and expressed relative to control (ctrl). Results represent mean values ± SEM, n=6.). Representative Blots are shown top (b) (e+f) Nile Red Staining was performed to assess lipid droplet diameter and 5 randomly taken pictures (40x magnification) were analyzed per treatment. Data represent mean values ± SEM, n=4. *p<0.05, **p<0.01, ***p<0.001 vs. vehicle; #p<0.05, ##p<0.01, ###p<0.001 vs. control.*

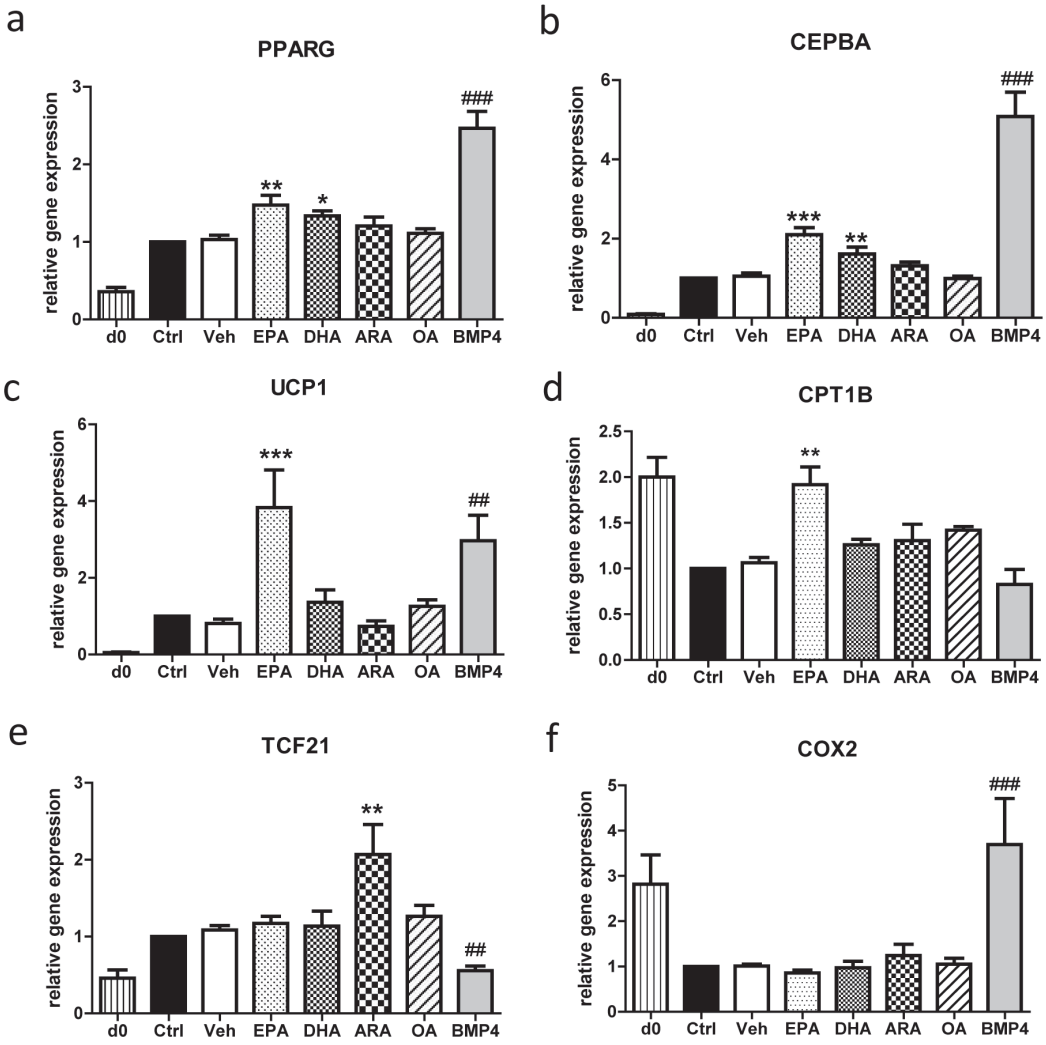

Figure 2: EPA induces a brite gene expression pattern in primary hASCs*. Gene expression of several white and brite marker genes was analyzed in hASCs chronically treated with EPA, DHA, ARA, OA (20 µM each) or BMP4 (50 ng/ml) via qRT-PCR. At day 12 of differentiation, mRNA expression levels of the adipogenic markers PPARG (a), CEPBA (b), UCP1 (c), the mitochondrial fatty acid transporter CPT1B (d), the white-specific marker TCF21 (e) and cyclooxygenase type 2 (COX2) (f) were measured. Expression levels of target genes are normalized to β-actin mRNA levels. Data represent mean values ± SEM and are expressed relative to control, n=7-8. *p<0.05, **p<0.01, ***p<0.001 vs. vehicle; #p<0.05, ##p<0.01, ###p<0.001 vs. control.*

aptive thermogenesis and browning of WAT (21;33), we assessed mRNA expression of this enzyme. *COX2* mRNA levels were not influenced by any of the LC-PUFAs, but were significantly higher in hASCs treated with the browning inducer BMP4 (Figure 2f). Similar to adipogenesis, OA had no effect on white and brown marker gene expression. Taken together, our data indicate that solely EPA induces a brite gene expression program in primary human adipocytes and that ARA rather promotes white adipogenesis.

Effect of EPA, DHA and ARA on mitochondrial function

In order to meet the requirements for thermogenesis, brown and also brite adipocytes have a higher number of mitochondria compared to white adipocytes. Thus, we assessed protein abundance of OXPHOS complexes after LC-PUFA treatment. While total OXPHOS complexes were not altered by any of the fatty acids (Figure 3a), we observed a differential regulation of the single OXPHOS complexes. Complex I showed a trend towards a decrease in ARA treated hASCs and complex IV was significantly downregulated in hASCs challenged with ARA and DHA (Suppl. figure 3b+e). In contrast, EPA increased complex III levels in hASCs, while no difference was observed in complex I and IV protein abundance (Suppl figure 3b-e). Activity of citrate synthase (CS) was measured as an additional indicator of mitochondrial content, and was significantly increased in hASCs exposed to EPA and BMP4. No effect of DHA, ARA and OA on CS activity was observed (Figure 3b).

To further assess mitochondrial bioenergetics, the influence of LC-PUFAs on oxygen consumption rate (OCR) in hASCs was analyzed in real-time. The components of total cellular OCR were determined using specific inhibitors for mitochondrial complexes (Figure 3c). Basal OCR was increased in differentiated hASCs after chronic treatment with all LC-PUFAs, but not after OA exposure. BMP4 and troglitazone, used as additional positive control, increased basal OCR in hASCs as well. Maximal respiration of differentiated hASCs was solely higher in EPA treated cells and in those exposed to BMP4 and troglitazone. Spare respiratory capacity, an indicator of metabolic flexibility, was significantly lower in ARA treated hASCs.

ARA abrogates the EPA-mediated effect on brite gene expression

Besides the total amounts of n-3 and n-6 LC-PUFA intake, it has been debated if rather a certain n-3/n-6 ratio is of importance to prevent metabolic diseases and we observed a differential regulation of brite gene expression by EPA and ARA. Therefore, we tested if EPA/ARA combination (ratio 1:2) could abrogate the EPA-mediated effects on marker gene expression. In-

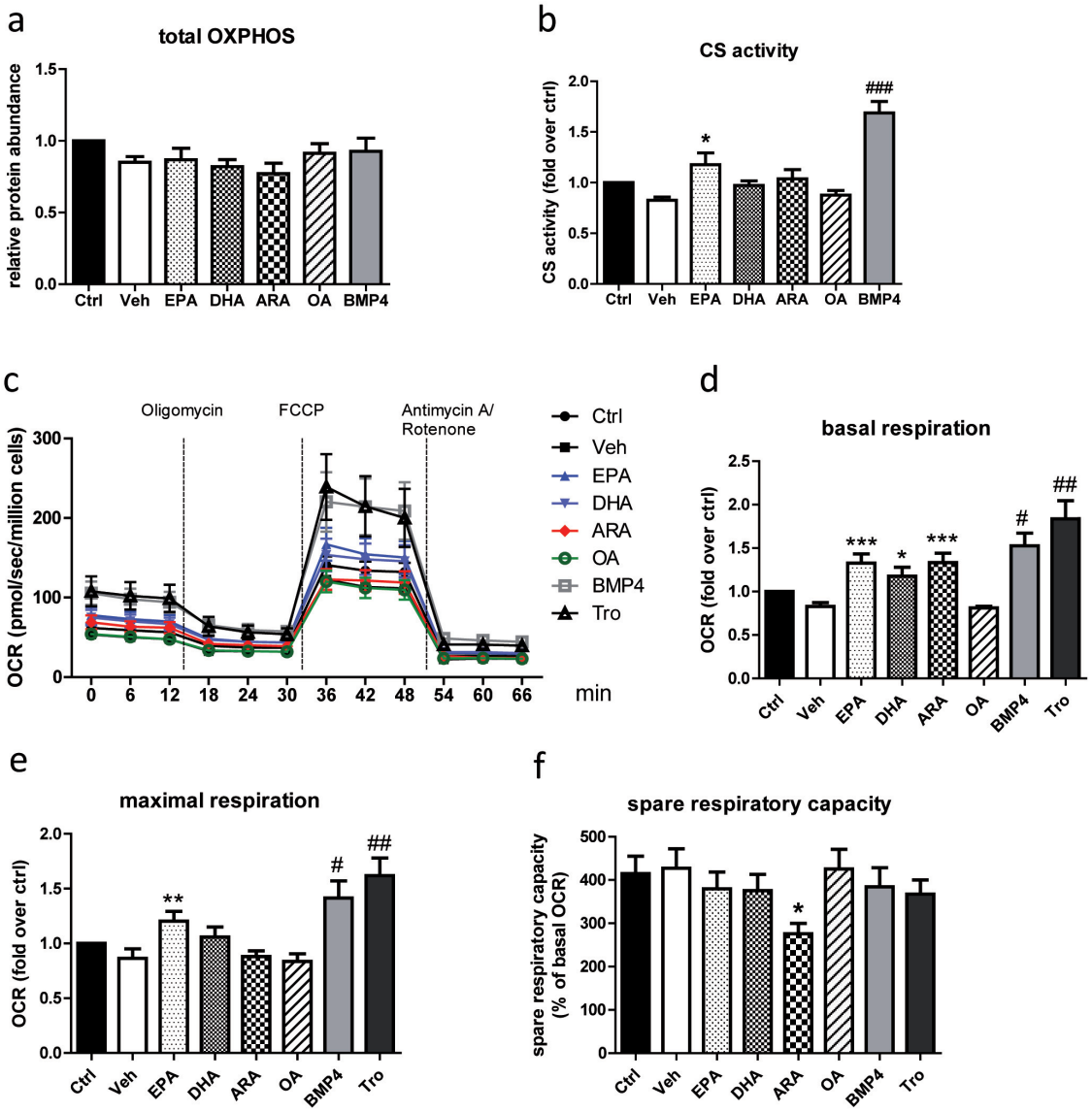

Figure 3: Effect of LC-PUFAs on mitochondrial content and function. *hASCs were challenged with fatty acids (20 µM), BMP4 (50 ng/ml) during the differentiation period of 12 days and several mitochondrial parameters were measured. (a) Protein abundance of total OXPHOS complexes by immunoblot with a commercially available OXPHOS antibody cocktail. Data are normalized to β-actin protein levels and expressed relative to control. Results represent mean values ± SEM, n=6. (b) Citrate Synthase (CS) activity in whole cell lysates. CS activity was normalized to the protein content of each sample. Values are means ± SEM out of n=5 independent experiments and expressed relative to control. (c) Real-time measurement of oxygen consumption rate (OCR), normalized to cell number, at baseline and after injection of different mitochondrial inhibitors. Chronic troglitazone treatment (1 µM) was included as additional positive control. (d-f) Calculations for basal respiration (d), maximal respiration (e) and spare respiratory capacity (f). Results represent mean values ± SEM, n=6-7, *p<0.05, **p<0.01, ***p<0.001 vs. vehicle; #p<0.05, ##p<0.01, ###p<0.001 vs. control.*

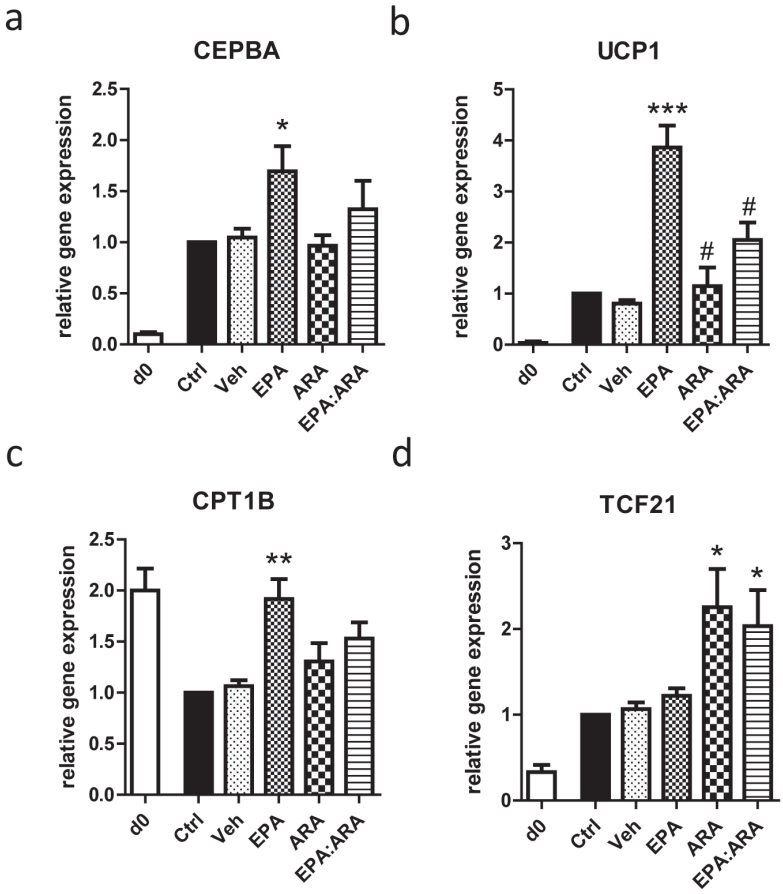

Figure 4: Combinatory effects of n-3 and n-6 LC-PUFAs on brite and white marker genes. *hASCs isolated from different donors were chronically treated (day 0-12 of differentiation) with EPA (n-3), ARA (n-6) or a combination of EPA:ARA (ratio 1:2) at a final concentration of 20 µM. After 12 days, RNA was isolated from differentiated hASCs and mRNA expression levels of CEPBA (a), UCP1 (b), CPT1B (c) and TCF21 (d) were assessed via qRT-PCR and normalized to β-actin mRNA levels. Data represent mean values ± SEM and are expressed relative to control, n=4-5, *p<0.05, **p<0.01 vs. vehicle; #p<0.05 vs. EPA.*

deed, the enhancement of *UCP1, C/EBPα* and *CPT1B* mRNA expression by EPA was strongly diminished in the EPA/ARA combination (Figure 4a-c). Moreover, relatively low levels of ARA in the combination were sufficient to increase *TCF21* expression to a similar degree as ARA alone (Figure 4d).

EPA but not BMP4 is able to trigger white-to-brown conversion of differentiated hASCs

In addition to brite adipogenesis, direct conversion of white to brite adipocytes has been discussed as a second process contributing to the browning of WAT during cold exposure (34). In order to investigate the effect of LC-PUFAs on direct conversion of differentiated white adipocytes to brite adipocytes, hASCs were exposed to LC-PUFAs or BMP4 from day 8 to 12 after induction of adipocyte differentiation. Again, 20 µM of LC-PUFAs was used, since 100 µM also reduced cell viability in this setting (Suppl. figure 1b). In contrast to the chronic treatment model, fatty acids or BMP4 treatment at later stages of differentiation had no effect on general adipogenesis. Lipid accumulation and HSL protein abundance in differentiated hASCs showed a trend, but no significant increase after LC-PUFA treatment from day 8-12 (Suppl. figure 4a+c). Nevertheless, adiponectin protein levels were still increased after the shorter EPA and DHA treatment (Suppl. figure 4d). Importantly, expression levels of white and brite marker genes after late LC-PUFA treatment showed the same effect (Figure 5) as under chronic treatment conditions (Figure 2). Hence, *UCP1* as well as *CPT1B* expression were still upregulated in differentiated hASCs after 4 days of EPA treatment, but not after exposure to DHA, ARA or OA (Figure 5c+d). Accordingly, mRNA levels of *TCF21* were significantly higher in ARA treated hASCs (Figure 5e). BMP4, which is able to induce a white-to-brown shift when added to hASCs from the beginning of adipocyte differentiation (Figure 2) (24), was not able to increase *UCP1* and *CPT1B* expression or decrease *TCF21* mRNA levels when applied in the late stage of adipocyte differentiation.

We next assessed if the 4 day treatment of hASCs at the late stage of differentiation also impacts mitochondrial functionality. Similar to the chronic setting, total OXPHOS complex abundance was not changed by any treatment (Figure 6a). However, single OXPHOS complexes (data not shown) and CS activity (Figure 6b) were also not affected after terminal LC-PUFA or BMP4 exposure. Real-time measurement of cellular OCR revealed that basal respiration was significantly increased after EPA, DHA and ARA treatment, but not after OA or BMP4 treatment (Figure 6c+d). However,

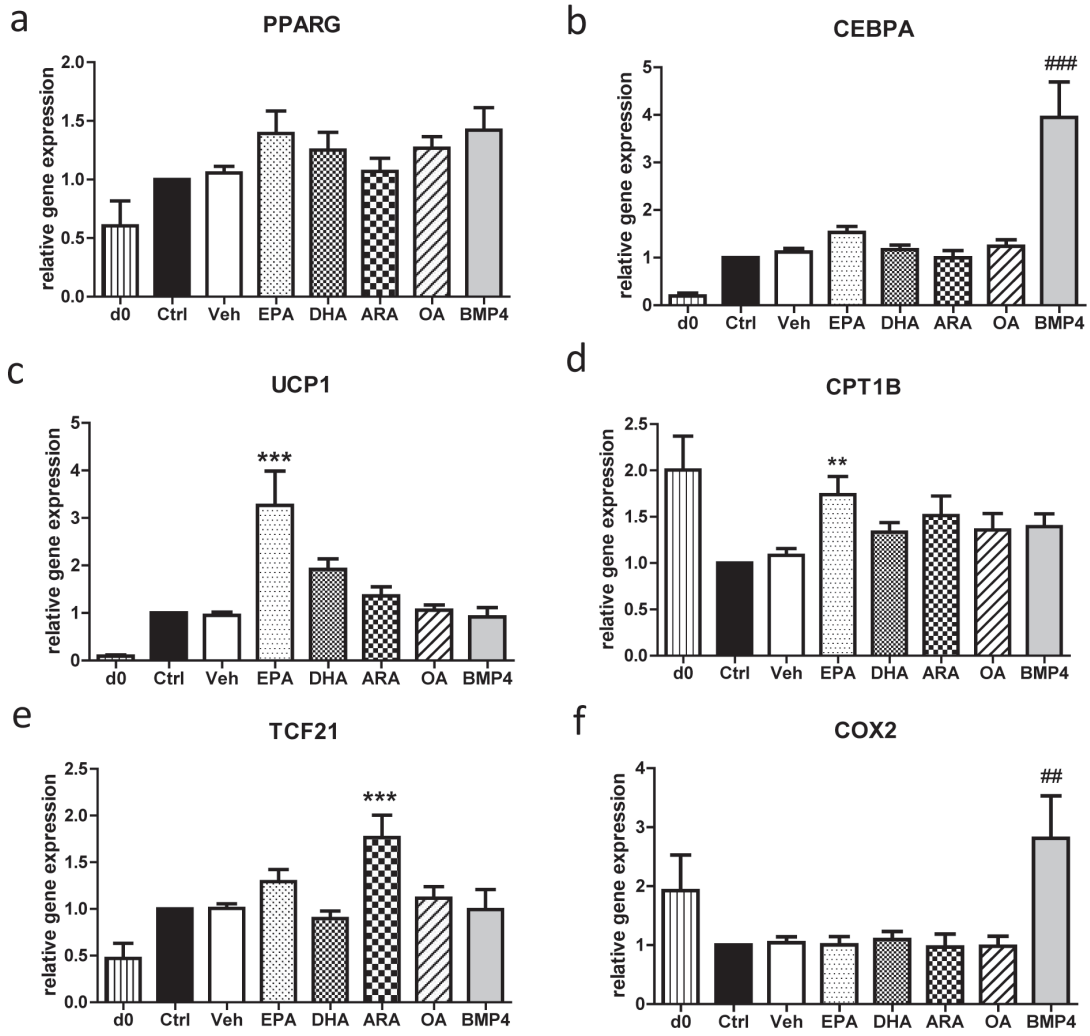

Figure 5: EPA, but not BMP4 triggers a brite gene expression pattern at a late stage of differentiation. *hASCs isolated from different donors were induced for adipogenic differentiation and EPA, DHA, ARA, OA (20 µM each) or BMP4 (50 ng/ml) were included in the medium from day 8 to 12 of differentiation. Total RNA was isolated and gene expression levels of PPARG (a), CEPBA (b), UCP1 (c), CPT1B (d), TCF21 (e) and COX2 (f) were measured via qRT-PCR. Expression levels of target genes are normalized to β-actin mRNA levels. Data represent mean values ± SEM and are expressed relative to control, n=7-8. **p<0.01, ***p<0.001 vs. vehicle; ##p<0.01, ###p<0.001 vs. control.*

maximal respiration was not changed by n-3 and n-6 LC-PUFAs and tended to be increased in EPA and DHA challenged hASCs (Figure 6e). As previously suggested (35), the positive control troglitazone increased basal and maximal respiration in hASCs. Interestingly, the 4 day treatment with ARA in the late stage of differentiation was sufficient to decrease spare respiratory capacity (Figure 6f).

Discussion

Opposing effects of dietary n-3 and n-6 LC-PUFAs on the development of obesity have been discussed (17;20). However, the underlying mechanisms are not fully understood and a potential impact of n-3 and n-6 LC-PUFAs on WAT browning in humans remains unknown. In the present work, we report for the first time that specifically EPA (n-3) and ARA (n-6) differentially regulate white-to-brown conversion and mitochondrial function in primary hASCs.

Many factors known to promote browning have been described to enhance adipogenesis, such as BMP4 and BMP7 (24;36) or rosiglitazone (5). We observed an augmented adipocyte differentiation by both n-3 and n-6 LC-PUFAs, indicated by increased lipid accumulation and HSL protein levels. This effect was comparable to the pro-adipogenic effect of BMP4, which is able to induce browning in murine and human white preadipocytes (24;37). In line, a recent study in 3T3-L1 adipocytes also observed a positive effect of EPA and DHA on adipocyte differentiation (38). In cont-

rast, it has been proposed, that the anti-obesity effect of EPA and DHA may be mediated by a decrease of total adipocyte cell number per fat pad (18) and other studies showed inhibitory actions of EPA and DHA (at 100 µM) on 3T3-L1 differentiation (26;39;40). DHA even exerted this effect by inhibiting mitotic clonal expansion and inducing apoptosis in 3T3-L1 cells (26). These heterogenous results may be due to different model systems and it has been shown that the adipogenic effect of LC-PUFAs *in vitro* depends on the medium composition (27). Moreover, we used relatively low concentrations of 20 µM, which did not reduce cell vitality, in contrast to at least 100 µM (26;39;40). Despite similar effects of EPA, DHA and ARA on adipocyte differentiation, we and others observed differential effects on protein expression of the insulin-sensitizing adipokine adiponectin (30-32).

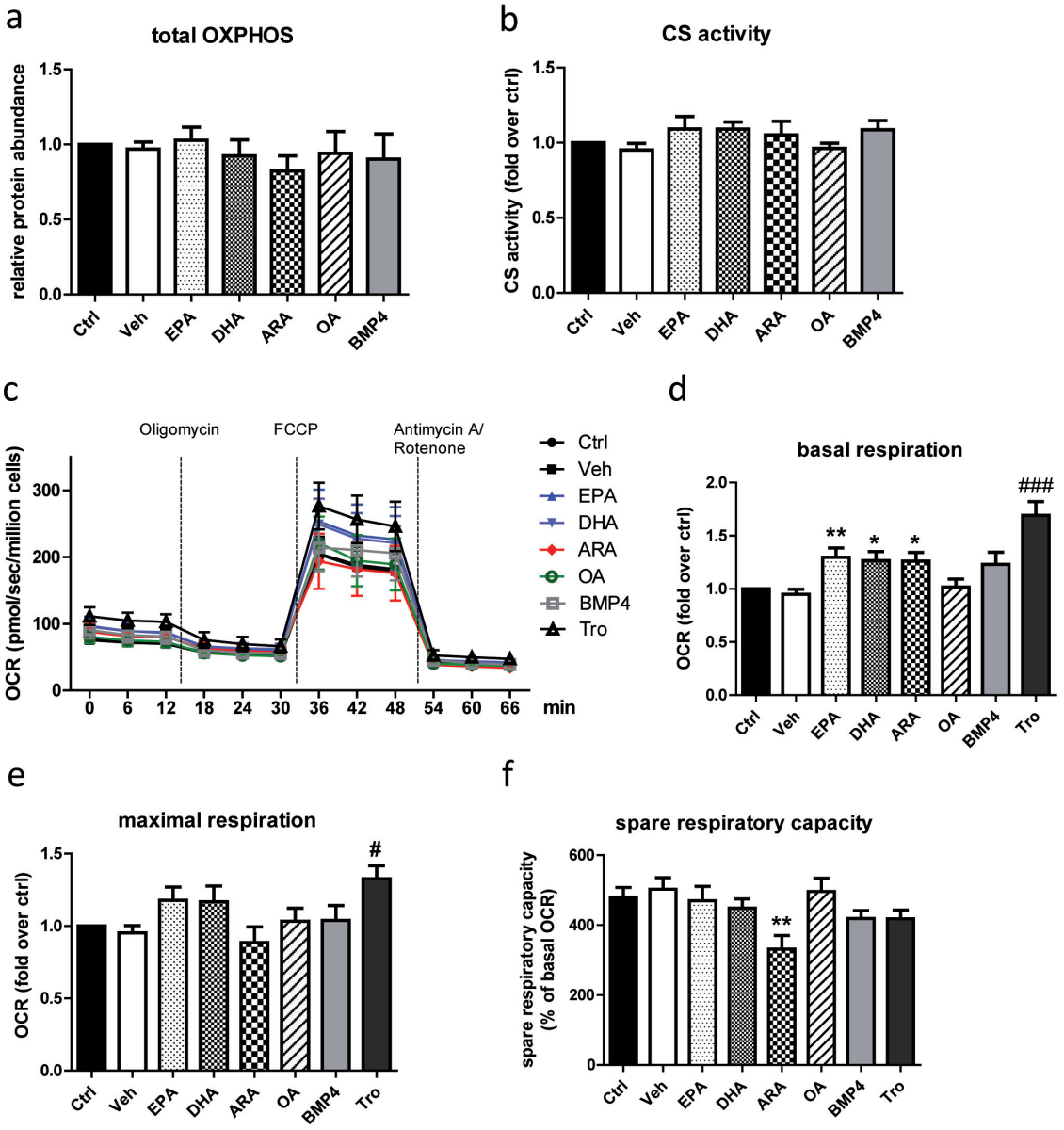

Figure 6: Effect of LC-PUFA treatment at the late stage of differentiation on mitochondrial content and function. *hASCs were challenged from day 8 to 12 of differentiation with the different fatty acids (20 µM) or BMP4 (50 ng/ml) prior to measurement of several mitochondrial parameters. (a) Protein levels of total OXPHOS complexes by immunoblot with a commercially available OXPHOS antibody cocktail. Data are normalized to ß-actin protein levels and expressed relative to control (ctrl). Results represent mean values ± SEM, n=6. (b) CS activity in whole cell lysates, normalized to the protein content of each sample. Values are means ± SEM out of n=5 independent experiments and expressed relative to control. (c) Real-time measurement of oxygen consumption rate (OCR), normalized to cell number, at baseline and after injection of different mitochondrial inhibitors. (d-f) Calculations for basal respiration (d), maximal respiration (e) and spare respiratory capacity (f). Results represent mean values ± SEM, n=6-7. *p<0.05, **p<0.01, ***p<0.001 vs. vehicle; ##p<0.01, ###p<0.001 vs. control.*

In addition to differential effects of n-3 and n-6 LC-PUFAs on adiponectin levels and lipid droplet size, we found opposing effects of EPA and ARA on brite marker gene expression. The n-3 LC-PUFA EPA upregulated *UCP1* and *CPT1B* expression confirming previous results obtained in mouse subcutaneous adipocytes, where EPA increased thermogenic gene expression (41). In contrast, ARA did not increase expression of any brite marker gene but did increase the expression of the white-specific marker *TCF21*. In line with this observation, a negative regulation of brite adipogenesis by ARA has been previously shown in human multipotent adipose-derived stem cells (hMADS), an established model to study browning (35). ARA inhibited white-to-brown conversion of hMADS when added simultaneously with rosiglitazone at the end of differentiation (42). Taken together, EPA and ARA differentially regulate brite adipogenesis, and ARA even inhibits the EPA mediated effects on brite gene expression when added in combination (EPA:ARA ratio1:2) to hASCs. Furthermore, EPA was still able to increase *UCP1* and *CPT1B* expression in the late stage of adipocyte differentiation in hASCs, similarly as recently observed in primary murine brown adipocytes (41). On the other hand, the growth factor BMP4 had no effect on mature adipocytes and is likely to act primarily on hASCs in the early stage of differentiation. Likewise, BMP7 induced commitment of murine precursor cells to brown adipocytes when added prior to the induction of differentiation (36).

The differential regulation of white-to-brown conversion by EPA and ARA was also translated into differences of mitochondrial function. Though protein levels of total OXPHOS complexes were not changed, EPA upregulated complex III levels. Moreover, increased CS activity in EPA challenged hASCs indicates a higher supply of NADH for oxidative phosphorylation. Indeed, maximal OCR was solely increased in EPA challenged cells. ARA on the other hand, decreased complex IV protein levels, had no impact on CS activity or maximal respiration, and decreased spare respiratory capacity. Surprisingly, the observed differences between EPA and ARA in terms of *CPT1B* expression, OXPHOS complexes and CS activity had no impact on basal OCR, which was equally increased by EPA, DHA and ARA. Only upon injection of the uncoupler FCCP, mimicking increased energy demand, the observed differences of EPA and ARA on mitochondrial markers get significant. Taking into account that spare respiratory capacity is an important determinant of metabolic flexibility in human adipocytes (43), ARA may promote mitochondrial dysfunction in adipocytes. Importantly, ARA was also able to impair mitochondrial function after treatment from day 8 to 12 of differentiation only, indicated by reduced spare respiratory capacity. However, the effects of EPA on brite gene expression in this shorter treatment model were not translated into significant changes of maximal OCR. Thus, longer treatment with EPA seems to be necessary to impact mitochondrial function.

It is well known that the anti- and pro-inflammatory effects of n-3 and n-6 LC-PUFAs are mostly due to the formation of a functionally different series of eicosanoids, involving the enzymes COX1 and COX2. Because EPA and ARA compete as substrates for COX1 and COX2, changing the ratio of n-3/n-6 intake and phospholipid composition will result in a modified eicosanoid pattern (17). The n-3 family member DHA is no substrate for COX enzymes and did neither alter brite gene expression nor mitochondrial function in hASCs, indicating a role for COX-mediated eicosanoid synthesis in brite adipogenesis. In line, COX2 has been implicated in adaptive thermogenesis (21;33) and the ARA-derived prostanoids PGE2 and PGF2α diminished *UCP1* expression and oxygen consumption in hMADS induced for brite adipogenesis (42). Although LC-PUFA treatment did not directly affect *COX2* expression in hASCs, a change in the EPA:ARA supply could modify prostaglandine composition. The observation that the EPA-induced promotion of brite adipocyte formation is inhibited when combined with ARA also supports an involvement of COX2.

Already in 1995, it has been speculated that PUFAs regulate BAT function. Feeding of mice with a diet rich in LA (18:2n-6) and ALA (18:3n-3) at a 2.3:1 ratio increased UCP1 protein content in BAT and raised capacity for NST (44). Later on differences between n-3 and n-6 PUFAs have been suggested for the first time, since UCP1 expression in BAT was greater after a diet rich in n-3 compared to n-6 PUFAs (45). However, these early studies could not narrow down the effects to a single PUFA. We here provide evidence that EPA rather than DHA regulates brown and brite adipocyte recruitment and function. Distinguishing the health benefits of EPA and DHA and refining dietary recommendations has also been a topic of a recent discussion (46). In addition to differentiating between the n-3 members EPA and DHA, our study indicates the importance of a specific n-3:n-6 ratio in the diet, especially that of EPA:ARA. This is further highlighted by recent clinical studies describing decreased EPA:ARA ratios in type 2 diabetic patients (22) and obese subjects (23).

In conclusion, differential effects of n-3 and n-6 LC-PUFAs on white-to-brown conversion are mainly determined by EPA and ARA and most likely mediated by their functionally different eicosanoids. Since EPA also partly promotes white-to-brown conversion of adipocytes in the late stage of differentiation, it may have a higher impact on whole adipose tissue function than BMP4, which only targets cells in the preadipocyte stage. Future studies should further analyze the health benefits of single LC-PUFAs to improve dietary recommendations in the context of obesity-associated diseases.

Acknowledgements

We thank J. Liebau (Department of Plastic Surgery, Florence-Nightingale-Hospital, Düsseldorf, Germany) and C. Andree (Department of Plastic Surgery, Sana-Hospital, Düsseldorf-Gerresheim, Germany) for support in obtaining AT samples. The secretarial assistance of B. Hurow and the technical help of A. Cramer are gratefully acknowledged. This work was supported by grants from the Ministerium für Wissenschaft und Forschung des Landes Nordrhein-Westfalen (Ministry of Science and Research of the State of North Rhine-Westphalia), the Bundesministerium für Gesundheit (Federal Ministry of Health), and by a Training and Feasibility Grant of the German Diabetes Center.

Conflict of interest

The authors have no conflict of interest to declare.

References

1 Stephens M, Ludgate M, Rees DA. Brown fat and obesity: the next big thing? Clinical Endocrinology 2011; 74/6: 661-670.

2 Cannon B, Nedergaard J. Brown adipose tissue: function and physiological significance. Physiol Rev 2004; 84/1: 277-359.

3 Seale P, Bjork B, Yang W, Kajimura S, Chin S, Kuang S et al. PRDM16 controls a brown fat/skeletal muscle switch. Nature 2008; 454/7207: 961-967.

4 Timmons JA, Wennmalm K, Larsson O, Walden TB, Lassmann T, Petrovic N et al. Myogenic gene expression signature establishes that brown and white adipocytes originate from distinct cell lineages. Proc Natl Acad Sci U S A 2007; 104/11: 4401-4406.

5 Petrovic N, Walden TB, Shabalina IG, Timmons JA, Cannon B, Nedergaard J. Chronic Peroxisome Proliferator-activated Receptor gamma (PPAR gamma) Activation of Epididymally Derived White Adipocyte Cultures Reveals a Population of Thermogenically Competent, UCP1-containing Adipocytes Molecularly Distinct from Classic Brown Adipocytes. Journal of Biological Chemistry 2010; 285/10: 7153-7164.

6 Smorlesi A, Frontini A, Giordano A, Cinti S. The adipose organ: white-brown adipocyte plasticity and metabolic inflammation. Obes Rev 2012; 13 Suppl 2: 83-96.

7 Bartelt A, Heeren J. Adipose tissue browning and metabolic health. Nat Rev Endocrinol 2014; 10/1: 24-36.

8 Cypess AM, Lehman S, Williams G, Tal I, Rodman D, Goldfine AB et al. Identification and importance of brown adipose tissue in adult humans. N Engl J Med 2009; 360/15: 1509-1517.

9 Saito M, Okamatsu-Ogura Y, Matsushita M, Watanabe K, Yoneshiro T, Nio-Kobayashi J et al. High incidence of metabolically active brown adipose tissue in healthy adult humans: effects of cold exposure and adiposity. Diabetes 2009; 58/7: 1526-1531.

10 van Marken Lichtenbelt WD, Vanhommerig JW, Smulders NM, Drossaerts JM, Kemerink GJ, Bouvy ND et al. Cold-activated brown adipose tissue in healthy men. N Engl J Med 2009; 360/15: 1500-1508.

11 Zingaretti MC, Crosta F, Vitali A, Guerrieri M, Frontini A, Cannon B et al. The presence of UCP1 demonstrates that metabolically active adipose tissue in the neck of adult humans truly represents brown adipose tissue. FASEB J 2009; 23/9: 3113-3120.

12 Virtanen KA, Lidell ME, Orava J, Heglind M, Westergren R, Niemi T et al. Brief Report: Functional Brown Adipose Tissue in Healthy Adults. New England Journal of Medicine 2009; 360/15: 1518-1525.

13 Cypess AM, White AP, Vernochet C, Schulz TJ, Xue R, Sass CA et al. Anatomical localization, gene expression profiling and functional characterization of adult human neck brown fat. Nat Med 2013; 19/5: 635-639.

14 Jespersen NZ, Larsen TJ, Peijs L, Daugaard S, Homoe P, Loft A et al. A classical brown adipose tissue mRNA signature partly overlaps with brite in the supraclavicular region of adult humans. Cell Metab 2013; 17/5: 798-805.

15 Lidell ME, Betz MJ, Dahlqvist LO, Heglind M, Elander L, Slawik M et al. Evidence for two types of brown adipose tissue in humans. Nat Med 2013; 19/5: 631-634.

16 Bonet ML, Oliver P, Palou A. Pharmacological and nut-

ritional agents promoting browning of white adipose tissue. Biochim Biophys Acta 2013; 1831/5: 969-985.

17 Flachs P, Rossmeisl M, Bryhn M, Kopecky J. Cellular and molecular effects of n-3 polyunsaturated fatty acids on adipose tissue biology and metabolism. Clin Sci (Lond) 2009; 116/1: 1-16.

18 Ruzickova J, Rossmeisl M, Prazak T, Flachs P, Sponarova J, Veck M et al. Omega-3 PUFA of marine origin limit diet-induced obesity in mice by reducing cellularity of adipose tissue. Lipids 2004; 39/12: 1177-1185.

19 Flachs P, Horakova O, Brauner P, Rossmeisl M, Pecina P, Franssen-van HN et al. Polyunsaturated fatty acids of marine origin upregulate mitochondrial biogenesis and induce beta-oxidation in white fat. Diabetologia 2005; 48/11: 2365-2375.

20 Ailhaud G, Massiera F, Weill P, Legrand P, Alessandri JM, Guesnet P. Temporal changes in dietary fats: role of n-6 polyunsaturated fatty acids in excessive adipose tissue development and relationship to obesity. Prog Lipid Res 2006; 45/3: 203-236.

21 Vegiopoulos A, Muller-Decker K, Strzoda D, Schmitt I, Chichelnitskiy E, Ostertag A et al. Cyclooxygenase-2 controls energy homeostasis in mice by de novo recruitment of brown adipocytes. Science 2010; 328/5982: 1158-1161.

22 Imamura S, Morioka T, Yamazaki Y, Numaguchi R, Urata H, Motoyama K et al. Plasma polyunsaturated fatty acid profile and delta-5 desaturase activity are altered in patients with type 2 diabetes. Metabolism 2014; 63/11: 1432-1438.

23 Inoue K, Kishida K, Hirata A, Funahashi T, Shimomura I. Low serum eicosapentaenoic acid / arachidonic acid ratio in male subjects with visceral obesity. Nutr Metab (Lond) 2013; 10/1: 25.

24 Elsen M, Raschke S, Tennagels N, Schwahn U, Jelenik T, Roden M et al. BMP4 and BMP7 induce the white-to-brown transition of primary human adipose stem cells. Am J Physiol Cell Physiol 2014; 306/5: C431-C440.

25 Romacho T, Glosse P, Richter I, Elsen M, Schoemaker MH, van Tol EA et al. Nutritional ingredients modulate adipokine secretion and inflammation in human primary adipocytes. Nutrients 2015; 7/2: 865-886.

26 Kim HK, Della-Fera M, Lin J, Baile CA. Docosahexaenoic acid inhibits adipocyte differentiation and induces apoptosis in 3T3-L1 preadipocytes. J Nutr 2006; 136/12: 2965-2969.

27 Madsen L, Petersen RK, Kristiansen K. Regulation of adipocyte differentiation and function by polyunsaturated fatty acids. Biochim Biophys Acta 2005; 1740/2: 266-286.

28 Schulz TJ, Tseng YH. Emerging role of bone morphogenetic proteins in adipogenesis and energy metabolism. Cytokine & Growth Factor Reviews 2009; 20/5-6: 523-531.

29 Gustafson B, Smith U. The WNT Inhibitor Dickkopf 1 and Bone Morphogenetic Protein 4 Rescue Adipogenesis in Hypertrophic Obesity in Humans. Diabetes 2012; 61/5.

30 Flachs P, Mohamed-Ali V, Horakova O, Rossmeisl M, Hosseinzadeh-Attar MJ, Hensler M et al. Polyunsaturated fatty acids of marine origin induce adiponectin in mice fed a high-fat diet. Diabetologia 2006; 49/2: 394-397.

31 Banga A, Unal R, Tripathi P, Pokrovskaya I, Owens RJ, Kern PA et al. Adiponectin translation is increased by the PPARgamma agonists pioglitazone and omega-3 fatty acids. Am J Physiol Endocrinol Metab 2009; 296/3: E480-E489.

32 Tishinsky JM, Ma DW, Robinson LE. Eicosapentaenoic acid and rosiglitazone increase adiponectin in an additive and PPARgamma-dependent manner in human adipocytes. Obesity (Silver Spring) 2011; 19/2: 262-268.

33 Madsen L, Pedersen LM, Lillefosse HH, Fjaere E, Bronstad I, Hao Q et al. UCP1 induction during recruitment of brown adipocytes in white adipose tissue is dependent on cyclooxygenase activity. PLoS One 2010; 5/6: e11391.

34 Rosenwald M, Perdikari A, Rulicke T, Wolfrum C. Bidirectional interconversion of brite and white adipocytes. Nat Cell Biol 2013; 15/6: 659-667.

35 Pisani DF, Djedaini M, Beranger GE, Elabd C, Scheideler M, Ailhaud G et al. Differentiation of Human Adipose-Derived Stem Cells into „Brite“ (Brown-in-White) Adipocytes. Front Endocrinol (Lausanne) 2011; 2: 87.

36 Tseng YH, Kokkotou E, Schulz TJ, Huang TL, Winnay JN, Taniguchi CM et al. New role of bone morphogenetic protein 7 in brown adipogenesis and energy expenditure. Nature 2008; 454/7207: 1000-1004.

37 Qian SW, Tang Y, Li X, Liu Y, Zhang YY, Huang HY et al. BMP4-mediated brown fat-like changes in white adipose tissue alter glucose and energy homeostasis. Proc Natl Acad Sci U S A 2013; 110/9: E798-E807.

38 Murali G, Desouza CV, Clevenger ME, Ramalingam R, Saraswathi V. Differential effects of eicosapentaenoic acid and docosahexaenoic acid in promoting

the differentiation of 3T3-L1 preadipocytes. Prostaglandins Leukot Essent Fatty Acids 2014; 90/1: 13-21.

39 Barber E, Sinclair AJ, Cameron-Smith D. Comparative actions of omega-3 fatty acids on in-vitro lipid droplet formation. Prostaglandins Leukot Essent Fatty Acids 2013; 89/5: 359-366.

40 Manickam E, Sinclair AJ, Cameron-Smith D. Suppressive actions of eicosapentaenoic acid on lipid droplet formation in 3T3-L1 adipocytes. Lipids Health Dis 2010; 9: 57.

41 Zhao M, Chen X. Eicosapentaenoic acid promotes thermogenic and fatty acid storage capacity in mouse subcutaneous adipocytes. Biochem Biophys Res Commun 2014; 450/4: 1446-1451.

42 Pisani DF, Ghandour RA, Beranger GE, Le FP, Chambard JC, Giroud M et al. The omega6-fatty acid, arachidonic acid, regulates the conversion of white to brite adipocyte through a prostaglandin/calcium mediated pathway. Mol Metab 2014; 3/9: 834-847.

43 Keuper M, Jastroch M, Yi CX, Fischer-Posovszky P, Wabitsch M, Tschop MH et al. Spare mitochondrial respiratory capacity permits human adipocytes to maintain ATP homeostasis under hypoglycemic conditions. FASEB J 2014; 28/2: 761-770.

44 Sadurskis A, Dicker A, Cannon B, Nedergaard J. Polyunsaturated fatty acids recruit brown adipose tissue: increased UCP content and NST capacity. Am J Physiol 1995; 269/2 Pt 1: E351-E360.

45 Takahashi Y, Ide T. Dietary n-3 fatty acids affect mRNA level of brown adipose tissue uncoupling protein 1, and white adipose tissue leptin and glucose transporter 4 in the rat. Br J Nutr 2000; 84/2: 175-184.

46 Russell FD, Burgin-Maunder CS. Distinguishing health benefits of eicosapentaenoic and docosahexaenoic acids. Mar Drugs 2012; 10/11: 2535-2559.

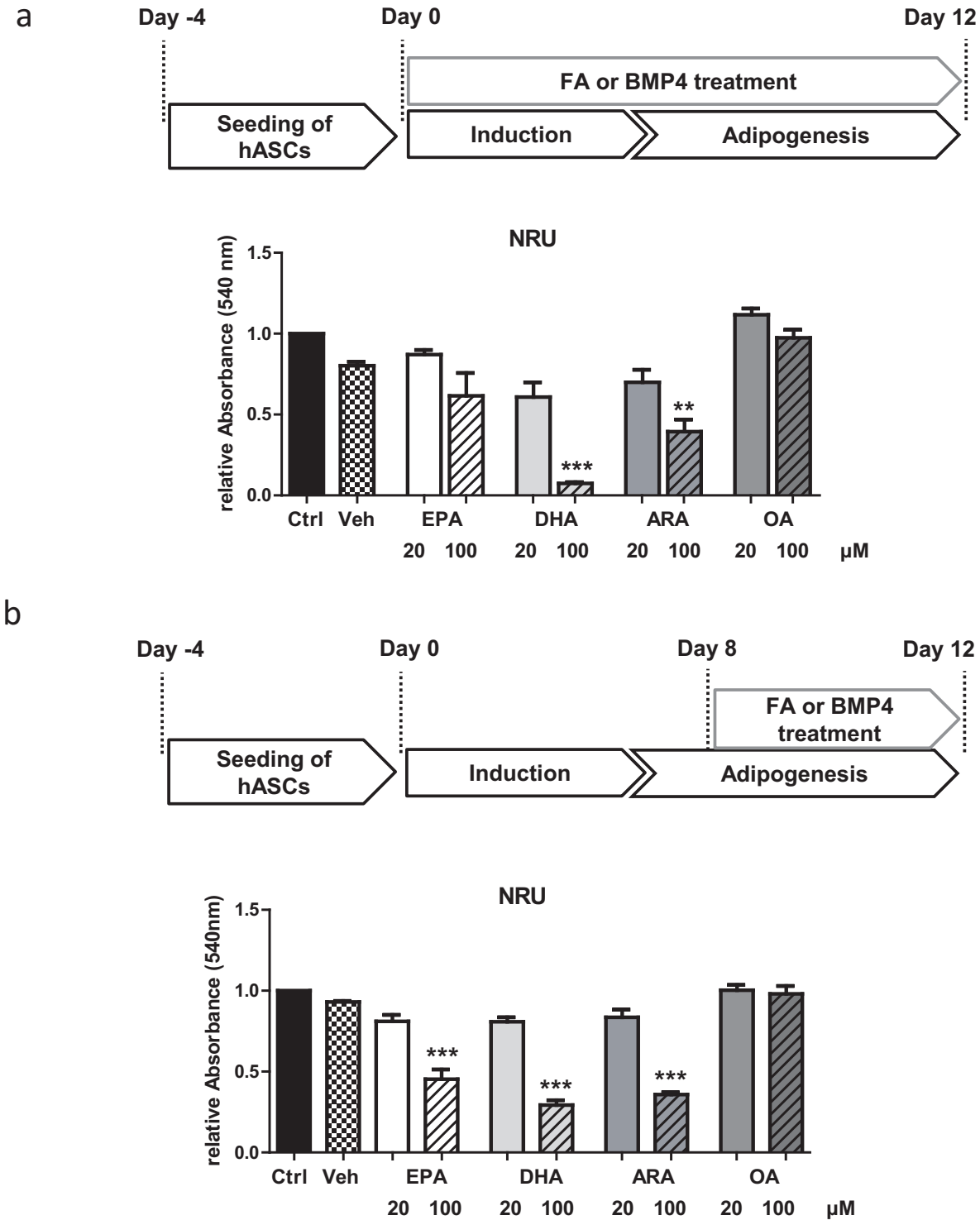

Suppl. Figure 1: Effect of chronic and shorter LC-PUFAs treatment on cell vitality. *(a) Model for chronic fatty acid (FA) treatment of hASCs. Neutral Red Staining was performed in hASCs treated with different fatty acids at concentrations of 20 µM and 100 µM. (b) Treatment of hASCs with different concentrations of FA at the late stage of differentiation (day 8-12) and assessment of cell viability by Neutral Red Uptake assay. Data represent mean values ± SEM, n=4,, **p<0.01, ***p<0.001 vs. vehicle*

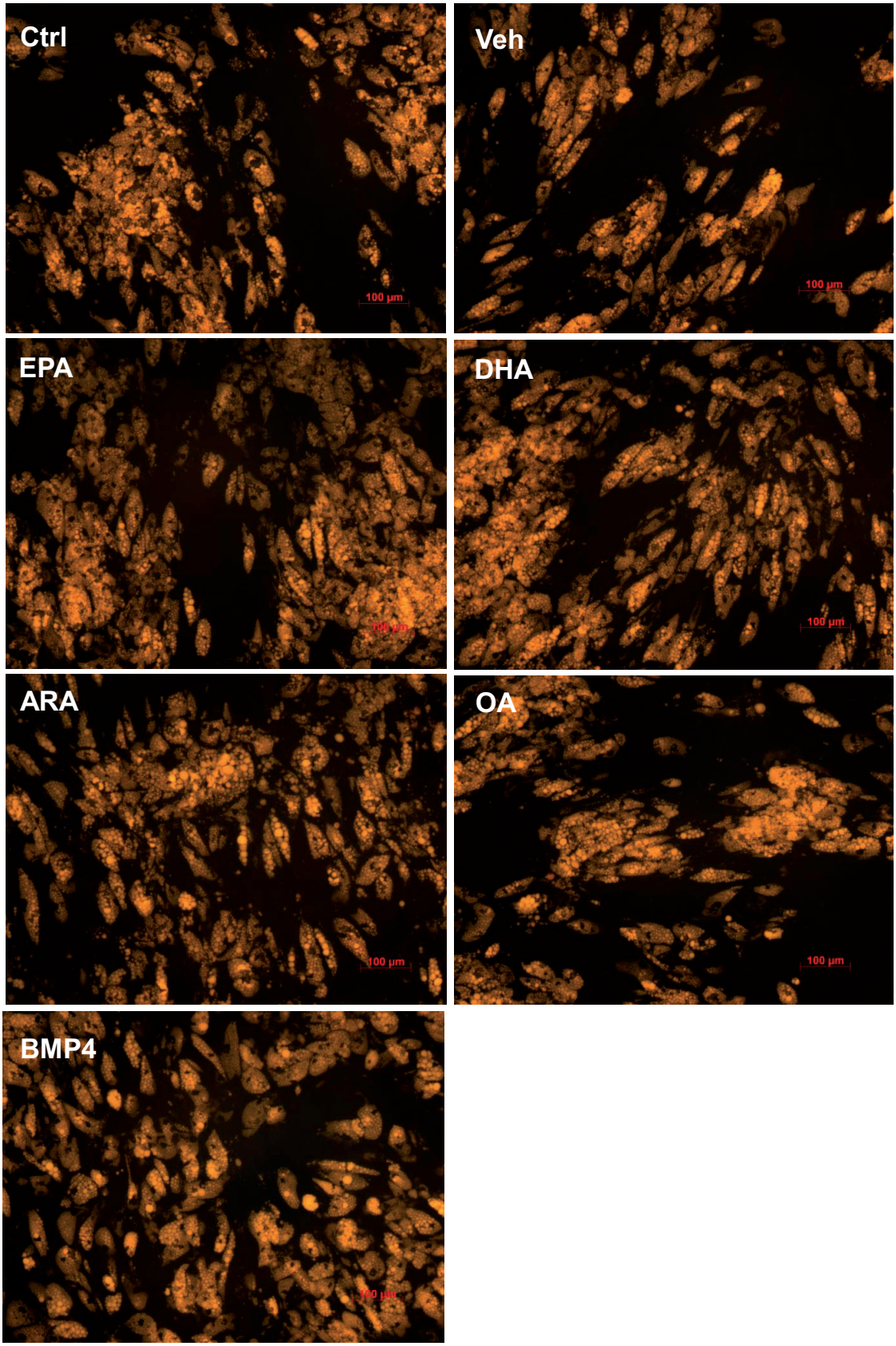

Suppl. Figure 2: Nile Red Staining of hASCs after chronic LC-PUFA treatment. *hASCs were treated with 20 µM of EPA, DHA, ARA or OA, and BMP4 (50 ng/ml) as positive control during the whole differentiation period. On day 12, cells were fixed and Nile Red Staining was performed. Representative images of one hASC donor at 10x magnification.*

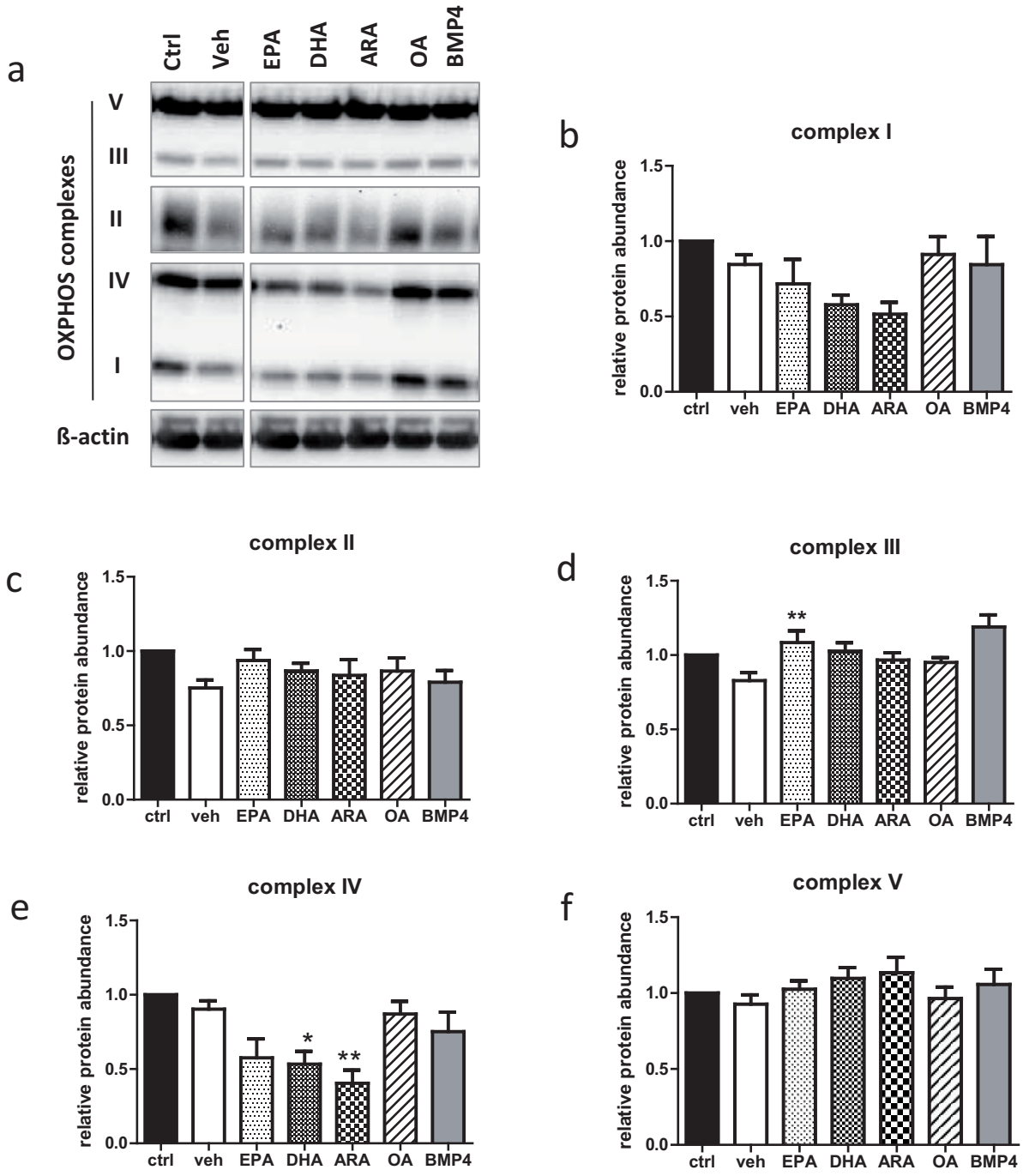

Suppl. Figure 3: Effect of LC-PUFAs on mitochondrial OXPHOS complexes. *After 12 days of differentiation hASCs challenged with the indicated treatments were analyzed for protein abundance of OXPHOS complexes by immunoblot with a commercially available OXPHOS antibody cocktail (a). Data are normalized to β-actin protein levels and expressed relative to control. Quantfication for single complexes (b-f). Results represent mean values ± SEM, n=6, *p<0.05 , **p<0.01 vs. vehicle.*

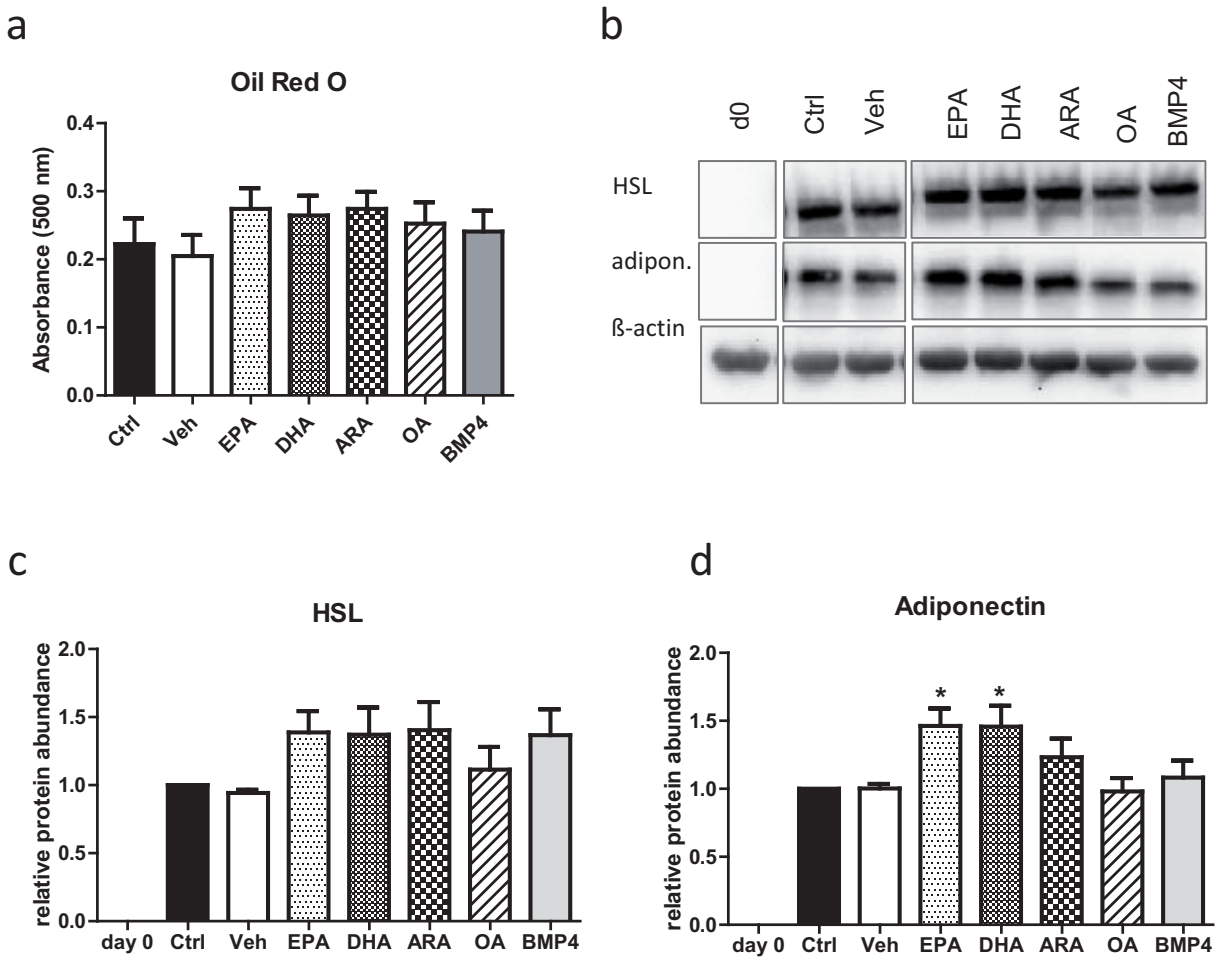

Suppl. Figure 4: Treatment with LC-PUFAs in the late stage of differentiation does not increase adipogenesis. *Quantification lipid accumulation by Oil Red O Staining (a), Western blot analysis (b-d) of HSL (c) and adiponectin (d) protein levels in hASCs exposed to fatty acids (20 μM) or BMP4 (50 ng/ml) from day 8-12 of differentiation. Protein levels of HSL and adiponectin were normalized to β-actin. Data respresent mean values ± SEM of n=6-8 independent experiments. *p<0.05 vs. vehicle.*

Evidence against a beneficial effect of irisin in humans

Silja Raschke[1], **Manuela Elsen**[1], Hans Gassenhuber[2], Mark Sommerfeld[2], Uwe Schwahn[2], Barbara Brockmann[2], Raphael Jung[1], Ulrik Wisløff[3], Arnt E. Tjønna[3], Truls Raastad[4], Jostein Hallén[4], Frode Norheim[5], Christian A. Drevon[5], Tania Romacho[1], Kristin Eckardt[1], Juergen Eckel[1*]

[1] *Paul-Langerhans-Group, Integrative Physiology, German Diabetes Center, Düsseldorf, Germany*
[2] *R&D Diabetes Division, Sanofi-Aventis Deutschland GmbH, Frankfurt, Germany*
[3] *K.G. Jebsen Center of Exercise in Medicine at Department of Circulation and Medical Imaging, Norwegian University of Science and Technology, Trondheim, Norway*
[4] *Norwegian School of Sport Sciences, Oslo, Norway*
[5] *Department of Nutrition, Institute of Basic Medical Sciences, Faculty of Medicine, University of Oslo, Oslo, Norway*

Abstract

Brown adipose tissue has gained interest as a potential target to treat obesity and metabolic diseases. Irisin is a newly identified hormone secreted from skeletal muscle enhancing browning of white fat cells, which improves systemic metabolism by increasing energy expenditure in mice. The discovery of irisin raised expectations of its therapeutic potential to treat metabolic diseases. However, the effect of irisin in humans is unclear. Analyses of genomic DNA, mRNA and expressed sequence tags revealed that *FNDC5*, the gene encoding the precursor of irisin, is present in rodents and most primates, but shows in humans a mutation in the conserved start codon ATG to ATA. HEK293 cells transfected with a human *FNDC5* construct with ATA as start codon resulted in only 1% full-length protein compared to human *FNDC5* with ATG. Additionally, in vitro contraction of primary human myotubes by electrical pulse stimulation induced a significant increase in *PGC1α* mRNA expression. However, *FNDC5* mRNA level was not altered. *FNDC5* mRNA expression in muscle biopsies from two different human exercise studies was not changed by endurance or strength training. Preadipocytes isolated from human subcutaneous adipose tissue exhibited differentiation to brite human adipocytes when incubated with bone morphogenetic protein (BMP) 7, but neither recombinant FNDC5 nor irisin were effective. In conclusion, our findings suggest that it is rather unlikely that the beneficial effect of irisin observed in mice can be translated to humans.

Introduction

Obesity and the involved risk of developing metabolic diseases represent a major global public health challenge. In obese patients glucose homeostasis is disturbed due to an imbalance between energy intake and energy expenditure. Although the understanding of the role of genetics in obesity and type 2 diabetes is increasing [1–3], roughly 60% of all cases of diabetes can be directly attributed to weight gain [4].

Brown adipose tissue (AT) has drawn attention as a novel preventive and therapeutic target to treat obesity and metabolic diseases like type 2 diabetes. Whereas white AT is the primary site of triglyceride storage, brown AT is specialized in energy expenditure. In order to maintain body temperature in a cold environment, brown AT oxidizes fatty acids and generates heat [5] by the mitochondrial uncoupling protein 1 (UCP1). Thus, UCP1 knock-out mice are cold sensitive and tend to develop obesity, even when fed a control diet [6], whereas experimental approaches aiming to increase the amount and activity of brown AT reduce the development of obesity [7]. Brown AT has also been detected in humans and is found in anatomically discrete depots, with the most common location in adults in the cervical-supraclavicular depot [8–12].

Brown adipocytes and skeletal muscle cells arise from progenitors expressing myf5 [13] and their differentiation is specifically controlled by transcriptional regulators like PRDM16 [14], PGC1α [15], and others [16–19]. Chronical stimulation of mouse preadipocytes derived from epididymal white AT with rosiglitazone, a PPARγ agonist, reveals a thermogenic competent population of *UCP1*-expressing adipocytes [20]. These cells do not represent classical brown adipocytes, because they do not express typical brown AT transcription factors such as *ZIC1* and *PRDM16.* Instead, these cells appear to be a particular type of adipocytes termed as 'brite' (brown-in-white) adipocytes. Thus, the possibility to switch from white AT

to brite AT and to identify mechanisms that can activate white to brown trans-differentiation in response to pharmacological compounds is highly attractive in the context of obesity treatment.

Boström *et al*. published a promising mechanism for the induction of brite adipocytes in white AT depots after exercise in mice. Overexpression of PGC1α in mice skeletal muscle as well as exercise induced expression of the *FNDC5* gene [21], a gene which has scarcely been studied before. In 2002 two different groups first described the mouse sequence of *FNDC5* [22,23]. In adult murine tissues, *FNDC5* is highly expressed in heart and brain and less in skeletal muscle [22,23]. FNDC5 is described as a protein containing a signal peptide, fibronectin type III repeats, and hydropathy analysis revealed a hydrophobic region, which is likely to encode a transmembrane domain. Previous studies linked the gene to differentiation of myoblasts and neurones [23,24], and it has been suggested that FNDC5 is located in the matrix of peroxisomes [23]. However, Boström *et al*. showed that the transmembrane protein is cleaved by transfected HEK293 cells and the extracellular part of the protein is released, which acts as novel molecule called irisin [21]. Viral delivery of *FNDC5* in mice caused browning of subcutaneous fat, stimulated oxygen consumption, and diminished diet-induced weight gain and metabolic dysfunction [21]. Thus, irisin induced a thermogenic mechanism in white AT, which improved whole body energy balance in mice. This initial report of irisin linked the *FNDC5* gene to browning in mice.

Furthermore, Boström *et al*. were the first to describe this gene in humans [21]. The bioinformatics analysis of the *FNDC5* gene performed by us revealed that divergent sequences have been published. Until the protein sequence was modified September 5, 2012 the UniProt database entry FNDC5/Q8NAU1 represented the full-length protein as described by Boström *et al*. [21]. The UniProt entry was modified, since the underlying transcript sequence was classified as artefact. Now, two potential protein sequences are available at the UniProt database. Ivanov *et al*. described human *FNDC5* as a gene with a mutation in the start codon to ATA [25], encoding isoleucin, instead of ATG, encoding methionine. Using this non-canonical start site would generate the full-length protein. The translation of the second protein sequence starts at the first in-frame ATG start codon of the *FNDC5* ORF, but as this ATG is located 76 codons downstream the resulting protein would be a truncated irisin protein.

Although, the initial description of irisin was focused on mice, Boström *et al*. raised the hope that exogenously administered irisin might have a therapeutic potential in the treatment of obesity and diabetes in humans. Thus, the aim of our present study was to analyze the human *FNDC5* gene and to explore its function in the human system. Our findings indicate that great caution is needed when extrapolating data regarding FNDC5/irisin from rodent to the human situation.

Materials and Methods

The study to obtain biopsies from m. vastus lateralis was approved by the Regional Committee for Research Ethics, Trondheim, Norway. Written informed consent was obtained from all participants. The study to obtain biopsies from m. trapezius was approved by the Regional Committee for Research Ethics, Oslo, Norway and written informed consent was obtained from all participants. The procedure to obtain subcutaneous adipose tissue was approved by the ethical committee of the Heinrich-Heine-University, Düsseldorf and all the donors provided written informed consent.

Sequence Alignment

ClustalW was used for multiple alignments. Blast searches were done using NCBI-BLAST interface. FNDC5 exon 1 sequences were obtained from ENSEMBL (Exon1_human: ENSE00001862258; Exon1_gorilla: ENSGGOE00000102667; Exon1_gibbon: ENSNLEE00000033119; Exon1_rat: ENSRNOE00000220327; Exon1_mouse: ENSMUSE00000333154. The Exon1_chimp had an gap. Therefore this gap was sequenced internally using 3 independent Chimp genomic DNAs (Exon1_chimp: ENSPTRE00000406642, ENSPTRE00000351668 and sequenced by us). All other Exon1 sequences were obtained from Ensembl. The protein sequences were obtained from Uniprot in case of the human, mouse and rat sequences (FNDC5_HUMAN_o: Q8NAU1 old version until 2012_08; FNDC5_HUMAN_c: Q8NAU1 current version since 2012_08; FNDC5_mouse: Q8K4Z2; FNDC5_rat: Q8K3V5). The gorilla and gibbon sequences were obtained from ENSEMBL (FNDC5_gorilla: ENSGGOP00000009792; FNDC5_gibbon: ENSNLEP00000003686), the chimp sequence was a combination of ENSEMBL and in-house sequence. Single nucleotide polymorphism data were obtained from NCBI and ENSEMBL. UNIPROT was searched for annotated non-canonical start sites in human proteins. The search for hairpin structures close to the start codon was done with the public tool AUG_hairpin (http://wwwmgs.bionet.nsc.ru/ mgs/programs/aug_hairpin/).

Overexpression of FNDC5 constructs in HEK293 cells

HEK293 cells were seeded in six-well plates coated with fibronectin at a density of $4x10^5$ cells/well in DMEM, high glucose containing 10% (vol./vol.) fetal calf serum and 1x Pen/Strep 24 h prior to transfection. The HEK293 cells were transfected with human or mouse *FNDC5* cloned into pcDNA5-FRT-TO_cEGFP expression vector (Figure S5). An additional vector was generated by single point mutation in the naturally occurring start codon ATA of human *FNDC5* to ATG. Transfection of HEK293 cells with 2 µg DNA was done as described by the manufacturer using jetPRIME reagent (Polyplus). After 24 h cells were lysed in an ice-cold lysis buffer containing 50 mmol/l Tris/HCl (pH 7.4), 1% (vol./vol.) NP-40, 0.25% (vol./vol.) sodium-deoxycholate, 150 mmol/l NaCl, 1 mmol/l EDTA, 1 mmol/l Na3VO4, and protease inhibitor cocktail (Roche). Deglycosylation of glycoproteins in the cell lysates using PNGase F was performed as specified by the manufacturer (New England Biolabs). Samples were analysed via SDS-PAGE and immunoblotting using standard methods. Antibodies against irisin/FNDC5 were from Phoenix Pharmaceuticals and against GFP from Rockland.

Culture of primary human skeletal muscle cells

Human skeletal muscle cells from five healthy donors (three males, 16, 21 and 47 years old; two females, 33 and 37 years old) were supplied as proliferating myoblasts (PromoCell, Lonza and Tebu). For an individual experiment, myoblasts were seeded in six-well culture dishes at a density of 1×105 cells/well and cultured to near-confluence in α-modified Eagle's medium (αMEM)/Ham's F-12 medium containing skeletal muscle cell growth medium supplement (PromoCell). The cells were then differentiated in αMEM containing 2% (vol/vol) horse serum (Gibco) until day 5 of differentiation and followed by overnight starvation in αMEM without serum.

Culture of murine C2C12 cells

C2C12 myoblasts were seeded in six-well culture dishes at a density of 1×105 cells/well and cultured to near-confluence in DMEM, high glucose containing 10% (vol./vol.) fetal calf serum (FCS). The cells were then differentiated in DMEM containing 2% (vol./vol.) horse serum until day 5 of differentiation and followed by overnight starvation in DMEM without serum.

Detection of irisin

Supernatants of primary human and C2C12 myotubes were collected for 24 h in serum free medium. The medium was centrifuged at 1,100 rpm for 5 min and afterwards concentrated using centrifugal filter devices with a cut off of 3 kDa (Millipore). Irisin protein levels in concentrated supernatants were quantified using EIA kit from Phoenix Pharmaceuticals according to the manufacturer´s instructions.

Electrical pulse stimulation

EPS was applied to fully differentiated myotubes in six-well dishes using a C-Dish combined with a pulse generator (C-Pace 100; IonOptix). The instrument emits bipolar stimuli to the carbon electrodes of the C-dish, which are placed in the cell culture medium. The human skeletal muscle cells were stimulated (1 Hz, 2 ms, 11.5 V) for 24 h after overnight starvation in serum-free αMEM [30]. The medium was changed directly before stimulation.

Human interval training study (endurance training)

Skeletal muscle biopsies were obtained from a subgroup of 6 untrained men (aged 40.8 ± 2.1 years; BMI: 26.1 ± 1.8 kg/m2) before and after 10 weeks of aerobic interval training (NCT00839579) [48]. Shortly, the participants performed endurance training on a treadmill 4 × 4 min intervals at ~90% of maximum heart frequency (HRpeak) with 3 min active recovery period at ~70% of HRpeak between each interval, 3 times weekly. Needle biopsies of m. vastus lateralis of fasting subjects were obtained at least 4 days after the last training session. Total RNA was extracted using Trizol and RNeasy Mini kit (Qiagen).

Human strength training study

Seven healthy, untrained men (aged 28.3 ± 4.2 years; BMI: 23.1 ± 2.4 kg/m2) participated in a strength-training program 3 times weekly for 11 weeks [32,49]. Before study start and at least 48 h after the last training session, needle biopsies were obtained from m. trapezius. Total RNA was prepared based on a modified version of the method described by Chomczynski and Sacchi [50].

Adipocyte culture and immunodetection

Subcutaneous AT was obtained from healthy lean or moderately overweight women (aged 40.4 ± 4.2 years, BMI 28.0 ± 1.1, n = 17) undergoing plastic surgery. Preadipocytes were isolated by collagenase digestion of AT as previously described by our group [51]. Isolated cell pellets were resuspended in basal medium (DMEM/F12 medium supplemented with 14 nmol/l NaHCO3, 33 mmol/l biotin, 17 mmol/l D-panthothenic-acid and 10% (vol./vol.) FCS, pH 7.4), seeded in six-well plates and maintained at 37°C with 5% CO2. After cells were grown until confluence, cultures were washed and further incubated in an adipocyte differentiation medium (basal medium supplemented with

66 nM insulin, 1 nM triiodo-L-thyronine, 100 nM cortisol, 10 mg/ml apo-transferrin, 50 mg/ml gentamycin) for 14 days. Medium was changed every 2–3 days with addition of 5 µM troglitazone for the first three days. Adipocytes were incubated with 50 ng/ml BMP7 (R&D systems), 200 and 1000 ng/ml FNDC5 (Abnova and Phoenix), 60 and 600 ng/ml irisin (Phoenix), and 60 and 600 ng/ml irisin (Cayman Chemical) during differentiation, respectively. Immunoblotting of lysates was performed as described in [30]. Oxphos antibody cocktail was provided by MitoSciences.

RNA-isolation and quantitative real-time PCR

Cells were lysed by Tripure (Roche Applied Science), RNA was isolated and reverse-transcribed using kits (RNeasy Mini, Omniscript Reverse Transcription, Qiagen) according to the manufacturer's instructions. Gene expression was determined by quantitative real-time PCR using primers as described in Table S1 and GoTaq qPCR Master Mix (Promega) with 0.016 to 20.00 ng cDNA on a cycler (Step One Plus; Applied Biosystems). Expression of the investigated genes was normalised to actin or GAPDH and analysed via the ΔΔCt method.

For human muscle biopsy samples, total RNA was reversely transcribed into cDNA on a Gene Amp PCR 9700 thermal cycler with the High Capacity cDNA reverse Transcription kit (Applied Biosystems Foster City, CA). Quantitative real-time PCR was performed with reagents and instruments from Applied Biosystems in the 96-well format using a 7900HT Fast instrument and the SDS 2.3 software (Applied biosystems) [52]. Predeveloped primers and probe sets (TaqMan assays, Applied Biosystems) were used to analyze mRNA levels of FNDC5 (Hs00401006_m1) and large ribosomal protein P0 (RPLP0, Hs99999902_m1). Relative target mRNA expression levels were calculated as 2-[Ct(target)-Ct(RPLP0))], thereby normalizing data to endogenous control RPLP0. For expression studies in human tissues the human FNDC5 probe set Hs00401006 from Life Technologies Corporation was used. Total RNA samples from different human tissues were purchased from Clontech Laboratories, Inc.

Microfluidic card TaqMan gene expression assay

RNA integrity was tested on an Agilent 2100 Bioanalyzer using Agilent RNA Nano chips. Only RNAs with a RIN score of 7.5 or higher were used for analysis. Synthesis of cDNA was done from 0.5 µg of each total RNA preparation in a volume of 20 µl with the Quantitect Reverse Transcription Kit from Qiagen according to the manufacturer's instructions. Thermal cycling of the PCR reactions was done in microfluidic cards on a ViiA7 Real Time PCR 384 well cycler and fluorescence plate reader from Applied Biosystems (see Table S2 for details on used gene specific TaqMan assays).

Statistics

Data are expressed as mean ± SEM. One-way ANOVA (post-hoc test: Tukey's multiple comparison test) and unpaired student's t-test were used to determine statistical significance. All statistical analyses were done using GraphPad Prism 5 considering a p-value of less than 0.05 as statistically significant.

Results

Start codon of FNDC5 gene is mutated in humans

A multi-species sequence alignment of the *FNDC5* exon 1 demonstrated that *FNDC5* genes from different species like rat, mouse, gibbon, gorilla and chimp display a conserved ATG translation start site, except for the human sequence (Figure 1A). In contrast, at the position of the start codon the human sequence shows an ATA, encoding isoleucin (I), instead of the conserved ATG, encoding methionine (M). Using 5′-RACE-PCR, we could confirm experimentally the mutation within the start codon as ATA in human brain and skeletal muscle samples (Figure S1). According to the current UniProt entry Q8NAU1 (Figure 1B, FNDC5_human_c) this is potentially a non-canonical start site and could still produce to full-length FNDC5, which might be later proteolytically cleaved to release irisin.

Before translation start, the ribosome recognizes a conserved mRNA sequence as the start site for protein translation, called Kozak consensus sequence (GCCXCCATGG, X=A or G). However, Kozak *et al*. showed that a mutated start codon to ATA, even in a perfect context (GCCXCCATAG, X=A or G, Figure 1A), was highly unlikely to serve as a translation site and resulted in low translation efficiency [26]. The next in-frame downstream ATG (M, marked in red in Figure 1B) is a non-Kozak ATG and located within the sequence that was annotated as irisin (irisin sequence marked in blue, Figure 1B). Thus, an N-terminal truncated FNDC5 (represented by cDNA sequences NP_715637/NM_153756) and truncated irisin would be generated. In addition there are three upstream partial Kozak ATGs in this mRNA that are not in frame with the *FNDC5* open reading frame (ORF) and would therefore strongly reduce translation from this new start site (Figure S3). It has been experimentally shown that the translation efficiency of non-canonical sites can be increased, if a hairpin slows down the scanning ribosome [27], as described for FGF2 (Figure S4A). Based on this observation, an ATG hairpin

program predicts if there are stem-loop structures in an appropriate distance to the ATA [28], which would increase the translation efficiency. However, for human *FNDC5* no eligible hairpin structures were found (Figure S4B).

A comparison of the full-length human FNDC5 protein sequence published by Boström *et al*. (Figure 1B, FNDC5_human_o, [21]) with mRNA, expressed sequence tags, genomic DNA and single-nucleotide polymorphism data revealed that the first three amino acids (MRR, Figure 1B) do not match human genomic DNA. We excluded that this is due to differential splicing, because 20 expressed sequence tags and two Ref_Seq cDNAs that cover this region, perfectly matched the annotated exon 1 region (Figure S2). We analyzed public single-nucleotide polymorphism data, but could not find a reference that this codon might be altered.

A

```
Exon1_human     ----------GCGGCCGCCGGGC-GCCGGAGCCGCGTCCCCCTGCGCCGCCCCGGGC--C
Exon1_chimp     ----------GCGGCCGCCGGGCGCCGGAGCCGCGTCCCCCTGCGACGCCCCGGGCC---
Exon1_gorilla   ----------GCGGCCGCCGGGC-GCCGAAGCCGCGTCCCCCTGCGCCGCCCCGGGC--C
Exon1_gibbon    ----------GCGGCCGCCGGGC-GCCGGAGCCGCGTCCCCCTGCGCCGCCCCGGGC--C
Exon1_mouse     GGGGCGGCGCGGGGCGGCCGGGCCGGGAGGGCCGCGGGCTGGAGCGTGAGTGCGAGCGGT
Exon1_rat       GGGGCGGCGCGGGGCGGCCCGGCCAAGAAAAACGCGGGCTGGAGCGAGAGTGCGAGCGGT

Exon1_human     TGCCGGCCGGAGGAGCCACCATACACCCCGGGTCGCCGAGCGCCTGGCCGCCCCGCGCCC
Exon1_chimp     TGCCGGCCGGAGGAGCCACCATGCACCCTGGGTCGCCGAGCGCCTGGCCGCCCCGCGCCC
Exon1_gorilla   TGCCGGCCGGAGGAGCCACCATGCACCCCGGGTCGCCGAGCGCCTGGCCGCCCCGCGCCC
Exon1_gibbon    TGCCGGCCGGAGGAGCCACCATGCACCCCGGGTCGCCCAGCGCCTGGCCGCCCCGCGCCC
Exon1_mouse     CACCGGGCCCAGGAGTCGCCATGCCCCCAGGG---CCGTGCGCCTGGCCGCCCCGCGC--
Exon1_rat       CACCCGGCGTAGGAGCCGCCATGCCCCCAGGG---CCGTGCGCCTGGCCGCCCCGCGC--
                                      ↓  ↓  ↓
                                     -3 +1 +4
```

B

```
FNDC5_HUMAN_o                   MRRWLGCVCFALVQADSPSAPVNVTVRHLKANSAVVSWDVLEDE
FNDC5_HUMAN_c   IHPGSPSAWPPRARAALRLWLGCVCFALVQADSPSAPVNVTVRHLKANSAVVSWDVLEDE
FNDC5_chimp     MHPGSPSAWPPRARAALRLWLGCVCFALVQADSPSAPVNVTVRHLKANSAVVSWDVLEDE
FNDC5_gorilla   MHPGSPSAWPPRAHAALRLWLGCVCFALVQADSPSAPVNVTVRHLKANSAVVSWDVLEDE
FNDC5_gibbon    MHPGSPSAWPPRARAALRLWLGCVCFALVQADSPSAPVNVTVRHLKANSAVVSWDVLEDE
FNDC5_MOUSE     -MPPGPCAWPP--RAALRLWLGCVCFALVQADSPSAPVNVTVRHLKANSAVVSWDVLEDE
FNDC5_RAT       -MPPGPCAWPP--RAALRLWLGCVCFALVQADSPSAPVNVTVRHLKANSAVVSWDVLEDE

FNDC5_HUMAN_o   VVIGFAISQQKKDVRMLRFIQEVNTTTRSCALWDLEEDTEYIVHVQAISIQGQSPASEPV
FNDC5_HUMAN_c   VVIGFAISQQKKDVRMLRFIQEVNTTTRSCALWDLEEDTEYIVHVQAISIQGQSPASEPV
FNDC5_chimp     VVIGFAISQQKKDVRMLRFIQEVNTTTRSCALWDLEEDTEYIVHVQAISIQGQSPASEPV
FNDC5_gorilla   VVIGFAISQQKKDVRMLRFIQEVNTTTRSCALWDLEEDTEYIVHVQAISIQGQSPASEPV
FNDC5_gibbon    VVIGFAISQQKKDVRMLRFIQEVNTTTRSCALWDLEEDTEYIVHVQAISIQGQSPASEPV
FNDC5_MOUSE     VVIGFAISQQKKDVRMLRFIQEVNTTTRSCALWDLEEDTEYIVHVQAISIQGQSPASEPV
FNDC5_RAT       VVIGFAISQQKKDVRMLRFIQEVNTTTRSCALWDLEEDTEYIVHVQAISIQGQSPASEPV

FNDC5_HUMAN_o   LFKTPREAEKMASKNKDEVTMKEMGRNQQLRTGEVLIIVVVLFMWAGVIALFCRQYDIIK
FNDC5_HUMAN_c   LFKTPREAEKMASKNKDEVTMKEMGRNQQLRTGEVLIIVVVLFMWAGVIALFCRQYDIIK
FNDC5_chimp     LFKTPREAEKMASKNKDEVTMKEMGRNQQLRTGEVLIIVVVLFMWAGVIALFCRQYDIIK
FNDC5_gorilla   LFKTPREAEKMASKNKDEVTMKEMGRNQQLRTGEVLIIVVVLFMWAGVIALFCRQYDIIK
FNDC5_gibbon    LFKTPREAEKMASKNKDEVTMKEMGRNQQLRTGEVLIIVVVLFMWAGVIALFCRQYDIIK
FNDC5_MOUSE     LFKTPREAEKMASKNKDEVTMKEMGRNQQLRTGEVLIIVVVLFMWAGVIALFCRQYDIIK
FNDC5_RAT       LFKTPREAEKMASKNKDEVTMKEMGRNQQLRTGEVLIIVVVLFMWAGVIALFCRQYDIIK

FNDC5_HUMAN_o   DNEPNNNKEKTKSASETSTPEHQGGGLLRSKI
FNDC5_HUMAN_c   DNEPNNNKEKTKSASETSTPEHQGGGLLRSKI
FNDC5_chimp     DNEPNNNKEKTKSASETSTPEHQGGGLLRSKI
FNDC5_gorilla   DNEPNNNKEKTKSASETSTPEHQGGGLLRSKI
FNDC5_gibbon    DNEPNNNKEKPKSASETSTPEHQGGGLLRSKI
FNDC5_MOUSE     DNEPNNNKEKTKSASETSTPEHQGGGLLRSKI
FNDC5_RAT       DNEPNNNKEKTKSASETSTPEHQGGGLLRSKI
```

Figure 1. The human FNDC5 gene differs from other species by a mutation in the start codon. *(A) Multiple alignment of the exon 1 sequences: the conserved partial Kozak ATG start sequence of FNDC5 is bold and red. The mutated ATG to ATA in human is bold and blue. There is no other ATG present in exon 1. (B) Multiple sequence alignment of FNDC5 proteins of different species including two human versions. FNDC5_human_o: sequence published by Boström et al.; FNDC5_human_c: current version in Uniprot; red M = start methionines including the potential downstream human start site; light blue = irisin sequence; blue I = mutated start site claimed to be a non canonical start site; purple LRL = sequence shown in UniProt (Q8NAU1_old) as MRR. The underlined sequence indicates the transmembrane part of the protein. Green sequence = peptide used for the generation of the Abcam FNDC5 antibody.*

Full-length human FNDC5 with ATA as start codon is not translated into protein

Nevertheless, *FNDC5* mRNA is expressed in human tissues, predominantly in the heart, less in muscle and brain (Figure S5). In certain cases, translation initiation can occur at codons differing from ATG by a single nucleotide, like ATA [25]. To verify whether human FNDC5 was translated into full-length protein with a non-ATG initiation, the human gene was cloned into the expression vector pcDNA5-FRT TO-cEGFP. In addition to this vector with ATA as start codon (ATA-hFNDC5-GFP), a second vector with ATG as classical start codon (ATG-hFNDC5-GFP) (Figure S6) and as a control murine FNDC5 (mFNDC5-GFP) was cloned. All vectors were transfected into HEK293 cells.

Although transient transfection of HEK293 cells with the expression vectors of mFNDC5-GFP and ATG-hFNDC5-GFP resulted in a clearly detectable fluorescence signal due to the expression of GFP-FNDC5 fusion protein, most importantly, for ATA-hFNDC5-

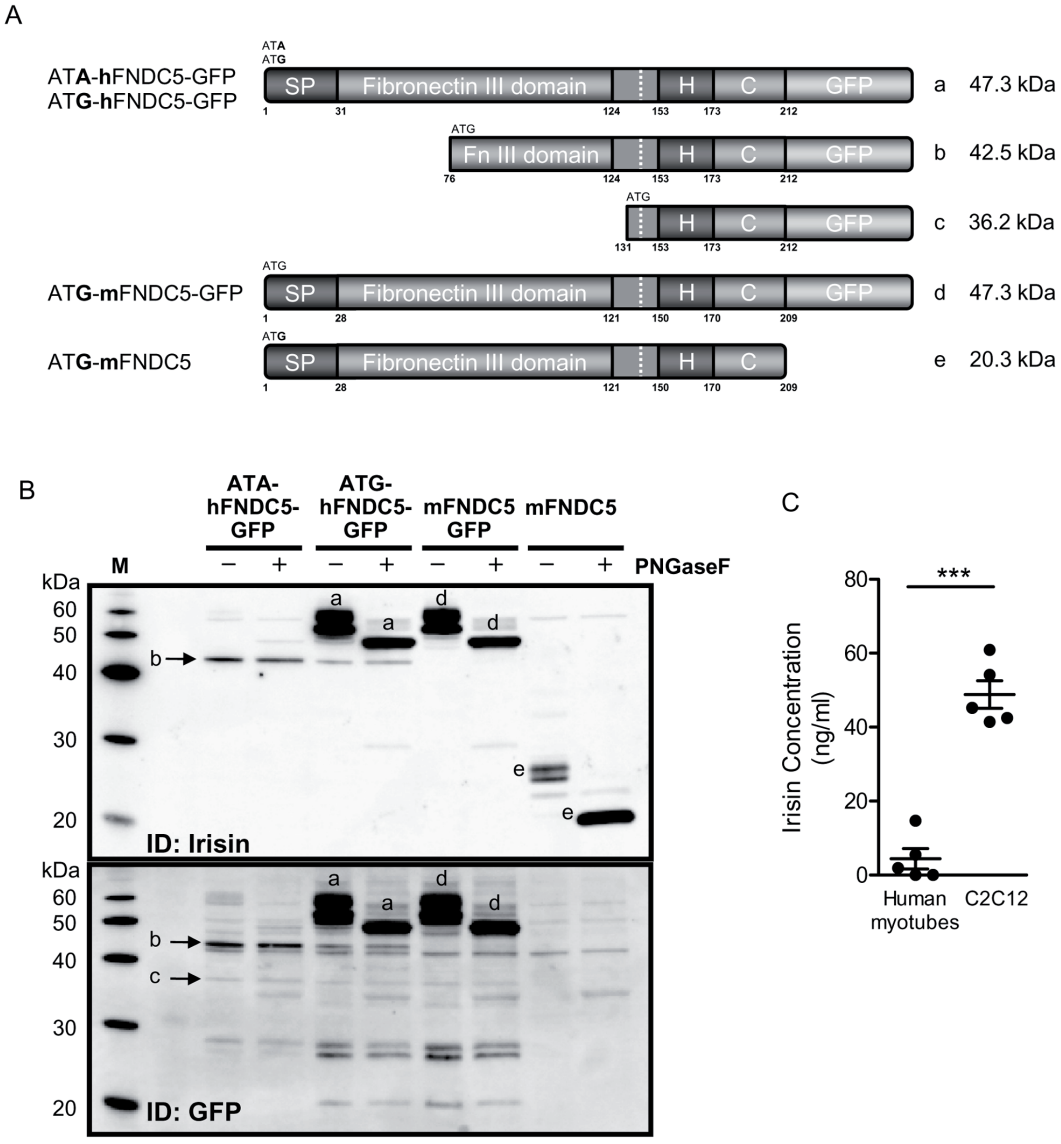

Figure 2. Human FNDC5 with an ATA start codon is translated into full-length protein only at very low abundance. *(A) Schematic representation of the predicted FNDC5 protein structures. Using the first ATG/ATA as start codon of human FNDC5 tagged with GFP would result in full-length FNDC5 protein (a). The use of downstream ATG as start codon would result in truncated FNDC5 protein isoforms (b and c). Murine FNDC5 with ATG as start codon tagged with GFP (d) or without GFP (e). (B) Expression of FNDC5 in HEK293 cells. Cells transfected with constructs containing human FNDC5-GFP gene with ATA and ATG as start codon as well as mouse FNDC5-GFP gene were analyzed 24 h after transfection. Cell lysates were analyzed by immunodetection using antibodies against irisin/FNDC5 and GFP. Cell lysates were treated with PNGaseF to deglycosylate proteins. (C) Supernatants of primary human and C2C12 myotubes were collected for 24 h in serum-free medium and concentrated 60fold using centrifugal filter devices. Irisin protein levels in concentrated supernatants were measured using EIA kit. Medium alone showed no cross-reactivity with the kit; n = 5, *** $p < 0.001$.*

GFP transfected cells the signal was hardly detectable (Figure S7A, B).

Analysing the protein level of transfected HEK293 cells revealed that the human construct with ATG as start codon produced similar amounts of full-length protein compared to murine FNDC5. The protein can be detected in two distinct bands of 52 and 56 kDa as shown by western blot analysis (Figure 2B). Full-length FNDC5 protein seems to be glycosylated, because incubation of cell lysates with N-glycosidase F (PNGase F) resulted in merging of the two bands into one signal with a significantly decreased size of 48 kDa. In contrast, the human transcript with ATA as start codon resulted only in 1% full-length protein as compared to ATG-hFNDC5-GFP. Instead the downstream in-frame ATG (represented by NP_715637, starting with MLRFIQEVN, Figure 2A (b)) was translated into a protein missing the first 76 amino acids. However, this ATG was used with strongly reduced efficiency and was apparently not glycosylated.

Additionally, at a molecular size of 36 kDa a very weak band was detected possibly representing the second downstream ATG of human FNDC5 (aa131) or murine FNDC5 (aa128), (Figure 2A (c), starting with MASKNKDE, Figure 1B).

A comparison of the irisin protein levels released by differentiated primary human skeletal muscle cells compared to murine C2C12 cells showed substantially lower irisin protein levels in the supernatant of human cells compared to murine cells (Figure 2C).

FNDC5 gene is not activated by contraction in humans

PGC1α gene expression is induced in muscle by exercise [29] and *FNDC5* gene expression was reported to be PGC1α-dependent in mice [21]. To study contraction-regulated gene expression, we previously developed an in vitro contraction model using electrical pulse stimulation (EPS) of primary human skeletal muscle cells [30]. By using this EPS model, *PGC1α* mRNA expression was significantly enhanced after 24 h of EPS in primary human skeletal muscle cells (1.5fold, Figure 3A). However, *FNDC5* mRNA expression was not altered (Figure 3A). This EPS-protocol, induced a significant upregulation of *MYH7* mRNA level (encoding myosin heavy chain (MHC) isoform 1 protein, 1.6fold), while *MYH2* (encoding MHC2a) and *MYH1* (encoding MHC2x) were unaltered (Figure 3B).

The gene expression of *FNDC5* in human muscle biopsies was examined before and after extensive and documented training in two different cohorts. We

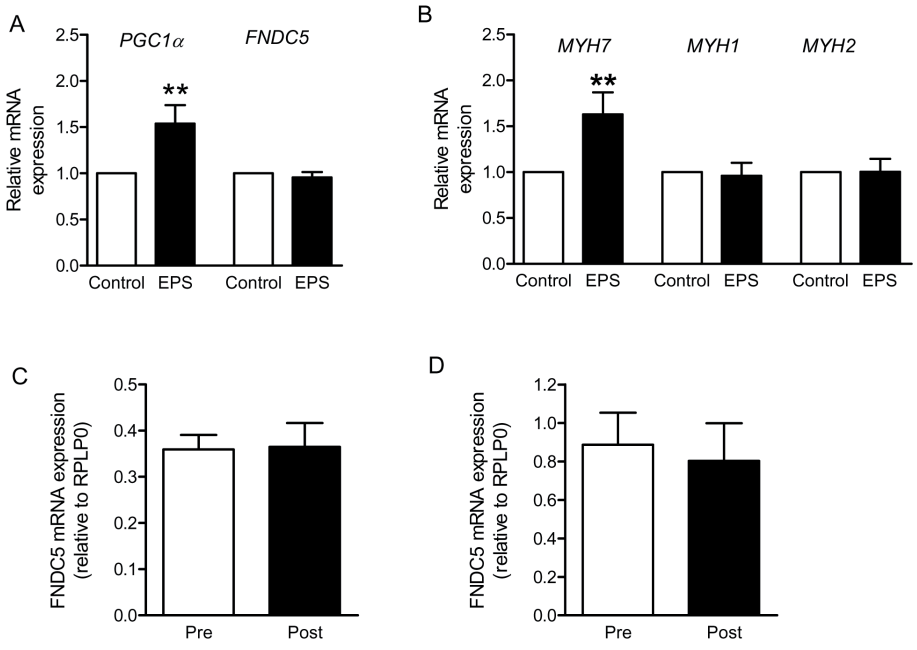

Figure 3. FNDC5 mRNA level is not contraction-regulated in skeletal muscle cells and is not increased by endurance or strength training in humans. *(A) and (B) Primary human skeletal muscle cells were differentiated in αMEM containing 2% (vol./vol.) horse serum, followed by overnight starvation, and subjected to EPS for 24 h in serum-free medium (1 Hz, 2 ms, 11.5 V). Relative gene expression of PGC1α, FNDC5 (A), MYH1, 2, and 7 (B) was measured by quantitative real-time PCR (qRT-PCR). All expression data were normalized to actin; n=5 (A), n=10 (B); **p < 0.01. White bars, control (non-EPS); black bars, EPS. (C) qRT-PCR analysis of FNDC5 expression in m. vastus lateralis from young sedentary males before (Pre) and after 10 weeks (Post) of aerobic interval training (n = 6). (D) qRT-PCR analysis of FNDC5 expression in m. trapezius from sedentary males before (Pre) and after 11 weeks (Post) of strength training (n = 7). All expression data were normalized to RPLP0. Data are presented as mean values ± SEM.*

found no *FNDC5* gene activation by neither 10 weeks of interval endurance training among 41±2 years old males (Figure 3C) nor 11 weeks of strength training in 28±4 years old males with normal body weight (Figure 3D).

Recombinant FNDC5 and irisin have no effect on the brite differentiation of human preadipocytes

We isolated preadipocytes from primary human subcutaneous AT and differentiated these cells to mature adipocytes in the presence of recombinant FNDC5 (200 ng/ml), irisin (60 ng/ml) or BMP7 (50 ng/ml) as a positive control, respectively. FNDC5 was obtained from Abnova, which also was used by Boström *et al*. [21] and Wu *et al*. [31]. In addition, we used recombinant FNDC5 protein obtained from Phoenix.

BMP7 potently induced a brite gene program in cultured adipocytes. Incubation with BMP7 during differentiation induced an increased expression of the general differentiation marker for adipogenesis PPARγ (3.6fold) (Figure 4A). Notably, *UCP1*, known as a brite marker, was even stronger enhanced (6.4 fold, Figure 4A). Additionally, the mRNA expression of *TCF21* [20], a marker for white AT, was significantly reduced after BMP7 incubation (Figure 4A). *ZIC1* is a marker for classical brown AT of myogenic origin in mice [20] and its expression was unaltered after BMP7 incubation of human adipocytes (Figure 4A). Neither recombinant FNDC5 nor irisin had an effect on mRNA expression of *PPARγ, UCP1, TCF21* or *ZIC1* (Figure 4A).

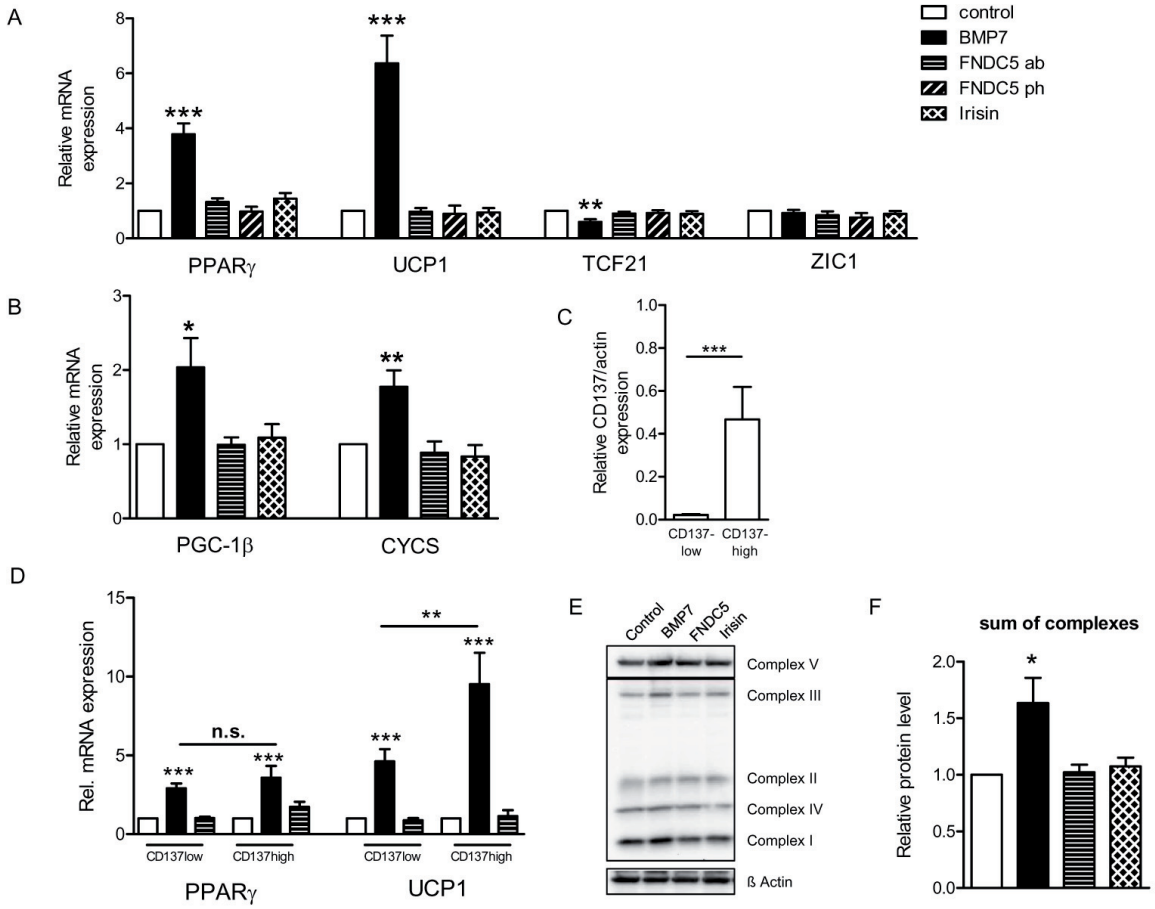

Figure 4. BMP7 activates the brite fat gene program in human adipocytes, but not FNDC5 and irisin. *Isolated preadipocytes from human subcutaneous preadipocytes of different donors were differentiated in the presence of 50 ng/ml BMP7, 200 ng/ml FNDC5 (Abnova), 200 ng/ml FNDC5 (Phoenix) and 60 ng/ml irisin (Phoenix). (A) Relative gene expression of PPARγ, UCP1, TCF21 and ZIC1 was measured by qRT-PCR after 12-14 days of differentiation. All expression data were normalized to actin; n≥4; ***p < 0.001. (B) PGC1β and CYCS mRNA expression was assessed by using microfluidic card TaqMan gene expression assay, n ≥ 4, *p < 0.05, **p < 0.01. (C) Relative gene expression of CD137 was measured by qRT-PCR on day 0 of differentiation; n=12; ***p < 0.001. (D) The increase of UCP1 and PPARγ expression in six individual donors was compared after BMP7 and FNDC5 (Abnova) incubation, respectively. Preadipocytes with high CD137 expression showed a more robust activation of UCP1 compared to PPARγ after BMP7 incubation. (E) Cell lysates were analysed by immunodetection using an oxidative phosphorylation antibody cocktail. A representative blot is shown. (F) Signal intensities of all complexes of the oxidative phosphorylation were quantified, summed up and normalized to ß-actin, n=3-5, *p < 0.05. (A-F) White bars, control; black bars, BMP7; horizontally hatched bar, FNDC5 (Abnova), diagonally hatched bar, FNDC5 (Phoenix); crossed bar, irisin. Data are presented as mean values ± SEM.*

In addition to *UCP1*, the transcription factor *PGC1β*, which regulates mitochondrial biogenesis, and *CYCS* (cytochrome c), an electron carrier protein of the mitochondrial electron transport chain, were both significantly enhanced by incubation with BMP7 (Figure 4B), while FNDC5 and irisin did not alter the mRNA level of these targets. Even higher concentrations of recombinant FNDC5 (1000 ng/ml) and irisin (600 ng/ml) as well as recombinant irisin obtained from a second company (Cayman Chemical, 60 and 600 ng/ml) had no effect on UCP-1 and PPARγ mRNA level (Figure S8).

The most prominent effect on *UCP1* mRNA expression was observed in cells highly expressing *CD137*, a novel recently described marker of preadipocytes which are susceptible to browning [31] (Figure 4C, D). Our present study includes experiments with adipocytes of more than 10 different donors. Analyzing expression of *CD137* on day 0 revealed that the donors may be clustered in a *CD137*-low expressing and a *CD137*-high expressing group (Figure 4C). *CD137*-high expressing adipocytes were more sensitive to BMP7-induced brite differentiation, as indicated by a higher *UCP1* induction compared to the expression of the general differentiation marker *PPARγ* (Figure 4D). In marked contrast to the gene activation by BMP7, no effect of FNDC5 and irisin on classical brown and brite AT markers could be observed (Figure 4A, B). The *CD137* expression level had no impact on the FNDC5 response of adipocytes (Figure 4D). Moreover, we monitored the protein level of all four complexes of the mitochondrial respiratory chain and the ATP synthase to evaluate the results of the expression of mitochondrial target genes. Incubation of adipocytes with BMP7 during differentiation led to significantly enhanced mitochondrial protein level (1.6fold), while FNDC5 and irisin had no effect (Figure 4E, F).

In order to assess the potential induction of genes by FNDC5 and irisin which are different from those previously measured (Figure 5), we performed a microfluidic card TaqMan gene expression assay including 37 genes associated with adipocyte differentiation or browning. Several genes were upregulated by incubation with BMP7 during differentiation including adiponectin (*ADIPOQ*), *C/EBPα*, *FABPB4*, leptin (*LEP*), and perilipins (*PLIN1, 2, 4* and *5*) (Figure 5A).

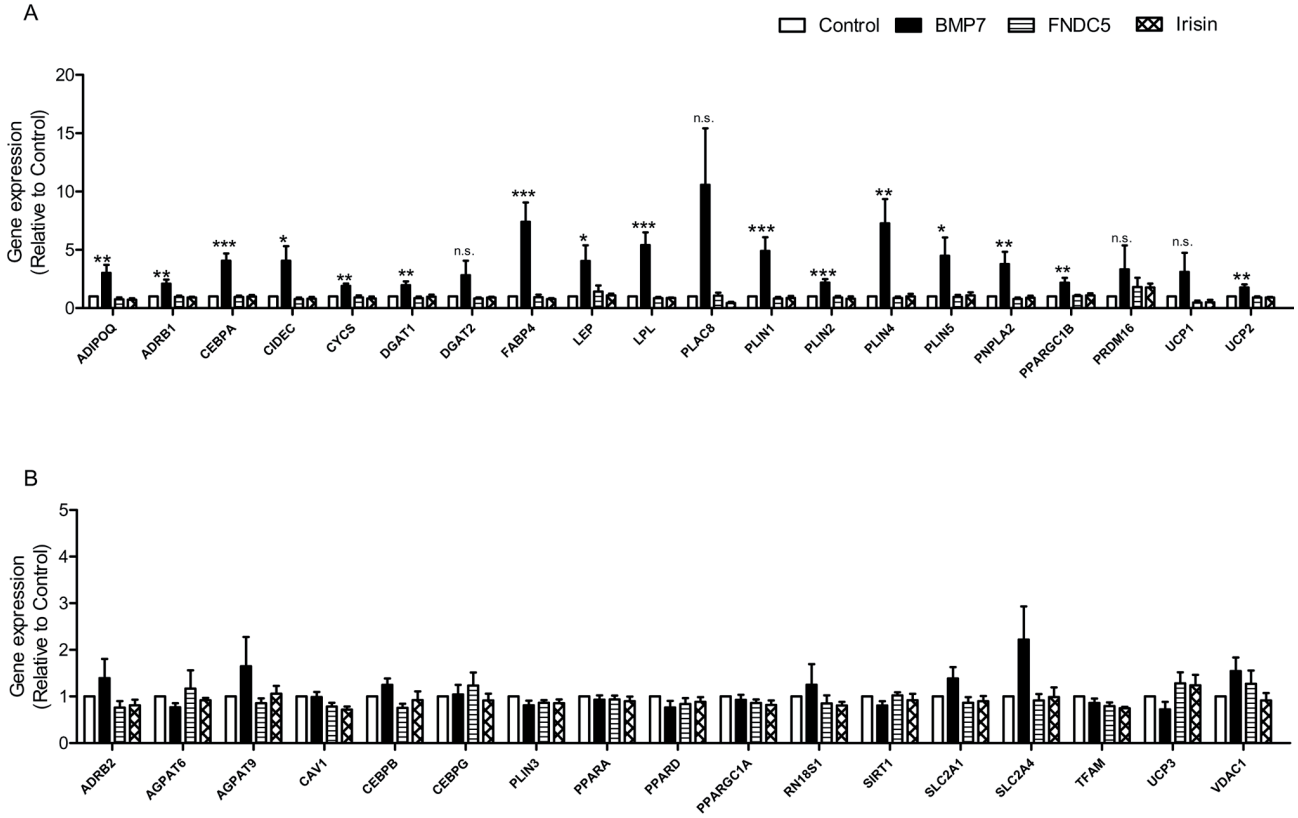

Figure 5. Gene expression analysis of human adipocytes after incubation with BMP7, FNDC5 and irisin. *Isolated preadipocytes from human subcutaneous AT of different donors were differentiated in the presence of 50 ng/ml BMP7, 200 ng/ml FNDC5 (Abnova), and 60 ng/ml irisin (Phoenix). Gene expression of 40 genes, related to adipocyte differentiation (A) and brite differentiation (B), was assessed by a microfluidic card TaqMan gene expression assay; n ≥ 4, *p < 0.05, **p < 0.01, ***p < 0.001 vs control; n.s., not significant. White bars, control; black bars, BMP7; horizontally hatched bar, FNDC5; crossed bar, irisin. Data are presented as mean values ± SEM.*

None of these genes were differentially regulated by FNDC5 or irisin. Genes that were not regulated by BMP7, FNDC5 and irisin are presented in figure 5B.

Discussion

Targeting irisin and its downstream signaling pathways might represent an interesting strategy to increase energy expenditure in humans and to combat obesity by inducing browning of white AT. Due to a high homology between the murine and human DNA sequence, it has been speculated that translation from the mouse model to a human therapeutic approach is possible. Boström *et al*. stated that the cleaved and released part of FNDC5, the hormone irisin, is highly conserved and identical in all mammalian species sequenced [21]. Indeed, the *FNDC5* gene is well conserved between organisms with one exception reported here, namely a mutation in the start codon of the human gene.

Examining the human genomic sequence revealed that the start from UniProt entry FNDC5/Q8NAU1 (full-length protein as described by Boström *et al*. [21]) is not matched by an ATG codon and that the upstream conserved ATG of other species is mutated to an ATA codon in humans. Ivanov *et al*. performed an algorithm based analysis of the 5'-UTRs of human GenBank RefSeq mRNAs to find non-ATG start codons in humans [25]. They used sequences 5′ of the annotated start-codon and compared these to other vertebrate sequences. In this bioinformatic analysis FNDC5 ranks high in their list, as the 5′ human amino acid sequence is almost identical to that in mouse.

Nevertheless, Kozak *et al*. have shown the presence of ATA causes low translation efficiency [26]. ATG hairpin program predicted no eligible stem-loop structure or hairpin for human *FNDC5*. These hairpin structures could increase the translation efficiency by slowing down the scanning process as helicases need time to resolve these structures and give the ribosome more time to misread the codon as an ATG start codon [27]. In higher eukaryotes non-canonical start sites are rare. A search using Uniprot and a specialized website that is based on NCBI data for annotated non-canonical ATA start sites (http://bioinfo.iitk.ac.in), resulted in only three human genes, which are translated to the protein level (Q02447, Q15561, Q99594).

Nevertheless, to challenge this bioinformatic analysis, we monitored the ability of the human transcript to be translated into protein. Overexpression of human FNDC5 in HEK293 cells with ATA as start codon provided the conclusive proof on the protein level. HEK293 cells transfected with the human expression vector using ATG as start codon produced similar amounts of full-length protein compared to mouse FNDC5. In contrast, the human transcript with ATA as start codon resulted in only 1% full-length protein compared to mouse FNDC5. Instead the downstream in-frame ATG (represented by the cDNA sequence NP_715637) was translated into protein. However, this ATG was used with highly reduced efficiency. Using this downstream ATG, the protein has lost the signal peptide, which leads proteins towards the secretory pathway, and almost 50% of the irisin sequence. Using an optimized expression system with a strong promoter as described here is certainly not reflecting the natural situation in human tissue. Our data support that in humans no or only very low translation of human *FNDC5* mRNA into protein is occurring and primarily a truncated version without signal peptide is produced. Consequently, irisin should not be detectable or at rather low concentrations.

Thus, we suggest that the human *FNDC5* gene might be a transcribed pseudogene that has substantially lost the ability to be translated into the full-length FNDC5 protein and possibly is unable to be processed to irisin. As a result, the mutation in the start codon of the human *FNDC5* gene may result in low translation efficiency and might explain the small release of irisin observed from primary human myotubes as compared to murine myotubes.

Physical activity promotes a more oxidative phenotype in skeletal muscle and is characterized by increased expression of *PGC1α* in skeletal muscle [29], which may enhance expression of *FNDC5* [21]. Inducing contractile activity in our in vitro model led to significantly enhanced secretion of the well-known myokines interleukin-6 and vascular endothelial growth factor [30]. Although using this protocol led to enhanced *PGC1α* expression in human myotubes, this did not result in a significantly enhanced *FNDC5* expression. This EPS model rather reflects a training model than acute exercise as shown by enhanced *MHCI* mRNA level and enhanced mitochondrial content [30]. Similar results were obtained from two different training cohorts. Neither 10 weeks of interval endurance training nor 11 weeks of strength training in healthy men resulted in increased *FNDC5* mRNA expression in skeletal muscle biopsies. However, strength training significantly upregulated the secretion of at least 11 myokines in m. trapezius such as plasminogen activator inhibitor 1, follistatin-like 1 and secreted protein, acidic and rich in cysteine [32]. Boström *et al*. observed enhanced *FNDC5* mRNA levels (2-fold) in a cohort of older, obese subjects after a 10-weeks pro-

tocol of endurance exercise [21]. However, using gene-chip probe sets Timmons *et al*. demonstrated that *FNDC5* induction in skeletal muscle occurred only in highly active elderly subjects compared to sedentary controls (1.3fold), which were a minority of examined subjects. Moreover, they failed to confirm increased *FNDC5* gene expression after aerobic exercise in younger subjects [33].

Another study showed that circulating irisin levels were only slightly increased (about 1.2fold) after 2 or 3 sets of double sprints after one week and not after 8 weeks of exercise [34]. However, this study measured circulating irisin levels after exercise in human plasma by using a commercially available ELISA kit. The reported irisin levels in human blood samples [34–37] are in conflict to our notion that human FNDC5 is not translated into full-length protein due to the non-ATG start codon. We recommend that these data has to be considered with caution and that available ELISA/EIA kits have to be reappraised by other methods e.g. mass spectrometry analysis.

Boström *et al*. [21] and Sharma *et al*. [38] used Western blot analyses to detect irisin in human and murine serum. The antibody used by the authors was obtained by Abcam and specifically detects the C-terminal region of the FNDC5 protein (the peptide used for immunization/antibody synthesis was sequenced and is highlighted in Figure 1C). FNDC5 is described as a transmembrane protein with the C-terminal tail located in the cytoplasm, whereas the extracellular N-terminal part is supposed to be cleaved and released as irisin. Thus, an antibody binding to the C-terminal region of the FNDC5 protein is unlikely to detect irisin in plasma samples.

A study with heart failure patients determined higher expression of both *PGC1α* and *FNDC5* in subjects with high aerobic performance, whereas no correlation was found in patients with low aerobic performance [39]. Nevertheless, muscle-specific overexpression of PGC1α in transgenic mice showed a significant increase in FNDC5 mRNA level [21] which might suggest that a profound induction of PGC1α is necessary to activate the downstream target *FNDC5*. Until now, only Boström *et al*. have reported a robust activation of *FNDC5* after exercise in humans as measured by quantitative real-time PCR in skeletal muscle biopsies [21].

Exercise enhanced the appearance of putative brown adipocyte progenitor cells in brown AT [40] and was described as novel physiological stimulus for browning of visceral fat in mice after controlled treadmill running [41] and free wheel running [21]. Several lines of evidence have suggested that bone morphogenetic proteins (BMP) induce adipose cell fate determination in mammalian cells (reviewed in [42]). BMP7 specifically triggers commitment of the multipotent mesenchymal cells into the brown adipocytes lineage, inducing the expression of brown fat-specific markers such as *PRDM16* and *UCP1* [7]. Embryos of BMP7 knockout mice exhibit a marked deficiency of brown AT and nearly complete absence of *UCP1* expression while adenoviral-mediated expression of BMP7 in mice results in significant increase in brown, but not in white AT and leads to an increase in energy expenditure [7]. Primary human adipocytes differentiated in vitro have a low basal level of *UCP1* gene expression, as described for white AT [43]. However, incubation of primary human preadipocytes with BMP7 during differentiation leads to an increase in PPARγ expression and an even more pronounced increase in *UCP1* and *CYCS* expression as well as enhanced mitochondrial content resulting in a brite phenotype of the adipocytes. Since *ZIC1*, a marker for classical brown adipocytes [20], was not altered by incubation with BMP7 and *PRDM16* was barely detectable, the differentiated adipocytes subjected to BMP7 incubation display no classical brown phenotype. In addition, BMP7 incubation decreased *TCF21* mRNA level, a marker for white adipocytes [20].

Wu *et al*. isolated adipose progenitor cells from murine subcutaneous white AT, immortalized the cells, generated clonal cell lines derived from single cells and analyzed the gene expression pattern of multiple cell lines after induction of differentiation and treatment with forskolin [31]. They identified a distinct pool of progenitors within white AT that can give rise to cells expressing *UCP1* upon an adequate stimulus. These brown-like or "brite" cells are similar, but not identical, to classical brown fat cells and express brite-selective genes, including a developmental transcription factor (*Tbx1*), a component of lipid metabolism pathways (*Slc27a1*), as well as molecules known to be important in immune und inflammatory pathways (*CD40* and *CD137*). Thus, murine brite cells have a gene expression pattern distinct from either white or brown AT. CD137 was then used to define primary brite adipocyte precursors and *CD137*-high expressing cells showed substantially elevated expression of *UCP1* after incubation with irisin-Fc and recombinant FNDC5 compared to *CD137*-low expressing cells [31]. In our study we observed a 'britening' effect of human adipocytes after incubation with BMP7 with the most prominent effect in *CD137*-high expressing cells. However, neither recombinant FNDC5 nor the

cleaved protein irisin triggered a brite differentiation of adipocytes in *CD137*-high- or *CD137*-low-expressing cells. Our results are supported by data recently presented at the Annual Meeting of the American Diabetes Association by Lee *et al*. showing that neither FNDC5 nor irisin induces browning of human and mouse adipocytes [44].

Wu *et al*. examined the gene expression profile of brown fat from 11 adult humans and unexpectedly found that the profile was closer to that of mouse brite cells than to that of mouse classical brown cells [31]. However, the presence of classical brown AT in humans has recently been shown by three independent groups [43,45,46]. The gene expression of classical markers of mouse brown, brite, and white adipocytes in adult human brown AT isolated from the supraclavicular region [43] or anatomically defined neck fat [45] suggests that human brown AT might consist of both classical brown and recruitable brite adipocytes. In addition, Lidell *et al*. provide evidence for an anatomically distinguishable interscapular brown AT depot in human infants that consists of classical brown adipocytes [46]. When thinking about pharmaceutically targeting brown and brite AT as a therapeutic approach to counteract human obesity it is of importance to clearly identify the developmental origin of these tissues in humans. Moreover, Cannon and Nedergaard raised the question how certain white-like adipocytes, which in general possess very few mitochondria, suddenly enhance their mitochondrial complement during the britening process and from where these adipocytes originate [47]. These crucial key questions should be addressed in future studies.

In conclusion, human *FNDC5* should be annotated as a transcribed pseudo-gene that has lost the ability to be effectively translated into full-length FNDC5 protein. A shorter protein version is translated only with low efficiency, but this protein has lost the signal peptide and almost 50% of the irisin sequence. Could irisin nevertheless be a potential drug in humans if downstream regulatory pathways might still exist? We observed no effect of recombinant FNDC5 and irisin on the britening of primary human adipocytes. Thus, we conclude that the function of irisin proposed for mice is lost in humans.

Acknowledgements

We thank J. Liebau (Department of Plastic Surgery, Florence-Nightingale-Hospital, Düsseldorf, Germany) and C. Andree (Department of Plastic Surgery, Sana-Hospital, Düsseldorf-Gerresheim, Germany) for support in obtaining AT samples. We thank Christian Roos (Gene Bank of Primates, Primate Genetics Laboratory, Göttingen, Germany) for providing chimpanzees DNA samples. The secretarial assistance of B. Hurow and the technical help of A. Cramer, K. Klein, M. Schmalz, S. Otto, S. Kauffelt and A. Schlüter are gratefully acknowledged.

References

1. Lyon HN, Hirschhorn JN (2005) Genetics of common forms of obesity: a brief overview. Am J Clin Nutr 82: 215S-217S.

2. Velho G, Robert JJ (2002) Maturity-onset diabetes of the young (MODY): genetic and clinical characteristics. Horm Res 57 Suppl 1: 29-33.

3. Naik RG, Brooks-Worrell BM, Palmer JP (2009) Latent autoimmune diabetes in adults. J Clin Endocrinol Metab 94: 4635-4644.

4. James W, Jackson-Leach R, Mhurchu CN, Kalamara E, Shayeghi M, et al. (2003) Overweight and obesity (high body mass index). Comparative Quantification of Health Risks: Global and Regional Burden of Disease Attributable to Selected Risk Factors Geneva, World Health Org.: 497-596.

5. Cannon B, Nedergaard J (2004) Brown adipose tissue: function and physiological significance. Physiol Rev 84: 277-359.

6. Feldmann HM, Golozoubova V, Cannon B, Nedergaard J (2009) UCP1 ablation induces obesity and abolishes diet-induced thermogenesis in mice exempt from thermal stress by living at thermoneutrality. Cell Metab 9: 203-209.

7. Tseng YH, Kokkotou E, Schulz TJ, Huang TL, Winnay JN, et al. (2008) New role of bone morphogenetic protein 7 in brown adipogenesis and energy expenditure. Nature 454: 1000-1004.

8. Cypess AM, Lehman S, Williams G, Tal I, Rodman D, et al. (2009) Identification and importance of brown adipose tissue in adult humans. N Engl J Med 360: 1509-1517.

9. Saito M, Okamatsu-Ogura Y, Matsushita M, Watanabe K, Yoneshiro T, et al. (2009) High incidence of metabolically active brown adipose tissue in healthy adult humans: effects of cold exposure and adiposity. Diabetes 58: 1526-1531.

10. van Marken Lichtenbelt WD, Vanhommerig JW, Smulders NM, Drossaerts JM, Kemerink GJ, et al. (2009) Cold-activated brown adipose tissue in healthy men. N Engl J Med 360: 1500-1508.

11. Virtanen KA, Lidell ME, Orava J, Heglind M, Westergren R, et al. (2009) Functional brown adipose tissue in healthy adults. N Engl J Med 360: 1518-1525.

12. Zingaretti MC, Crosta F, Vitali A, Guerrieri M, Frontini A, et al. (2009) The presence of UCP1 demonstrates that metabolically active adipose tissue in the neck of adult humans truly represents brown adipose tissue. FASEB J 23: 3113-3120.

13. Seale P, Bjork B, Yang W, Kajimura S, Chin S, et al. (2008) PRDM16 controls a brown fat/skeletal muscle switch. Nature 454: 961-967.

14. Seale P, Kajimura S, Yang W, Chin S, Rohas LM, et al. (2007) Transcriptional control of brown fat determination by PRDM16. Cell Metab 6: 38-54.

15. Puigserver P, Wu Z, Park CW, Graves R, Wright M, Spiegelman BM (1998) A cold-inducible coactivator of nuclear receptors linked to adaptive thermogenesis. Cell 92: 829-839.

16. Picard F, Gehin M, Annicotte J, Rocchi S, Champy MF, et al. (2002) SRC-1 and TIF2 control energy balance between white and brown adipose tissues. Cell 111: 931-941.

17. Wang Z, Qi C, Krones A, Woodring P, Zhu X, et al. (2006) Critical roles of the p160 transcriptional coactivators p/CIP and SRC-1 in energy balance. Cell Metab 3: 111-122.

18. Hansen JB, Kristiansen K (2006) Regulatory circuits controlling white versus brown adipocyte differentiation. Biochem J 398: 153-168.

19. Schulz TJ, Tseng YH (2009) Emerging role of bone morphogenetic proteins in adipogenesis and energy metabolism. Cytokine Growth Factor Rev 20: 523-531.

20. Petrovic N, Walden TB, Shabalina IG, Timmons JA, Cannon B, Nedergaard J (2010) Chronic peroxisome proliferator-activated receptor gamma (PPARgamma) activation of epididymally derived white adipocyte cultures reveals a population of thermogenically competent, UCP1-containing adipocytes molecularly distinct from classic brown adipocytes. J Biol Chem 285: 7153-7164.

21. Bostrom P, Wu J, Jedrychowski MP, Korde A, Ye L, et al. (2012) A PGC1-alpha-dependent myokine that drives brown-fat-like development of white fat and thermogenesis. Nature 481: 463-468.

22. Teufel A, Malik N, Mukhopadhyay M, Westphal H (2002) Frcp1 and Frcp2, two novel fibronectin type III repeat containing genes. Gene 297: 79-83.

23. Ferrer-Martinez A, Ruiz-Lozano P, Chien KR (2002) Mouse PeP: a novel peroxisomal protein linked to myoblast differentiation and development. Dev Dyn 224: 154-167.

24. Hashemi MS, Ghaedi K, Salamian A, Karbalaie K, Emadi-Baygi M, et al. (2013) Fndc5 knockdown significantly decreased neural differentiation rate of mouse embryonic stem cells. Neuroscience 231: 296-304.

25. Ivanov IP, Firth AE, Michel AM, Atkins JF, Baranov PV (2011) Identification of evolutionarily conserved non-AUG-initiated N-terminal extensions in human coding sequences. Nucleic Acids Res 39: 4220-4234.

26. Kozak M (1989) Context effects and inefficient initiation at non-AUG codons in eucaryotic cell-free translation systems. Mol Cell Biol 9: 5073-5080.

27. Kozak M (1990) Downstream secondary structure facilitates recognition of initiator codons by eukaryotic ribosomes. Proc Natl Acad Sci U S A 87: 8301-8305.

28. Kochetov AV, Palyanov A, Titov II, Grigorovich D, Sarai A, Kolchanov NA (2007) AUG_hairpin: prediction of a downstream secondary structure influencing the recognition of a translation start site. BMC Bioinformatics 8: 318.

29. Pilegaard H, Saltin B, Neufer PD (2003) Exercise induces transient transcriptional activation of the PGC-1alpha gene in human skeletal muscle. J Physiol 546: 851-858.

30. Lambernd S, Taube A, Schober A, Platzbecker B, Gorgens SW, et al. (2012) Contractile activity of human skeletal muscle cells prevents insulin resistance by inhibiting pro-inflammatory signalling pathways. Diabetologia 55: 1128-1139.

31. Wu J, Bostrom P, Sparks LM, Ye L, Choi JH, et al. (2012) Beige adipocytes are a distinct type of thermogenic fat cell in mouse and human. Cell 150: 366-376.

32. Norheim F, Raastad T, Thiede B, Rustan AC, Drevon CA, Haugen F (2011) Proteomic identification of secreted proteins from human skeletal muscle cells and expression in response to strength training. Am J Physiol Endocrinol Metab 301: E1013-E1021.

33. Timmons JA, Baar K, Davidsen PK, Atherton PJ (2012) Is irisin a human exercise gene? Nature 488: E9-10.

34. Huh JY, Panagiotou G, Mougios V, Brinkoetter M, Vamvini MT, et al. (2012) FNDC5 and irisin in humans: I. Predictors of circulating concentrations in serum and plasma and II. mRNA expression and circulating concentrations in response to weight loss and exercise. Metabolism 61: 1725-1738.

35. Choi YK, Kim MK, Bae KH, Seo HA, Jeong JY, et al. (2013) Serum irisin levels in new-onset type 2 diabetes. Diabetes Res Clin Pract .

36. Moreno-Navarrete JM, Ortega F, Serrano M, Guerra E, Pardo G, et al. (2013) Irisin Is Expressed and Produced by Human Muscle and Adipose Tissue in Association With Obesity and Insulin Resistance. J Clin Endocrinol Metab 98: E769-78.

37. Stengel A, Hofmann T, Goebel-Stengel M, Elbelt U,

Kobelt P, Klapp BF (2013) Circulating levels of irisin in patients with anorexia nervosa and different stages of obesity--correlation with body mass index. Peptides 39: 125-130.

38. Sharma N, Castorena CM, Cartee GD (2012) Greater insulin sensitivity in calorie restricted rats occurs with unaltered circulating levels of several important myokines and cytokines. Nutr Metab (Lond) 9: 90.

39. Lecker SH, Zavin A, Cao P, Arena R, Allsup K, et al. (2012) Expression of the Irisin Precursor FNDC5 in Skeletal Muscle Correlates With Aerobic Exercise Performance in Patients With Heart Failure. Circ Heart Fail 5: 812-818.

40. Xu X, Ying Z, Cai M, Xu Z, Li Y, et al. (2011) Exercise ameliorates high-fat diet-induced metabolic and vascular dysfunction, and increases adipocyte progenitor cell population in brown adipose tissue. Am J Physiol Regul Integr Comp Physiol 300: R1115-R1125.

41. De Matteis R, Lucertini F, Guescini M, Polidori E, Zeppa S, et al.(2012) Exercise as a new physiological stimulus for brown adipose tissue activity. Nutr Metab Cardiovasc Dis 23: 582-90.

42. Schulz TJ, Tseng YH (2009) Emerging role of bone morphogenetic proteins in adipogenesis and energy metabolism. Cytokine Growth Factor Rev 20: 523-531.

43. Jespersen NZ, Larsen TJ, Peijs L, Daugaard S, Homoe P, et al. (2013) A classical brown adipose tissue mRNA signature partly overlaps with brite in the supraclavicular region of adult humans. Cell Metab 17: 798-805.

44. Lee D, Zhou Y, Tu M, Ishino T, Rukstalis M, et al. (2013) Irisin Does Not Induce Browning of Mouse or Human Adipocytes. Diabetes 62: A25.

45. Cypess AM, White AP, Vernochet C, Schulz TJ, Xue R, et al. (2013) Anatomical localization, gene expression profiling and functional characterization of adult human neck brown fat. Nat Med 19: 635-639.

46. Lidell ME, Betz MJ, Dahlqvist LO, Heglind M, Elander L, et al. (2013) Evidence for two types of brown adipose tissue in humans. Nat Med 19: 631-634.

47. Cannon B, Nedergaard J (2012) Cell biology: Neither brown nor white. Nature 488: 286-287.

48. Gjelstad IM, Haugen F, Gulseth HL, Norheim F, Jans A, et al. (2012) Expression of perilipins in human skeletal muscle in vitro and in vivo in relation to diet, exercise and energy balance. Arch Physiol Biochem 118: 22-30.

49. Ronnestad BR, Egeland W, Kvamme NH, Refsnes PE, Kadi F, Raastad T (2007) Dissimilar effects of one- and three-set strength training on strength and muscle mass gains in upper and lower body in untrained subjects. J Strength Cond Res 21: 157-163.

50. Gauthier ER, Madison SD, Michel RN (1997) Rapid RNA isolation without the use of commercial kits: application to small tissue samples. Pflugers Arch 433: 664-668.

51. Sell H, Laurencikiene J, Taube A, Eckardt K, Cramer A, et al. (2009) Chemerin is a novel adipocyte-derived factor inducing insulin resistance in primary human skeletal muscle cells. Diabetes 58: 2731-2740.

52. Haugen F, Norheim F, Lian H, Wensaas AJ, Dueland S, et al. (2010) IL-7 is expressed and secreted by human skeletal muscle cells. Am J Physiol Cell Physiol 298: C807-C816.

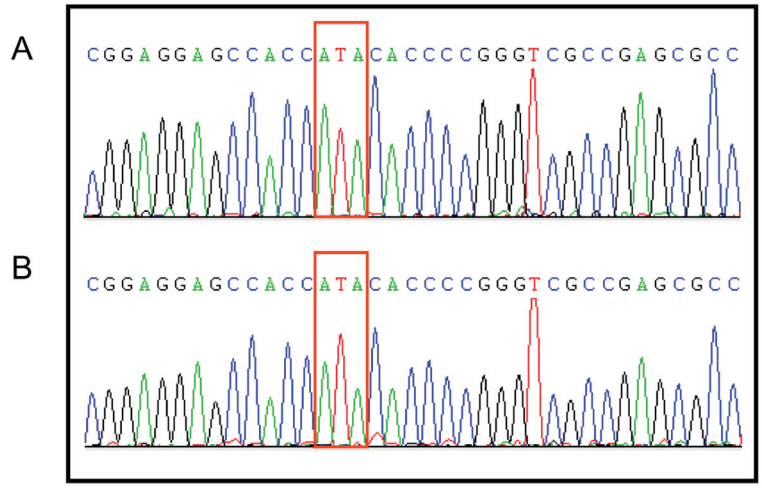

Figure S1. *Genotyping of human FNDC5 exon 1 sequence. Source of mRNA for 5′-RACE was (A) human skeletal muscle and (B) human cerebellum. Tissue samples were obtained from Clontech. Identified sequences with bp 55-91 of human FNDC5 variant 2 (NM_153756) and variant 3 (NM_001171940).*

```
NM_001171940     GAGCCACCATACACCCCGGGTCGCCGAGCGCCTGGCCGCCCCGCGCCCGCGCCGCGCTCC
NM_153756        GAGCCACCATACACCCCGGGTCGCCGAGCGCCTGGCCGCCCCGCGCCCGCGCCGCGCTCC
BF221649         GAGCCACCATACACCCCGGGTCGCCGAGCGCCTGGCCGCCCCGCGCCCGCGCCGCGCTCC
AA908225         GAGCCACCATACACCCCGGGTCGCCGAGCGCCTGGCCGCCC-GCGCCCGCGC-GCGCTCC
BE467868         GAGCCACCATACACCCCGGGTCGCCGAGCGCCTGGCCGCCCCGCGCCCGCGCCGCGCTCC
AA931673         GAGCCACCATACACCCCGGGTCGCCGAGCGCCTGGCCGCCCCGC-CCCG-GCCG-GCTCC
BE502835         GAGCCACCATACACCCCGGGTCGCCGAGCGCCTGGCCGCCCCGCGCCCGCGCCGCGCTCC
BF433165         GAGCCACCATACACCCCGGGTCGCCGAGCGCCTGGCCGCCCCGCGCCCGCGCCGCGCTCC
BF108485         GAGCCACCATACACCCCGGGTCGCCGAGCGCCTGGCCGCCCCGCGCCCGCGCCGCGCTCC
AI798367         GAGCCACCATACACCCCGGGTCGCCGAGCGCCTGGCCGCCCCGCGCCCGCGCCGCGCTCC
AA913809         GAGCCACCATACACCCCGGGTCGCCGAG-GCCTGGCCGCCCCGCGCCCG-GCCG-GCTCC
BF445046         GAGCCACCATACACCCCGGGTCGCCGAGCGCCTGGCCGCCCCGCGCCCGCGCCGCGCTCC
AI971851         GAGCCACCATACACCCCGGGTCGCCGAGCGCCTGGCCGCCCCGCGCCCGCGCCGCGCTCC
BE468219         GAGCCACCATACACCCCGGGTCGCCGAGCGCCTGGCCGCCCCGCGCCCGCGCCGCGCTCC
BE218308         GAGCCACCATACACCCCGGGTCGCCGAGCGCCTGGCCGCCCCGCGCCCGCGCCGCGCTCC
BE551417         GAGCCACCATACACCCCGGGTCGCCGAGCGCCTGGCCGCCCCGCGCCCGCGCCGCGCTCC
AI391724         GAGCCACCATACACCCCGGGTCGCCGAGCGCCTGGCCGCCCCGCGCCCGCGCCGCGCTCC
AI937294         GAGCCACCATACACCCCGGGTCGCCGAGCGCCTGGCCGCCCCGCGCCCGCGCCGCGCTCC
AW612671         GAGCCACCATACACCCCGGGTCGCCGAGCGCCTGGCCGCCCCGCGCCCGCGCCGCGCTCC
AI458319         GAGCCACCATACACCCCGGGTCGCCGAGCGCCTGGCCGCCCCGCGCCCGCGCCGCGCTCC
AI694150         GAGCCACCATACACCCCGGGTCGCCGAGCGCCTGGCCGCCCCGCGCCCGCGCCGCGCTCC
DA685889         --------ATACACCCCGGGTCGCCGAGCGCCTGGCCGCCCCGCGCCCGCGCCGCGCTCC
DA070643         ----------------------------GCGCCTGGCCGCCCCGCGCCCGCGCCGCGCTCC
```

Figure S2. *Alignment of two Ref_Seq cDNAs (NM 001171940.1 and NM_153756.2) and 20 expressed sequence tags sequences. The alignment covers the mutated start ATG to ATA codon and the CTC codon in purple that should be the start ATG, if the FNDC5 protein sequence published by Böstrom et al. [21] is forced to match the exon1 sequence.*

```
  1 GCGGCCGCCGGGCGCCGGAGCCGCGTCCCCCTGCGCCGCCCCGGGCCTGCCGGCCGGAGG

 61 AGCCACCATACACCCCGGGTCGCCGAGCGCCTGGCCGCCCCGCGCCCGCGCCGCGCTCCG

121 CCTGTGGCTGGGCTGCGTCTGCTTCGCGCTGGTGCAGGCGGACAGTCCCTCAGCCCCAGT

181 GAACGTCACCGTCAGGCACCTCAAGGCCAACTCTGCAGTGGTGAGCTGGGATGTTCTGGA

241 GGATGAGGTTGTCATCGGATTTGCCATCTCCCAGCAGAAGAAGGATGTGCGGATGCTGCG
                                                      M  L  R

301 CTTCATCCAGGAGGTGAACACCACCACCCGCTCATGTGCCCTCTGGGACCTGGAGGAGGA
      F  I  Q  E  V  N  T  T  T  R  S  C  A  L  W  D  L  E  E D
```

Figure S3*. cDNA sequence showing the non-Kozak start ATG of NP_ 715637/NM_153756. The 3 partial Kozak ATGs and the common stop codon (in yellow) for these 3 uORFs are boxed.*

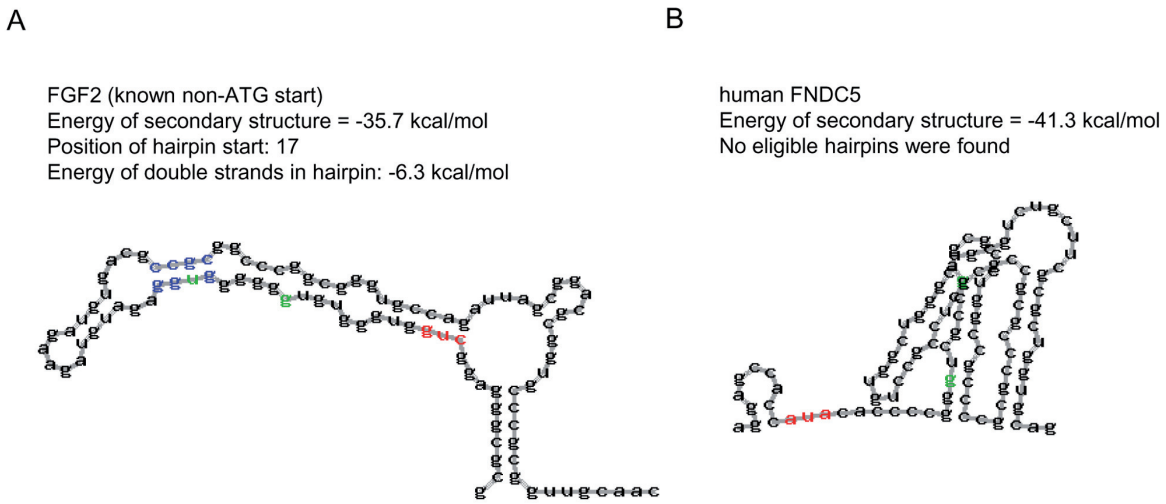

Figure S4. *Secondary structure of FGF2 and human FNDC5 mRNA. Using a program for prediction of a downstream hairpin which potentially increases initiation of translation at start AUG codon in a suboptimal context showed a positive result for FGF2 (A) and no result for FNDC5 (B).*

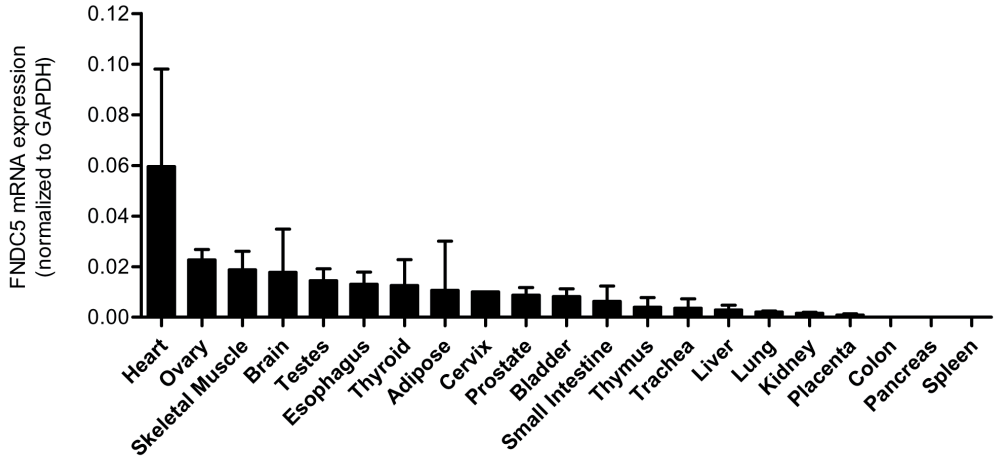

Figure S5. *Human FNDC5 mRNA expression levels in different human tissues. The expression was measured by qRT-PCR and expressed relative to mRNA levels of GAPDH, shown are means +/- SD from two measurements. Total RNA samples pooled from several donors were purchased from Clontech Laboratories, Inc.*

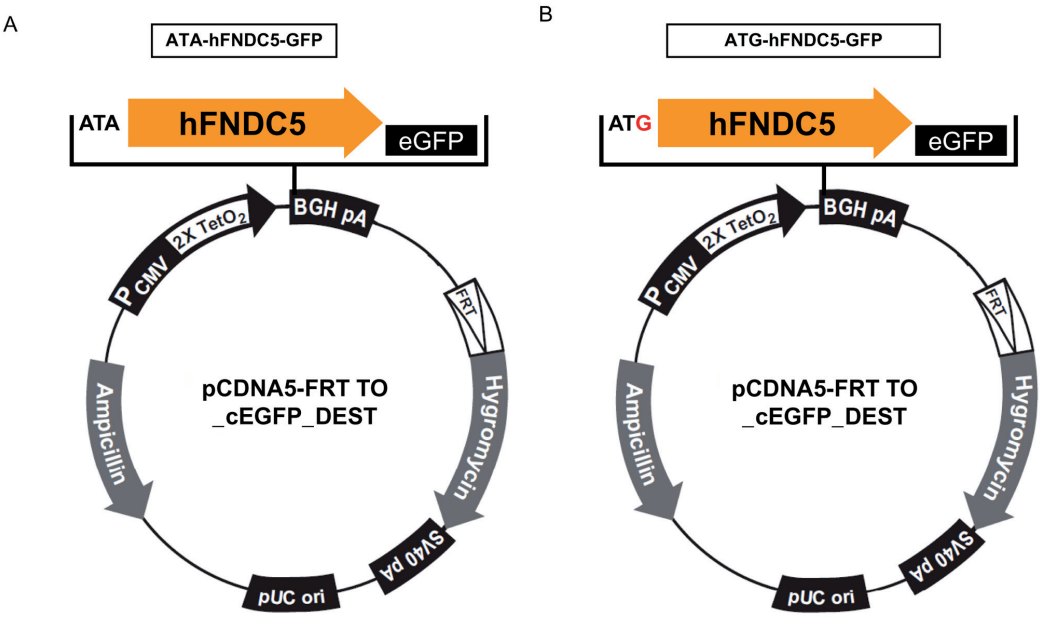

Figure S6. *Vectors maps of ATA-hFNDC5-GFP (A) and ATG-hFNDC5-GFP (B).*

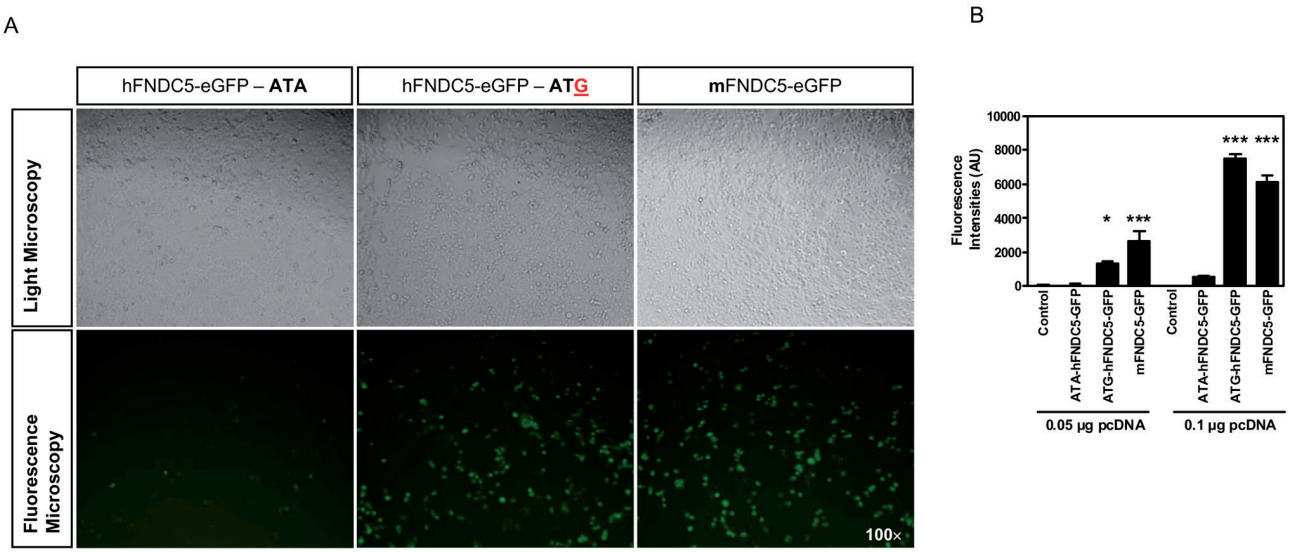

Figure S7*. Quantification of GFP fluorescence in HEK293 cells. (A) In 96 well plate format HEK293 cells were seeded at a density of 2x104/well and transiently transfected with 0.05 µg of the indicated expression vector using jetPRIME reagent. 24 h later cells were visualized using 100x magnification on an inverted fluorescence microscope. (B) Quantification of GFP signal was measured with an Ultra Evolution Tecan at 485 and 520 nm. Data are presented as mean values ± SEM.*

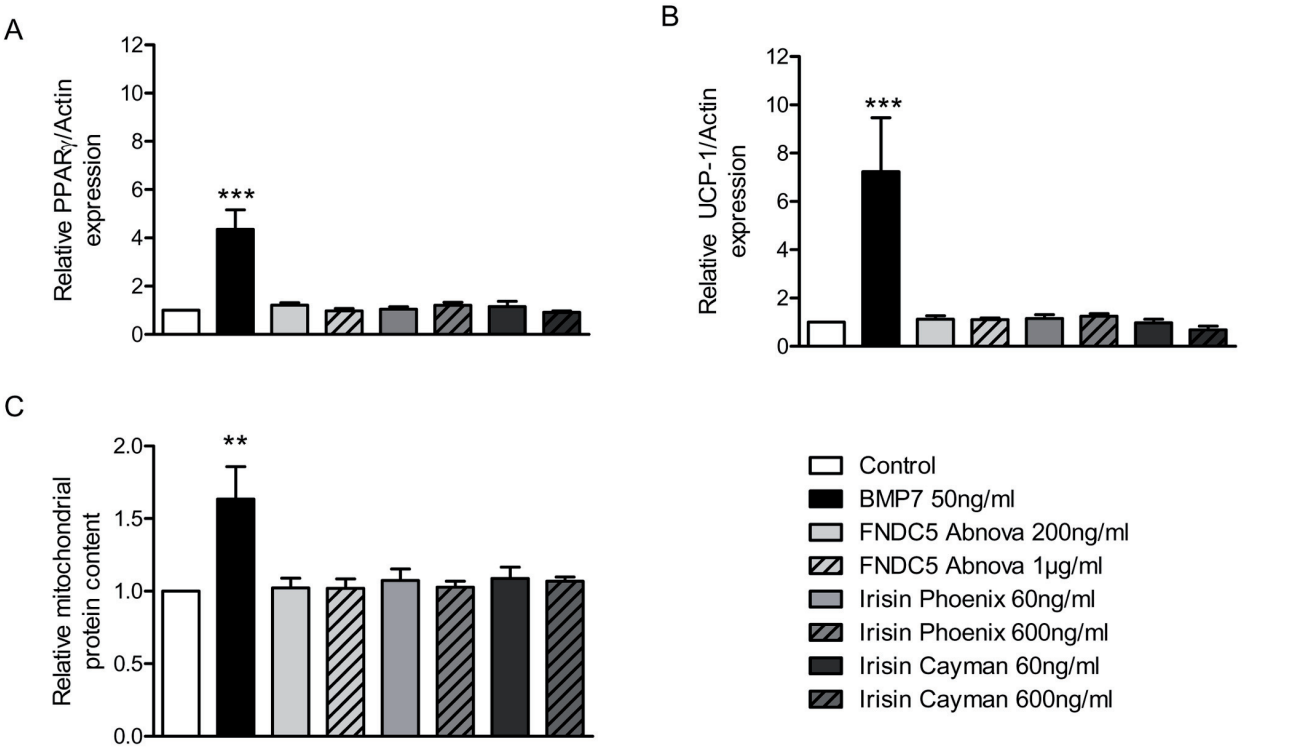

Figure S8. *Isolated preadipocytes from human subcutaneous preadipocytes of different donors were differentiated in the presence of 50 ng/ml BMP7, 200 and 1000 ng/ml FNDC5 (Abnova), 60 and 600 ng/ml irisin (Phoenix) and 60 and 600 ng/ml irisin (Cayman Chemical). (A, B) Relative gene expression of PPARγ (A) and UCP1 (B) was measured by qRT-PCR after 12-14 days of differentiation. All expression data were normalized to the mRNA level of actin; n=5-6 (for treatment with irisin provided by Cayman Chemical n=3); ***p < 0.001. (C) Cell lysates were analysed by immunodetection using an oxidative phosphorylation antibody cocktail. Signal intensities of all complexes of the oxidative phosphorylation were quantified and normalized to ß-actin, n=3-5, **p < 0.01.*

Table S1. *Overview of used primers.*

Gene	Supplier: Identifier	Forward Primer Sequenz (5‘→3‘)	Reverse Primer Sequenz (5‘→3‘)
Actin (human)	Qiagen: Hs_ACTB_2_SG	Sequence not provided by supplier	
Adiponectin (human)	Qiagen: Hs_ADIPOQ_1 SG	Sequence not provided by supplier	
C/EBPα (human)	Qiagen: Hs_CEBPA_1_SG	Sequence not provided by supplier	
CD137 human)	Eurofins MWG Operon	AGCTGTTACAACA-TAGTAGCCAC	TCCTGCAAT-GATCTTGTCCTCT
FNDC5 (human)	Qiagen: Hs_FNDC5_1_SG	Sequence not provided by supplier	
MYH1 (human)	Eurofins MWG Operon	CCAGACTGTGTCTG-CTCTCTTCAG	C A G G A C A A G C T-CATGCTCCAT
MYH2 (human)	Eurofins MWG Operon	A A G G T C G G C A A T-GAGTATGTCA	CAACCATCCACAGG-AACATCTTC
MYH7 (human)	Qiagen: Hs_MYH7_1_SG	Sequence not provided by supplier	
PGC1α (human)	Qiagen: Hs_PPARGC1A_1 SG	Sequence not provided by supplier	
PPARγ (human)	Qiagen: Hs_PPARG_1 SG	Sequence not provided by supplier	
TCF21 (human)	Qiagen: Hs_TCF21_2_SG	Sequence not provided by supplier	
UCP1 (human)	Qiagen: Hs_UCP1_3_SG	Sequence not provided by supplier	
ZIC1 (human)	Qiagen: Hs_ZIC1_1_SG	Sequence not provided by supplier	

Table S2. *Gene symbols and corresponding TaqMan assay IDs provided by Applied Biosystems used for microfluidic card real-time PCR analysis.*

Gene Symbol	*Assay ID*
ADIPOQ	*Hs00605917_m1*
ADRB1	*Hs02330048_s1*
ADRB2	*Hs00240532_s1*
CAV1	*Hs00971716_m1*
CEBPA	*Hs00269972_s1*
CEBPB	*Hs00270923_s1*
CEBPG	*Hs01922818_s1*
CIDEC	*Hs01032998_m1*
CPT1A	*Hs00912671_m1*
CYCS	*Hs01588974_g1*
DGAT1	*Hs00201385_m1*
DGAT2	*Hs01045913_m1*
FABP4	*Hs01086177_m1*
LEP	*Hs00174877_m1*
LPL	*Hs00173425_m1*
NRF1	*Hs00192316_m1*
OXR1	*Hs00250562_m1*
PLIN1	*Hs00160173_m1*
PLIN2	*Hs00605340_m1*
PLIN3	*Hs00998421_m1*
PLIN4	*Hs00287411_m1*
PLIN5	*Hs00965990_m1*
PNPLA2	*Hs00386101_m1*
PPARA	*Hs00947539_m1*
PPARD	*Hs04187066_g1*
PPARGC1A	*Hs01016719_m1*
PPARGC1B	*Hs00991677_m1*
PRDM16	*Hs00922674_m1*
RN18S1	*Hs03928985_g1*
SIRT1	*Hs01009005_m1*
SLC2A1	*Hs00892681_m1*
SLC2A4	*Hs00168966_m1*
TFAM	*Hs00273372_s1*
UCP1	*Hs00222453_m1*
UCP2	*Hs01075227_m1*
UCP3	*Hs01106052_m1*
VDAC1	*Hs01631624_gH*

Browning of white fat: does irisin play a role in humans?

Manuela Elsen, Silja Raschke, Jürgen Eckel

Paul-Langerhans-Group, German Diabetes Center, Duesseldorf, Germany

Abstract

The discovery of irisin as an exercise-regulated myokine inducing browning of WAT has gained interest as a potential new strategy to combat obesity and its associated disorders, such as type 2 diabetes. However, there are inconsistencies regarding the relevance of irisin in humans. The regulation of *FNDC5* mRNA expression by exercise and contraction could not be reproduced by a number of human studies using several exercise protocols and *in vitro* approaches. Furthermore, the nature of FNDC5 fragments and the presence of irisin in humans are questionable and probably contribute to conflicting data obtained with commercially available ELISA kits. Most importantly, the information regarding the concentration of circulating irisin in humans is not clear, as different studies using different kits measure irisin levels in a wide range. Data about the role of irisin in states of human obesity and metabolic diseases are conflicting and, in some cases, changes in irisin levels have been observed; they were only moderate in 10–20%. Independent of the presence and regulation of FNDC5/irisin in humans, the application of recombinant irisin could still represent a therapeutic strategy to fight obesity. However, the current data obtained from human cell models reveal that FNDC5/irisin has no effect on browning of the major WAT depots in humans and is likely to selectively target a small subpopulation of adipocytes, which are located in classical BAT regions, such as the supraclavicular adipose tissue. Thus, other candidates, such as BMP7 or CNPs, seem to be more prominent candidates as inducers of browning in humans.

Keywords: adipocyte, diabetes, exercise, obesity, muscle

Introduction

White adipose tissue (WAT) and brown adipose tissue (BAT) exert inverse functions in that WAT stores energy, whereas BAT, characterized by a large number of mitochondria containing uncoupling protein 1 (UCP1), mediates adaptive thermogenesis and contributes to the maintenance of body temperature. In 2009, five independent studies demonstrated the presence of BAT in adult humans (Cypess *et al*. 2009, van Marken Lichtenbelt *et al*. 2009, Saito *et al*. 2009, Virtanen *et al*. 2009, Zingaretti *et al*. 2009) and confirmed the existence of an inverse correlation between BMI and BAT activity. These observations have aroused considerable interest in the therapeutic potential of brown adipocytes for inducing weight loss, and recent data have confirmed that BAT oxidative metabolism contributes significantly to energy expenditure (Ouellet *et al*. 2012). The classical view of brown and white fat cells was modified in 2010 by a publication of the Cannon/Nedergaard group describing a third type of fat cells termed 'brite' (brown-in-white) adipocytes (Petrovic *et al*. 2010). These cells share biochemical features and the thermogenic potential with brown adipocytes, but are derived from different precursor cells (Seale *et al*. 2008).

The possibility to differentiate adipose stem cells into brite adipocytes (browning of white fat) and to induce thermogenic activation and augment energy expenditure is currently considered as an important promising approach to combat obesity and obesity-related complications.

A novel hormone-like myokine termed irisin has recently been described to activate such a white-to-brown shift in adipocytes (Boström *et al*. 2012a). As this molecule was originally reported to be released after physical activity, it gained huge interest as a potential mediator of the health-promoting effects of physical exercise. Irisin is a 112 amino acid peptide cleaved from fibronectin type III domain containing protein 5 (FNDC5), a type I membrane protein which was claimed to be upregulated by exercise training in both mice and humans (Boström *et al*. 2012a). When writing this review, more than 100 papers dealing with irisin have been found in PubMed. However, the physiological role and the potential therapeutic value of irisin have remained highly controversial. In this review, we analyzed the current literature regarding exercise regulation and the functional impact of irisin in humans. We conclude that: i) the nature and con-

centration of circulating FNDC5 fragments remain unclear and ii) irisin has no effect on major WAT depots in humans and may only target a small subpopulation of adipocytes.

Impact of exercise on browning of white adipose tissue

As noticed before, the exercise-regulated myokine irisin was identified and described as a link between exercise and the promotion of WAT browning (Boström *et al*. 2012a). It is well known that the transcriptional coregulator PGC1α is induced in muscle in response to exercise in rodents and humans (Goto *et al*. 2000, Pilegaard *et al*. 2003). Therefore, transgenic mice overexpressing *Pgc1a (Ppargc1a)* in skeletal muscle can be used as an exercise model (Boström *et al*. 2012a). Interestingly, these transgenics exhibited increased expression of the brown marker genes *Ucp1* and cell death-inducing DFFA-like effector A (*Cidea*) only in the inguinal depot, suggesting that muscle activity promotes remodeling of subcutaneous WAT. Indeed, UCP1 expression was also strongly upregulated in the subcutaneous inguinal depot of mice after 3 weeks of wheel running.

From a physiological point of view, the induction of brown-like fat in response to exercise appears to be surprising due to several factors. First, exercise itself is an energy-consuming process and skeletal muscle is supplied with energy sources from other organs, such as free fatty acids released from WAT during physical activity. In this context, Kelly (2012) raised the question as to why physical activity would induce a program that burns fat stores, which are needed for the exercising muscle. Secondly, it has been discussed by Cannon & Nedergaard (2004) that there should be a diminished demand for non-shivering thermogenesis during exercise, as heat is generated by skeletal muscle contraction. In accordance, several studies on rats have demonstrated that treadmill running has no effect on *Ucp1* mRNA levels in BAT (Scarpace *et al*. 1994, Segawa *et al*. 1998, De Matteis *et al*. 2013) as well as on BAT mass (Segawa *et al*. 1998). The interscapular BAT of the *Pgc1a* transgenic mice used by Boström *et al*. (2012a) was also not altered when compared with WT mice. Furthermore, even a trend toward a decrease in *Ucp1* mRNA expression in BAT has been observed in rats after 3 weeks of endurance exercise (Roca-Rivada *et al*. 2013). By contrast, only one study demonstrated that treadmill exercise training of mice leads to enhanced expression of certain brown adipocyte-specific genes in BAT (Xu *et al*. 2011). Thus, exercise intervention is likely to have no effect on classical BAT in rodents. Regarding the browning of WAT, an increase in the number of mitochondria and enhanced expression of brown-specific genes in the visceral epididymal WAT of mice have been demonstrated after exercise (Xu *et al*. 2011). Another study carried out on rats also observed induction of UCP1 expression in the visceral but not the subcutaneous WAT after 3 weeks of training (Roca-Rivada *et al*. 2013). Boström *et al*. (2012a) demonstrated the most prominent effect of exercise on the subcutaneous WAT and the data obtained were in contrast to the two above-mentioned studies.

In addition to these studies on rodents, a potential induction of WAT browning in response to exercise remains to be clarified in case of humans. A recent study performing a 12-week training intervention in humans could not detect any alterations in WAT. Thus, expression of several brown adipocyte-specific marker genes, such as *UCP1* and *PRDM16*, were not significantly changed in subcutaneous adipose tissue after the intervention (Norheim *et al*. 2014). Hence, studies assessing the impact of exercise on WAT browning in rodents are conflicting, especially with regard to the WAT depot that undergoes remodeling in response to exercise. Furthermore, the browning of WAT in response to exercise has not yet been demonstrated in humans and, hence, further studies in humans are necessary.

Exercise regulation of FNDC5 mRNA in skeletal muscle - *in vivo* studies

In the initial report by Boström *et al*. (2012a), irisin is proposed to be a novel PGC1α-dependent and exercise-responsive myokine. This conclusion was based on the finding that skeletal muscle *Fndc5* mRNA levels from mice after 3 weeks of free wheel running were enhanced compared with sedentary mice (about 2.8-fold). Moreover, enhanced *Fndc5* expression was accompanied by increased *Pgc1a* mRNA levels (about 2.5-fold). Additionally, the expression levels of *FNDC5* and *PGC1A* were examined in muscle biopsies from human subjects before and after 10 weeks of endurance training. Expression of both genes was enhanced after the training session (about twofold) (Bostro¨m *et al*. 2012a).

After this initial description of FNDC5 and irisin as exercise-regulated proteins in mice and humans, *FNDC5* mRNA expression in skeletal muscle was analyzed in several human exercise cohorts (Table 1).

Intriguingly, most of these studies performed in humans failed to reproduce enhanced *FNDC5* mRNA levels after exercise. The upregulation of FNDC5 in skeletal muscle by exercise was only demonstrated in four out of 15 studies, including the study by Bostro¨m *et al*. In this context, they reported the most prominent increase in *FNDC5* mRNA expression after exercise (twofold) (Boström *et al*. 2012a), whereas three other studies reported only a moderate increase of 1.3- to 1.4-fold (Timmons *et al*. 2012, Pekkala *et al*. 2013, Norheim *et al*. 2014).

Timmons *et al*. (2012) were the first unable to reproduce a substantial training-induced increase in *FNDC5* expression, neither in young men after endurance training nor in a different cohort (20–80 years old subjects) after resistance training. However, it is possible that *FNDC5* mRNA expression can be induced by exercise in a subset of individuals, as older active subjects had a 30% higher *FNDC5* expression than sedentary control subjects, while no difference was observed in younger subjects (Timmons *et al*. 2012). As FNDC5 has been described to be PGC1α-dependent (Boström *et al*. 2012a), this early study by Timmons *et al*. (2012) has been criticized for including exercise intervention studies without reported induction of *PGC1A* expression in muscle (Boström *et al*. 2012b). Thus, a lack of PGC1α induction in some of the exercise cohorts may explain the conflicting results.

In line with this suggestion, exercise intervention studies reporting increased muscle *PGC1A* expression would potentially clarify the relation between *FNDC5* and *PGC1A* mRNA expression in skeletal muscle. Recently, Norheim *et al*. (2014) compared the effects of acute and chronic exercise and assessed the correlation between *PGC1A* and *FNDC5* expression in these exercise types. Therefore, a cohort of 13 sedentary

Table 1: *Human exercise cohorts analyzed for FNDC5 mRNA expression in skeletal muscle after different modes of exercise*

Study (reference)	Patients/subjects	n	Exercise mode	Intervention	Main results
Boström *et al*. 2012a	Healthy adults	8	A	10 weeks of supervised endurance training	2fold increase of *FNDC5* mRNA expression in muscle
Besse-Patin *et al*. 2014	Obese, non-diabetic subjects	11	A	8 weeks of supervised endurance training	No change of *FNDC5* mRNA expression in muscle
Kurdiova *et al*. 2014	Sedentary, obese individuals	16	A	12 week strength/endurance training	No change of *FNDC5* mRNA expression in muscle
	Sedentary vs Trained	7 vs 8	B	1h 75% of maximal capacity	No change of *FNDC5* mRNA expression in muscle
Norheim *et al*. 2014	Normoglycaemic, sedentary men	13	A	12 week combined endurance and strength training	1.4fold increase of *FNDC5* mRNA expression in muscle
	Normoglycaemic, sedentary men	13	B	45 min cycling at 70% VO2 max	No change of *FNDC5* mRNA expression in muscle
Pekkala *et al*. 2013	Healthy, untrained male	17	B	1 hour acute low intensity aerobic exercise	No change of *FNDC5* mRNA expression in muscle
	Healthy, young male	10	B	single resistance exercise bout	1.4fold increase of *FNDC5* mRNA expression in muscle
	Healthy, old male	10	B	single resistance exercise bout	No change of *FNDC5* mRNA expression in muscle
	Healthy, untrained middle-aged male	9	A	21 weeks combined endurance and resistance exercise	No change of *FNDC5* mRNA expression in muscle
Raschke *et al*. 2013	Young, sedentary males	6	A	10 weeks of aerobic interval training	No change of *FNDC5* mRNA expression in muscle
	Young, sedentary males	7	A	11 weeks of strength training	No change of *FNDC5* mRNA expression in muscle
Timmons *et al*. 2012	Young sedentary males)	24	A	6 weeks intense endurance cycling	No change of *FNDC5* mRNA expression in muscle
	20-80 years old subjects	43	A	20 weeks supervised resistance exercise study	No change of *FNDC5* mRNA expression in muscle
	Young vs older sedentary and age-matched endurance trained	10 vs 10	-	-	1.3fold increase of *FNDC5* mRNA expression in muscle of older trained compared to older sedentary subjects

A: long-term exercise intervention; B: acute exercise

men, aged 40–65 years, underwent a 12-week intervention of combined endurance and strength training. Muscle biopsies were taken after an acute endurance workload, both before (acute) and after (chronic) the 12-week intervention period. Interestingly, after 12 weeks of exercise, *PGC1A* was slightly activated (1.2-fold) and *FNDC5* mRNA levels were additionally increased (1.4-fold) (Norheim *et al*. 2014), being in line with the initial report by Boström *et al*. However, acute exercise intervention performed by the same subjects gave different results. Regardless of the prominent increase in *PGC1A* mRNA levels (7.4-fold), *FNDC5* mRNA expression levels did not differ at all (Norheim *et al*. 2014). Prominent effects on PGC1A mRNA expression have also been described in other acute exercise cohorts (twofold and fourfold (Pekkala *et al*. 2013)), whereas chronic exercise had a moderate effect (1.2-fold (Norheim *et al*. 2014) and 1.5-fold (Boström *et al*. 2012a)).

In conclusion, the regulation of *FNDC5* expression by exercise could not be reproduced by the majority of studies performed in humans (Table 1). Furthermore, even a strong increase in gene expression of the transcriptional coactivator *PGC1A* occurring after acute exercise does not necessarily lead to an activation of *FNDC5* expression (Pekkala *et al*. 2013, Norheim *et al*. 2014).

Exercise regulation of FNDC5 mRNA in skeletal muscle: *in vitro* models

To further investigate the effect of PGC1α on FNDC5 expression in human skeletal muscle cells, *in vitro* studies were performed on primary human myotubes (Besse-Patin *et al*. 2014, Raschke *et al*. 2013, Norheim *et al*. 2014).

Treatment of primary human myotubes with drugs mimicking the activation of exercise signaling pathways, namely caffeine, ionomycin, and forskolin, significantly increased *PGC1A* expression. However, this induction of *PGC1A* mRNA expression was not accompanied by enhanced *FNDC5* expression. Indeed, *FNDC5* mRNA was reduced after incubating the myotubes for 24 h with these exercise mimetics (Norheim *et al*. 2014). In line with this, a second study also demonstrated significantly decreased *FNDC5* expression levels in primary human myotubes challenged with ionomycin and forskolin (Besse-Patin *et al*. 2014).

To circumvent exercise mimetics as an *in vitro* exercise model, electrical pulse stimulation (EPS) has been performed to induce muscle contraction *in vitro*. This model is well established and primary human myotubes subjected to EPS are characterized by enhanced PGC1A mRNA expression, enhanced mitochondrial biogenesis as well as enhanced secretion of the well-known myokines IL6 and VEGFA (Lambernd *et al*. 2012). Moreover, this EPS model reflects a training model rather than acute exercise as shown by the enhanced *MYH1* mRNA level and enhanced mitochondrial content (Lambernd *et al*. 2012, Raschke *et al*. 2013). Similar to the results obtained with exercise mimetics, *FNDC5* mRNA expression was not significantly enhanced in primary human myotubes after EPS, although *PGC1A* expression was significantly increased (Raschke *et al*. 2013).

To sum up, all of these *in vitro* studies performed with primary human skeletal muscle cells failed to demonstrate an increase in *FNDC5* expression using several approaches to mimic exercise *in vitro*. The lack of PGC1α induction as a potential reason for the absence of augmented *FNDC5* expression can be excluded, as *PGC1A* gene expression was significantly enhanced in all models.

Taken all described human *in vivo* and *in vitro* studies together, discussing all these discrepancies between PGC1A activation and *FNDC5* mRNA expression, Norheim *et al*. (2014) speculated that *FNDC5* is not a direct PGC1α target gene but is rather upregulated in skeletal muscle *in vivo* via secondary mechanisms.

The initial characterization of a candidate myokine is frequently limited to the detection of mRNA expression in skeletal muscle tissue, as it has also been done for *FNDC5*. Moreover, determination of gene expression or protein level in skeletal muscle biopsies is critical, as besides skeletal muscle fibers, skeletal muscle contains extended layers of connective tissues, capillaries, and nerve cells among others. Thus, gene expression studies must be followed by the detection of the encoded protein specifically in skeletal muscle fibers, e.g., by additional immunostaining of the skeletal muscle tissue sections. Finally, for full validation of a protein as a myokine, secretion from skeletal muscle cells has to be demonstrated.

Exercise regulation of circulating irisin in humans

Key points in the study by Boström *et al*. (2012a) were that the irisin fragment was present in the plasma of mouse and and humans and that circulating levels were enhanced following exercise, as observed for skeletal muscle *FNDC5* expression in this study (Bo-

ström *et al*. 2012a). The presence of irisin protein in plasma was based on Western blots using an antibody which detects the transmembrane segment of FNDC5 and thus would fail to detect the C-terminally cleaved, secreted irisin fragment (Erickson 2013; Raschke *et al*. 2013). However, later on, several ELISA assays to detect circulating irisin became commercially available and were used to quantify irisin concentrations in human exercise studies (Table 2).

Using these ELISA kits, some of these human studies reported moderately increased serum irisin levels after exercise intervention. Thus, Kraemer *et al*. (2014) reported transiently elevated circulating irisin levels in response to moderate aerobic exercise during the first hour after exercise (20% increase) (Kraemer *et al*. 2014). In line with this finding, Huh *et al*. (2012) observed a moderate increase in circulating irisin level 30 min after a sprint running session (18% increase) (Huh *et al*. 2012) and Norheim *et al*. (2014) demonstrated slightly increased irisin levels after 45 min cycling (20% increase) (Norheim *et al*. 2014). In contrast to *FNDC5* mRNA data, enhanced circulating irisin levels were found in acute exercise studies rather than in long-term training studies.

Despite these three reports, 12 out of 15 studies failed to demonstrate that exercise affects circulating irisin levels in humans, neither after an acute bout of exercise nor after chronic exercise training (Huh *et al*. 2012, Aydin *et al*. 2013, Hecksteden *et al*. 2013, Moraes *et al*. 2013, Pekkala *et al*. 2013, Kurdiova *et al*. 2014, Norheim *et al*. 2014). Recently, Hecksteden *et al*. (2013) have published a randomized control trial and focused on the serum irisin concentrations. Subjects performed two guideline-conforming training interventions, either endurance or strength endurance training for 26 weeks. Once again, a training-induced increase in circulating irisin levels could not be confirmed (Hecksteden *et al*. 2013). Interestingly, although Norheim *et al*. (2014) observed an increased expression of PGC1A and *FNDC5* after 12 weeks of exercise, this was not translated into chronically increased levels of irisin in plasma and training for 12 weeks even tended to reduce irisin levels.

Summarizing the above-mentioned ELISA results, the current data provide equivocal results for regulation of circulating irisin levels after exercise. Only some studies reported slightly increased irisin levels after acute exercise, while the majority of studies failed to reproduce the results obtained by Boström *et al*. (summarized in Table 2).

Impact of irisin on WAT browning

The idea of irisin as an exercise-regulated myokine in humans and the physiological role of exercise-mediated browning of WAT have been discussed in the previous section. Independent of the potential regulation of circulating irisin and skeletal muscle *FNDC5* expression in response to acute or chronic exercise, the functionality of irisin in humans remains to be elucidated. Boström *et al*. (2012a) initially demonstrated that recombinant irisin and FNDC5 induce browning of WAT-derived murine preadipocytes *in vitro*. In the context of irisin as a therapeutic approach in the fight against obesity and its associated metabolic diseases, it is crucial to prove that irisin has an effect on white-to-brown transition in human cell models. Therefore, functional studies investigating the potency of irisin as an inducer of browning, performed in rodents and humans, will be discussed in this section.

After selection of secreted PGC1α- and exercise-regulated proteins/myokines in mice, Boström *et al*. (2012a) assessed their potential as inducers of browning and identified FNDC5 as a promising candidate. To study browning of WAT *in vitro*, murine preadipocytes were isolated from the inguinal fat depot and treated with commercially available recombinant FNDC5 (Abnova, Taiwan, China) during adipogenic differentiation. The inguinal depot is regarded as a subcutaneous and generally white fat depot, but has a high ability to undergo browning in response to a cold environment (Walden *et al*. 2012) and hormonal stimuli such as BMP7 (Schulz *et al*. 2011). Treatment of primary murine subcutaneous preadipocytes with 20 nM recombinant FNDC5 increased the expression of the BAT marker genes *Ucp1, Cidea, and Pgc1a* as well as oxygen consumption as a functional readout (Boström *et al*. 2012a). By contrast, FNDC5 failed to enhance brown marker genes in classical brown adipocytes isolated from the interscapular depot, suggesting tissue- and/or lineage-specific effects for FNDC5. The beneficial effect of irisin has also been demonstrated *in vivo*, as high-fat diet-induced obesity was reduced by adenoviral-mediated overexpression of FNDC5 in mice (Boström *et al*. 2012a).

The idea of a tissue-dependent impact of FNDC5 on browning was further elucidated by a second study from the same group. They proposed that brite or beige adipocytes display a distinct subpopulation within white adipose tissue and are highly responsive to β-adrenergic stimulation similar to classical brown adipocytes (Wu *et al*. 2012). In this context, *CD137 (TNFRSF9)* and *TMEM26* were identified as selective cell surface marker genes highly expressed in bri-

Table 2: *Human exercise cohorts analyzed for circulating irisin levels after different modes of exercise.*

Study (reference)	Patients/subjects	n	Exercise mode	Intervention	Main result
Boström *et al*. 2012a	Healthy adults	8	A	10 weeks of supervised endurance training	WB with Abnova antibody -> does not detect irisin
Hecksteden *et al*. 2013	Healthy adults: control aerobic training strength training	39 23 40	A	26 weeks of supervised aerobic endurance or strength endurance training	No change in circulating irisin levels between groups
Huh *et al*. 2012	Young, moderately trained, healthy males	15	B	1 week of exercise (2-3 sets of two 80-m sprints)	Circulating irisin levels were significantly induced (18%) 30 min after the exercise
	Young, moderately trained, healthy males	15	A	8 weeks of exercise (three times a week, 2-3 sets of two 80-m sprints)	No change in circulating irisin levels
Kraemer *et al*. 2014	Healthy, young male	7	B	90 min treadmill exercise	Circulating irisin levels were significantly induced (20%) by 54 min exercise
Kurdiova *et al*. 2014	Sedentary vs Trained	7 vs 8	B	1h 75% of maximal capacity	No change in circulating irisin levels
Moraes *et al*. 2013	Hemodialysis patients	26	A	6 months supervised resistance exercise	No change in circulating irisin levels
Norheim *et al*. 2014	Normoglycaemic, sedentary men	13	A	12 week combined endurance and strength training	No change in or trend to reduced circulating irisin levels
	Normoglycaemic, sedentary men	13	B	45 min cycling at 70% VO2 max	1.2fold increase in circulating irisin levels directly after exercise
Pekkala *et al*. 2013	Healthy, untrained male	17	B	1 hour acute low intensity aerobic exercise	No change in circulating irisin levels
	Healthy, young male	14	B	single resistance exercise bout	No change in circulating irisin levels
	Healthy, young male	10	B	single resistance exercise bout	No change in circulating irisin levels
	Healthy, untrained middle-aged male	9	A	21 weeks heavy-intensity endurance exercise	No change in circulating irisin levels
	Healthy, untrained middle-aged male	9	A	21 weeks combined endurance and resistance exercise	No change in circulating irisin levels
Aydin *et al*. 2013	obese males vs healthy males	7 vs 7	B	45 min of moderate outdoor running (5.5 km/45 min)	No change in circulating irisin levels

A: long-term exercise intervention; B: acute exercise

te adipocytes, but with a low expression in classical brown and white adipocytes. Interestingly, CD137-sorted cells from the stromal vascular fraction isolated from the inguinal depot of mice display a strong browning response toward 20 nM FNDC5 (Abnova) or 100 nM of the fusion protein irisin-Fc. On the other hand, cells expressing CD137 to a lesser extent did not show any significant response toward FNDC5 or irisin-Fc, indicating that only a subpopulation of preadipocytes isolated from the subcutaneous depot, which highly express CD137, is responsible for the browning effect of irisin (Wu *et al*. 2012).

Another study using murine 3T3-L1 adipocytes and primary rat adipocytes also observed a white-to-brown shift after exposure to 20 nM recombinant irisin, which was produced in yeast using the human irisin cDNA sequence (Zhang *et al*. 2014). Notably, the irisin-mediated increase in *Ucp1* mRNA expression was higher in 3T3-L1 adipocytes compared with primary rat adipocytes (sevenfold vs fourfold), indicating potential differences in the action of irisin between species. Unfortunately, *CD137* expression was not assessed in this study. In line with these results in murine and rat cell systems, a third study demonstrated the impact of irisin on browning of murine WAT. Treatment of primary murine preadipocytes isolated from the inguinal depot with 20 nM of a commercially available FNDC5 peptide (Abcam, ab117436) enhanced the expression of *Ucp1* and other brown marker genes (Shan *et al*. 2013). However, the synthetic peptide from Abcam used for this study corresponds to the C-terminal region of human FNDC5 and comprises the amino acids 149–178. This peptide is a part of the transmembrane domain and does not share any sequences with the irisin fragment, which comprises amino acids 32–143 (UniProt entry Q8NAU1). There-

fore, the results observed by Shan *et al*. (2013) with this peptide are surprising and not related to the irisin fragment.

Summarizing the current data assessing the role of irisin in rodents, there is evidence for an impact of irisin on the browning of WAT. However, the function of irisin has not yet been validated in a human cell system and remains unclear. In addition to the previously described lineage-selective effect of FNDC5, potential differences in the molecular signature of adipose tissue depots between mice and humans have been proposed. Thus, Wu *et al*. (2012) observed that human adipose tissue from the supraclavicular region, and proven to be BAT positive by [18F]FDG-PET/CT, shares the molecular signature of murine beige adipose tissue rather than murine classical BAT with a myogenic origin (Wu *et al*. 2012). However, three recent studies have provided evidence for the existence of classical brown adipocytes in humans, suggesting that the human neck adipose tissue depot is composed of both classical and brite adipocytes (Cypess *et al*. 2013, Jespersen *et al*. 2013, Lidell *et al*. 2013). In conclusion, these studies raise the question of whether results about browning obtained in murine models can be extrapolated to the human situation.

Relevance of irisin as an inducer of browning in humans

Studies investigating the functionality of FNDC5 and/or irisin in humans are rare and criticism has been raised regarding the relevance of irisin in humans. In this context, primary human preadipocytes isolated from the subcutaneous depot of different donors did not exhibit browning in response to irisin or FNDC5 (Raschke *et al*. 2013). The effects of three different recombinant proteins obtained from several sources (Phoenix, Abnova, and Caymen Chemicals) were compared in this study to exclude any potential differences between the suppliers. However, none of the proteins were able to induce browning, even when applied at high concentrations (1000 ng/ml for FNDC5 and 600 ng/ml for irisin). Moreover, preadipocytes isolated from donors highly expressing *CD137* strongly induced the browning program in response to BMP7, while no response toward irisin or FNDC5 was observed (Raschke *et al*. 2013).

Until recently, this was the sole study assessing the direct effect of FNDC5/irisin on browning in primary human adipocytes. More recently, a second study was published investigating the potency of FNDC5 to induce browning in primary human adipocytes from different depots. Lee *et al*. (2014) demonstrated a strong induction of several brown marker genes in primary human adipocytes isolated from neck biopsies after FNDC5 treatment for 6 days. Moreover, FNDC5 treatment of neck adipocytes increased basal and uncoupled oxygen consumption rates and FNDC5-treated cells were able to respond to b-adrenergic stimulation, a crucial feature of brown adipocyte functionality. As the myogenic marker *ZIC1* was not detectable, these neck adipocytes represent brite adipocytes rather than the classical brown ones. Interestingly, the effect of FNDC5 was only marginal or completely absent in primary adipocytes isolated from the subcutaneous and omental depots (Lee *et al*. 2014). In line with the study by Raschke *et al*. (2013), adipocytes from the subcutaneous depot do not appear to be able to undergo browning in response to FNDC5/irisin. One explanation could be the low expression of the brite-specific marker genes *TMEM26* and *CD137* in the subcutaneous depot compared with deep neck adipose tissue depots (Cypess *et al*. 2013, Lee *et al*. 2014). However, high *CD137* expression in human subcutaneous adipose tissue was not associated with a browning effect of FNDC5/irisin (Raschke *et al*. 2013).

The current data dealing with the effect of FNDC5/irisin on browning in humans lead to the suggestion that the sensitivity toward FNDC5/irisin is potentially dependent on the adipocyte lineage and in consequence the adipose tissue depot and the species (Fig. 1). Thus, FNDC5/irisin does not activate classical brown adipocytes (Boström *et al*. 2012a) and has no effect on pure white adipocytes (Wu *et al*. 2012, Raschke *et al*. 2013, Lee *et al*. 2014). It is likely that only a small subpopulation of adipocytes, which are highly expressing brite-specific markers, is responsible for the irisin effect (Wu *et al*. 2012). In this case, the relevance of irisin in humans and its potency as a pharmacological agent to treat obesity is questionable, as the major human adipose tissue depots (subcutaneous and omental) are pure white depots with a low expression of brite-specific markers and do not undergo browning upon FNDC5/irisin treatment. Probably, a subpopulation of cells present in deep neck adipose tissue from humans, which is suggested to be composed of classical brown and brite adipocytes, responds to FNDC5/irisin. However, the contribution of these cells to whole-body energy expenditure is not clearly determined. Moreover, other candidates seem to be more promising and have been shown to induce browning in human subcutaneous adipocytes, such as CNPs (Bordicchia *et al*. 2012) or BMP7 (Schulz *et al*. 2011, Elsen *et al*. 2014).

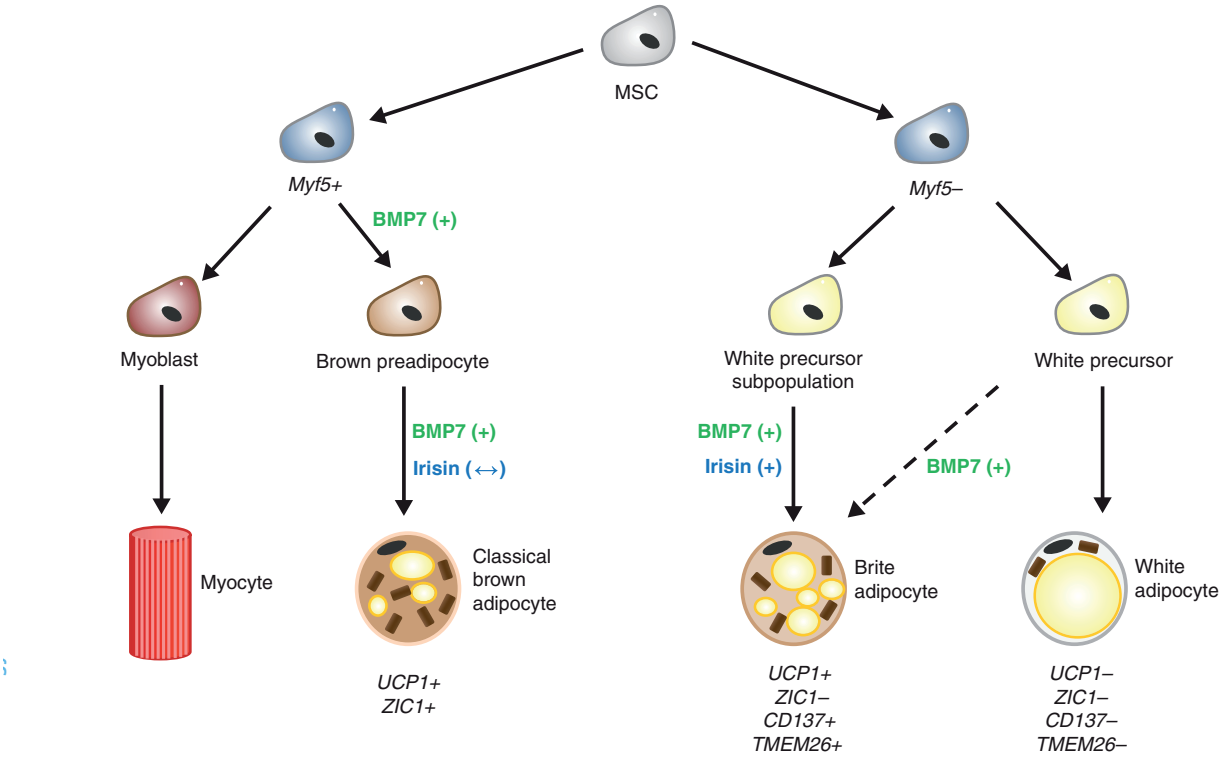

Figure 1: *Classical brown adipocytes share a developmental origin with skeletal muscle cells and are derived from Myf5+ precursor cells. BMP7 is involved in lineage determination as well as differentiation of classical brown adipocytes which express UCP1 and myogenic markers like ZIC1, while irisin does not promote classical brown adipocyte differentiation. White adipocytes develop from Myf5- precursor and give also rise to beige adipocytes in response to certain stimuli, such as BMP7. Only a subpopulation of white precursor cells, potentially characterized by high expression of beige markers such as CD137 and TMEM26, is likely to undergo browning in response to irisin, as proposed by Wu et al. (2012). (+), positive effect; (↔), no effect.*

Role of irisin in metabolic diseases

In addition to the discovery of irisin as an exercise-regulated myokine, which induced browning of WAT, Boström *et al*. (2012a) demonstrated the beneficial effects of irisin on whole-body metabolism. Thus, adenoviral-mediated FNDC5 overexpression led to browning of WAT in lean mice as well as diet-induced obese mice. In addition, a moderate increase in circulating irisin levels by threefold augmented energy expenditure, reduced the body weight gain under high-fat diet, and improved dietinduced insulin resistance (Boström *et al*. 2012a). These results suggested a potential protective role of irisin in the development of type 2 diabetes, one of the major obesity-associated metabolic diseases. In order to investigate the relevance of irisin in humans, many clinical studies have focused on the relation between circulating irisin levels and metabolic parameters and diseases. The following section will give a comprehensive overview about the correlation of circulating irisin with metabolic parameters in humans and highlight existing discrepancies (Table 3).

As irisin has initially been described to protect against diet-induced weight gain, mediated by browning of WAT and thus increased energy expenditure, many studies have investigated the correlation of circulating irisin with obesity in humans. In line with the suggested protective role of the myokine irisin in the development of obesity, negative correlations of circulating irisin levels with the BMI have been reported in humans (Aydin *et al*. 2013, Choi *et al*. 2013, Moreno-Navarrete *et al*. 2013, Polyzos *et al*. 2014). However, controversy exists regarding the relation between irisin levels and the BMI. Several studies reported a positive correlation of serum irisin levels with BMI (Liu *et al*. 2013, Stengel *et al*. 2013, Crujeiras *et al*. 2014a, Liu *et al*. 2014, Park *et al*. 2014) or could not detect a change in circulating irisin in obesity (Huh *et al*. 2012, Gouni-Berthold *et al*. 2013, Kurdiova *et al*. 2014). This could be related to different populations analyzed in the different studies, as some include obese subjects without metabolic disorders whereas others enclose obese patients with metabolic diseases such as type 2 diabetes.

However, recent intervention studies provide evidence for a positive correlation between BMI and circulating irisin levels, which is in conflict with the proposed anti-obesity effect of irisin. The earliest intervention study by Huh *et al*. (2012) assessed morbidly obese subjects undergoing gastric banding or gastric bypass and blood samples were collected at baseline and 6 months after surgery. Bariatric surgery led to a significant weight loss after 6 months, which was accompanied by decreased circulating irisin levels. These lower irisin levels were attributed to a lower fat-free mass and decreased *FNDC5* mRNA expression in skeletal muscle (Huh *et al*. 2012). However, the reduction of fat mass was not analyzed as a factor causing lower circulating irisin levels. The recent observation that irisin is not only a myokine but also an adipokine (Roca-Rivada *et al*. 2013) raises the question if circulating irisin can be solely attributed to skeletal muscle. Moreover, secretion of irisin is higher from WAT of diet-induced obese rats compared with lean controls (Roca-Rivada *et al*. 2013), suggesting that adipose tissue, especially in states of obesity, represents an important source of irisin besides skeletal muscle. Two other interventional studies, both with 8 weeks of hypocaloric diet, observed decreased irisin levels after weight loss (de la Iglesia *et al*. 2013, Crujeiras *et al*. 2014b). In addition to a positive association between irisin and BMI, irisin has been described to be positively associated with waist circumference and fat mass. (Crujeiras *et al*. 2014a). In summary, there is stronger evidence for a positive correlation of circulating irisin with adiposity markers. Nevertheless, data are still conflicting and it is not clear which organ is the major source of irisin.

Besides the association of irisin with obesity, many studies assessed the regulation of irisin in type 2 diabetes and other metabolic diseases. Similar to the conflicting observations regarding BMI, which have been discussed above, controversy exists. While some studies reported decreased irisin levels in type 2 diabetic subjects compared with lean subjects (Choi *et al*. 2013, Liu *et al*. 2013, Kurdiova *et al*. 2014) and a negative correlation of HOMA-IR with circulating irisin levels in girls (Al-Daghri *et al*. 2013), other studies demonstrated a positive correlation of circulating irisin with HOMA-IR (Park *et al*. 2013, Ebert *et al*. 2014a).

Table 3: *Correlation of circulating irisin with metabolic parameters*

Metabolic parameter	Correlation with circulating irisin	reference
BMI	Pos. correlation (T2DM cohort)	Liu *et al*. 2014
	Pos. correlation (non-diabetics)	Liu *et al*. 2013
	Pos. correlation (cross-sectional)	Park *et al*. 2014
	Pos. correlation	Stengel *et al*. 2013
	Pos. correlation	Crujeiras *et al*. 2014a
	↑ (before vs. after weight loss)	De Iglesia *et al*. 2013
	Neg. correlation (non-diabetics)	Moreno-Navarette *et al*. 2013
	Neg. correlation	Choi *et al*. 2013
	↓ (obese vs. lean)	Polyzos *et al*. 2014
	↓ (obese vs. lean)	Aydin *et al*. 2013
	No correlation	Huh *et al*. 2012
	No correlation	Gouni-Berthold *et al*. 2013
T2DM	↓ (T2DM vs. lean)	Kurdiova *et al*. 2014
	↓ (T2DM vs. lean)	Choi *et al*. 2013
	↓ (T2DM vs. lean)	Liu *et al*. 2013
	↓ (T2DM with renal insufficiency vs. T2DM)	Liu *et al*. 2014
GDM	↑ (prior GDM vs. no GDM)	Ebert *et al*. 2014b
MetS	↑ (MetS vs. lean)	Park *et al*. 2013
HOMA-IR	Pos. correlation	Park *et al*. 2013
	Pos. correlation	Ebert *et al*. 2014a
	Neg. correlation (girls)	Al-Daghri *et al*. 2013
NAFLD	No difference (NAFLD obese vs. obese)	Polyzos *et al*. 2013
	↓ (NAFLD obese vs. obese)	Zhang *et al*. 2013
CKD	↓ (CKD vs. control)	Wen *et al*. 2013
	↓ (CKD stage 5 vs. CKD stage 1)	Ebert *et al*. 2014a

T2DM: Type 2 diabetes; GDM: gestational diabetes mellitus; MetS: Metabolic syndrome; HOMA-IR: homeostasis model assessment-estimated insulin resistance; NAFLD: Non-alcoholic fatty liver disease; CKD: Chronic kidney disease.

In line, increased irisin levels were found in subjects with metabolic syndrome (Park *et al*. 2013) and higher circulating irisin concentrations have been reported in mothers with prior gestational diabetes (GDM) compared with those without prior GDM (Ebert *et al*. 2014b). Besides, reduced circulating irisin levels have been demonstrated in patients with chronic kidney disease (CKD) (Zhang *et al*. 2013) and non-alcoholic fatty liver disease (NAFLD) (Wen *et al*. 2013, Ebert *et al*. 2014a).

In addition to the different study populations, the different assays used to detect irisin may be a reason for these controversial results. Criticism regarding the reliability of commercially available irisin/FNDC5 antibodies and non-validated ELISA kits has already been raised (Erickson 2013). In this context, we summarized the cohort, the irisin concentrations measured, and the assay used in each study to gain an overview about the range of detected irisin concentrations (Supplementary Table 1, see section on supplementary data given at the end of this article). Interestingly, there is a wide range of irisin concentrations measured, from very low concentrations of 38.86 ± 2.48 pg/ml (Choi *et al*. 2013) to relatively high concentrations of 2157.9 ± 600.7 ng/ml (Moreno-Navarrete *et al*. 2013) in lean individuals. The concentrations measured in these different studies differ strongly, with about 50 000 times higher concentrations measured in the study by Moreno-Navarette *et al*. compared with those values originating from Choi *et al*. This tremendous difference between the circulating irisin concentrations indicates that at least some of the available ELISAs are unspecific and may have a high cross-reactivity to other proteins present in serum and plasma. Moreover, striking differences are observed even when using the same kit (Supplementary Table 1).

Is the irisin fragment present in humans?

Based on the huge variation in the current studies assessing circulating irisin concentrations in humans, the physiological circulating irisin levels in humans remain unclear. Moreover, the term irisin is often incorrectly and indistinctly used with FNDC5. The secretion mechanism of irisin by extracellular cleavage of FNDC5 proposed by Boström *et al*. (2012a) and the presence of a 12.6 kDa irisin fragment (theoretical molecular weight of the irisin chain amino acids 32–142 according to UniProt entry Q8NAU1) in the circulation has not been proven. As mentioned previously, for the initial description of irisin. an antibody raised against a peptide corresponding to amino acids 149–178 and thus mainly located in the transmembrane domain was used (Erickson 2013, Raschke *et al*. 2013). This antibody (ab117436, Abcam) is not predicted to detect irisin and is no longer available at Abcam. Nevertheless, a band of 22 kDa was designated to irisin, which was detected in western blot of deglycosylated cell media from HEK293 cells transfected with FNDC5 (Boström *et al*. 2012a). This molecular weight of 22 kDa is more likely to reflect full-length FNDC5 (23.7 kDa, according to Q8NAU1) than irisin (12.6 kDa, see above), which would not be in conflict with the used antibody. A later study by Roca-Rivada *et al*. (2013) used two different antibodies, one solely against full-length FNDC5 (Abcam, raised against amino acids 149–178) and the other also detecting the irisin fragment (Phoenix Pharmaceuticals, raised against amino acids 42–142), to discriminate between these two proteins. With both antibodies, a band of 25 kDa was observed in conditioned media from rat skeletal muscle corresponding to full-length FNDC5. Interestingly, no additional band at the predicted lower molecular weight of irisin was observed with the anti-irisin antibody (Roca-Rivada *et al*. 2013), questioning the release of the initially described irisin fragment. Recently, a mass spectrometry approach has been used to clarify the identity of FNDC5-immunoreactive bands in human serum samples, which underwent deglycosylation. Several bands were observed with an anti-FNDC5 antibody from Abcam (ab131390) detecting both FNDC5 and the irisin fragment; but exclusively in a band of 24 kDa, a unique peptide located in the irisin sequence was identified by mass spectrometry, confirming that this band represents FNDC5 or fragments of FNDC5 (Lee *et al*. 2014). Unfortunately, this band was also designated as the irisin fragment, although the molecular weight is 24 kDa and the band could also represent other forms of FNDC5. Summarizing these studies, it remains unclear which fragments of FNDC5 are present in the circulation of humans.

Additionally, sequence differences between species have been reported. *FNDC5* has already been described in 2011 to contain a non-canonical ATG start codon in humans (Ivanov *et al*. 2011). In line, multispecies alignment of the *FNDC5* exon 1 revealed that the canonical ATG start site is conserved in mouse, rat, gorilla, and chimp, but displays a mutation in the human sequence to ATA (Raschke *et al*. 2013). *In vitro* studies demonstrated that the translational efficiency of full-length *FNDC5* is strikingly reduced in this case and in consequence also the release of FNDC5 fragments. Usage of the next in-frame ATG as an alternative start site would lead to a truncated form

of FNDC5 lacking the first 76 amino acids (Raschke *et al*. 2013). Interestingly, the specific fragment in the FNDC5-immunoreactive band with a molecular weight of 24 kDa identified by mass spectrometry (Lee *et al*. 2014) is a part of this truncated form (represented by NP_715637) described by Raschke *et al*. Taken together, FNDC5 fragments are present in humans, but the nature and the secretion mode have to be clarified in future studies and the presence of the initially described irisin peptide in humans is unclear.

Summary and conclusion

The discovery of irisin as an exercise-regulated myokine inducing browning of WAT has gained interest as a potential new strategy to combat obesity and its associated disorders, such as type 2 diabetes. However, there are inconsistencies regarding the relevance of irisin in humans. The regulation of *FNDC5* mRNA expression by exercise and contraction could not be reproduced by a number of human studies using several exercise protocols and *in vitro* approaches. Furthermore, the nature of FNDC5 fragments and the presence of irisin in humans are questionable and probably contribute to conflicting data obtained with commercially available ELISA kits. Most importantly, the information regarding the concentration of circulating irisin in humans is not clear, as different studies using different kits measure irisin levels in a wide range. Data about the role of irisin in states of human obesity and metabolic diseases are conflicting and, in some cases, changes in irisin levels have been observed; they were only moderate with 10–20%. Independent of the presence and regulation of FNDC5/irisin in humans, the application of recombinant irisin could still represent a therapeutic strategy to fight obesity. However, the current data obtained from human cell models reveal that FNDC5/irisin has no effect on browning of the major WAT depots in humans and is likely to selectively target a small subpopulation of adipocytes, located in classical BAT regions, such as the supraclavicular adipose tissue. Thus, other candidates, such as BMP7 or CNPs, seem to be more prominent candidates as inducers of browning in humans.

Declaration of interest

The authors declare that there is no conflict of interest that could be perceived as prejudicing the impartiality of the review reported.

Funding

This work was supported by the Ministerium für Wissenschaft und Forschung des Landes Nordrhein-Westfalen (Ministry of Science and Research of the State of North Rhine-Westphalia), the Bundesministerium für Gesundheit (Federal Ministry of Health), and the Leibniz Gemeinschaft (SAW-FBN-2013-3).

References

Al-Daghri NM, Alkharfy KM, Rahman S, Amer OE, Vinodson B, Sabico S, Milan P, Harte AL, McTernan PG, Alokail MS *et al*. 2013 Irisin as a predictor of glucose metabolism in children: sexually dimorphic effects. European Journal of Clinical Investigation [in press]. (doi:10.1111/eci.12196)

Aydin S, Aydin S, Kuloglu T, Yilmaz M, Kalayci M, Sahin I & Cicek D 2013 Alterations of irisin concentrations in saliva and serum of obese and normal-weight subjects, before and after 45 min of a Turkish bath or running. Peptides 50 13–18. (doi:10.1016/j.peptides.2013.09.011)

Besse-Patin A, Montastier E, Vinel C, Castan-Laurell I, Louche K, Dray C, Daviaud D, Mir L, Marques MA, Thalamas C *et al*. 2014 Effect of endurance training on skeletal muscle myokine expression in obese men: identification of apelin as a novel myokine. International Journal of Obesity 38 707–713. (doi:10.1038/ijo.2013.158)

Bordicchia M, Liu D, Amri EZ, Ailhaud G, Dessi-Fulgheri P, Zhang C, Takahashi N, Sarzani R & Collins S 2012 Cardiac natriuretic peptides act via p38 MAPK to induce the brown fat thermogenic program in mouse and human adipocytes. Journal of Clinical Investigation 122 1022–1036. (doi:10.1172/JCI59701)

Boström P, Wu J, Jedrychowski MP, Korde A, Ye L, Lo JC, Rasbach KA, Boström EA, Choi JH, Long JZ *et al*. 2012a A PGC1-a-dependent myokine that drives brown-fat-like development of white fat and thermogenesis. Nature 481 463–468. (doi:10.1038/nature10777)

Boström P, Wu J, Jedrychowski MP, Korde A, Ye L, Lo JC, Rasbach KA, Boström EA, Choi JH, Long JZ *et al*. 2012b Bostro¨m *et al*. reply. Nature 488 E10–E11. (doi:10.1038/nature11365)

Cannon B & Nedergaard J 2004 Brown adipose tissue: function and physiological significance. Physiological Reviews 84 277–359. (doi:10.1152/physrev.00015.2003)

Choi YK, Kim MK, Bae KH, Seo HA, Jeong JY, Lee WK, Kim JG, Lee IK & Park KG 2013 Serum irisin levels in new-onset type 2 diabetes. Diabetes Research and Clinical Practice 100 96–101. (doi:10.1016/j.diabres.2013.01.007)

Crujeiras AB, Pardo M, Arturo RR, Santiago NC, Zulet MA, Martinez JA & Casanueva FF 2014a Longitudinal variation of circulating irisin after an energy restriction-induced weight loss and following weight regain in obese men and women. American Journal of Human Biology 26 198–207. (doi:10.1002/ajhb.22493)

Crujeiras AB, Zulet MA, Lopez-Legarrea P, de la Iglesia I, Pardo M, Carreira MC, Martinez JA & Casanueva FF 2014b Association between circulating irisin levels and the promotion of insulin resistance during the weight maintenance period after a dietary weight-lowering program in obese patients. Metabolism 63 520–531. (doi:10.1016/j.metabol.2013.12.007)

Cypess AM, Lehman S,Williams G, Tal I, Rodman D, Goldfine AB, Kuo FC, Palmer EL, Tseng YH, Doria A *et al*. 2009 Identification and importance of brown adipose tissue in adult humans. New England Journal of Medicine 360 1509–1517. (doi:10.1056/NEJMoa0810780)

Cypess AM, White AP, Vernochet C, Schulz TJ, Xue R, Sass CA, Huang TL, Roberts-Toler C, Weiner LS, Sze C *et al*. 2013 Anatomical localization, gene expression profiling and functional characterization of adult human neck brown fat. Nature Medicine 19 635–639. (doi:10.1038/nm.3112)

De Matteis R, Lucertini F, GuesciniM, Polidori E, Zeppa S, Stocchi V, Cinti S & Cuppini R 2013 Exercise as a new physiological stimulus for brown adipose tissue activity. Nutrition, Metabolism, and Cardiovascular Diseases 23 582–590. (doi:10.1016/j.numecd.2012.01.013)

Ebert T, Focke D, Petroff D, Wurst U, Richter J, Bachmann A, Lossner U, Kralisch S, Kratzsch J, Beige J *et al*. 2014a Serum levels of the myokine irisin in relation to metabolic and renal function. European Journal of Endocrinology 170 501–506. (doi:10.1530/EJE-13-1053)

Ebert T, Stepan H, Schrey S, Kralisch S, Hindricks J, Hopf L, Platz M, Lossner U, Jessnitzer B, Drewlo S *et al*. 2014b Serum levels of irisin in gestational diabetes mellitus during pregnancy and after delivery. Cytokine 65 153–158. (doi:10.1016/j.cyto.2013.11.009)

Elsen M, Raschke S, Tennagels N, Schwahn U, Jelenik T, Roden M, Romacho T & Eckel J 2014 BMP4 and BMP7 induce the white-to-brown transition of primary human adipose stem cells. American Journal of Physiology. Cell Physiology 306 C431–C440. (doi:10.1152/ajpcell.00290.2013)

Erickson HP 2013 Irisin and FNDC5 in retrospect: an exercise hormone or a transmembrane receptor? Adipocytes 2 289–293. (doi:10.4161/adip.26082)

Goto M, Terada S, Kato M, Katoh M, Yokozeki T, Tabata I & Shimokawa T 2000 cDNA cloning and mRNA analysis of PGC-1 in epitrochlearis muscle in swimming-exercised rats. Biochemical and Biophysical Research Communications 274 350–354. (doi:10.1006/bbrc.2000.3134)

Gouni-Berthold I, Berthold HK, Huh JY, Berman R, Spenrath N, Krone W & Mantzoros CS 2013 Effects of lipid-lowering drugs on irisin in human subjects in vivo and in human skeletal muscle cells ex vivo. PLoS ONE 8 e72858. (doi:10.1371/journal.pone.0072858)

Hecksteden A, Wegmann M, Steffen A, Kraushaar J, Morsch A, Ruppenthal S, Kaestner L & Meyer T 2013 Irisin and exercise training in humans – results from a randomized controlled training trial. BMC Medicine 11 235. (doi:10.1186/1741-7015-11-235)

Huh JY, Panagiotou G, Mougios V, Brinkoetter M, Vamvini MT, Schneider BE & Mantzoros CS 2012 FNDC5 and irisin in humans: I. Predictors of circulating concentrations in serum and plasma and II. mRNA expression and circulating concentrations in response to weight loss and exercise. Metabolism 61 1725–1738. (doi:10.1016/j.metabol.2012.09.002)

de la Iglesia R, Lopez-Legarrea P, Crujeiras AB, Pardo M, Casanueva FF, Zulet MA & Martinez JA 2013 Plasma irisin depletion under energy restriction is associated with improvements in lipid profile inmetabolic syndrome patients. Clinical Endocrinology [in press]. (doi:10.1111/cen.12383)

Ivanov IP, Firth AE, Michel AM, Atkins JF & Baranov PV 2011 Identification of evolutionarily conserved non-AUG-initiated N-terminal extensions in human coding sequences. Nucleic Acids Research 39 4220–4234. (doi:10.1093/nar/gkr007)

Jespersen NZ, Larsen TJ, Peijs L, Daugaard S, Homoe P, Loft A, de Jong JJ, Mathur N, Cannon B, Nedergaard J *et al*. 2013 A classical brown adipose tissue mRNA signature partly overlaps with brite in the supraclavicular region of adult humans. Cell Metabolism 17 798–805. (doi:10.1016/j.cmet.2013.04.011)

Kelly DP 2012 Irisin, light my fire. Science 336 42–43. (doi:10.1126/science.1221688)

Kraemer RR, Shockett P, Webb ND, Shah U & Castracane VD 2014 A transient elevated irisin blood concentration in response to prolonged, moderate aerobic exercise in young men and women. Hormone and Metabolic Research 46 150–154. (doi:10.1055/s-0033-1355381)

Kurdiova T, Balaz M, Vician M, Maderova D, Vlcek M, Valkovic L, Srbecky M, Imrich R, Kyselovicova O, Belan V *et al*. 2014 Effects of obesity, diabetes and exercise on Fndc5 gene expression and irisin release in human skeletal muscle and adipose tissue: in vivo and in vitro studies. Journal of Physiology 592 1091–1107. (doi:10.1113/jphysiol.2013.264655)

Lambernd S, Taube A, Schober A, Platzbecker B, Gorgens SW, Schlich R, Jeruschke K, Weiss J, Eckardt K & Eckel J 2012 Contractile activity of human skeletal muscle cells prevents insulin resistance by inhibiting pro-inflammatory signalling pathways. Diabetologia 55 1128–1139. (doi:10.1007/s00125-012-2454-z)

Lee P, Linderman JD, Smith S, Brychta RJ, Wang J, Idelson C, Perron RM, Werner CD, Phan GQ, Kammula US *et al*. 2014 Irisin and FGF21 are cold-induced endocrine activators of brown fat function in humans. Cell Metabolism 19 302–309. (doi:10.1016/j.cmet.2013.12.017)

Lidell ME, Betz MJ, Dahlqvist LO, Heglind M, Elander L, Slawik M, Mussack T, Nilsson D, Romu T, Nuutila P *et al*. 2013 Evidence for two types of brown adipose tissue in humans. Nature Medicine 19 631–634. (doi:10.1038/nm.3017)

Liu JJ, Wong MD, Toy WC, Tan CS, Liu S, Ng XW, Tavintharan S, Sum CF & Lim SC 2013 Lower circulating irisin is associated with type 2 diabetes mellitus. Journal of Diabetes and its Complications 27 365–369. (doi:10.1016/j.jdiacomp.2013.03.002)

Liu JJ, Liu S, Wong MD, Tan CS, Tavintharan S, Sum CF & Lim SC 2014 Relationship between circulating irisin, renal function and body composition in type 2 diabetes. Journal of Diabetes and its Complications 28 208–213. (doi:10.1016/j.jdiacomp.2013.09.011)

van Marken Lichtenbelt WD, Vanhommerig JW, Smulders NM, Drossaerts JM, Kemerink GJ, Bouvy ND, Schrauwen P & Teule GJ 2009 Cold-activated brown adipose tissue in healthy men. New England Journal of Medicine 360 1500–1508. (doi:10.1056/NEJMoa0808718)

Moraes C, Leal VO, Marinho SM, Barroso SG, Rocha GS, Boaventura GT & Mafra D 2013 Resistance exercise training does not affect plasma irisin levels of hemodialysis patients. Hormone and Metabolic Research 45 900–904. (doi:10.1055/s-0033-1354402)

Moreno-Navarrete JM,Ortega F, Serrano M, Guerra E, Pardo G, Tinahones F, RicartW& Fernandez-Real JM 2013 Irisin is expressed and produced by human muscle and adipose tissue in association with obesity and insulin resistance. Journal of Clinical Endocrinology and Metabolism 98 E769–E778. (doi:10.1210/jc.2012-2749)

Norheim F, Langleite TM, Hjorth M, Holen T, Kielland A, Stadheim HK, Gulseth HL, Birkeland KI, Jensen J & Drevon CA 2014 The effects of acute and chronic exercise on PGC-1a, irisin and browning of subcutaneous adipose tissue in humans. FEBS Letters 281 739–749. (doi:10.1111/febs.12619)

Ouellet V, Labbe SM, Blondin DP, Phoenix S, Guerin B, Haman F, Turcotte EE, Richard D & Carpentier AC 2012 Brown adipose tissue oxidative metabolism contributes to energy expenditure during acute cold exposure in humans. Journal of Clinical Investigation 122 545–552. (doi:10.1172/JCI60433)

Park KH, Zaichenko L, Brinkoetter M, Thakkar B, Sahin-Efe A, Joung KE, Tsoukas MA, Geladari EV, Huh JY, Dincer F *et al*. 2013 Circulating irisin in relation to insulin resistance and the metabolic syndrome. Journal of Clinical Endocrinology and Metabolism 98 4899–4907. (doi:10.1210/jc.2013-2373)

Park KH, Zaichenko L, Peter P, Davis CR, Crowell JA & Mantzoros CS 2014 Diet quality is associated with circulating C-reactive protein but not irisin levels in humans. Metabolism 63 233–241. (doi:10.1016/j.metabol.2013.10.011)

Pekkala S, Wiklund PK, Hulmi JJ, Ahtiainen JP, Horttanainen M, Pollanen E, Makela KA, Kainulainen H, Hakkinen K, Nyman K *et al*. 2013 Are skeletal muscle FNDC5 gene expression and irisin release regulated by exercise and related to health? Journal of Physiology 591 5393–5400. (doi:10.1113/jphysiol.2013.263707)

Petrovic N, Walden TB, Shabalina IG, Timmons JA, Cannon B & Nedergaard J 2010 Chronic peroxisome proliferator-activated receptor gamma (PPARgamma) activation of epididymally derived white adipocyte cultures reveals a population of thermogenically competent, UCP1-containing adipocytes molecularly distinct from classic brown adipocytes. Journal of Biological Chemistry 285 7153–7164. (doi:10.1074/jbc.M109.053942)

Pilegaard H, Saltin B & Neufer PD 2003 Exercise induces transient transcriptional activation of the PGC-1a gene in human skeletal muscle. Journal of Physiology 546 851–858. (doi:10.1113/jphysiol.2002.034850)

Polyzos SA, Kountouras J, Anastasilakis AD, Geladari EV & Mantzoros CS 2014 Irisin in patients with nonalcoholic fatty liver disease. Metabolism 63 207–217. (doi:10.1016/j.metabol.2013.09.013)

Raschke S, Elsen M, Gassenhuber H, Sommerfeld M, Schwahn U, Brockmann B, Jung R, Wisloff U, Tjonna AE, Raastad T *et al*. 2013 Evidence against a beneficial effect of irisin in humans. PLoS ONE 8 e73680. (doi:10.1371/journal.pone.0073680)

Roca-Rivada A, Castelao C, Senin LL, Landrove MO, Baltar J, Belen CA, Seoane LM, Casanueva FF & Pardo M 2013 FNDC5/irisin is not only a myokine but also an adipokine. PLoS ONE 8 e60563. (doi:10.1371/journal.pone.0060563)

Saito M, Okamatsu-Ogura Y, Matsushita M, Watanabe K, Yoneshiro T, Nio-Kobayashi J, Iwanaga T, Miyagawa M, Kameya T, Nakada K *et al*. 2009 High incidence of metabolically active brown adipose tissue in healthy adult humans: effects of cold exposure and

adiposity. Diabetes 58 1526–1531. (doi:10.2337/db09-0530)

Scarpace PJ, Yenice S& Tumer N 1994 Influence of exercise training and age on uncoupling protein mRNA expression in brown adipose tissue. Pharmacology, Biochemistry, and Behavior 49 1057–1059. (doi:10.1016/0091-3057(94)90264-X)

Schulz TJ, Huang TL, Tran TT, Zhang H, Townsend KL, Shadrach JL, Cerletti M, McDougall LE, Giorgadze N, Tchkonia T *et al*. 2011 Identification of inducible brown adipocyte progenitors residing in skeletal muscle and white fat. PNAS 108 143–148. (doi:10.1073/pnas.1010929108)

Seale P, Bjork B, Yang W, Kajimura S, Chin S, Kuang S, Scime A, Devarakonda S, Conroe HM, Erdjument-Bromage H *et al*. 2008 PRDM16 controls a brown fat/skeletal muscle switch. Nature 454 961–967.

(doi:10.1038/nature07182) Segawa M, Oh-Ishi S, Kizaki T, Ookawara T, Sakurai T, Izawa T, Nagasawa J, Kawada T, Fushiki T & Ohno H 1998 Effect of running training on brown adipose tissue activity in rats: a reevaluation. Research Communications in Molecular Pathology and Pharmacology 100 77–82.

Shan T, Liang X, Bi P & Kuang S 2013 Myostatin knockout drives browning of white adipose tissue through activating the AMPK–PGC1α–Fndc5 pathway in muscle. FASEB Journal 27 1981–1989. (doi:10.1096/fj.12-225755)

Stengel A, Hofmann T, Goebel-Stengel M, Elbelt U, Kobelt P & Klapp BF 2013 Circulating levels of irisin in patients with anorexia nervosa and different stages of obesity – correlation with body mass index. Peptides 39 125–130. (doi:10.1016/j.peptides.2012.11.014)

Timmons JA, Baar K, Davidsen PK & Atherton PJ 2012 Is irisin a human exercise gene? Nature 488 E9–10. (doi:10.1038/nature11364)

Virtanen KA, Lidell ME, Orava J, Heglind M, Westergren R, Niemi T, Taittonen M, Laine J, Savisto NJ, Enerback S *et al*. 2009 Functional brown adipose tissue in healthy adults. New England Journal of Medicine 360 1518–1525. (doi:10.1056/NEJMoa0808949)

Walden TB, Hansen IR, Timmons JA, Cannon B & Nedergaard J 2012 Recruited vs. nonrecruited molecular signatures of brown, ”brite”, and white adipose tissues. American Journal of Physiology. Endocrinology and Metabolism 302 E19–E31. (doi:10.1152/ajpendo.00249.2011)

Wen MS, Wang CY, Lin SL & Hung KC 2013 Decrease in irisin in patients with chronic kidney disease. PLoS ONE 8 e64025. (doi:10.1371/journal.pone.0064025)

Wu J, Boström P, Sparks LM, Ye L, Choi JH, Giang AH, Khandekar M, Virtanen KA, Nuutila P, Schaart G *et al*. 2012 Beige adipocytes are a distinct type of thermogenic fat cell in mouse and human. Cell 150 366–376. (doi:10.1016/j.cell.2012.05.016)

Xu X, Ying Z, Cai M, Xu Z, Li Y, Jiang SY, Tzan K,Wang A, Parthasarathy S, He G *et al*. 2011 Exercise ameliorates high-fat diet-induced metabolic and vascular dysfunction, and increases adipocyte progenitor cell population in brown adipose tissue. American Journal of Physiology. Regulatory, Integrative and Comparative Physiology 300 R1115–R1125. (doi:10.1152/ajpregu.00806.2010)

Zhang HJ, Zhang XF,Ma ZM, Pan LL, Chen Z, Han HW, Han CK, Zhuang XJ, Lu Y, Li XJ *et al*. 2013 Irisin is inversely associated with intrahepatic triglyceride contents in obese adults. Journal of Hepatology 59 557–562. (doi:10.1016/j.jhep.2013.04.030)

Zhang Y, Li R, Meng Y, Li S, Donelan W, Zhao Y, Qi L, Zhang M, Wang X, Cui T *et al*. 2014 Irisin stimulates browning of white adipocytes through mitogen-activated protein kinase p38 MAP kinase and ERK MAP kinase signaling. Diabetes 63 514–525. (doi:10.2337/db13-1106)

Zingaretti MC, Crosta F, Vitali A, Guerrieri M, Frontini A, Cannon B, Nedergaard J & Cinti S 2009 The presence of UCP1 demonstrates that metabolically active adipose tissue in the neck of adult humans truly represents brown adipose tissue. FASEB Journal 23 3113–3120. (doi:10.1096/fj.09-133546)

***Suppl. Table 1**: Range of circulating irisin levels in humans*

Study (reference)	Patients/subjects	Circulating Concentration (ng/ml)	sample	Assay supplier
Al-Daghri et al. 2013	153 Saudi-Arab children: 81 boys (age 12.4±3.2 years, BMI: 19.5±5.9) 72 girls (age: 12.9±3.2 years, BMI: 20.6±5.2)	 930 ±? 1570±?	serum	Phoenix
Aydin et al. 2013	Middle-aged obese male subjects (n=14), normal weight male subjects (n=14)	~ 65	serum	Phoenix (EK-067-52)
Choi et al. 2012	Healthy adults (n=104) New onset of type 2 diabetes (n=104)	0.0389 0.0245	serum	USCN LifeScience
Crujeiras et al. 2014a	Obese subjects (n=94): BMI 35.6 ± 4.5 kg/m^2 Lean subjects (n=48): BMI 22.9 ± 2.2 kg/m^2	353.1 ± 18.06 198.4 ± 7.8	plasma	Phoenix (EK-067-52)
De la Iglesia et al. 2013	84 caucasian adults with metabolic syndrome control diet group (n=42) RESMENA diet group (n=42)	Baseline irisin levels: 423.8 ± 220.0 300.3 ± 118.6	plasma	Phoenix (EK-067-52)
Ebert et al. 2014a	532 CKD patients (CKD stage 1-5)	392.6 (median) CKD1 females - 307.9 (median) CKD5 males	serum	Phoenix
Ebert et al. 2014b	74 pregnant women with gestational DM 74 NGT pregnant control subjects	482.1 (median) 466.6 (median)	serum	Phoenix
Gouni-Berthold et al. 2013	Healthy males with mild hypercholesterolemia (n=70)	265 ±102	serum	Aviscera Bioscience
Huh et al. 2012	117 greek middle-aged women (age 49.3±8.6 years, BMI 30.2±5.3) Morbidly obese subjects (n=14) (age 53.1±8.9, BMI 50.2±10.6)	113.12±20.62 112.67±32.19	plasma	Aviscera Bioscience
Kurdiova et al. 2014	99 middle-aged sedentary men were into 4 groups: (i) lean healthy (control) individuals (n=29) (ii) healthy overweight/obese patients (n=29) (iii) patients with impaired glucose tolerance (n=25) (iv) newly diagnosed, untreated type 2 diabetes (n=16)	~ 5 ng/ml	plasma	Phoenix (RK-067-16)
Kraemer et al. 2014	Healthy, young male (n=7)	~ 50	plasma	Aviscera Bioscience
Liu et al. 2013	Healthy subjects (n=60) Type 2 Diabetics (n=96)	257 ±24 204 ± 72	plasma	USCN LifeScience
Liu et al. 2014	365 T2DM sujects	63.3 – 117.3	plasma	Aviscera Bioscience
Moraes et al. 2013	Healthy subjects (n=18) Hemodialysis patients (n=26)	101.3 ± 12.5 71.0 ± 41.6	plasma	Phoenix
Moreno-Navarette et al. 2013	Healthy subjects (n=18) Obese subjects (n=17)	2157.9 ± 600.7 1783.7 ± 426.9	plasma	Aviscera Bioscience

Suppl. Table 1: Range of circulating irisin levels in humans

Study (reference)	Patients/subjects	Circulating Concentration (ng/ml)	sample	Assay supplier
Park et al. 2013	Healthy subjects (n=107) Subjects with metabolic syndrome (n=44)	162.2 214.4	serum/plasma	Phoenix (EK-067-52)
Park et al. 2014	Caucasians (n=72), BMI = 28.6 ± 6.5 African-Americans (n=79), BMI = 31.7 ± 7.8	166.0 ± 1.4 196.5 ± 1.4	serum/plasma	Pheonix (EK-067-52)
Pekkala et al. 2013	Healthy, middle-aged untrained males (n=17)	~1000	serum	Phoenix
Polyzos et al. 2014	Nonalcoholic fatty liver disease (NAFLD) patients Obese controls (similar BMI as NAFLD group) Lean controls	30.5 ± 1.5 (NAFLD) 33.7 ± 2.7 49.7 ± 2.0	serum	Phoenix (EK-067-52)
Stengel et al. 2013	Normal weight (n=8), BMI = 22.6 ± 0.9 Obese (n=8), BMI = 36.9 ± 1.2 Morbid Obese (n=8), BMI = 45.9 ± 5	774.5 ± 46.2 794.9 ± 64.8 917.2 ± 67.4	plasma	Phoenix (EK-067-16)
Wen et al. 2013	Healthy, older subjects (n=19) Chronic kidney disease patients (n=38)	108.5 ± 3.6 91.2 ± 3.1	plasma	Aviscera Bioscience
Zhang et al. 2013	Obese subjects (n=74)	9.01 (3.57-18.88)	serum	Aviscera Bioscience

The ELISA kit EK-067–52 distributed by Phoenix is manufactured by Aviscera (Santa Clara, CA.) and corresponds to the Aviscera ELISA kit.

2.6 Contribution statement

Functional annotation of the human fat cell secretome

Dahlman I, **Elsen M**, Tennagels N, Korn M, Brockmann B, Sell H, Eckel J & Arner P (2012). Arch.Physiol Biochem. 118 84-91.

Impact factor: to be released

Contribution	Total: 27.5 % Conceived / designed experiments: 25 % Performed experiments: 25 % Analysed data: 35 % Contributed to discussion: 35 % Wrote the manuscript: 20 % Reviewed / edited manuscript: 35% Author: 2nd author

BMP4 and BMP7 induce the white-to-brown transition of primary human adipose stem cells

Elsen M, Raschke S, Tennagels N, Schwahn U, Jelenik T, Roden M, Romacho T, Eckel J (2014) Am.J.Physiol Cell Physiol 306 C431-C440.

Impact factor: 3.674

Contribution	Total: 86.6 % Conceived / designed experiments: 90 % Performed experiments: 90 % Analysed data: 90 % Contributed to discussion: 70 % Wrote the manuscript: 90 Reviewed / edited manuscript: 90% Author: 1st author

Eicosapentaenoic acid and arachidonic acid differentially regulate white-to-brown conversion and mitochondrial function in primary human adipocytes

Fleckenstein-Elsen M, Dinnies D, Jelenik T, Roden M, Romacho T, Eckel J (2015) International Journal of Obesity, submitted

Impact factor: 5.386

Contribution	Total: 83.3 % Conceived / designed experiments: 90 % Performed experiments: 70 % Analysed data: 70 % Contributed to discussion: 90 % Wrote the manuscript: 90 Reviewed / edited manuscript: 90% Author: 1st author

Evidence against a beneficial effect of irisin in humans

Raschke S, **Elsen M**, Gassenhuber H, Sommerfeld M, Schwahn U, Brockmann B, Jung R, Wisløff U, Tjønna AE, Raastad T, Hallén J, Norheim F, Drevon CA, Romacho T, Eckardt K, Eckel J (2013). PLoS.One. 8 e73680.

Impact factor: 3.534

Contribution	Total: 37.5 % Conceived / designed experiments: 35 % Performed experiments: 40 % Analysed data: 40 % Contributed to discussion: 40 % Wrote the manuscript: 30 % Reviewed / edited manuscript: 40% Author: 2nd author

Browning of white fat: does irisin play a role in humans?

Elsen M, Raschke S, Eckel J (2014) J.Endocrinol. 222 R25-R38.

Impact factor: 3.586

Contribution	Total: 76.6 % Conceived / designed experiments: - Performed experiments: - Analysed data: - Contributed to discussion: 60 % Wrote the manuscript: 80 % Reviewed / edited manuscript: 90% Author: 1st author

3 Discussion

3.1 Characterization of the adipose tissue secretome – identification of novel adipokines regulating adipogenesis

Obesity-related metabolic disturbances are linked to the dysfunction of WAT (12;108). WAT is now recognized as active endocrine organ, secreting more than 300 different proteins (10). The adipokine secretion pattern is altered in the obese state and plays a major role in the development of type 2 diabetes (108). In particular, an increased secretion of inflammatory cytokines is associated with WAT dysfunction and promotes insulin resistance (109). In contrast, the adipokine adiponectin is one of the few factors whose secretion from WAT is downregulated in obesity and which exerts beneficial effects on insulin sensitivity (110). Despite the ongoing characterization of single adipose tissue-derived factors, there is limited knowledge about the broad regulation of the whole secretome in human adipocytes. Several *in vitro* studies contributed to describe the regulation of potential adipokines during adipocyte differentiation (111-113), induced insulin resistance (114) or under *in vitro* hypoxic conditions (111). However, the clinical role of the majority of these secreted factors and their regulation in obesity *in vivo* is largely unknown. Therefore, we performed an *in silico* analysis of the recently identified 347 adipocyte-derived proteins (10) in order to analyze their regulation in obesity *in vivo*, and to score and identify adipokine candidates of high interest for further functional analysis (11).

In order to identify novel adipokines of high interest, we have chosen scoring categories which would describe a classical adipokine like adiponectin (11). Different cells present in WAT contribute to the whole adipose tissue secretome, comprising cytokines, chemokines and other hormones (8). However, it has been recommended to define a true adipokine as factor being produced and secreted primarily from mature adipocytes (5). Therefore, the main scoring criteria (i) regulated during differentiation of human adipocytes, (ii) regulated in obesity (using human WAT samples and an obese animal model), (iii) highly expressed in adipose tissue compared to other tissues, and (iv) annotated to be a secreted protein, were defined. Proving the validity of this scoring system, adiponectin and leptin reached a high score.

Expression levels of most of the 347 candidate adipokines were upregulated in subcutaneous and visceral WAT from obese compared to lean female subjects (11). Adipose tissue undergoes structural changes during expansion of fat mass and progression of obesity (8). The

chronic low-grade inflammation of WAT, an enlargement of adipocytes and alterations of extracellular matrix (ECM) components represent the main aspects of WAT remodeling (115). Accordingly, numerous of the adipokine candidates which were strongly upregulated in WAT from obese versus lean subjects could be allocated to ECM components, adhesion molecules or factors of the acute inflammatory response (11).

An "unhealthy" expansion of fat mass due to a reduced generation of new adipocytes may enhance the development of adipocyte hypertrophy, which is linked to WAT inflammation (115) and metabolic dysfunction (18). Recent studies revealed that the annual adipocyte turnover *in vivo*, and the capacity of subcutaneous preadipocytes to differentiate *in vitro* is impaired in hypertrophic obesity (17;18). In line with these findings, several cytokines which are upregulated in adipose tissue dysfunction exert inhibitory action on adipocyte differentiation (116). Promoting adipocyte differentiation, as triggered by the PPARγ agonist drugs TZD, leads to hyperplasia of WAT along with the presence of smaller adipocytes and allowing a "healthy" fat mass expansion (117). Recent research provided evidence that certain adipose tissue-derived factors regulating adipogenesis in an auto-/paracrine manner are dysregulated in the obese state (18;118). Hence, the identification of novel adipokine candidates involved in the regulation of adipocyte differentiation is of particular interest in the context of adipose tissue expansion.

WNT1-inducible signaling pathway protein 2 (WISP2)

The wingless-type mouse mammary tumor virus integration site family (WNT)-signaling pathway governs several developmental processes and is highly conserved between species (119). Secreted proteins of the WNT family activate canonical WNT/β-catenine signaling by binding to the transmembrane receptors of the Frizzled family and its coreceptor lipoprotein receptor-related protein (LRP). In contrast to BMP signaling, WNT/β-catenine signaling negatively regulates adipogenesis by inhibition of PPARγ and C/EBPα (120), the key transcription factors of adipogenesis (58). WNT-signaling needs to be abrogated to allow induction of adipocyte differentiation. This is partially mediated by increased secretion of the extracellular WNT antagonist Dickkopf-1 (DKK1) upon induction of adipogenesis of human subcutaneous preadipocytes (118). However, other factors secreted from adipose tissue may affect WNT-signaling and thereby regulate adipocyte differentiation in an auto-/paracrine manner.

WISP2 was one of the top score candidate adipokines in our study (11) and could represent a novel factor regulating adipogenesis. Gene expression of *WISP2* is induced by WNT-signaling (121). On the contrary, *WISP2* mRNA expression has been described to be suppressed during 3T3-L1 adipocyte differentiation along with inhibition of the WNT-signaling pathway (122;123). Accordingly, we also observed that *WISP2* is regulated during differentiation of primary human adipocytes. WISP2 has been previously validated as adipokine primarily secreted from preadipocytes which inhibits adipocyte differentiation (123). Secreted WISP2 activated canonical WNT/β-catenine signaling (124) and overexpression of *WISP2* or addition of recombinant WISP2 protein inhibited differentiation of 3T3-L1 adipocytes (123). Besides secreted WISP2, a cytosolic form of WISP2 coexists which also suppresses adipocyte differentiation by binding the PPARγ activator zinc finger protein 423 (Znf423) (123). Interestingly, the proadipogenic growth factor BMP4 (83;118;125) is able to rescue a reduced adipogenesis mediated by WISP2 (118). We found that *WISP2* expression is upregulated in WAT from obese compared to lean subjects (11) and a positive correlation between adipocyte size and *WISP2* expression in subcutanoeus WAT has been described (123). Keeping the concept of an "unhealthy" fat expansion in mind, WISP2 might be a promising adipokine dysregulated in obesity and contributing to the development of adipocyte hypertrophy by inhibition of *de novo* adipogenesis.

Chordin-like 1 (CHRDL1)

Another top score adipokine candidate found upregulated in the obese state was CHRDL1 (11). CHRDL1, alternatively called ventroptin or neurogenesin-1, gained our interest due to its function as extracellular BMP antagonist (126-129).

BMP signaling plays a role in adipogenesis and other developmental processes. Temporal and spatial regulation of the BMP ligand availability and the secretion of extracellular BMP antagonists allows tight control of BMP signaling (78). BMP antagonists directly bind to the BMP ligand in the extracellular space, thereby preventing or dampening binding of BMPs to their cognate receptors (78). CHRDL1 was initially described as a secreted BMP4 antagonist in chicken embryos and may be involved in the regulation of topographic retinotectal projection (127). Besides BMP4, CHRDL1 has been shown to interact with other BMP family members. The BMP2-induced osteogenic differentiation in MC3T3-E1 (130) as well as the BMP7-induced osteoblastic trans-differentiation of myogenic C2C12 cells were inhibited by CHRDL1 (131). BMP antagonists are very complex in their action and have partially been

described to exert agonistic effects on BMP signaling as well (78). This may also be true for CHRDL1, which enhanced BMP2-mediated effects on C2C12 cells while inhibiting those effects induced by BMP7 (131). Since the BMP family members BMP4 and BMP7 are assumed to have opposing effects on white and brite adipocyte differentiation (79), we hypothesized that CHRDL1 may differentially regulate BMP4 and BMP7 action in adipocytes.

To validate CHRDL1 as adipokine, we assessed expression of CHRDL1 on the mRNA and protein level during differentiation of primary human adipocytes. We observed that CHRDL1 mRNA and protein expression were upregulated during *in vitro* differentiation of human subcutaneous preadipocytes (Figure 5 a+b). This finding was confirmed by a recent study assessing the expression pattern of several BMP antagonists during adipogenesis. Interestingly, all antagonists were downregulated during adipocyte differentiation, except CHRDL1 and noggin (132). Taking into account that CHRDL1 may have a dual function as BMP agonist or antagonist (128;131), the strong upregulation of CHRDL1 during adipogenesis raised the question if it is an endogenous antagonist of BMPs. To address this question, we tested if recombinant CHRDL1 could affect the BMP4- or BMP7-induced SMAD1/5/8 phosphorylation in primary human preadipocytes. We observed no impact of recombinant CHRDL1 on canonical BMP-signaling (Figure 5 c+d). In accordance, a previous study by Gustafson and colleagues found that overexpression of *CHRDL1* in preadipocytes did not alter adipocyte differentiation and no effect on BMP4-mediated SMAD1/5/8 phosphorylation was observed (132). Moreover, silencing of *CHRDL1* even decreased adipocyte differentiation and this effect was not rescued by addition of BMP4 (132).

In summary, the current data about the role of CHRDL1 in adipogenesis strongly indicate, that CHRDL1 does not interfere with the BMP4-induced promotion of differentiation. Moreover, CHRDL1 is likely to be no endogenous factor differentially regulating BMP4 and BMP7 action on white and brite adipocyte differentiation. Nevertheless, expression of the adipokine *CHRDL1* is strongly upregulated in subcutaneous WAT from obese patients compared to lean (11;132) and its function in adipose tissue should be further investigated.

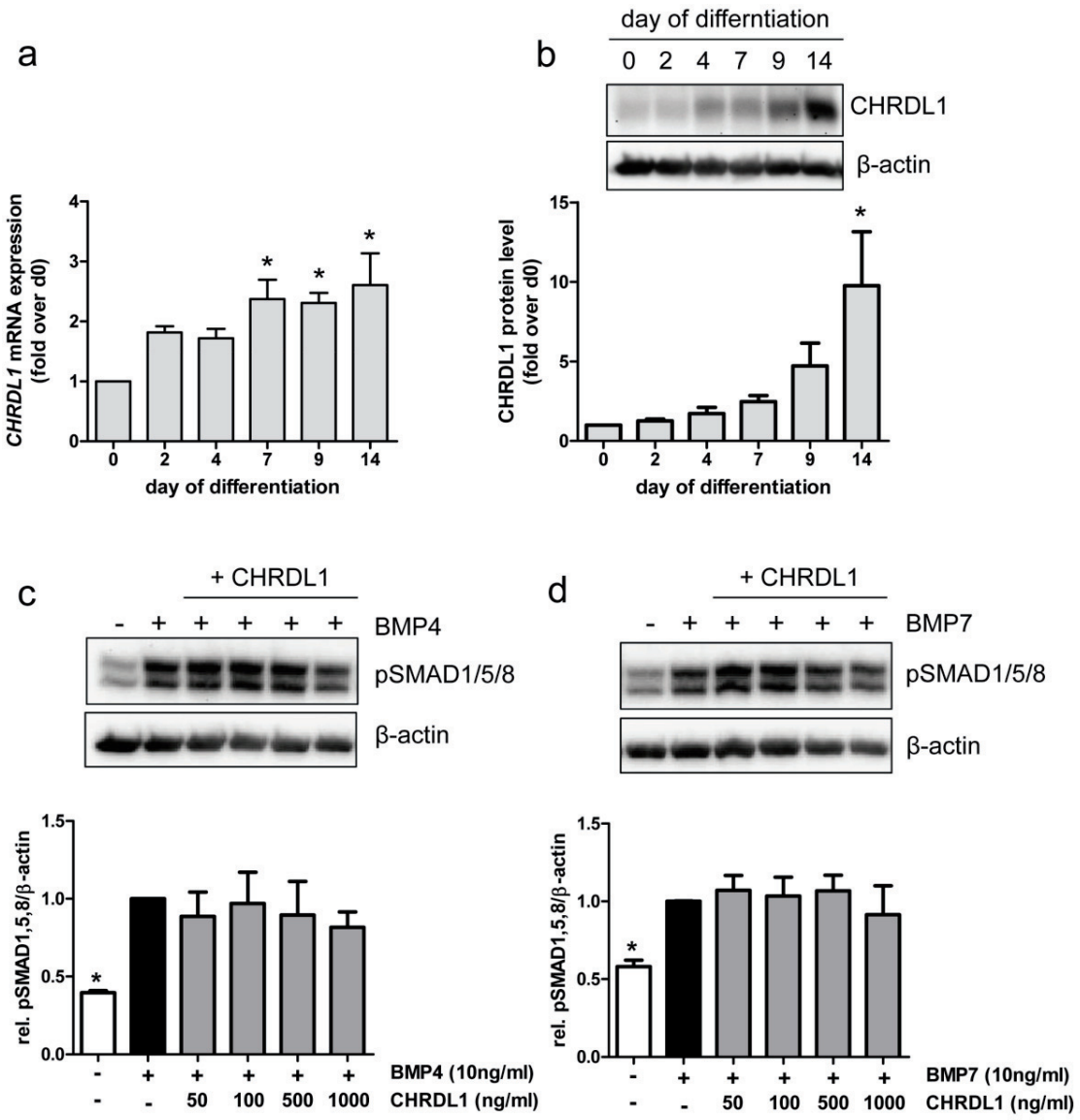

Figure 5: Regulation of CHRDL1 during adipogenesis and its effect on BMP signaling. (a+b) Primary human preadipocytes were isolated from subcutaneous WAT of different lean female subjects and *in vitro* differentiated for the indicated time points. CHRDL1 mRNA expression was assessed via qRT-PCR and normalized to β-actin mRNA levels (a). Protein levels of CHRDL1 during adipogenesis were analyzed by Western Blot and normalized to β-actin abundance (b). Data represent mean values ± SEM and are expressed relative to day 0 of differentiation, n=4-5, *p<0.05 vs. day 0 (c+d) Subcutaneous preadipocytes were challenged with 10 ng/ml BMP4 (c) or BMP7 (d) for 1 hour with or without the addition of different concentrations of the potential agonist CHRDL1. SMAD1/5/8 phosphorylation was determined via Western Blot. Values are normalized to β-actin protein levels and expressed relative to BMP treatment alone. Data represent means ± SEM, n=3, *p<0.05 vs. BMP treatment alone.

3.2 Role of BMP4 and BMP7 on white, brite and brown adipogenesis

The two BMP family members BMP4 and BMP7 were and may still be assumed to differentially regulate white and brown adipocyte differentiation (79;83). The identification of different developmental origins of brown and white adipocytes, the discovery of the brite

adipocyte and the existence of potential differences between mice und human adipose tissue depots complicated the interpretation of the role of BMP4 and BMP7 in the regulation of adipocyte differentiation.

BMP4, but not BMP7 is an endogenous factor regulating adipogenesis

In 2004, BMP4 was initially proposed to induce commitment of murine pluripotent C3H10T1/2 cells to the adipocyte lineage, indicated by the formation of lipid-laden cells and increased expression of the key transcription factors PPARγ and C/EBPα (133). Moreover, BMP signaling is required for stem cell commitment since overexpression of constitutively active BMP receptor 1a (BMPR1A) or BMP receptor 1b (BMPR1B) allows adipogenic differentiation of C3H10T1/2 cells in the absence of BMP2 or BMP4 (134). BMP4 is expressed and secreted from A33 cells, an adipogenic subclone from murine pluripotent 10T1/2 cells. Adipocyte differentiation can be blocked in these cells by addition of the BMP4 inhibitor noggin (135), suggesting that BMP4 is a secreted factor regulating adipogenesis in an auto-/paracrine manner. In line with this finding, BMP4 mRNA expression has also been shown in primary human preadipocytes and adipogenesis was blocked after exposure to noggin (118). Interestingly, the regulation of BMP4 during adipogenesis seems to be dependent on the cell type and/or species. BMP4 mRNA expression is strongly suppressed upon induction of differentiation in 3T3-L1 preadipocytes (118;136), while primary human preadipocytes displayed increased BMP4 expression levels after adipogenic induction (118). In contrast, we observed that BMP4 protein is constitutively expressed during differentiation of primary human preadipocytes (125). Differences in the regulation of BMP4 expression may be explained by the use of different cell culture media containing distinct supplements. Nevertheless, we confirmed that BMP4 is a secreted factor by Western blot detection of BMP4 in concentrated supernatants from *in vitro* differentiated human adipose-derived stem cells (hASCs) (125).

In contrast to BMP4, less is known about the relevance of BMP7 as endogenous factor released from adipose tissue. We were able to detect mature BMP7 protein in whole cell lysates from hASCs as well as from differentiated hASCs, but failed to show secretion of BMP7 (125). BMP7 mRNA and protein have also been detected in a subset of precursor cells isolated from subcutaneous WAT from different female subjects (137), while a recent study even found no mRNA expression of BMP7 at all in primary human preadipocytes and adipocytes (132). Taken together, BMP7 has not been proven to be secreted from

preadipocytes or mature adipocytes until now and one study was not able to show mRNA expression at all. BMP4 and BMP7 are found in the circulation of humans (138;139) and may therefore impact adipose tissue in an endocrine manner. However, BMPs are mainly acting locally through formation of a growth factor gradient during adipose tissue development (83). Given that BMP7 secretion from human adipocytes remains unclear, BMP7 is not likely to be an important auto-/paracrine regulator of WAT plasticity, at least in humans.

BMP4 and BMP7 as regulators of white versus brite/brown differentiation

The initial studies describing BMP4 as a trigger for the commitment to the white adipocyte lineage were mainly based on the assessment of lipid accumulation and expression of PPARγ and C/EBPα (133-135). These are common features of *in vitro* differentiated white, brite and brown adipocytes. Measurement of specific marker gene expression and functional features is necessary to distinguish different types of adipocytes. Since knowledge about white, brite and brown marker genes began to increase after 2009, it is possible that a potential effect of BMP4 on brite adipogenesis has not been recognized before.

However, the fact that C3H10T1/2 cells pretreated with BMP4 and implanted into BALB/c athymic mice developed into unilocular adipocytes strongly indicated that BMP4 promotes commitment of pluripotent stem cells to the white adipocyte lineage (133). Further evidence was provided by Tseng and colleagues in 2008, showing that BMP4 inhibited *UCP1* expression in brown preadipocytes isolated from the interscapular BAT of lean mice, while BMP7 increased *UCP1* expression in those cells. Importantly, both BMP members induced general adipocyte differentiation and lipid accumulation to the same extent (80). Supporting a role for BMP7 in BAT development, implantation of BMP7 pretreated C3H10T1/2 cells into BALB/c athymic mice leads to the appearance of multilocular UCP1-positive adipocytes in regions of implantation (80). A recent study by Qian and colleagues highlighted that the effect of BMP4 on the adipocyte phenotype may be dependent on the cell type, in particular regarding the different developmental origins of classical brown and white adipocytes (84). Thus, adipose tissue-specific fatty acid binding protein 4 (FABP4)-driven overexpression of BMP4, resulting in equally increased BMP4 expression in WAT and BAT, had differential effects in those tissues. BMP4 triggered the appearance of multilocular lipid droplets and expression of *UCP1* in WAT of transgenic mice, while decreasing *UCP1* mRNA levels in classical BAT (84). Therefore, the actions of BMP4 and BMP7 need to be compared within the same cell system to conclude differences in their function.

We showed for the first time that equipotent concentrations of BMP4 and BMP7 (50 ng/ml each), determined by equal activation of canonical SMAD1/5/8 phosphorylation, exerted the same effects on brite marker gene expression, mitochondrial abundance and function in hASCs isolated from subcutaneous WAT (125). In line with previous observations in murine brown preadipocytes (80), BMP4 and BMP7 both increased lipid accumulation and expression of general markers of adipocyte differentiation in hASCs. In parallel, another study directly comparing the effects of BMP4 and BMP7 was published. Xue and colleagues proposed that both BMP4 and BMP7 induce the commitment of pluripotent C3H10T1/2 to brown-like adipocytes. Supporting our findings, both BMP4 and BMP7 triggered expression of thermogenic genes, mitochondrial genes and enhanced oxygen consumption in C3H10T1/2 cells (140). Moreover, BMP4 and BMP7 equally increased basal *UCP1* expression in 3T3-L1 adipocytes (140). This novel role of BMP4 as a potential endogenous regulator of brite or brown-like adipogenesis in humans is supported by a recent characterization of precursor cells isolated from different human adipose depots. Adipocyte progenitor cells isolated from the subcutaneous and deep neck depot display a distinct gene expression pattern. BMP4 was identified as gene enriched in precursor cells from the deep neck depot, which underwent differentiation into brown-like adipocytes (141).

BMP signaling is a complex scenario which is controlled on several levels. The secretion of extracellular antagonists and the receptor composition of a certain cell type allow precise regulation of a certain BMP ligand. Therefore, one could speculate that the differential functions of BMP4 in white and classical brown adipocytes may be due to distinct BMP receptor compositions. However, the expression pattern of BMP receptor isoforms displayed no striking differences between murine white and classical brown adipocytes (80). BMP4 and BMP7 share several BMP receptors (77). Nevertheless, BMP7 but not BMP4 has been shown to activate the p38 MAPK/ATF2/PGC1α axis in brown preadipocytes (80), which is also activated by β-adrenergic control of *UCP1* transcription (Chapter 1). In line with its beneficial effects in WAT, BMP4 has also been shown to activate p38 MAPK signaling in murine white preadipocytes (84), suggesting that other factors of the complex BMP signaling machinery contribute to the cell-specific effects of BMP4 and BMP7. In contrast to these studies in mice, we were neither able to show activation of p38 MAPK nor increased *PGC1α* expression in primary hASCs after BMP4 or BMP7 treatment. Moreover, BMP4 and BMP7 did not induce the full browning program with enhanced mitochondrial biogenesis, in accordance with the lack of *PGC1α* upregulation (125). Our results indicate that the plasticity of precursor cells isolated from human subcutaneous adipose tissue is lower than those from rodents.

Supporting this idea, Schulz and colleagues showed that BMP7 treatment during the whole differentiation is necessary to induce *UCP1* mRNA in human precursor cells, while pretreatment prior to the start of differentiation is sufficient in murine cells (82).

In conclusion, BMP4 is likely to play a minor role in the activation and recruitment of classical BAT, which is mainly regulated by BMP7. In contrast to BAT, we and others have shown that both BMP4 and BMP7 promote browning in WAT-derived precursor cells in mice and men. The potency of BMP4 to induce browning and/or the ability to undergo browning seems to be lower in human WAT precursor cells. The fact that BMP4 but not BMP7 is expressed and secreted from murine and human *in vitro* differentiated adipocytes indicates a role for BMP4 as endogenous factor regulating WAT plasticity in an auto-/paracrine manner. Further studies should aim to understand the regulation of BMP4 expression itself as well as the expression and function of endogenous regulators of BMP signaling. Moreover, a potential dysregulation of BMP4 signaling in WAT in states of obesity and other metabolic diseases should be assessed.

3.3 Differential impact of n-3 and n-6 LC-PUFAs on WAT plasticity

Adipogenesis and white-to-brown conversion is enhanced by several endogenous hormones and pharmacological agents. Some dietary factors have been described to induce brite adipocytes, such as resveratrol (142). Studies in rodents have shown that a HFD leads to an increase of WAT mass and BAT mass as well (50;85;87). However, there is little knowledge about the effect of specific fatty acids on BAT activity and their impact on white-to-brown conversion has not been investigated so far. LC-PUFAs from the n-3 and n-6 family exert divergent effects on several biological processes, due to the formation of different classes of lipid-derived mediators (93) or activation of different receptors, such as the n-3 specific receptor GPR120 (94). In the context of obesity, divergent functions of n-3 and n-6 LC-PUFAs have been described as well. HFD-induced fat mass and body weight gain was reduced in mice when HFD was supplemented with the n-3 LC-PUFAs EPA and DHA (88;95). Analogously, transgenic fat-1 mice which are able to synthesize n-3 LC-PUFAs endogenously are partially protected against HFD-induced obesity (143). In contrast to these anti-obesity effects of n-3 LC-PUFAs, n-6 LC-PUFAs, in particular ARA, are suggested to promote the development of obesity (144). In addition, decreased circulating EPA:ARA ratios have been found in human subjects with visceral obesity (145) and type 2 diabetes (146). Therefore, we hypothesized that n-3 and n-6 LC-PUFAs have divergent effects on WAT

plasticity and aimed to assess potential differential effects of single LC-PUFAs on brite adipocyte differentiation in primary human cells.

Adipose tissue expansion and adipogenesis

Many factors promoting brite adipocyte formation enhance general adipogenesis (69), as also observed for BMP4 and BMP7 in the second study of this thesis. Thus, the impact of the n-3 family members EPA and DHA and the n-6 member ARA on general adipocyte differentiation was investigated prior to the assessment of brite gene expression. We observed increased adipocyte differentiation in hASCs after challenge with both n-3 (EPA and DHA) and n-6 (ARA) LC-PUFAs, indicated by lipid accumulation and HSL protein abundance (Study 3, (147)). There is a bulk of *in vitro* studies analyzing the role of EPA, DHA and ARA on adipogenesis with highly contradictory results. Some studies describe an inhibition of adipocyte differentiation by EPA and DHA (148-150), supporting the idea that the anti-obesity effects of n-3 LC-PUFAs are partially due to inhibition of WAT growth and cellularity (88;95). Along with our results, EPA and DHA have also been reported to promote adipocyte differentiation in 3T3-L1 adipocytes (151). The same controversy exists for ARA. Initially identified as one of the adipogenic components of serum and required for the induction of adipogenesis (152), other studies reported inhibitory actions of ARA on adipocyte differentiation (153;154). A recent study showed that the ability of LC-PUFAs to induce adipocyte differentiation *in vitro* is dependent on the media composition (96), providing a possible explanation for the abovementioned results. Moreover, different ARA-derived prostanoids have divergent effects on adipocyte differentiation (154-156), indicating that metabolism of ARA in a certain cell type may also affect the obtained results. Nevertheless, we observed differences between individual LC-PUFAs on adiponectin expression. EPA and DHA increased adiponectin protein levels in hASCs in accordance with previous studies (157-159). ARA on the other hand, did not increase protein expression of the insulin-sensitizing adipokine adiponectin and led to enlarged lipid droplets. Promotion of adipocyte hypertrophy and alteration of the adipokine profile mediated by ARA could link high dietary intake and circulating levels of ARA with obesity (145) and type 2 diabetes (146).

Though no differences between EPA and DHA treatment on lipid accumulation, lipid droplet size, and other aspects of adipogenesis were observed, *in vivo* studies in rodents indicate differences between these two n-3 family members. The decreased HFD-induced growth and

cellularity of WAT by n-3 PUFA supplementation is dependent on the abundance of EPA and DHA in diet. Mice fed a HFD rich in DHA displayed a decreased total DNA content per fat depot, while a HFD mainly supplemented with EPA did not decrease total DNA content (88). Therefore, anti-obesity effects cannot be attributed to n-3 LC-PUFAs in general. Specific differences between the impact of EPA and DHA on adipose tissue growth and other processes may exist (160) and should be further explored.

Browning of WAT

In addition to their divergent impact on adiponectin and lipid droplet size, LC-PUFAs from the n-3 and n-6 family may also differentially regulate white-to-brown conversion. By using molecular and functional approaches, we could show for the first time that n-3 and n-6 LC-PUFAs differentially regulate white and brite adipocyte differentiation in primary hASCs (147).

Assessment of marker gene expression revealed that the n-3 LC-PUFA EPA increased *UCP1* and *CPT1B* mRNA levels in hASCs, genes enriched in brite and brown adipocytes. In support of our study, EPA has previously been shown to increase thermogenic gene expression in murine adipocytes isolated from the subcutaneous depot as well (161). Besides these effects on white-to-brown conversion, n-3 LC-PUFAs seem to be positive regulators of classical BAT function. Accordingly, the increase of BAT mass and UCP1 content observed in mice in response to HFD is further augmented when HFD is enriched with n-3 LC-PUFAs (87). However, n-3 enriched diets contain a mixture of different n-3 PUFAs, not allowing the attribution of the observed effects to a specific fatty acid. In this context, one major finding of our study was that the induction of a brite phenotype was specific for EPA, while DHA failed to alter *UCP1* and *CPT1B* expression (147). Therefore EPA and not DHA seems to be the active representative of n-3 PUFAs triggering WAT browning, as recently proposed in murine cells (161). In contrast to EPA, ARA did not affect brite marker gene expression in hASCs but increased expression of the white-specific marker TCF21. The observed gene expression pattern of hASCs treated with ARA together with larger lipid droplets compared to EPA or DHA treated cells indicates a promotion of a white adipocyte phenotype by ARA. This concept is endorsed by the fact, that ARA decreases TZD-induced brite adipocyte formation in human multipotent adipose-derived stem cells (hMADS) (162). Moreover, mice display only a slight increase of UCP1 content in BAT in response to HFD enriched with a n-6 PUFA mixture in comparison to a high UCP1 upregulation by n-3 PUFAs (87). Likewise, expression

of the WAT-enriched marker gene leptin (53) was upregulated by the n-6 but not the n-3 containing HFD (87). Taken together, specifically EPA and ARA seem to have divergent effects on white and brite adipocyte formation in humans.

The underlying mechanisms for the described effects of individual LC-PUFAs have not been analyzed in this study, but the participation of COX-mediated formation of eicosanoids could be speculated. Both EPA and DHA compete for incorporation into phospholipids with ARA, but only EPA and ARA are substrates for COX1 and COX2 giving rise to functionally different mediators. In addition, COX2 has been implicated in the regulation of cold-induced thermogenesis (44;97). A potential role for COX-mediated synthesis of eicosanoids is supported by the observation, that the ARA-mediated downregulation of *UCP1* expression in hMADS was abrogated by inhibition of COX enzymes (162). Thus, it is likely that COX action contributes to the described differential regulation of white and brite adipocyte differentiation by EPA and ARA in hASCs. Further experiments combining EPA treatment with specific COX1 and COX2 inhibitors in hASCs should be performed to confirm this idea.

Mitochondrial function

In addition to the assessment of white-to-brown conversion based on gene expression functional analyses were performed. Increased mitochondrial content and function in brown and brite adipocytes is a prerequisite to meet the requirements for UCP1-mediated thermogenesis. Following the described differences between EPA and DHA on *UCP1* and *CPT1B* gene expression, only EPA increased activity of the mitochondrial enzyme citrate synthase and augmented OXPHOS complex III protein levels. This was translated into a higher maximal oxygen consumption rate in EPA challenged hASCs. DHA had no influence on citrate synthase activity, OXPHOS complexes or maximal respiration. In contrast to our results obtained after long-term treatment in human cells, DHA as well as the basic n-3 family member ALA increased expression of *PGC1α* and *NRF1* in 3T3-L1 adipocytes after 24 hours (95). However, EPA and DHA were not compared in this murine cell model and concentrations were 10-fold higher compared to what applied by us (200 µM versus 20 µM, respectively).

Independent of UCP1-mediated thermogenesis, improved oxidative metabolism in WAT has been discussed to contribute to a “healthy” phenotype (163). On the contrary, obese rodents (164;165) and humans (166;167) display a reduced mitochondrial content and impaired

function in WAT. In contrast to an increased oxidative metabolism in hASCs triggered by EPA, we observed that ARA significantly lowered OXPHOS complex IV levels and decreased spare respiratory capacity in hASCs. Given that spare respiratory capacity is an indicator of metabolic flexibility and stress resistance of cells (168;169), ARA triggered impaired mitochondrial function in hASCs. Interestingly, spare respiratory capacity was already decreased after a shorter ARA challenge at later stages of differentiation (day 8 to 12) (147). In accordance with our findings in hASCs, ARA has been related to mitochondrial dysfunction in other cell types. Mitochondrial activity declines with age in WAT (164;166) and skeletal muscle (170). In this context, activity of OXPHOS complex I and IV have been reported to decrease with age in skeletal muscle, along with increased presence of ARA and DHA in muscle homogenates (170). ARA metabolism has also been linked to impaired mitochondrial respiration in HepG2 cells (171;172), potentially mediated by ARA-induced enhancement of ROS production (172). Although we did not directly measure ROS production, this could be a potential cause of ARA-induced mitochondrial impairment in hASCs. Hence, *COX1* mRNA levels were upregulated in ARA challenged hASCs (Figure 6) while *COX2* expression was not altered. COX1 rather than COX2 has been implicated in the oxidative stress response in endothelial cells (173), indicating different biological functions of these two enzymes. In accordance, COX2 but not COX1 is considered to participate in the regulation of adaptive thermogenesis (44) and brown adipocyte differentiation (174).

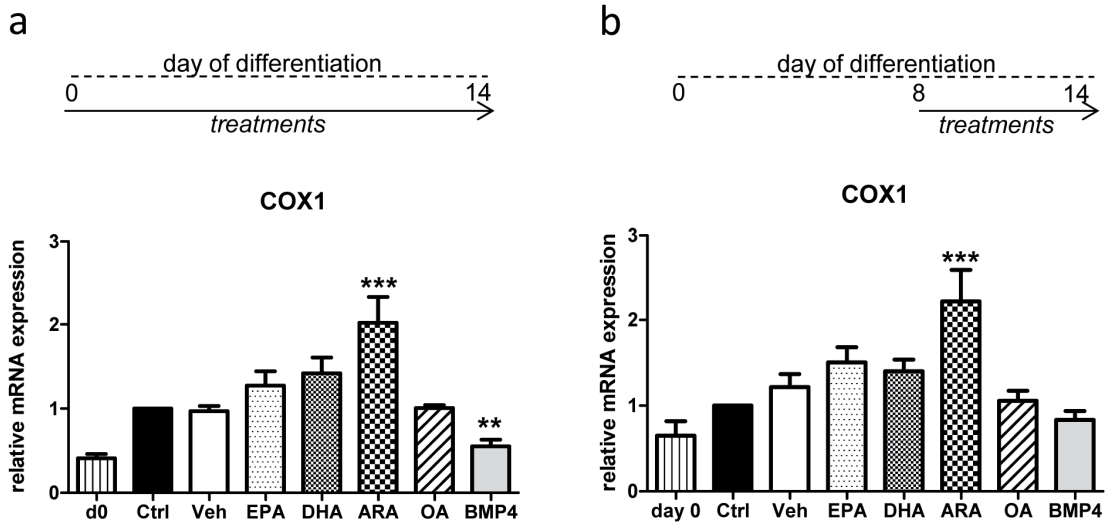

Figure 6: Effect of LC-PUFAs on COX1 gene expression. Primary hASCs were challenged during the whole differentiation period (a) or from day 8 to 12 of differentiation (b) with 20 µM of EPA, DHA, ARA or OA. Afterwards, COX1 expression was determined by qRT-PCR and normalized to expression levels of β-actin. Values represent mean values ± SEM, n=7, **p<0.01, ***p<0.001.

In summary, this study showed that EPA and ARA exert divergent functions on white-to-brown conversion and mitochondrial function of primary human adipocytes. EPA triggered a white-to-brown shift on the molecular and functional level, providing a novel underlying mechanism for the anti-obesity effects of n-3 LC-PUFAs. A positive effect of n-3 LC-PUFAs on browning may be mainly mediated by EPA, since DHA had no effect on brite adipogenesis in hASCs. ARA on the other hand, induced aspects of WAT dysfunction, mainly indicated by enlarged lipid droplet size and impaired mitochondrial function. These differential effects of EPA and ARA contribute to explain the presence of decreased circulating EPA:ARA ratios found in obese and type 2 diabetic patients and highlight the importance of a certain EPA:ARA ratio in diet. Future dietary intervention studies should pay attention to the exact LC-PUFA composition and consider specific effects of single LC-PUFAs.

3.4 Impact of the exercise-regulated myokine irisin on WAT browning

In addition to a balanced nutrition, physical activity is major aspect of lifestyle and exhibits several health benefits. Regular exercise increases muscle strength and fitness, dissipates energy, counteracts the development of obesity and type 2 diabetes and also improves glucose metabolism in subjects with existing metabolic disturbances. These health benefits cannot solely be assigned to increased energy expenditure and changes in skeletal muscle function after exercise, and other tissues/organs undergo changes in response to regular exercise. In rats, regular training prevented HFD-induced WAT hypertrophy and glucose-intolerance (175). Several studies in rodents provide evidence that exercise also alters the plasticity of white and brown adipose tissue. Classical BAT has been shown to be reduced in response to exercise training (85) or was not affected (101;102;106). On the other hand, several studies reported induction of brown-like features in the subcutaneous or visceral WAT depot after exercise (85;103-105). These observations raised the question which factors are mediating changes in the adipose organ in response to muscle contraction. Skeletal muscle has been recognized as an endocrine organ releasing a vast amount of functionally different myokines partly mediating the beneficial effects of exercise. In this context, Boström and colleagues identified irisin, a cleaved product from fibronectin domain-containing protein 5 (FNDC5), as an exercise-regulated myokine linking training to WAT browning (106). As novel factor promoting browning in mice, irisin gained our interest and we aimed to validate its function on white-to-brown transition in primary human cells.

FNDC5 and irisin – does irisin exist?

During muscle contraction, *PGC1α* mRNA expression is upregulated in mice and men. Transgenic mice specifically overexpressing *PGC1α* in skeletal muscle are considered as a model mimicking exercise, and display protection against age-related obesity (176) and browning of subcutaneous WAT (106). In order to screen for proteins regulated by exercise in skeletal muscle and potentially mediating WAT browning, the irisin precursor FNDC5 was identified as a promising candidate strongly upregulated in myotubes from PGC1α transgenics (106). The sequence of murine *FNDC5* has already been described in 2002, containing a signal peptide, a fibronectin type III (FNIII) domain, a hydrophobic region likely to be a transmembrane domain and a short cytoplasmic domain (177;178). However, the function of FNDC5 remained unclear.

Boström *et al.* reported that FNDC5 cleavage in the extracellular domain by an unkown protease leads to the release of irisin (106), comprising the amino acids (aa) 29-140 of the extracellular domain in mice (UniProt entry Q8K4Z2). Moreover, they were able to detect the irisin fragment in human plasma samples and found increased circulating irisin levels after exercise (106). However, several concerns about the concept of irisin as an exercise-regulated myokine mediating browning of WAT have been raised. In particular the validity of the tools to measure FNDC5/irisin protein has been questioned (179). Boström and colleagues detected irisin with a commercially available antibody made against an extracellular part of FNDC5 (aa 149-178), not predicted to detect irisin (aa 29-140). Furthermore, an immuno-reactive band of 22 kDa much larger than its theoretical molecular weight (~13 kDa) was designated to irisin, doubting the nature of the initially described irisin fragment. Until now, several studies failed to detect immuno-reactive bands corresponding to the molecular weight of irisin in serum samples or supernatants from skeletal muscle cells (104;180;181). The presence of multiple bands in Western blots indicates that the polyclonal antibodies used were highly unspecific. Nevertheless, commercial ELISA kits based on these antibodies became available and have been extensively used to analyze the association between circulating irisin levels and exercise or several metabolic parameters. Keeping the antibody issue in mind, it seems not surprising that the obtained results were highly controversial, as reviewed in study 5 of this thesis (182) and by others (183). Importantly, circulating irisin levels even analyzed with the same kits differed in a non-physiological range, strongly questioning the reliability of these tools and in consequence the attained results.

The existence and relevance of FNDC5 and irisin in humans was further criticized by a major finding of this thesis (Study 4). Thus, the ATG start codon of the human *FNDC5* gene is mutated to a non-canonical ATA start codon (184). Although non-canonical start codons can efficiently give rise to a protein due to the formation of hairpin structures (185), we observed a negligible production of full-length FNDC5 protein from the human expression vector construct (1% compared to the murine construct). Moreover, truncated forms of FNDC5 were detected in lysates from cells containing the human construct, likely due to usage of the next in-frame ATG as start codon (184). Based on these findings, we concluded that full-length FNDC5 is not efficiently translated into protein in humans and consequently irisin is not or only marginally produced by cleavage from FNDC5. However, a previous study claimed the presence of irisin or at least fragments of FNDC5 in human plasma, by analyzing bands corresponding to the theoretical molecular weights of FNDC5/irisin via mass spectrometry (181). In support with our findings, Albrecht *et al.* recently failed to detect peptides corresponding to FNDC5 or irisin in human serum samples by performing mass spectrometry as well (180). Accordingly, irisin concentrations determined by ELISA did not correlate with those obtained by Western blot quantification of bands potentially corresponding to FNDC5/irisin (180). Taken together, no reliable and consistent data on the existence of irisin in humans are available until now, strongly indicating that irisin is not an exercise-regulated myokine in humans mediating WAT browning in an endocrine manner. Nevertheless, the role of irisin in humans is still debated and polarizes the research community (186-189).

Irisin as inducer of browning in mice and men

Although there is evidence against the presence of irisin in humans and its regulation by exercise, application of irisin and FNDC5 may represent a strategy to promote browning of WAT in humans. In mice, recombinant FNDC5 has initially been described to induce browning of subcutaneous preadipocytes, indicated by increased expression of *UCP1*, *PRDM16*, *PGC1α* and other brown/brite marker genes. These changes were detected after FNDC5 treatment (20 nM) during the whole differentiation period of 6 days. FNDC5 seems to exert its effects during differentiation or rather in later stages, since challenge of murine preadipocytes from day 3 to 6 was sufficient to enhance *UCP1* expression (106). Interestingly, FNDC5 or irisin had no impact on gene expression of murine classical brown adipocytes (106). This would be in line with the notion that training of mice has no effect on classical BAT while promoting WAT browning (85), as outlined above. Supporting a role of

FNDC5 and irisin in the white-to-brown conversion in rodents, later studies were able to reproduce the induction of *UCP1* expression in 3T3-L1 adipocytes (190;191) and primary rat adipocytes (190) by FNDC5 or irisin treatment in later stages of differentiation. However, results obtained in the adipogenic 3T3-L1 cell line have to be interpreted carefully, since stem cell-specific effects for FNDC5/irisin have been described. The study from Wu *et al.* proposed the existence of a certain brite precursor cell, characterized by high expression of CD137 or TMEM26 and displaying a strong browning response to FNDC5 and irisin exposure (43). In contrast, CD137 low-expressing cells are not able undergo browning in response FNDC5 or irisin (43). Taking potential cell- and depot-specific differences of the action of FNDC5/irisin into account, studies in primary cells from different depots seem better suited to understanding the impact of irisin on WAT browning.

In contrast to these studies in mice, there is less evidence for a role of FNDC5/irisin in browning in human cell systems (Table 2). Using primary human preadipocytes isolated from the subcutaneous depot of different donors, we were not able to show induction of *UCP1* expression and other brite marker genes by FNDC5 or irisin treatment (184). Even in CD137 high-expressing donors, displaying a strong response to the positive control BMP7, *UCP1* expression was not enhanced after FNDC5/irisin treatment during the whole differentiation period. In accordance with our observations, Lee and colleagues also observed no significant induction of *UCP1* expression in human subcutaneous preadipocytes after 6 days treatment with a high concentration of 100 nM FNDC5 (181). Supporting the proposed concept of cell-/depot-specific effects of FNDC5/irisin, 100 nM FNDC5 has been shown to mediate a strong browning response in human preadipocytes isolated from the cervical depot. These preadipocytes possessed a classical brown and brite molecular signature (181), in line with the idea that human deep neck adipose tissue is likely to be composed of brite and classical brown preadipocytes (53). In contrast, one study claimed that irisin induces white-to-brown transdifferentiation of mature human adipocytes (192). However, these primary cells were isolated from the subcutaneous depot of severely obese individuals and classical brown or brite marker gene expression, such as CD137, were not assessed to characterize the cells. Moreover, and in contrast to all other studies in murine and human cell models, a strong inhibition of adipogenesis by irisin was observed (192) (Table 2).

Table 2: Effect of FNDC5/irisin on white-to-brown conversion *in vitro*

Study	Species	Cell type	Treatment	Duration	Effect
Boström et al. 2012	Mouse	Subc preadipocytes	20 nM FNDC5	Day 0-6	UCP1↑ (~45fold), leptin ↓, Differentiation ↔
			20 nM FNDC5	Day 3-4	UCP1↑ (~20fold)
				Day 5-6	UCP1↑ (~18fold)
		Interscapular preadipocytes	20 nM FNDC5	Day 0-6	UCP1↔
Zhang et al.2014	Mouse	3T3-L1	20 nM irisin	Day 3-7	UCP1↑ (7fold), Differentiation ↔
	Rat	Subc preadipocytes	20 nM irisin	6 hrs	UCP1↑ (4fold)
Wang et al. 2014	Mouse	3T3-L1	20 nM irisin	Day 10-12	UCP1↑ (1.4fold)
Wu et al. 2013	Mouse	Subc preadipocytes – CD137 high	20 nM FNDC5	Day 0-6	UCP1↔ Differentiation ↔
		Subc preadipocytes – CD137 low	20 nM FNDC5	Day 0-6	UCP1↑ (~25fold), Differentiation ↔
Huh et al. 2014	Mouse	3T3-L1	50 nM irisin	Day 0-8	Strong inhibition of differentiation
Raschke et al. 2013	Human	Subc preadipocytes	~45nM FNDC5*	Day 0-14	UCP1↔ Differentiation ↔
			~50 nM irisin**	Day 0-14	UCP1↔ Differentiation ↔
		Subc preadipocytes – CD137 high	~5nM irisin***	Day 0-14	UCP1↔ Differentiation ↔
Lee et al. 2014	Human	Subc preadipocytes	100 nM FNDC5	Day 5-11	UCP1↑ (2fold, n.s.)
		Omental preadipocytes	100 nM FNDC5	Day 5-11	UCP1↔
		Cervical preadipocytes	100 nM FNDC5	Day 5-11	UCP1↑ (~50fold), differentiation ↔
Huh et al. 2014	Human	Subc preadipocytes (from obese subjects)	50 nM irisin	Day 0-28	Strong inhibition of differentiation
			10 nM irisin	Day 28-36	UCP1↑ (~23fold), leptin ↑ (~35fold)

* corresponds to 1000 ng/ml FNDC5; **corresponds to 600 ng/ml irisin and ***60 ng/ml irisin. ↑upregulation, ↓downregulation, ↔ no effect, subc: subcutaneous.

In conclusion, FNDC5 protein expression in humans is marginal due to a mutation in the start codon and truncated forms of FNDC5 and thus irisin may exist. Moreover, the therapeutic potential of irisin as inducer of WAT browning to counteract obesity remains unclear based on the current data. FNDC5/irisin may only target a small subpopulation of cells present in BAT of the neck region and its impact on whole body metabolism has to be elucidated. Besides irisin, other skeletal muscle-derived factors, such as FGF21 (181) and the small molecule myokine β-aminoisobutyric acid (193) have been proposed to couple exercise to WAT browning. Nevertheless, future studies should prioritize the question if exercise *per se* alters BAT activity in humans and mediates recruitment of brite adipocytes, as observed in rodents.

3.5 Hormones, nutrition or exercise – different potentials to induce browning?

In this thesis, the impact of endogenous hormones and nutritional factors on white-to-brown conversion was assessed in human adipogenic precursor cells isolated from the subcutaneous fat pad, a depot displaying a high ability to undergo browning (30;82). Brite adipocytes can either appear by *de novo* recruitment and differentiation from precursor cells or by direct conversion of mature adipocytes (48;49). Since adipocyte cell number in WAT is kept relatively constant in human adults (13), approaches promoting both brite differentiation as well as white-to-brown conversion of mature adipocytes would represent the most effective strategies. In this context, the present thesis revealed differences between the investigated endogenous and nutritional factors on white-to-brown transition.

BMPs play an important role in the regulation of developmental processes and mediate commitment of pluritpotent cells to a certain lineage. Thus, pretreatment of murine pluripotent C3H10T1/2 cells with BMP7 triggers commitment to the brown adipocyte lineage (80). In human preadipocytes isolated from the subcutaneous depot, long-term treatment with BMP7 during the whole differentiation period is necessary to induce *UCP1* expression (82). Similar to BMP7, we identified BMP4 as promoter of browning in primary subcutaneous hASCs when applied during the whole differentiation period (125). Since shorter BMP4 treatment of hASCs in the terminal stage of differentiation had no impact on brite gene expression or mitochondrial function (147), BMP4 is likely to have no impact on transdifferentiation of mature white adipocytes.

In contrast to BMP4, the n-3 LC-PUFA EPA was able to induce *UCP1* and *CPT1B* expression in the late stage of differentiation. Hence, EPA may target both preadipocytes as well as mature adipocytes within WAT. Moreover, EPA also enhances *UCP1* expression in murine classical brown adipocytes (161), while BMP4 is likely to exert divergent effects on classical brown and brite adipocytes (as outlined in chapter 3.2). Comparing BMP4 and EPA, dietary EPA may represent a more potent regulator of adipose tissue plasticity and whole-body energy metabolism (Figure 7). An induction of brite gene expression in hASCs with physiologically low concentrations of 20 µM EPA underlines the relevance of fatty acid composition in diet.

Coherent with the beneficial effects of the n-3 LC-PUFA EPA on mature adipocytes, the n-6 LC-PUFA ARA exerts rather negative effects on mature adipocytes. Besides the induction of the white marker TCF21, we show an impairment of mitochondrial function in differentiated hASCs after 4 days ARA treatment. The fact that ARA inhibits the positive effects on brite

gene expression and mitochondrial function mediated by EPA highlights the role of a balanced n-3/n-6 ratio in diet, and represents an additional mechanism for the opposing effects of n-3 and n-6 LC-PUFAs. Intriguingly, ARA has even been shown to inhibit the TZD-induced white-to-brown conversion in hMADS (162), suggesting that the impact of a certain browning inducer can be influenced by other factors. Thus, the effectiveness and success of a pharmacological approach to increase thermogenesis in humans may be dependent on nutrition and could be diminished by dietary ARA. This notion should be considered when performing clinical trials and interpreting the results.

The exercise-regulated myokine irisin has gained considerable interest due to its function as browning inducer in rodents and was regarded as a promising target to treat obesity in humans. However, irisin is not likely to be expressed at physiologically relevant levels in humans and seems to trigger white-to-brown conversion only in a specific subset of precursor cells. The contribution of irisin-mediated browning of a subpopulation of precursor cells to total thermogenic activity and whole body energy metabolism is questionable and remains unclear.

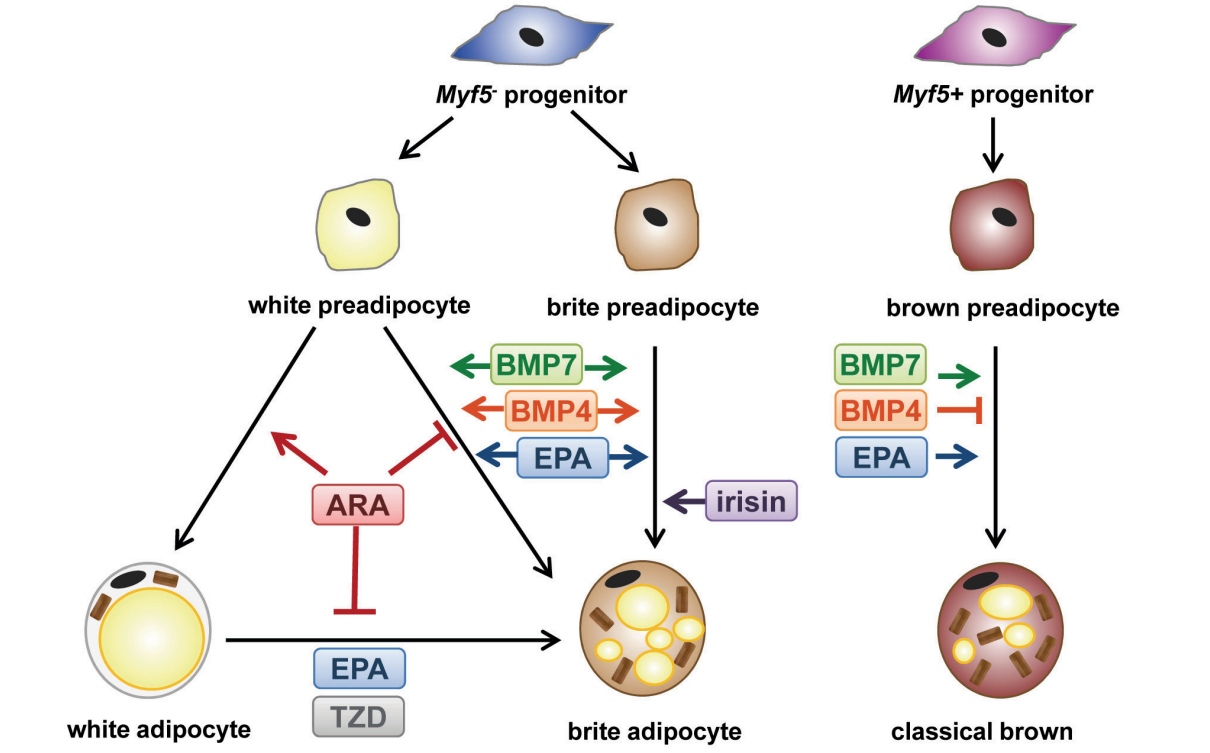

Figure 7: Different potential of BMPs, LC-PUFAs and irisin to promote browning. The growth factors BMP4 and BMP7 enhance brite adipocyte differentiation, but have no effect on white-to-brown transdifferentiation of mature white adipocytes. Differentiation of classical brown adipocytes is likely to be triggered only by BMP7, while BMP4 may have inhibitory effects on classical brown adipocytes. The n-3 LC-PUFA EPA has beneficial effects on both brite and brown adipocyte differentiation and may even induce white-to-brown conversion of mature adipocytes, similar as TZDs. In contrast to EPA, the n-6 LC-PUFA ARA promotes white adipogenesis and inhibits the action of EPA and TZDs.

Summing up the currently available data about the role of BMP4, EPA and irisin in WAT browning, EPA seems to be the most potent candidate since it impacts precursor cells and mature adipocytes present in WAT depots and may also have positive effects on classical BAT (Figure 7).

3.6 Perspective

In the first study of this thesis top score adipokine candidates playing a potential role in the regulation of adipose tissue growth and obesity were identified. WISP2 was one of the top score adipokines found upregulated in the obese state. In parallel, WISP2 was validated as adipokine and characterized as an important factor regulating adipogenesis by the group of Ulf Smith at the University of Gothenburg. Another candidate, CHRDL1 turned out to be no inhibitor of the proadipogenic factor BMP4 in human adipocytes. Nevertheless, CHRDL1 is strongly regulated in obesity and its paracrine function in adipose tissue as well as its endocrine effects on other organs should be assessed in future studies.

The identification of the brite adipocyte and the possibility to induce brite adipocytes within WAT depots gained considerable interest as potential strategy to prevent the development of obesity. We here showed that BMP4 is produced and secreted from adipocytes. Different from previous assumptions, BMP4 had similar effects as BMP7 and induced a brite phenotype in hASCs from subcutaneous WAT. On the contrary, BMP4 and BMP7 seem to have opposing functions in classical BAT. Thus, future studies should aim to understand which intrinsic differences between white and classical brown adipocytes determine the specific effect of BMP4. The regulation of BMP4 in obesity, WAT inflammation or insulin resistance should be further assessed.

In the third study of this thesis the n-3 and n-6 LC-PUFAs EPA and ARA were identified as regulators of brite and white adipocyte differentiation. In the near future, we will assess the underlying mechanisms, especially the involvement of COX2-mediated synthesis of lipid derived mediators. Another major finding of this study was that the n-3 LC-PUFA DHA had no specific effect on white-to-brown conversion. Extrapolating our *in vitro* results to the *in vivo* situation, dietary intervention studies should distinguish between single n-3 LC-PUFAs to identify the active component within a fatty acid mixture. Dietary supplemention with EPA rather than DHA may represent a non-pharmacological approach to reduce the development of obesity and its associated metabolic disorders.

Finally, we provide evidence that FNDC5 and irisin seem not to be expressed in humans, or if at all, at marginal concentrations. Reviewing the currently available data about circulating irisin levels, tools to measure irisin levels seem to be unreliable and irisin is no contraction-regulated myokine in humans. Functionally, we and others observed that FNDC5 or irisin are no potent inducers of WAT browning in humans. Importantly, the concept that exercise itself mediates browning of WAT remains to be elucidated in humans. Thus, future studies should assess if long-term exercise intervention has an impact on (i) BAT activity using PET-CT scans and (ii) browning of WAT by analyzing expression levels of marker genes in biopsies from subcutaneous WAT.

4 References for Introduction and Discussion

1 World Health Organization. Obesity and overweight. Fact sheet N°311. 2015.

2 World Health Organization. Global status report on noncommunicable diseases. 2014.

3 Romacho T, Elsen M, Rohrborn D, Eckel J. Adipose tissue and its role in organ crosstalk. *Acta Physiol (Oxf)* 2014; **210/4**: 733-753.

4 Finkelstein EA, Trogdon JG, Cohen JW, Dietz W. Annual medical spending attributable to obesity: payer-and service-specific estimates. *Health Aff (Millwood)* 2009; **28/5**: w822-w831.

5 Trayhurn P, Wood IS. Adipokines: inflammation and the pleiotropic role of white adipose tissue. *Br J Nutr* 2004; **92/3**: 347-355.

6 Scherer PE. Adipose tissue: from lipid storage compartment to endocrine organ. *Diabetes* 2006; **55/6**: 1537-1545.

7 Peinado JR, Pardo M, de la Rosa O, Malagon MM. Proteomic characterization of adipose tissue constituents, a necessary step for understanding adipose tissue complexity. *Proteomics* 2012; **12/4-5**: 607-620.

8 Ouchi N, Parker JL, Lugus JJ, Walsh K. Adipokines in inflammation and metabolic disease. *Nat Rev Immunol* 2011; **11/2**: 85-97.

9 Samaras K, Botelho NK, Chisholm DJ, Lord RV. Subcutaneous and visceral adipose tissue gene expression of serum adipokines that predict type 2 diabetes. *Obesity (Silver Spring)* 2010; **18/5**: 884-889.

10 Lehr S, Hartwig S, Lamers D, Famulla S, Muller S, Hanisch FG et al. Identification and validation of novel adipokines released from primary human adipocytes. *Mol Cell Proteomics* 2012; **11/1**: M111.

11 Dahlman I, Elsen M, Tennagels N, Korn M, Brockmann B, Sell H et al. Functional annotation of the human fat cell secretome. *Arch Physiol Biochem* 2012; **118/3**: 84-91.

12 Goossens GH. The role of adipose tissue dysfunction in the pathogenesis of obesity-related insulin resistance. *Physiol Behav* 2008; **94/2**: 206-218.

13 Spalding KL, Arner E, Westermark PO, Bernard S, Buchholz BA, Bergmann O et al. Dynamics of fat cell turnover in humans. *Nature* 2008; **453/7196**: 783-787.

14 Hirsch J, Batchelor B. Adipose tissue cellularity in human obesity. *Clin Endocrinol Metab* 1976; **5/2**: 299-311.

15 Bjorntorp P. Effects of age, sex, and clinical conditions on adipose tissue cellularity in man. *Metabolism* 1974; **23/11**: 1091-1102.

16 Roden M, Price TB, Perseghin G, Petersen KF, Rothman DL, Cline GW et al. Mechanism of free fatty acid-induced insulin resistance in humans. *J Clin Invest* 1996; **97/12**: 2859-2865.

17 Arner E, Westermark PO, Spalding KL, Britton T, Ryden M, Frisen J et al. Adipocyte turnover: relevance to human adipose tissue morphology. *Diabetes* 2010; **59/1**: 105-109.

18 Gustafson B, Hammarstedt A, Hedjazifar S, Smith U. Restricted Adipogenesis in Hypertrophic Obesity: The Role of WISP2, WNT, and BMP4. *Diabetes* 2013; **62/9**: 2997-3004.

19 Skurk T, Alberti-Huber C, Herder C, Hauner H. Relationship between adipocyte size and adipokine expression and secretion. *J Clin Endocrinol Metab* 2007; **92/3**: 1023-1033.

20 Xu H, Barnes GT, Yang Q, Tan G, Yang D, Chou CJ et al. Chronic inflammation in fat plays a crucial role in the development of obesity-related insulin resistance. *J Clin Invest* 2003; **112/12**: 1821-1830.

21 Cancello R, Henegar C, Viguerie N, Taleb S, Poitou C, Rouault C et al. Reduction of macrophage infiltration and chemoattractant gene expression changes in white adipose tissue of morbidly obese subjects after surgery-induced weight loss. *Diabetes* 2005; **54/8**: 2277-2286.

22 Giordano A, Smorlesi A, Frontini A, Barbatelli G, Cinti S. White, brown and pink adipocytes: the extraordinary plasticity of the adipose organ. *Eur J Endocrinol* 2014; **170/5**: R159-R171.

23 Wronska A, Kmiec Z. Structural and biochemical characteristics of various white adipose tissue depots. *Acta Physiol (Oxf)* 2012; **205/2**: 194-208.

24 Tchkonia T, Tchoukalova YD, Giorgadze N, Pirtskhalava T, Karagiannides I, Forse RA et al. Abundance of two human preadipocyte subtypes with distinct capacities for replication, adipogenesis, and apoptosis varies among fat depots. *Am J Physiol Endocrinol Metab* 2005; **288/1**: E267-E277.

25 Fontana L, Eagon JC, Trujillo ME, Scherer PE, Klein S. Visceral fat adipokine secretion is associated with systemic inflammation in obese humans. *Diabetes* 2007; **56/4**: 1010-1013.

26 McQuaid SE, Hodson L, Neville MJ, Dennis AL, Cheeseman J, Humphreys SM et al. Downregulation of adipose tissue fatty acid trafficking in obesity: a driver for ectopic fat deposition? *Diabetes* 2011; **60/1**: 47-55.

27 Bluher M. The distinction of metabolically 'healthy' from 'unhealthy' obese individuals. *Curr Opin Lipidol* 2010; **21/1**: 38-43.

28 Cannon B, Nedergaard J. Brown adipose tissue: function and physiological significance. *Physiol Rev* 2004; **84/1**: 277-359.

29 Forner F, Kumar C, Luber CA, Fromme T, Klingenspor M, Mann M. Proteome differences between brown and white fat mitochondria reveal specialized metabolic functions. *Cell Metab* 2009; **10/4**: 324-335.

30 Walden TB, Hansen IR, Timmons JA, Cannon B, Nedergaard J. Recruited vs. nonrecruited molecular signatures of brown, "brite," and white adipose tissues. *Am J Physiol Endocrinol Metab* 2012; **302/1**: E19-E31.

31 Cypess AM, Lehman S, Williams G, Tal I, Rodman D, Goldfine AB et al. Identification and importance of brown adipose tissue in adult humans. *N Engl J Med* 2009; **360/15**: 1509-1517.

32 van Marken Lichtenbelt WD, Vanhommerig JW, Smulders NM, Drossaerts JM, Kemerink GJ, Bouvy ND et al. Cold-activated brown adipose tissue in healthy men. *N Engl J Med* 2009; **360/15**: 1500-1508.

33 Saito M, Okamatsu-Ogura Y, Matsushita M, Watanabe K, Yoneshiro T, Nio-Kobayashi J et al. High incidence of metabolically active brown adipose tissue in healthy adult humans: effects of cold exposure and adiposity. *Diabetes* 2009; **58/7**: 1526-1531.

34 Virtanen KA, Lidell ME, Orava J, Heglind M, Westergren R, Niemi T et al. Functional brown adipose tissue in healthy adults. *N Engl J Med* 2009; **360/15**: 1518-1525.

35 Zingaretti MC, Crosta F, Vitali A, Guerrieri M, Frontini A, Cannon B et al. The presence of UCP1 demonstrates that metabolically active adipose tissue in the neck of adult humans truly represents brown adipose tissue. *FASEB J* 2009; **23/9**: 3113-3120.

36 Nicholls DG. Hamster brown-adipose-tissue mitochondria. The chloride permeability of the inner membrane under respiring conditions, the influence of purine nucleotides. *Eur J Biochem* 1974; **49/3**: 585-593.

37 Fedorenko A, Lishko PV, Kirichok Y. Mechanism of fatty-acid-dependent UCP1 uncoupling in brown fat mitochondria. *Cell* 2012; **151/2**: 400-413.

38 Gesner C. De Quadrupedibus viviparis. In: *Historiae Animalium.* 1551.

39 Seale P, Bjork B, Yang W, Kajimura S, Chin S, Kuang S et al. PRDM16 controls a brown fat/skeletal muscle switch. *Nature* 2008; **454/7207**: 961-967.

40 Timmons JA, Wennmalm K, Larsson O, Walden TB, Lassmann T, Petrovic N et al. Myogenic gene expression signature establishes that brown and white adipocytes originate from distinct cell lineages. *Proc Natl Acad Sci U S A* 2007; **104/11**: 4401-4406.

41 Smorlesi A, Frontini A, Giordano A, Cinti S. The adipose organ: white-brown adipocyte plasticity and metabolic inflammation. *Obes Rev* 2012; **13 Suppl 2**: 83-96.

42 Petrovic N, Walden TB, Shabalina IG, Timmons JA, Cannon B, Nedergaard J. Chronic Peroxisome Proliferator-activated Receptor gamma (PPAR gamma) Activation of Epididymally Derived White Adipocyte Cultures Reveals a Population of Thermogenically Competent, UCP1-containing Adipocytes Molecularly Distinct from Classic Brown Adipocytes. *Journal of Biological Chemistry* 2010; **285/10**: 7153-7164.

43 Wu J, Bostrom P, Sparks LM, Ye L, Choi JH, Giang AH et al. Beige adipocytes are a distinct type of thermogenic fat cell in mouse and human. *Cell* 2012; **150/2**: 366-376.

44 Vegiopoulos A, Muller-Decker K, Strzoda D, Schmitt I, Chichelnitskiy E, Ostertag A et al. Cyclooxygenase-2 controls energy homeostasis in mice by de novo recruitment of brown adipocytes. *Science* 2010; **328/5982**: 1158-1161.

45 Bordicchia M, Liu D, Amri EZ, Ailhaud G, Dessi-Fulgheri P, Zhang C et al. Cardiac natriuretic peptides act via p38 MAPK to induce the brown fat thermogenic program in mouse and human adipocytes. *J Clin Invest* 2012; **122/3**: 1022-1036.

46 Lee JY, Takahashi N, Yasubuchi M, Kim YI, Hashizaki H, Kim MJ et al. Triiodothyronine induces UCP-1 expression and mitochondrial biogenesis in human adipocytes. *Am J Physiol Cell Physiol* 2012; **302/2**: C463-C472.

47 Lee YH, Petkova AP, Mottillo EP, Granneman JG. In vivo identification of bipotential adipocyte progenitors recruited by beta3-adrenoceptor activation and high-fat feeding. *Cell Metab* 2012; **15/4**: 480-491.

48 Himms-Hagen J, Melnyk A, Zingaretti MC, Ceresi E, Barbatelli G, Cinti S. Multilocular fat cells in WAT of CL-316243-treated rats derive directly from white adipocytes. *Am J Physiol Cell Physiol* 2000; **279/3**: C670-C681.

49 Rosenwald M, Perdikari A, Rulicke T, Wolfrum C. Bi-directional interconversion of brite and white adipocytes. *Nat Cell Biol* 2013; **15/6**: 659-667.

50 Feldmann HM, Golozoubova V, Cannon B, Nedergaard J. UCP1 ablation induces obesity and abolishes diet-induced thermogenesis in mice exempt from thermal stress by living at thermoneutrality. *Cell Metab* 2009; **9/2**: 203-209.

51 Kopecky J, Clarke G, Enerback S, Spiegelman B, Kozak LP. Expression of the mitochondrial uncoupling protein gene from the aP2 gene promoter prevents genetic obesity. *J Clin Invest* 1995; **96/6**: 2914-2923.

52 Stephens M, Ludgate M, Rees DA. Brown fat and obesity: the next big thing? *Clin Endocrinol (Oxf)* 2011; **74/6**: 661-670.

53 Cypess AM, White AP, Vernochet C, Schulz TJ, Xue R, Sass CA et al. Anatomical localization, gene expression profiling and functional characterization of adult human neck brown fat. *Nat Med* 2013; **19/5**: 635-639.

54 Jespersen NZ, Larsen TJ, Peijs L, Daugaard S, Homoe P, Loft A et al. A classical brown adipose tissue mRNA signature partly overlaps with brite in the supraclavicular region of adult humans. *Cell Metab* 2013; **17/5**: 798-805.

55 Lidell ME, Betz MJ, Dahlqvist LO, Heglind M, Elander L, Slawik M et al. Evidence for two types of brown adipose tissue in humans. *Nat Med* 2013; **19/5**: 631-634.

56 Blondin DP, Labbe SM, Tingelstad HC, Noll C, Kunach M, Phoenix S et al. Increased brown adipose tissue oxidative capacity in cold-acclimated humans. *J Clin Endocrinol Metab* 2014; **99/3**: E438-E446.

57 Vijgen GH, Bouvy ND, Teule GJ, Brans B, Hoeks J, Schrauwen P et al. Increase in brown adipose tissue activity after weight loss in morbidly obese subjects. *J Clin Endocrinol Metab* 2012; **97/7**: E1229-E1233.

58 Farmer SR. Transcriptional control of adipocyte formation. *Cell Metab* 2006; **4/4**: 263-273.

59 Kajimura S, Seale P, Spiegelman BM. Transcriptional control of brown fat development. *Cell Metab* 2010; **11/4**: 257-262.

60 Siersbaek MS, Loft A, Aagaard MM, Nielsen R, Schmidt SF, Petrovic N et al. Genome-wide profiling of peroxisome proliferator-activated receptor gamma in primary epididymal, inguinal, and brown adipocytes reveals depot-selective binding correlated with gene expression. *Mol Cell Biol* 2012; **32/17**: 3452-3463.

61 Linhart HG, Ishimura-Oka K, DeMayo F, Kibe T, Repka D, Poindexter B et al. C/EBPalpha is required for differentiation of white, but not brown, adipose tissue. *Proc Natl Acad Sci U S A* 2001; **98/22**: 12532-12537.

62 Karamanlidis G, Karamitri A, Docherty K, Hazlerigg DG, Lomax MA. C/EBPbeta reprograms white 3T3-L1 preadipocytes to a Brown adipocyte pattern of gene expression. *J Biol Chem* 2007; **282/34**: 24660-24669.

63 Kajimura S, Saito M. A new era in brown adipose tissue biology: molecular control of brown fat development and energy homeostasis. *Annu Rev Physiol* 2014; **76**: 225-249.

64 Scarpulla RC. Metabolic control of mitochondrial biogenesis through the PGC-1 family regulatory network. *Biochim Biophys Acta* 2011; **1813/7**: 1269-1278.

65 Puigserver P, Wu Z, Park CW, Graves R, Wright M, Spiegelman BM. A cold-inducible coactivator of nuclear receptors linked to adaptive thermogenesis. *Cell* 1998; **92/6**: 829-839.

66 Uldry M, Yang W, St-Pierre J, Lin J, Seale P, Spiegelman BM. Complementary action of the PGC-1 coactivators in mitochondrial biogenesis and brown fat differentiation. *Cell Metab* 2006; **3/5**: 333-341.

67 Seale P, Conroe HM, Estall J, Kajimura S, Frontini A, Ishibashi J et al. Prdm16 determines the thermogenic program of subcutaneous white adipose tissue in mice. *J Clin Invest* 2011; **121/1**: 96-105.

68 Elabd C, Chiellini C, Carmona M, Galitzky J, Cochet O, Petersen R et al. Human multipotent adipose-derived stem cells differentiate into functional brown adipocytes. *Stem Cells* 2009; **27/11**: 2753-2760.

69 Bonet ML, Oliver P, Palou A. Pharmacological and nutritional agents promoting browning of white adipose tissue. *Biochim Biophys Acta* 2013; **1831/5**: 969-985.

70 Cao W, Daniel KW, Robidoux J, Puigserver P, Medvedev AV, Bai X et al. p38 mitogen-activated protein kinase is the central regulator of cyclic AMP-dependent transcription of the brown fat uncoupling protein 1 gene. *Mol Cell Biol* 2004; **24/7**: 3057-3067.

71 Arch JR. beta(3)-Adrenoceptor agonists: potential, pitfalls and progress. *Eur J Pharmacol* 2002; **440/2-3**: 99-107.

72 Pfeifer A, Hoffmann LS. Brown, beige, and white: the new color code of fat and its pharmacological implications. *Annu Rev Pharmacol Toxicol* 2015; **55**: 207-227.

73 Sell H, Berger JP, Samson P, Castriota G, Lalonde J, Deshaies Y et al. Peroxisome proliferator-activated receptor gamma agonism increases the capacity for sympathetically mediated thermogenesis in lean and ob/ob mice. *Endocrinology* 2004; **145/8**: 3925-3934.

74 Ohno H, Shinoda K, Spiegelman BM, Kajimura S. PPARgamma agonists induce a white-to-brown fat conversion through stabilization of PRDM16 protein. *Cell Metab* 2012; **15/3**: 395-404.

75 Blind E, Dunder K, de Graeff PA, Abadie E. Rosiglitazone: a European regulatory perspective. *Diabetologia* 2011; **54/2**: 213-218.

76 Bogacka I, Xie H, Bray GA, Smith SR. Pioglitazone induces mitochondrial biogenesis in human subcutaneous adipose tissue in vivo. *Diabetes* 2005; **54/5**: 1392-1399.

77 Bragdon B, Moseychuk O, Saldanha S, King D, Julian J, Nohe A. Bone morphogenetic proteins: a critical review. *Cell Signal* 2011; **23/4**: 609-620.

78 Walsh DW, Godson C, Brazil DP, Martin F. Extracellular BMP-antagonist regulation in development and disease: tied up in knots. *Trends Cell Biol* 2010; **20/5**: 244-256.

79 Modica S, Wolfrum C. Bone morphogenic proteins signaling in adipogenesis and energy homeostasis. *Biochim Biophys Acta* 2013; **1831/5**: 915-923.

80 Tseng YH, Kokkotou E, Schulz TJ, Huang TL, Winnay JN, Taniguchi CM et al. New role of bone morphogenetic protein 7 in brown adipogenesis and energy expenditure. *Nature* 2008; **454/7207**: 1000-1004.

81 Townsend KL, Suzuki R, Huang TL, Jing E, Schulz TJ, Lee K et al. Bone morphogenetic protein 7 (BMP7) reverses obesity and regulates appetite through a central mTOR pathway. *FASEB J* 2012; **26/5**: 2187-2196.

82 Schulz TJ, Huang TL, Tran TT, Zhang H, Townsend KL, Shadrach JL et al. Identification of inducible brown adipocyte progenitors residing in skeletal muscle and white fat. *Proc Natl Acad Sci U S A* 2011; **108/1**: 143-148.

83 Schulz TJ, Tseng YH. Emerging role of bone morphogenetic proteins in adipogenesis and energy metabolism. *Cytokine Growth Factor Rev* 2009; **20/5-6**: 523-531.

84 Qian SW, Tang Y, Li X, Liu Y, Zhang YY, Huang HY et al. BMP4-mediated brown fat-like changes in white adipose tissue alter glucose and energy homeostasis. *Proc Natl Acad Sci U S A* 2013; **110/9**: E798-E807.

85 Wu MV, Bikopoulos G, Hung S, Ceddia RB. Thermogenic capacity is antagonistically regulated in classical brown and white subcutaneous fat depots by high fat diet and endurance training in rats: impact on whole-body energy expenditure. *J Biol Chem* 2014; **289/49**: 34129-34140.

86 Sadurskis A, Dicker A, Cannon B, Nedergaard J. Polyunsaturated fatty acids recruit brown adipose tissue: increased UCP content and NST capacity. *Am J Physiol* 1995; **269/2 Pt 1**: E351-E360.

87 Takahashi Y, Ide T. Dietary n-3 fatty acids affect mRNA level of brown adipose tissue uncoupling protein 1, and white adipose tissue leptin and glucose transporter 4 in the rat. *Br J Nutr* 2000; **84/2**: 175-184.

88 Ruzickova J, Rossmeisl M, Prazak T, Flachs P, Sponarova J, Veck M et al. Omega-3 PUFA of marine origin limit diet-induced obesity in mice by reducing cellularity of adipose tissue. *Lipids* 2004; **39/12**: 1177-1185.

89 Catala A. Five decades with polyunsaturated Fatty acids: chemical synthesis, enzymatic formation, lipid peroxidation and its biological effects. *J Lipids* 2013; **2013**: 710290.

90 Lorente-Cebrian S, Costa AG, Navas-Carretero S, Zabala M, Martinez JA, Moreno-Aliaga MJ. Role of omega-3 fatty acids in obesity, metabolic syndrome, and cardiovascular diseases: a review of the evidence. *J Physiol Biochem* 2013; **69/3**: 633-651.

91 Guichardant M, Calzada C, Bernoud-Hubac N, Lagarde M, Vericel E. Omega-3 polyunsaturated fatty acids and oxygenated metabolism in atherothrombosis. *Biochim Biophys Acta* 2015; **1851/4**: 485-495.

92 Monteiro J, Leslie M, Moghadasian MH, Arendt BM, Allard JP, Ma DW. The role of n - 6 and n - 3 polyunsaturated fatty acids in the manifestation of the metabolic syndrome in cardiovascular disease and non-alcoholic fatty liver disease. *Food Funct* 2014; **5/3**: 426-435.

93 Flachs P, Rossmeisl M, Bryhn M, Kopecky J. Cellular and molecular effects of n-3 polyunsaturated fatty acids on adipose tissue biology and metabolism. *Clin Sci (Lond)* 2009; **116/1**: 1-16.

94 Oh DY, Talukdar S, Bae EJ, Imamura T, Morinaga H, Fan W et al. GPR120 is an omega-3 fatty acid receptor mediating potent anti-inflammatory and insulin-sensitizing effects. *Cell* 2010; **142/5**: 687-698.

95 Flachs P, Horakova O, Brauner P, Rossmeisl M, Pecina P, Franssen-van HN et al. Polyunsaturated fatty acids of marine origin upregulate mitochondrial biogenesis and induce beta-oxidation in white fat. *Diabetologia* 2005; **48/11**: 2365-2375.

96 Madsen L, Petersen RK, Kristiansen K. Regulation of adipocyte differentiation and function by polyunsaturated fatty acids. *Biochim Biophys Acta* 2005; **1740/2**: 266-286.

97 Madsen L, Pedersen LM, Lillefosse HH, Fjaere E, Bronstad I, Hao Q et al. UCP1 induction during recruitment of brown adipocytes in white adipose tissue is dependent on cyclooxygenase activity. *PLoS One* 2010; **5/6**: e11391.

98 Pedersen BK. The diseasome of physical inactivity--and the role of myokines in muscle--fat cross talk. *J Physiol* 2009; **587/Pt 23**: 5559-5568.

99 Raschke S, Eckel J. Adipo-myokines: two sides of the same coin--mediators of inflammation and mediators of exercise. *Mediators Inflamm* 2013; **2013**: 320724.

100 Eckardt K, Gorgens SW, Raschke S, Eckel J. Myokines in insulin resistance and type 2 diabetes. *Diabetologia* 2014; **57/6**: 1087-1099.

101 Scarpace PJ, Yenice S, Tumer N. Influence of exercise training and age on uncoupling protein mRNA expression in brown adipose tissue. *Pharmacol Biochem Behav* 1994; **49/4**: 1057-1059.

102 Segawa M, Oh-Ishi S, Kizaki T, Ookawara T, Sakurai T, Izawa T et al. Effect of running training on brown adipose tissue activity in rats: a reevaluation. *Res Commun Mol Pathol Pharmacol* 1998; **100/1**: 77-82.

103 De MR, Lucertini F, Guescini M, Polidori E, Zeppa S, Stocchi V et al. Exercise as a new physiological stimulus for brown adipose tissue activity. *Nutr Metab Cardiovasc Dis* 2013; **23/6**: 582-590.

104 Roca-Rivada A, Castelao C, Senin LL, Landrove MO, Baltar J, Belen CA et al. FNDC5/irisin is not only a myokine but also an adipokine. *PLoS One* 2013; **8/4**: e60563.

105 Xu X, Ying Z, Cai M, Xu Z, Li Y, Jiang SY et al. Exercise ameliorates high-fat diet-induced metabolic and vascular dysfunction, and increases adipocyte progenitor cell population in brown adipose tissue. *Am J Physiol Regul Integr Comp Physiol* 2011; **300/5**: R1115-R1125.

106 Bostrom P, Wu J, Jedrychowski MP, Korde A, Ye L, Lo JC et al. A PGC1-alpha-dependent myokine that drives brown-fat-like development of white fat and thermogenesis. *Nature* 2012; **481/7382**: 463-468.

107 Kelly DP. Medicine. Irisin, light my fire. *Science* 2012; **336/6077**: 42-43.

108 Arner P. Insulin resistance in type 2 diabetes -- role of the adipokines. *Curr Mol Med* 2005; **5/3**: 333-339.

109 Bouloumie A, Curat CA, Sengenes C, Lolmede K, Miranville A, Busse R. Role of macrophage tissue infiltration in metabolic diseases. *Curr Opin Clin Nutr Metab Care* 2005; **8/4**: 347-354.

110 Koerner A, Kratzsch J, Kiess W. Adipocytokines: leptin--the classical, resistin--the controversical, adiponectin--the promising, and more to come. *Best Pract Res Clin Endocrinol Metab* 2005; **19/4**: 525-546.

111 Rosenow A, Noben JP, Bouwman FG, Mariman EC, Renes J. Hypoxia-mimetic effects in the secretome of human preadipocytes and adipocytes. *Biochim Biophys Acta* 2013; **1834/12**: 2761-2771.

112 Kim J, Choi YS, Lim S, Yea K, Yoon JH, Jun DJ et al. Comparative analysis of the secretory proteome of human adipose stromal vascular fraction cells during adipogenesis. *Proteomics* 2010; **10/3**: 394-405.

113 Zhong J, Krawczyk SA, Chaerkady R, Huang H, Goel R, Bader JS et al. Temporal profiling of the secretome during adipogenesis in humans. *J Proteome Res* 2010; **9/10**: 5228-5238.

114 Lim JM, Wollaston-Hayden EE, Teo CF, Hausman D, Wells L. Quantitative secretome and glycome of primary human adipocytes during insulin resistance. *Clin Proteomics* 2014; **11/1**: 20.

115 Sun K, Kusminski CM, Scherer PE. Adipose tissue remodeling and obesity. *J Clin Invest* 2011; **121/6**: 2094-2101.

116 Karastergiou K, Mohamed-Ali V. The autocrine and paracrine roles of adipokines. *Mol Cell Endocrinol* 2010; **318/1-2**: 69-78.

117 Okuno A, Tamemoto H, Tobe K, Ueki K, Mori Y, Iwamoto K et al. Troglitazone increases the number of small adipocytes without the change of white adipose tissue mass in obese Zucker rats. *J Clin Invest* 1998; **101/6**: 1354-1361.

118 Gustafson B, Smith U. The WNT inhibitor Dickkopf 1 and bone morphogenetic protein 4 rescue adipogenesis in hypertrophic obesity in humans. *Diabetes* 2012; **61/5**: 1217-1224.

119 Gordon MD, Nusse R. Wnt signaling: multiple pathways, multiple receptors, and multiple transcription factors. *J Biol Chem* 2006; **281/32**: 22429-22433.

120 Ross SE, Hemati N, Longo KA, Bennett CN, Lucas PC, Erickson RL et al. Inhibition of adipogenesis by Wnt signaling. *Science* 2000; **289/5481**: 950-953.

121 Jackson A, Vayssiere B, Garcia T, Newell W, Baron R, Roman-Roman S et al. Gene array analysis of Wnt-regulated genes in C3H10T1/2 cells. *Bone* 2005; **36/4**: 585-598.

122 Waki H, Park KW, Mitro N, Pei L, Damoiseaux R, Wilpitz DC et al. The small molecule harmine is an antidiabetic cell-type-specific regulator of PPARgamma expression. *Cell Metab* 2007; **5/5**: 357-370.

123 Hammarstedt A, Hedjazifar S, Jenndahl L, Gogg S, Grunberg J, Gustafson B et al. WISP2 regulates preadipocyte commitment and PPARgamma activation by BMP4. *Proc Natl Acad Sci U S A* 2013; **110/7**: 2563-2568.

124 Grunberg JR, Hammarstedt A, Hedjazifar S, Smith U. The Novel Secreted Adipokine WNT1-inducible Signaling Pathway Protein 2 (WISP2) Is a Mesenchymal Cell Activator of Canonical WNT. *J Biol Chem* 2014; **289/10**: 6899-6907.

125 Elsen M, Raschke S, Tennagels N, Schwahn U, Jelenik T, Roden M et al. BMP4 and BMP7 induce the white-to-brown transition of primary human adipose stem cells. *Am J Physiol Cell Physiol* 2014; **306/5**: C431-C440.

126 Gao WL, Zhang SQ, Zhang H, Wan B, Yin ZS. Chordin-like protein 1 promotes neuronal differentiation by inhibiting bone morphogenetic protein-4 in neural stem cells. *Mol Med Rep* 2013; **7/4**: 1143-1148.

127 Sakuta H, Suzuki R, Takahashi H, Kato A, Shintani T, Iemura S et al. Ventroptin: a BMP-4 antagonist expressed in a double-gradient pattern in the retina. *Science* 2001; **293/5527**: 111-115.

128 Larman BW, Karolak MJ, Adams DC, Oxburgh L. Chordin-like 1 and twisted gastrulation 1 regulate BMP signaling following kidney injury. *J Am Soc Nephrol* 2009; **20/5**: 1020-1031.

129 Kane R, Godson C, O'Brien C. Chordin-like 1, a bone morphogenetic protein-4 antagonist, is upregulated by hypoxia in human retinal pericytes and plays a role in regulating angiogenesis. *Mol Vis* 2008; **14**: 1138-1148.

130 Fernandes H, Dechering K, van SE, Steeghs I, Apotheker M, Mentink A et al. Effect of chordin-like 1 on MC3T3-E1 and human mesenchymal stem cells. *Cells Tissues Organs* 2010; **191/6**: 443-452.

131 Chandra A, Itakura T, Yang Z, Tamakoshi T, Xue X, Wang B et al. Neurogenesin-1 differentially inhibits the osteoblastic differentiation by bone morphogenetic proteins in C2C12 cells. *Biochem Biophys Res Commun* 2006; **344/3**: 786-791.

132 Gustafson B, Hammarstedt A, Hedjazifar S, Hoffmann JM, Svensson PA, Grimsby J et al. BMP4 and BMP antagonists regulate human white and beige adipogenesis. *Diabetes* 2015.

133 Tang QQ, Otto TC, Lane MD. Commitment of C3H10T1/2 pluripotent stem cells to the adipocyte lineage. *Proc Natl Acad Sci U S A* 2004; **101/26**: 9607-9611.

134 Huang H, Song TJ, Li X, Hu L, He Q, Liu M et al. BMP signaling pathway is required for commitment of C3H10T1/2 pluripotent stem cells to the adipocyte lineage. *Proc Natl Acad Sci U S A* 2009; **106/31**: 12670-12675.

135 Bowers RR, Kim JW, Otto TC, Lane MD. Stable stem cell commitment to the adipocyte lineage by inhibition of DNA methylation: role of the BMP-4 gene. *Proc Natl Acad Sci U S A* 2006; **103/35**: 13022-13027.

136 Suenaga M, Matsui T, Funaba M. BMP Inhibition with dorsomorphin limits adipogenic potential of preadipocytes. *J Vet Med Sci* 2010; **72/3**: 373-377.

137 Boulet N, Esteve D, Bouloumie A, Galitzky J. BMP7 is produced by a specific human adipose tissue progenitor cell subset and promotes human progenitor cell brite adipogenesis. Diabetologia Abstract volume EASD. 2014.

138 Zeng J, Jiang Y, Xiang S, Chen B. Serum bone morphogenetic protein 7, insulin resistance, and insulin secretion in non-diabetic individuals. *Diabetes Res Clin Pract* 2011; **93/1**: e21-e24.

139 Son JW, Kim MK, Park YM, Baek KH, Yoo SJ, Song KH et al. Association of serum bone morphogenetic protein 4 levels with obesity and metabolic syndrome in non-diabetic individuals. *Endocr J* 2011; **58/1**: 39-46.

140 Xue R, Wan Y, Zhang S, Zhang Q, Ye H, Li Y. Role of bone morphogenetic protein 4 in the differentiation of brown fat-like adipocytes. *Am J Physiol Endocrinol Metab* 2014; **306/4**: E363-E372.

141 Tews D, Schwar V, Scheithauer M, Weber T, Fromme T, Klingenspor M et al. Comparative gene array analysis of progenitor cells from human paired deep neck and subcutaneous adipose tissue. *Mol Cell Endocrinol* 2014; **395/1-2**: 41-50.

142 Wang S, Liang X, Yang Q, Fu X, Rogers CJ, Zhu M et al. Resveratrol induces brown-like adipocyte formation in white fat through activation of AMP-activated protein kinase (AMPK) alpha1. *Int J Obes (Lond)* 2015.

143 Belchior T, Paschoal VA, Magdalon J, Chimin P, Farias TM, Chaves-Filho AB et al. Omega-3 fatty acids protect from diet-induced obesity, glucose intolerance, and adipose tissue inflammation through PPARgamma-dependent and PPARgamma-independent actions. *Mol Nutr Food Res* 2015.

144 Ailhaud G, Massiera F, Weill P, Legrand P, Alessandri JM, Guesnet P. Temporal changes in dietary fats: role of n-6 polyunsaturated fatty acids in excessive adipose tissue development and relationship to obesity. *Prog Lipid Res* 2006; **45/3**: 203-236.

145 Inoue K, Kishida K, Hirata A, Funahashi T, Shimomura I. Low serum eicosapentaenoic acid / arachidonic acid ratio in male subjects with visceral obesity. *Nutr Metab (Lond)* 2013; **10/1**: 25.

146 Imamura S, Morioka T, Yamazaki Y, Numaguchi R, Urata H, Motoyama K et al. Plasma polyunsaturated fatty acid profile and delta-5 desaturase activity are altered in patients with type 2 diabetes. *Metabolism* 2014; **63/11**: 1432-1438.

147 Fleckenstein-Elsen M, Dinnies D, Jelenik T, Roden M, Romacho T, Eckel J. Eicosapentaenoic acid and arachidonic acid differentially regulate white-to-brown conversion and mitochondrial function in primary human adipocytes. *Int J Obes (Lond)* 2015; **submitted**.

148 Kim HK, Della-Fera M, Lin J, Baile CA. Docosahexaenoic acid inhibits adipocyte differentiation and induces apoptosis in 3T3-L1 preadipocytes. *J Nutr* 2006; **136/12**: 2965-2969.

149 Barber E, Sinclair AJ, Cameron-Smith D. Comparative actions of omega-3 fatty acids on in-vitro lipid droplet formation. *Prostaglandins Leukot Essent Fatty Acids* 2013; **89/5**: 359-366.

150 Manickam E, Sinclair AJ, Cameron-Smith D. Suppressive actions of eicosapentaenoic acid on lipid droplet formation in 3T3-L1 adipocytes. *Lipids Health Dis* 2010; **9**: 57.

151 Murali G, Desouza CV, Clevenger ME, Ramalingam R, Saraswathi V. Differential effects of eicosapentaenoic acid and docosahexaenoic acid in promoting the differentiation of 3T3-L1 preadipocytes. *Prostaglandins Leukot Essent Fatty Acids* 2014; **90/1**: 13-21.

152 Gaillard D, Negrel R, Lagarde M, Ailhaud G. Requirement and role of arachidonic acid in the differentiation of pre-adipose cells. *Biochem J* 1989; **257/2**: 389-397.

153 Petersen RK, Jorgensen C, Rustan AC, Froyland L, Muller-Decker K, Furstenberger G et al. Arachidonic acid-dependent inhibition of adipocyte differentiation requires PKA activity and is associated with sustained expression of cyclooxygenases. *J Lipid Res* 2003; **44/12**: 2320-2330.

154 Casimir DA, Miller CW, Ntambi JM. Preadipocyte differentiation blocked by prostaglandin stimulation of prostanoid FP2 receptor in murine 3T3-L1 cells. *Differentiation* 1996; **60/4**: 203-210.

155 Vassaux G, Gaillard D, Ailhaud G, Negrel R. Prostacyclin is a specific effector of adipose cell differentiation. Its dual role as a cAMP- and Ca(2+)-elevating agent. *J Biol Chem* 1992; **267/16**: 11092-11097.

156 Negrel R, Gaillard D, Ailhaud G. Prostacyclin as a potent effector of adipose-cell differentiation. *Biochem J* 1989; **257/2**: 399-405.

157 Banga A, Unal R, Tripathi P, Pokrovskaya I, Owens RJ, Kern PA et al. Adiponectin translation is increased by the PPARgamma agonists pioglitazone and omega-3 fatty acids. *Am J Physiol Endocrinol Metab* 2009; **296/3**: E480-E489.

158 Romacho T, Glosse P, Richter I, Elsen M, Schoemaker MH, van Tol EA et al. Nutritional ingredients modulate adipokine secretion and inflammation in human primary adipocytes. *Nutrients* 2015; **7/2**: 865-886.

159 Tishinsky JM, Ma DW, Robinson LE. Eicosapentaenoic acid and rosiglitazone increase adiponectin in an additive and PPARgamma-dependent manner in human adipocytes. *Obesity (Silver Spring)* 2011; **19/2**: 262-268.

160 Russell FD, Burgin-Maunder CS. Distinguishing health benefits of eicosapentaenoic and docosahexaenoic acids. *Mar Drugs* 2012; **10/11**: 2535-2559.

161 Zhao M, Chen X. Eicosapentaenoic acid promotes thermogenic and fatty acid storage capacity in mouse subcutaneous adipocytes. *Biochem Biophys Res Commun* 2014; **450/4**: 1446-1451.

162 Pisani DF, Ghandour RA, Beranger GE, Le FP, Chambard JC, Giroud M et al. The omega6-fatty acid, arachidonic acid, regulates the conversion of white to brite adipocyte through a prostaglandin/calcium mediated pathway. *Mol Metab* 2014; **3/9**: 834-847.

163 Flachs P, Rossmeisl M, Kuda O, Kopecky J. Stimulation of mitochondrial oxidative capacity in white fat independent of UCP1: a key to lean phenotype. *Biochim Biophys Acta* 2013; **1831/5**: 986-1003.

164 Wilson-Fritch L, Nicoloro S, Chouinard M, Lazar MA, Chui PC, Leszyk J et al. Mitochondrial remodeling in adipose tissue associated with obesity and treatment with rosiglitazone. *J Clin Invest* 2004; **114/9**: 1281-1289.

165 Valerio A, Cardile A, Cozzi V, Bracale R, Tedesco L, Pisconti A et al. TNF-alpha downregulates eNOS expression and mitochondrial biogenesis in fat and muscle of obese rodents. *J Clin Invest* 2006; **116/10**: 2791-2798.

166 Hallgren P, Sjostrom L, Hedlund H, Lundell L, Olbe L. Influence of age, fat cell weight, and obesity on O2 consumption of human adipose tissue. *Am J Physiol* 1989; **256/4 Pt 1**: E467-E474.

167 Pietilainen KH, Naukkarinen J, Rissanen A, Saharinen J, Ellonen P, Keranen H et al. Global transcript profiles of fat in monozygotic twins discordant for BMI: pathways behind acquired obesity. *PLoS Med* 2008; **5/3**: e51.

168 Keuper M, Jastroch M, Yi CX, Fischer-Posovszky P, Wabitsch M, Tschop MH et al. Spare mitochondrial respiratory capacity permits human adipocytes to maintain ATP homeostasis under hypoglycemic conditions. *FASEB J* 2014; **28/2**: 761-770.

169 Sriskanthadevan S, Jeyaraju DV, Chung TE, Prabha S, Xu W, Skrtic M et al. AML cells have low spare reserve capacity in their respiratory chain that renders them susceptible to oxidative metabolic stress. *Blood* 2015; **125/13**: 2120-2130.

170 Bronnikov GE, Kulagina TP, Aripovsky AV. Dietary supplementation of old rats with hydrogenated peanut oil restores activities of mitochondrial respiratory complexes in skeletal muscles. *Biochemistry (Mosc)* 2010; **75/12**: 1491-1497.

171 Bajpai P, Srinivasan S, Ghosh J, Nagy LD, Wei S, Guengerich FP et al. Targeting of splice variants of human cytochrome P450 2C8 (CYP2C8) to mitochondria and their role in arachidonic acid metabolism and respiratory dysfunction. *J Biol Chem* 2014; **289/43**: 29614-29630.

172 Dong GZ, Lee JH, Ki SH, Yang JH, Cho IJ, Kang SH et al. AMPK activation by isorhamnetin protects hepatocytes against oxidative stress and mitochondrial dysfunction. *Eur J Pharmacol* 2014; **740**: 634-640.

173 Toniolo A, Buccellati C, Pinna C, Gaion RM, Sala A, Bolego C. Cyclooxygenase-1 and prostacyclin production by endothelial cells in the presence of mild oxidative stress. *PLoS One* 2013; **8/2**: e56683.

174 Sharma A, Huard C, Vernochet C, Ziemek D, Knowlton KM, Tyminski E et al. Brown fat determination and development from muscle precursor cells by novel action of bone morphogenetic protein 6. *PLoS One* 2014; **9/3**: e92608.

175 Gollisch KS, Brandauer J, Jessen N, Toyoda T, Nayer A, Hirshman MF et al. Effects of exercise training on subcutaneous and visceral adipose tissue in normal- and high-fat diet-fed rats. *Am J Physiol Endocrinol Metab* 2009; **297/2**: E495-E504.

176 Wenz T, Rossi SG, Rotundo RL, Spiegelman BM, Moraes CT. Increased muscle PGC-1alpha expression protects from sarcopenia and metabolic disease during aging. *Proc Natl Acad Sci U S A* 2009; **106/48**: 20405-20410.

177 Teufel A, Malik N, Mukhopadhyay M, Westphal H. Frcp1 and Frcp2, two novel fibronectin type III repeat containing genes. *Gene* 2002; **297/1-2**: 79-83.

178 Ferrer-Martinez A, Ruiz-Lozano P, Chien KR. Mouse PeP: a novel peroxisomal protein linked to myoblast differentiation and development. *Dev Dyn* 2002; **224/2**: 154-167.

179 Erickson HP. Irisin and FNDC5 in retrospect: An exercise hormone or a transmembrane receptor? *Adipocyte* 2013; **2/4**: 289-293.

180 Albrecht E, Norheim F, Thiede B, Holen T, Ohashi T, Schering L et al. Irisin - a myth rather than an exercise-inducible myokine. *Sci Rep* 2015; **5**: 8889.

181 Lee P, Linderman JD, Smith S, Brychta RJ, Wang J, Idelson C et al. Irisin and FGF21 are cold-induced endocrine activators of brown fat function in humans. *Cell Metab* 2014; **19/2**: 302-309.

182 Elsen M, Raschke S, Eckel J. Browning of white fat: does irisin play a role in humans? *J Endocrinol* 2014; **222/1**: R25-R38.

183 Sanchis-Gomar F, Alis R, Pareja-Galeano H, Romagnoli M, Perez-Quilis C. Inconsistency in circulating irisin levels: what is really happening? *Horm Metab Res* 2014; **46/8**: 591-596.

184 Raschke S, Elsen M, Gassenhuber H, Sommerfeld M, Schwahn U, Brockmann B et al. Evidence against a beneficial effect of irisin in humans. *PLoS One* 2013; **8/9**: e73680.

185 Kozak M. Downstream secondary structure facilitates recognition of initiator codons by eukaryotic ribosomes. *Proc Natl Acad Sci U S A* 1990; **87/21**: 8301-8305.

186 Servick K. Biomedicine. Woes for 'exercise hormone'. *Science* 2015; **347/6228**: 1299.

187 Wu J, Spiegelman BM. Irisin ERKs the fat. *Diabetes* 2014; **63/2**: 381-383.

188 Elsen M, Raschke S, Sommerfeld M, Gassenhuber H, Eckel J. Comment on Wu and Spiegelman. Irisin ERKs the fat. Diabetes 2014;63:381-383. *Diabetes* 2014; **63/9**: e16.

189 Spiegelman BM, Wrann C. Response to Comment on Wu and Spiegelman. Irisin ERKs the fat. Diabetes 2014;63:381-383. *Diabetes* 2014; **63/9**: e17.

190 Zhang Y, Li R, Meng Y, Li S, Donelan W, Zhao Y et al. Irisin stimulates browning of white adipocytes through mitogen-activated protein kinase p38 MAP kinase and ERK MAP kinase signaling. *Diabetes* 2014; **63/2**: 514-525.

191 Wang C, Wang L, Li W, Yan F, Tian M, Wu C et al. Irisin has no effect on lipolysis in 3T3-L1 adipocytes or fatty acid metabolism in HepG2 hepatocytes. *Endocrine* 2014.

192 Huh JY, Dincer F, Mesfum E, Mantzoros CS. Irisin stimulates muscle growth-related genes and regulates adipocyte differentiation and metabolism in humans. *Int J Obes (Lond)* 2014; **38/12**: 1538-1544.

193 Roberts LD, Bostrom P, O'Sullivan JF, Schinzel RT, Lewis GD, Dejam A et al. beta-Aminoisobutyric acid induces browning of white fat and hepatic beta-oxidation and is inversely correlated with cardiometabolic risk factors. *Cell Metab* 2014; **19/1**: 96-108.

Danksagung

Mein besonderer Dank gilt Prof. Dr. Jürgen Eckel, insbesondere für die Möglichkeit als Ernährungswissenschaftlerin in der Biologie promovieren zu können. Nachdem die Umsetzung von Plan A eher schleppend verlief haben wir gemeinsam einen für mich perfekten Plan B entwickelt. Ich habe mich immer für mein Thema begeistert und der Abschluss meiner Arbeit hätte mit meinem Studienhintergrund nicht besser sein können. Weiterhin möchte ich mich auch für die persönliche Weiterentwicklung bedanken, die ich durch zahlreiche nationale und international Kongresse sowie die Arbeit innerhalb verschiedener Industrieprojekte durchlaufen durfte.

Vielen Dank an Prof. Dr. Eckhard Lammert für die Hilfe bei der Durchführung des Anerkennungsverfahrens an der Heinrich-Heine-Universität Düsseldorf, die Übernahme des Korreferats und für sein Interesse an dieser Arbeit.

Ein großer Dank gilt auch den industriellen Kooperationspartnern in Frankfurt und Nijmegen, die durch Diskussionen und ihrem experimentellen Einsatz zum Erfolg dieser Arbeit beigetragen haben.

Weiterhin möchte ich mich bei Henrike und insbesondere bei Tanya für die geduldige Beantwortung meiner Fragen, gemeinsame wissenschaftliche Diskussionen und die Betreuung während meiner Doktorarbeit bedanken. Tomas Jelenik möchte ich für die erfolgreiche, unkomplizierte Zusammenarbeit und die Hilfe am Oxygraphen bedanken. Andrea, Marlis und Angelika danke ich dafür, dass sie mich zu einem Fettzellexperten gemacht haben und für ihre Hilfe im Labor. Bei allen gegenwärtigen und früheren Doktoranden der PLG bedanke ich mich für die Unterstützung in den letzten vier Jahren, das Feiern von Höhen und die Motivation in schlechten Zeiten. Insbesondere Susanne und Silja gilt mein Dank, die ich in meinem ersten Jahr mit tausend Fragen gelöchert habe. Ein großes Dankeschön an meine Masterstudentin Daniela. Du hast einen super Job gemacht! Danke an Birgit für die Hilfe bei bürokratischen Angelegenheiten.

Zuletzt möchte ich mich bei meiner Familie für die Ermöglichung meines Studiums, Auslandssemesters und die große Unterstützung während meiner Promotion bedanken. An dieser Stelle geht auch ein Dankeschön an Prof. Dr. Hartmut Land, der den Forschergeist in mir geweckt und an mich geglaubt hat. Liebe Spiekeroog Truppe, Bonner Mädels, Tennisfreunde, Nachbarn, Daniela und Thomas; Danke für eure Freundschaft!

Lieber Martin, Danke für Alles. Du hast nie an meiner Kompetenz gezweifelt.

Eidesstattliche Erklärung

Die vorliegende Dissertation habe ich eigenständig und ohne unerlaubte Hilfe angefertigt. Die Dissertation wurde in der vorgelegten oder in ähnlicher Form noch bei keiner anderen Institution eingereicht. Ich habe bisher keine erfolglosen Promotionsversuche unternommen.

(Manuela Fleckenstein-Elsen)

Düsseldorf, den 27.04.2015